BOEING

Volume VII

Phase I, Final Briefing
SPS and Rectenna Systems Analyses
D180-25037-7

Solar Power Satellite System Definition Study

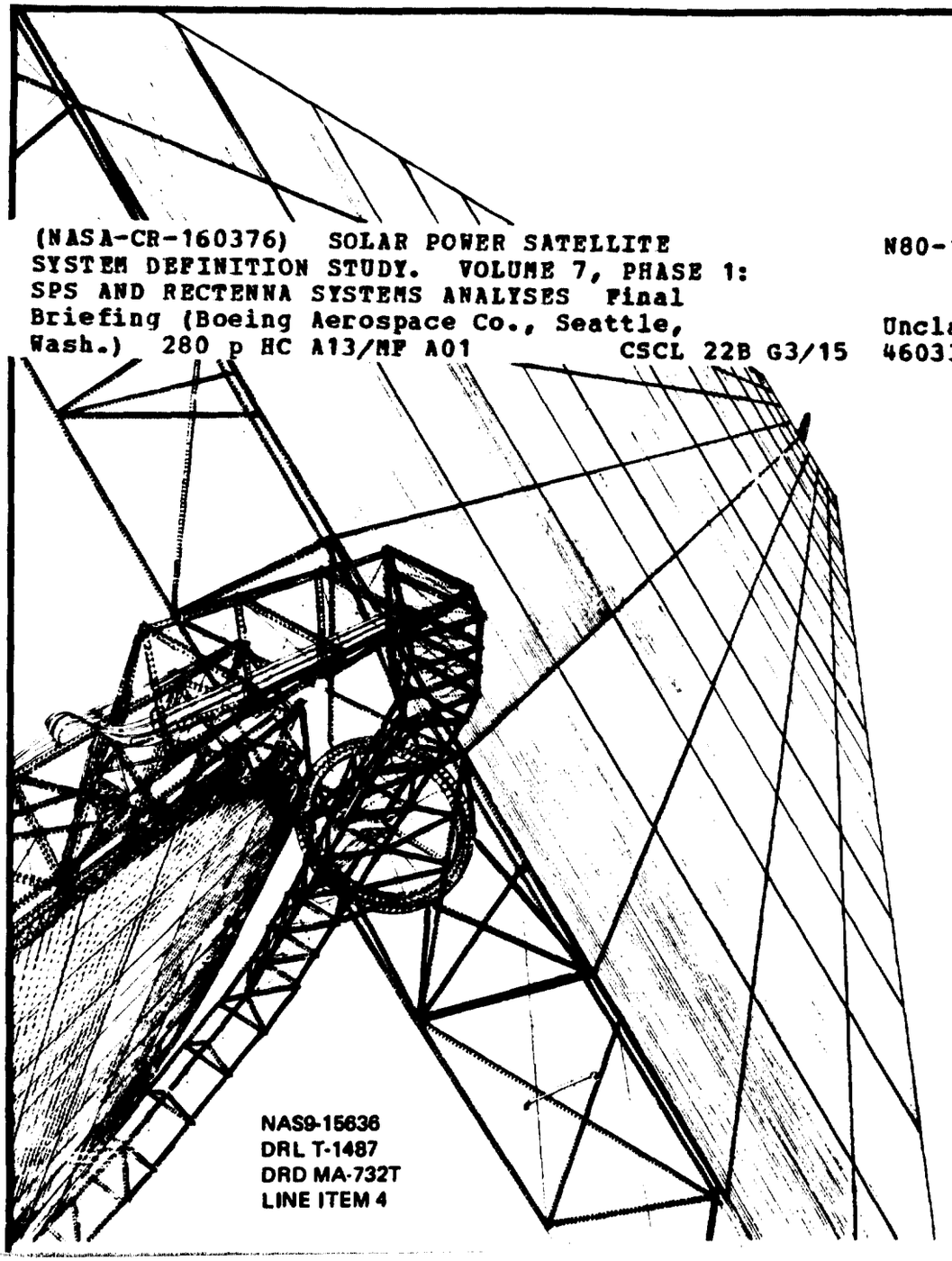

NAS9-15636
DRL T-1487
DRD MA-732T
LINE ITEM 4

BOEING

GENERAL ELECTRIC

GRUMMAN

Arthur D Little, Inc

TRW

Solar Power Satellite
System Definition Study

Volume VII
PHASE I FINAL BRIEFING
SPS and Rectenna Systems Analyses
D180-25037-7

Approved By: G R Woodcock
G. R. Woodcock
Study Manager

Boeing Aerospace Company
Ballistic Missiles and Space Division
P.O. Box 3999
Seattle, Washington 98124

FOREWORD

The SPS System Definition Study was initiated in June of 1978. Phase I of this effort was completed in December of 1978 and is herewith reported. This study is a follow-on effort to an earlier study of the same title completed in March of 1978. These studies are a part of an overall SPS evaluation effort sponsored by the U. S. Department of Energy (DOE) and the National Aeronautics and Space Administration.

This study is being managed by the Lyndon B. Johnson Space Center. The Contracting Officer is Thomas Mancuso. The Contracting Officer's representative and Study Technical Manager is Harold Benson. The study is being conducted by The Boeing Company with Arthur D. Little, General Electric, Grumman, and TRW as subcontractors. The study manager for Boeing is Gordon Woodcock. Subcontractor managers are Dr. Philip Chapman (ADL), Roman Andryczyk (GE), Ronald McCaffrey (Grumman), and Ronal Crisman (TRW).

This report includes a total of seven volumes:

I - Executive Summary
II - Phase I Systems Analyses and Tradeoffs
III - Reference System Description
IV - Silicon Solar Cell Annealing Tests
V - Phase I Final Briefing Executive Summary
VI - Phase I Final Briefing: Space Construction and Transportation
VII - Phase I Final Briefing: SPS and Rectenna Systems Analyses

In addition, General Electric will supply a supplemental briefing on rectenna construction.

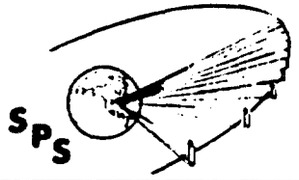

Agenda

BOEING

SPS-2525

THURSDAY, DEC 14TH

*	0900	EXECUTIVE SUMMARY	G. WOODCOCK
		TOPICAL REPORT I: SPACE OPERATIONS	
▶	1045	CONSTRUCTION LOCATION ANALYSIS	E. DAVIS
	1200	(LUNCH)	
▶	1300	SATELLITE CONSTRUCTION ANALYSIS	K. MILLER, R. McCAFFREY
●	1430	ALUMINUM SATELLITE STRUCTURE	R. McCAFFREY
		TOPICAL REPORT II: GROUND OPERATIONS	
▶	1500	INDUSTRIAL INFRASTRUCTURE	P. CHAPMAN
▶	1530	RECTENNA SITING	D. GREGORY

FRIDAY, DEC 15TH

		TOPICAL REPORT III: SATELLITE & RECETNNA SYSTEMS	
●	0900	SOLAR ARRAYS AND ANNEALING	O. DENMAN
●	0930	ONBOARD POWER HANDLING	O. DENMAN
●	0945	ONBOARD DATA & COMMUNICATIONS	R. CRISMAN
●	1015	POWER TRANSMISSION SYSTEM	E. NALOS
●	1100	POWER RECEPTION SYSTEM	R. ANDRYCZYK
	1200	(LUNCH)	
		TOPICAL REPORT IV: DEVELOPMENT PLANNING	
*	1300	TECHNOLOGY ADVANCEMENT	G. WOODCOCK
▶	1330	FLIGHT PROJECTS	D. GREGORY

* = VOLUME V

▶ = VOLUME VI

● = VOLUME VII

STUDY
ALUMINUM STRUCTURE
10 GW SOLAR
POWER SATELLITE

GROUNDRULES

- LEO CONSTRUCTION 4 BY 8 MODULE 2673 m x 5348 m
- FABRICATION IN DIRECTION OF MAJOR AXIS OF MODULE
- CONSTRUCTION BASE MAJOR AXIS IS EARTH POINTING-CONSTRUCTED IN DIRECTION OF VELOCITY VECTOR
- SOLAR BLANKET PRELOADED UNIAXIALLY
- BEAMS ATTACHED CENTROIDALLY
- FLATNESS REQUIREMENT

DESIGN DATA

- MASS DATA

SOLAR ARRAYS	5.178×10^7 kg
MW ANTENNAS	2.521×10^7 kg
WT GROWTH	2.051×10^7 kg
TOTAL	9.75×10^7 kg

- SOLAR ARRAY BLANKET UNIT WEITHT – 0.427 kg/m^2
- T/W IN TRANSPORT FROM LEO TO GEO – 0.0001
- SPS NATURAL FREQUENCY INCLUDING SOLAR CELLS & ANTENNAS – 0.0012 Hz
- SOLAR BLANKET NATURAL FREQUENCY – 0.0024 Hz
- SOLAR BLANKET PRELOAD NEEDED TO OBTAIN FREQUENCY = 4.285 N/m (0.0245 LB./IN.)
- FACTOR OF SAFETY – 1.4
- 30 YEAR SERVICE LIFE

GRUMMAN

DESIGN CONDITIONS

The more significant structural loading conditions currently are the solar array blanket preload and loads caused by transport of the 4 bay x 8 bay module to GEO. The first condition causes a high local cap load in the 7.5 meter beam; the second induces the highest column compression load in the 7.5 m by 667.5 m beam. In as much as aluminum has a coefficient of thermal expansion (CTE) greater than the advanced structural composites, the effect of gradients on distortions, stresses etc., are under evaluation. Thermal control features will be incorporated in the design to minimize thermal/structural response. These include thermal coatings, incorporation of lightening holes in members, etc. Loads induced during fabrication and handling will also require assessment.

DESIGN CONDITIONS

- SOLAR BLANKET PRE-LOAD
- TEMPERATURES & THERMAL GRADIENT TIME HISTORIES
- TRANSPORT ACCELERATION TO GEO
- ATTITUDE CONTROL & STATION KEEPING TORQUES
- STIFFNESS
- INTERFACE LOADS BETWEEN MODULE & CONSTRUCTION BASE; BEAM HANDLING

SOLAR ARRAY PRELOAD DESIGN CONDITION

The LEO baseline configuration utilizes a four bay wide construction base to fabricate the 4 bay by 8 bay module. During module construction, the 15 meter wide solar array blankets are installed on the two end bays of the 8 bay length as shown. The 15 meter arrays are interconnected along their lengths and uniaxially pretensioned such that the blanket natural frequency is 8.64 cph. Bending moments, caused by the pretension result in high axial compression loads in the caps of the 667.5 m beam. This condition gives the critical load in the cap.

SOLAR ARRAY PRE-LOAD DESIGN CONDITION

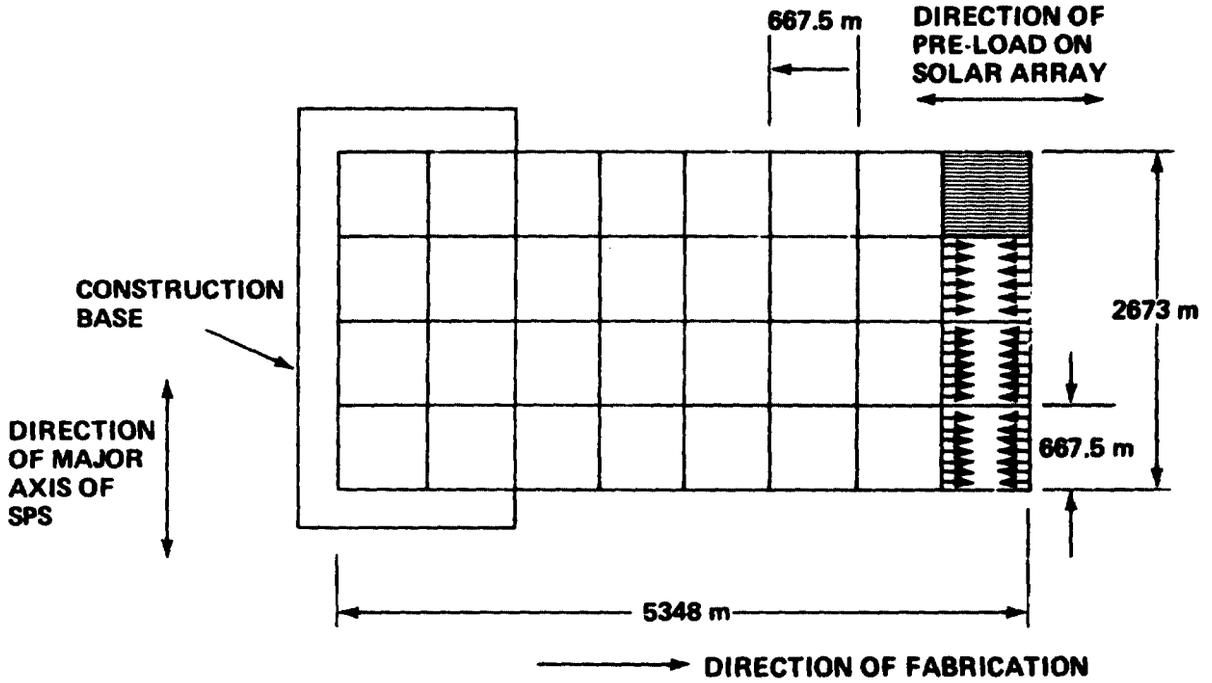

FREQUENCY OF UNIAXIALLY LOADED MEMBRANE

$$f_n = \frac{3600}{2\ell}\sqrt{\frac{S}{W}} \text{ cph}$$

ℓ = LENGTH METERS

S = TENSION PER UNIT WIDTH

W = ARRAY UNIT WEIGHT

REQUIRED f_n = 8.64 cph

LOADS APPLIED TO BEAM BY SOLAR ARRAY

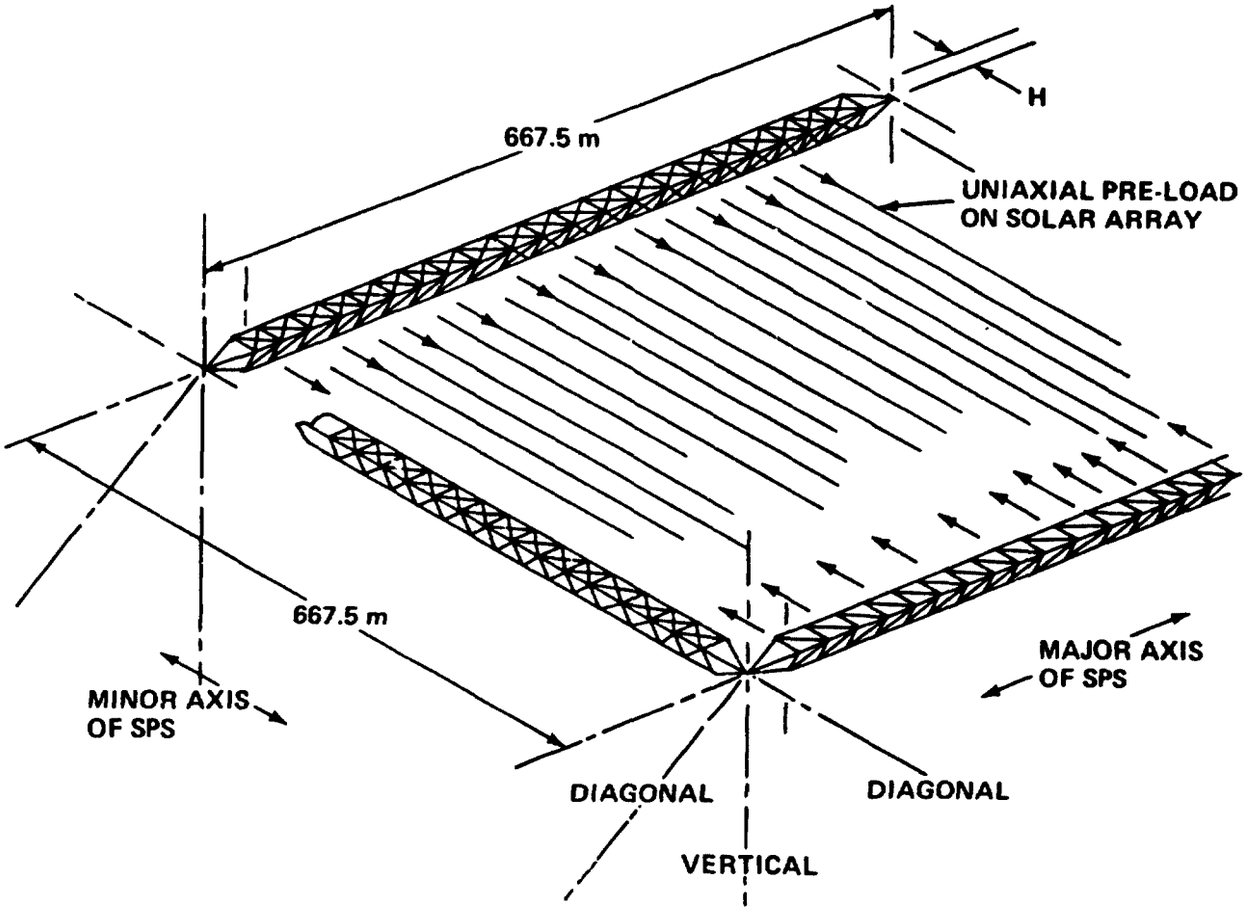

4 BAY BY 8 BAY MODULE

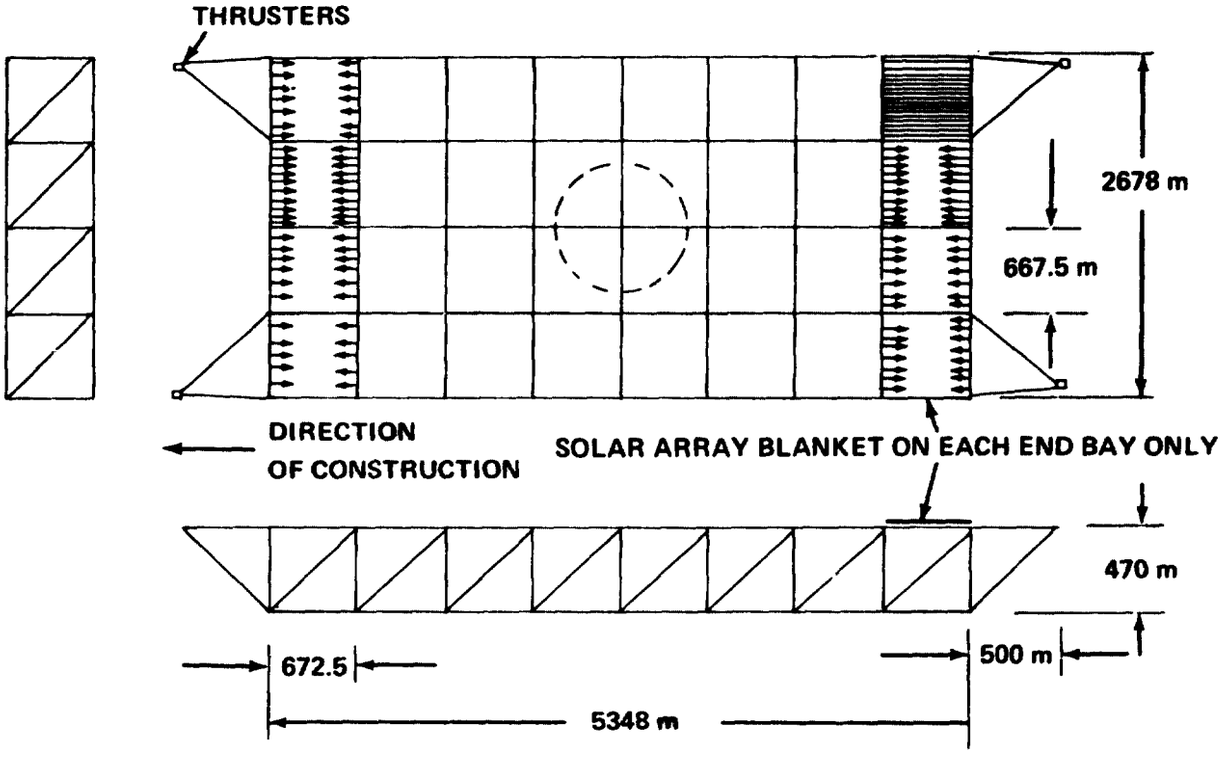

MODULE MASS – 6,500,000 kg
ANTENNA MASS – 12,200,000 kg

MAXIMUM THRUST TO WEIGHT RATIO = 0.0001

GRUMMAN

MODULE SELF TRANSPORT TO GEO DESIGN CONDITION

The maximum compression load in the 667.5 meter member results from the module transfer from LEO to GEO. The four thruster forces are applied to the module and antenna masses as shown in the figure. A dynamic magnification factor of 2.0 and a factor of 1.4 are applied to the member loads. The maximum compression load in the 667.5 meter beam is -7544 lbs.

DESIGN LOADS ON MODULE

CONDITION: SELF-TRANSPORT TO GEO

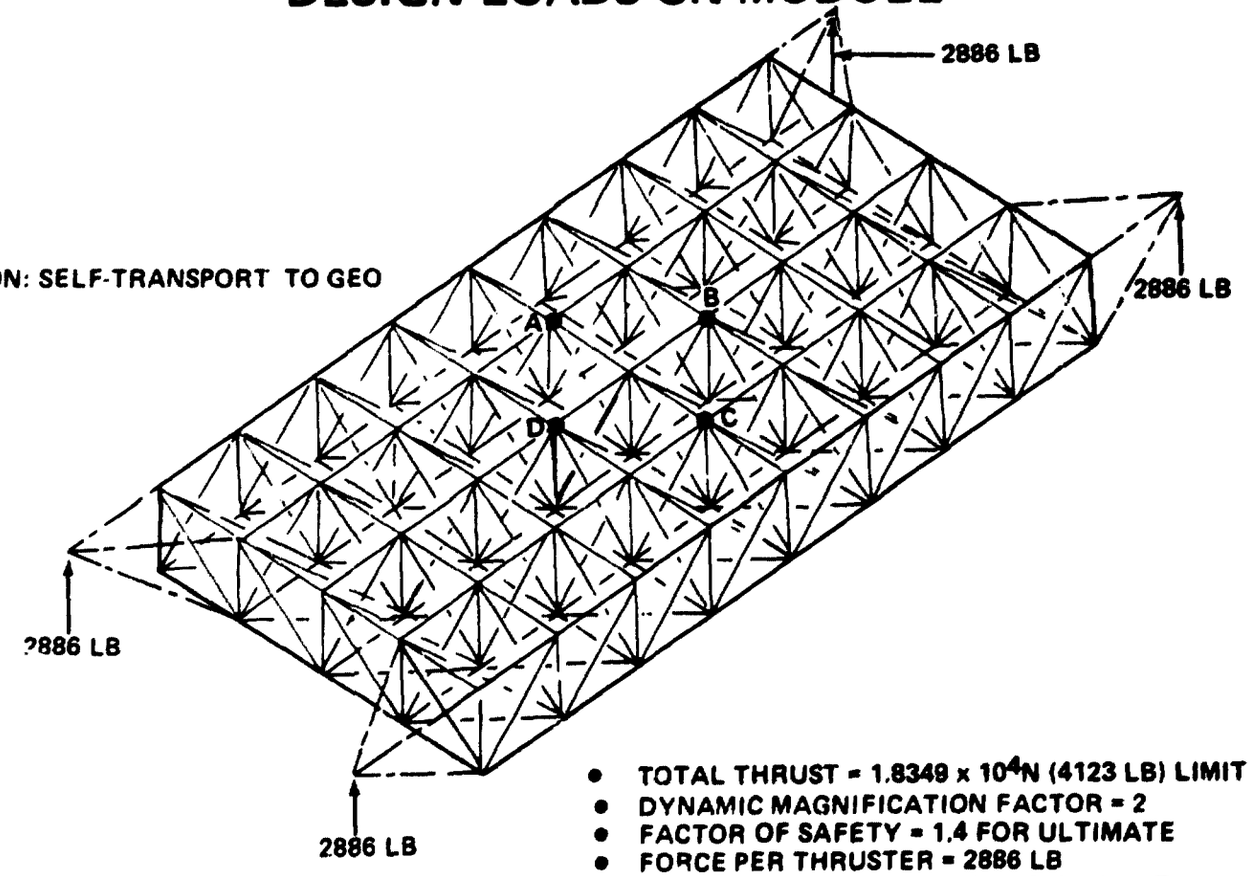

- TOTAL THRUST = 1.8349×10^4N (4123 LB) LIMIT
- DYNAMIC MAGNIFICATION FACTOR = 2
- FACTOR OF SAFETY = 1.4 FOR ULTIMATE
- FORCE PER THRUSTER = 2886 LB
- ANTENNA INERTIA FORCE = 7532 LB ULT.
- MODULE INERTIA FORCE = 4013 LB ULT.
- ANTENNA SUPPORTED AT POINTS A, B, C, D

GRUMMAN

SUMMARY TRUSS LOADS DUE TO ORBIT TRANSFER FROM LEO TO GEO

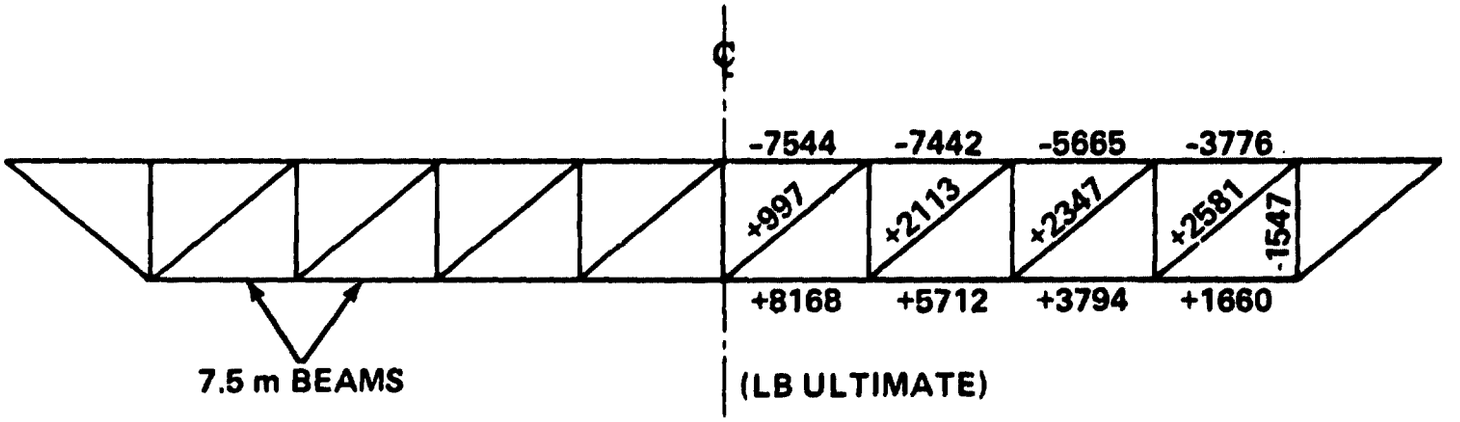

NOTE:
- PRETENSION UNIAXIAL SOLAR BLANKET LOADS ON UPPER BEAMS DO NOT ACT ON ABOVE MEMBERS. BENDING CAUSED BY SOLAR ARRAY PRETENSION OCCURS ON 7.5 m BEAMS NORMAL TO ABOVE BEAMS.
- INCLUDES MODULE & ANTENNA MASSES

VARIATION OF CRITICAL CAP COMPRESSION LOAD VS BEAM DEPTH

MAX MOMENT ON 667.5 m BEAM = 2.96 x 10^6 IN.-LB ULTIMATE

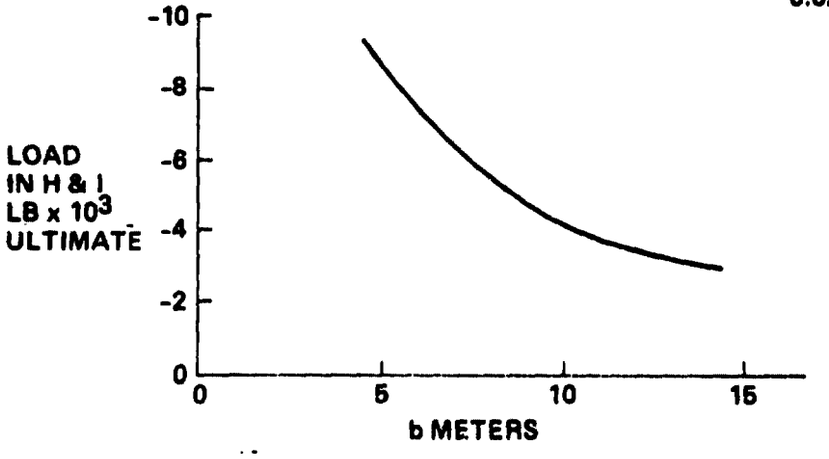

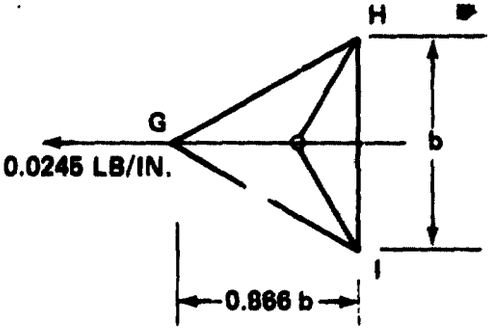

$$C_{H,I} = -\frac{M_{\mathbb{C}}}{1.732\,b}$$

ALUMINUM BEAM DESIGN 7.5 METER

The aluminum triangular cross section beam design incorporates three roll formed closed section caps interconnected by battens spaced at 7.5 meters. Shear stiffness can be provided by either preloaded cross cables or compression/tension members. The cable concept is approximately 20% lighter and has been selected for the baseline aluminum structure. However, pretensioned cables for shear stiffening may induce potential problems such as: adjustment of all cable tensions to the proper preloads to prevent slack at any time, failure of cable attachments, potential for excessive material creep deformation under sustained load and temperature for 30 years increased by an appropriate scatter factor, effect of selected cable system on lattice column capability, etc.

The selected cap size for the design loads is 7.5 inches deep and has a thickness of .028 inches. The batten is also a closed section with the bottom flanges extending outward for attachment to the cap. The depth is 4 inches and thickness of 0.020 inches.

In order to minimize thermal gradients in members and between members, lightening holes have been spaced to reduce shadowing as much as possible. Thermal coatings are also being evaluated to maintain temperatures and gradients within acceptable limits.

The roll formed cap incorporates longitudinal stiffening beads near the corner sections in order to provide a high compression capability in the corners. Between the lightening holes, beads are rolled into the section for stiffening. The section is formed on a mandrel which is used for support during the attachment operation. The lower attachment on the centerline is not completed until after the battens are connected. The gap between flanges permits the mandrel support to extend inward to the beam machine; the mandrel support ends, and the two flanges are joined.

ALUMINUM BEAM DESIGN (7.5 METERS)

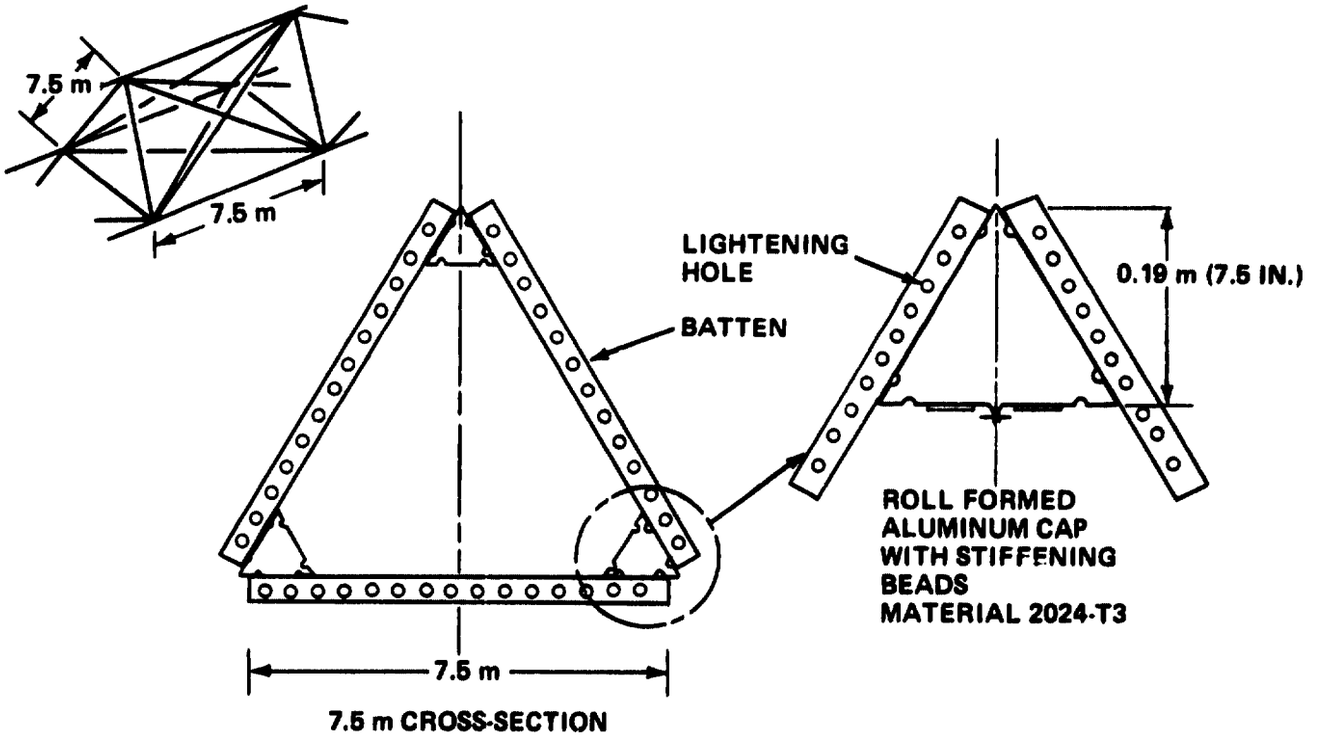

BEAM CAP SECTION ROLL-FORMED ALUMINUM ALLOY

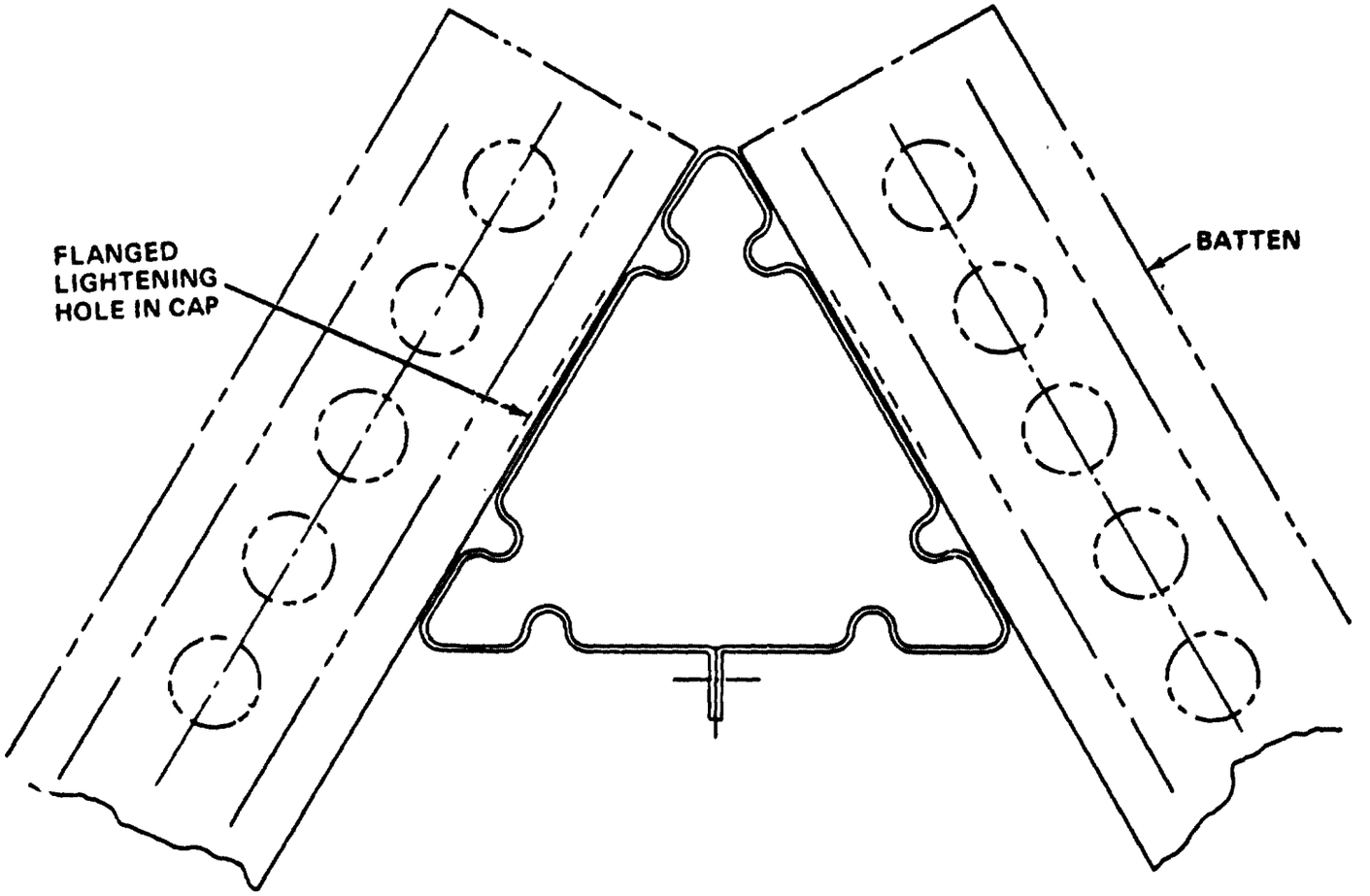

GRUMMAN

BATTEN SECTION ROLL-FORMED

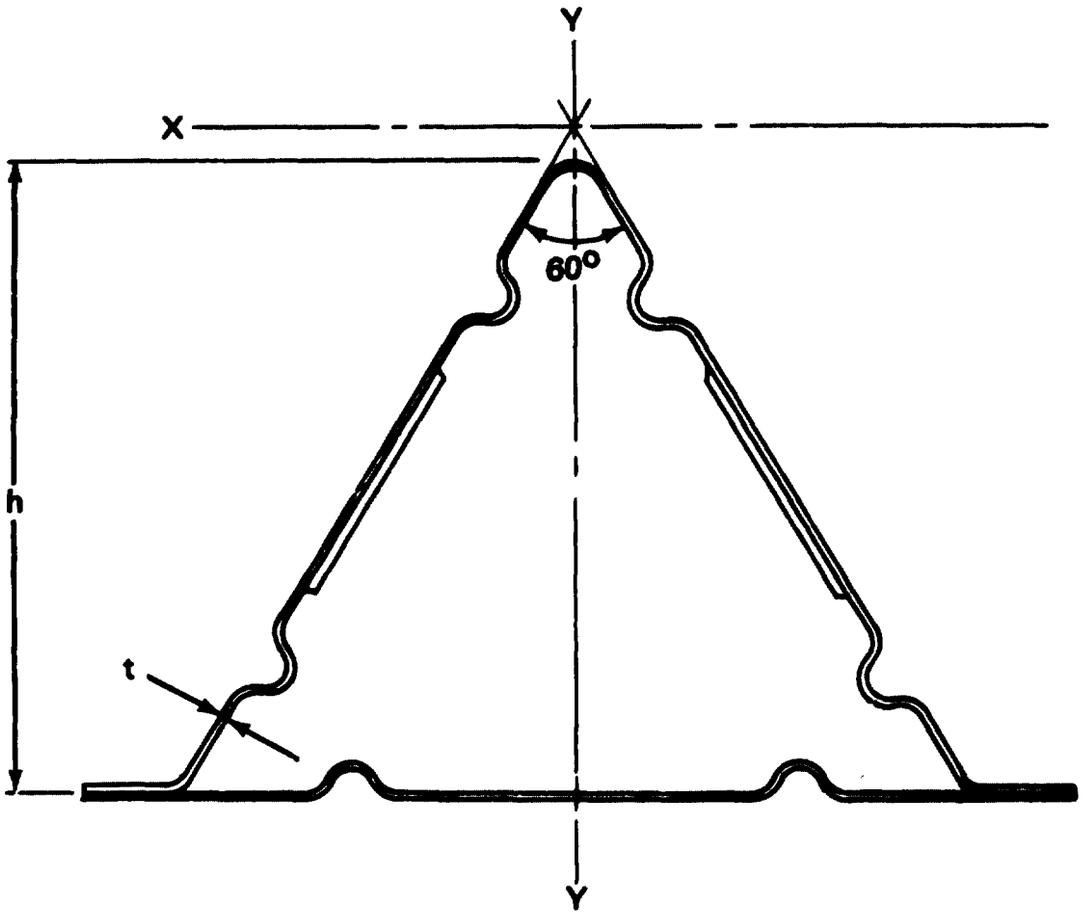

CANDIDATE MATERIAL PROPERTY DATA

	2024-T3	2219-T6	6061-T6
• F_{TU} ksi	64	54	42
• F_{TY} ksi	47	36	36
• F_{CY} ksi	39	38	35
• E_C ksi	10.7×10^3	10.8×10^3	10.1×10^3
• ρ LB/IN.^{3}	0.100	0.102	0.098
• α IN./IN./°F x 10^{-6} @ 200°F	12.9	12.4	13
• K BTU/(HR) (FT^2) (°F)/FT	80	74	96
• C BTU/(LB) (°F) @ 200 °F	0.22	0.23	0.23

ALUMINUM CLOSED SECTION BEAM CAP THICKNESS & DEPTH VS CRITICAL LOAD; L = 7.5 m

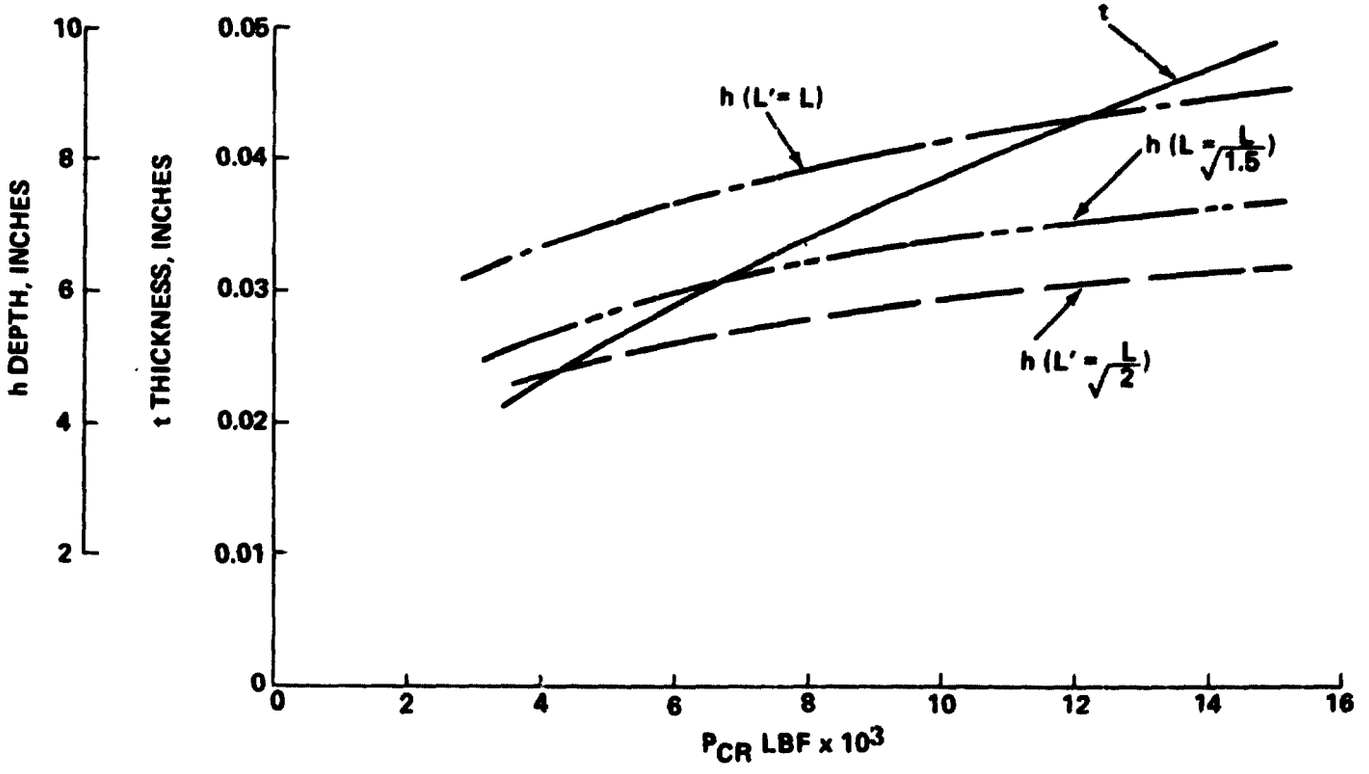

CANDIDATE TRUSS CONFIGURATIONS

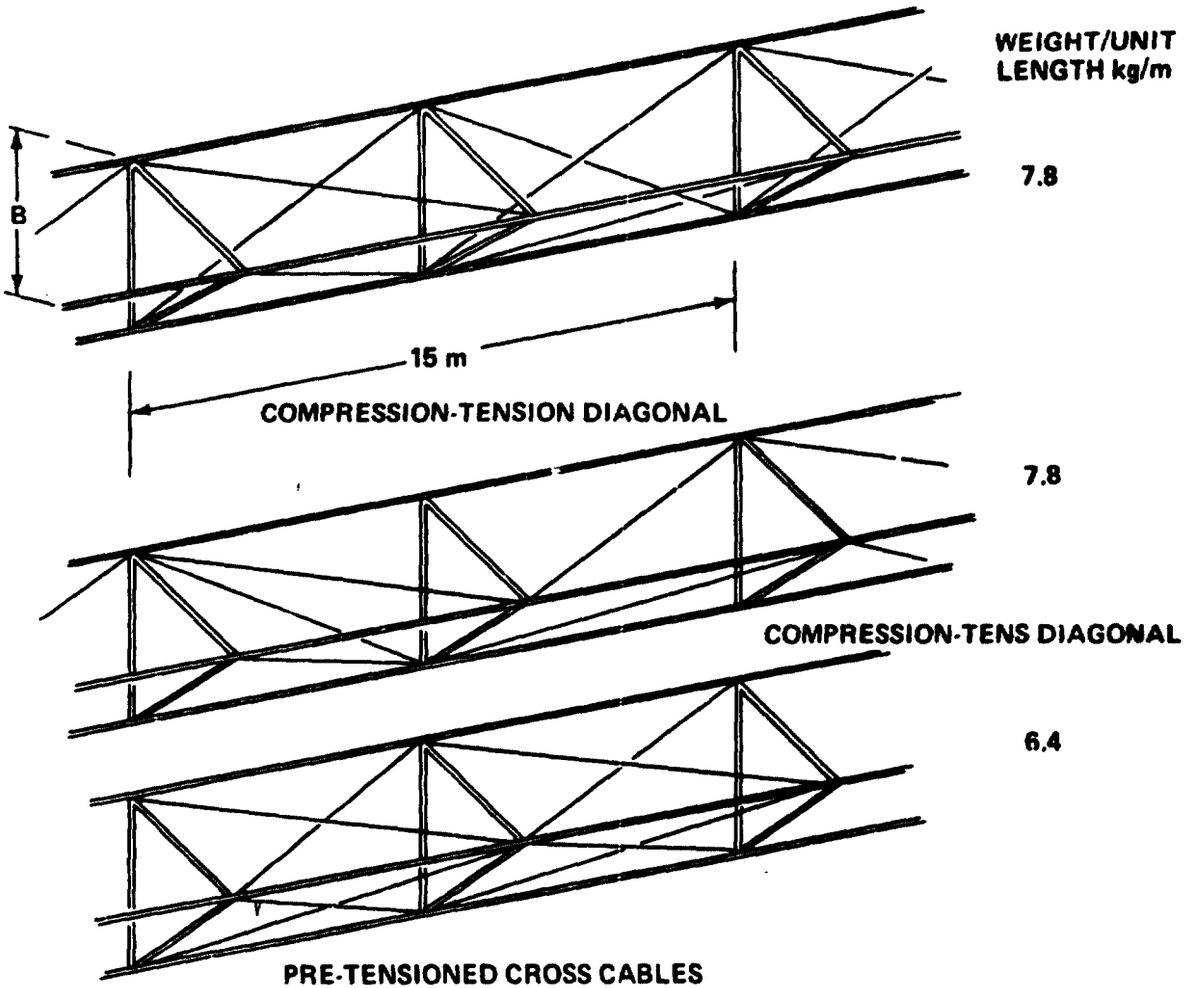

PRELIMINARY ESTIMATE OF MODULE SLOPES FOR VARIOUS THERMAL GRADIENTS

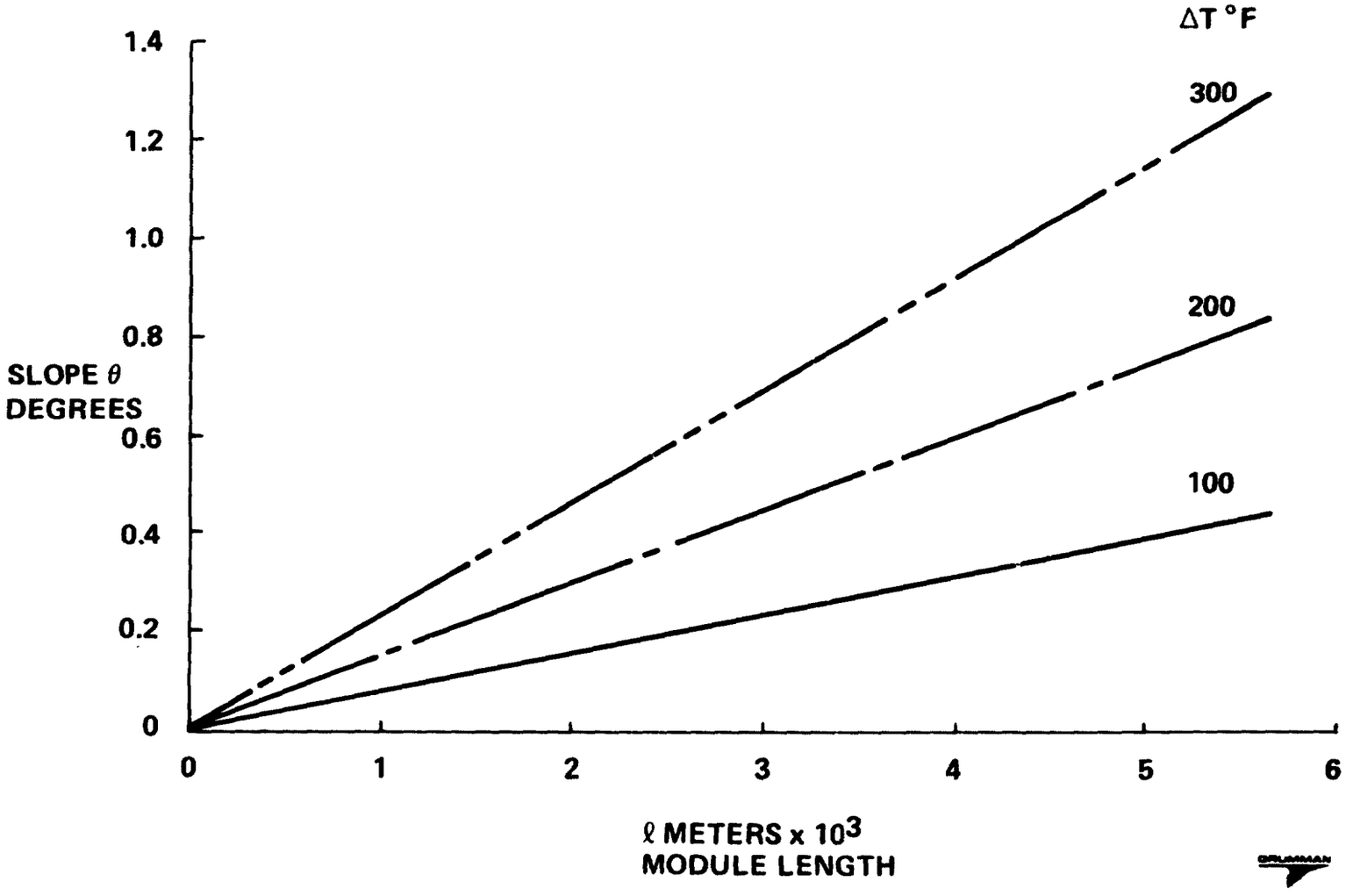

ESTIMATED DEFLECTION DUE TO THERMAL GRADIENT

An estimate of the solar array module slopes and deflections was calculated for various temperature gradients. The analysis was based on the following assumptions:

- o The module structure was cantilevered from the construction base.
- o The temperature gradient between upper and lower surface did not vary spanwise.

The results show that for a temperature difference between upper and lower members of 200°F the tip deflection relative to the base is 8 meters; the slope is 0.8 degrees.

Updated thermal data will be used to reevaluate these estimates.

PRELIMINARY ESTIMATE OF MODULE DEFLECTIONS FOR VARIOUS THERMAL GRADIENTS

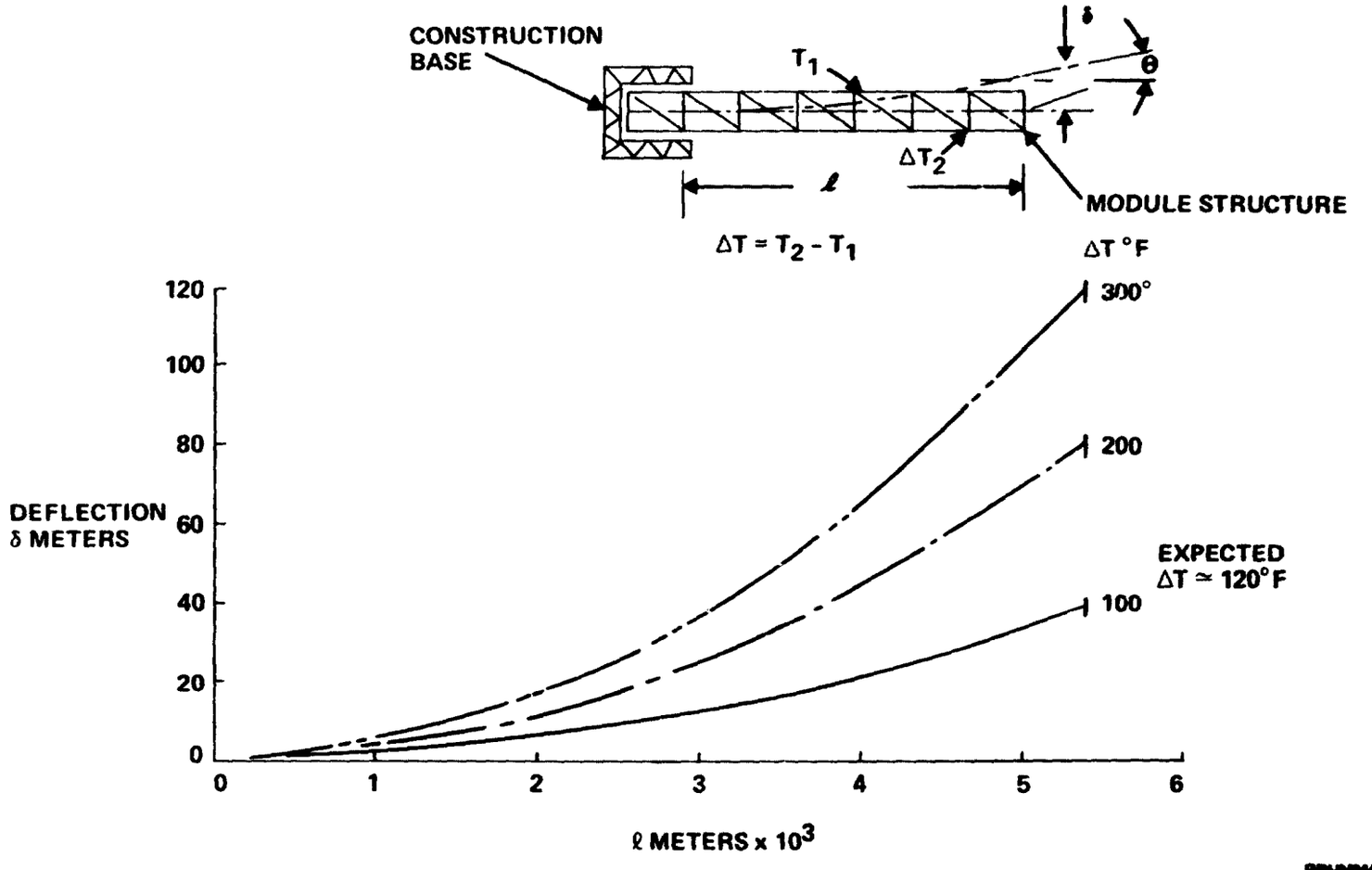

ORBITAL ATTITUDE DURING CONSTRUCTION

Thermal analysis of the construction phase is being performed to yield the structural temperature distribution necessary to perform the distortion/stress analysis. Both horizontal and vertical beam orientations will be investigated for the first part of this study, to minimize thermal grandients, the horizontal beams were oriented so that the axes of the elements were aligned with the sun's rays so that the sun entering the holes in the two sun-facing surfaces impinged on the third (back) at 0° orbit angle (see sketch). At the back side of the orbit (before entering the earth's shadow) solar energy enters the holes in the back surface to impinge on the other two.

Other arrangements to be considered are the severe cases where the sun is normal to one of the surfaces at 0° orbit angle and where one element shadows another. The vertical beams where intermittent shadowing takes place, is also to be investigated.

For the construction phase, a 300 n. Mi circular orbit is considered.

In GEO-synchronous orbit, the gradients between the sun-side horizontal beams, and those opposite will be calculated.

For this study, the inside of the elements are coated with black anodize (ϵ = .83, α = .86) and the outside surface with Z-93 white paint (ϵ =.90, α =.17).

ORBITAL ATTITUDE DURING CONSTRUCTION

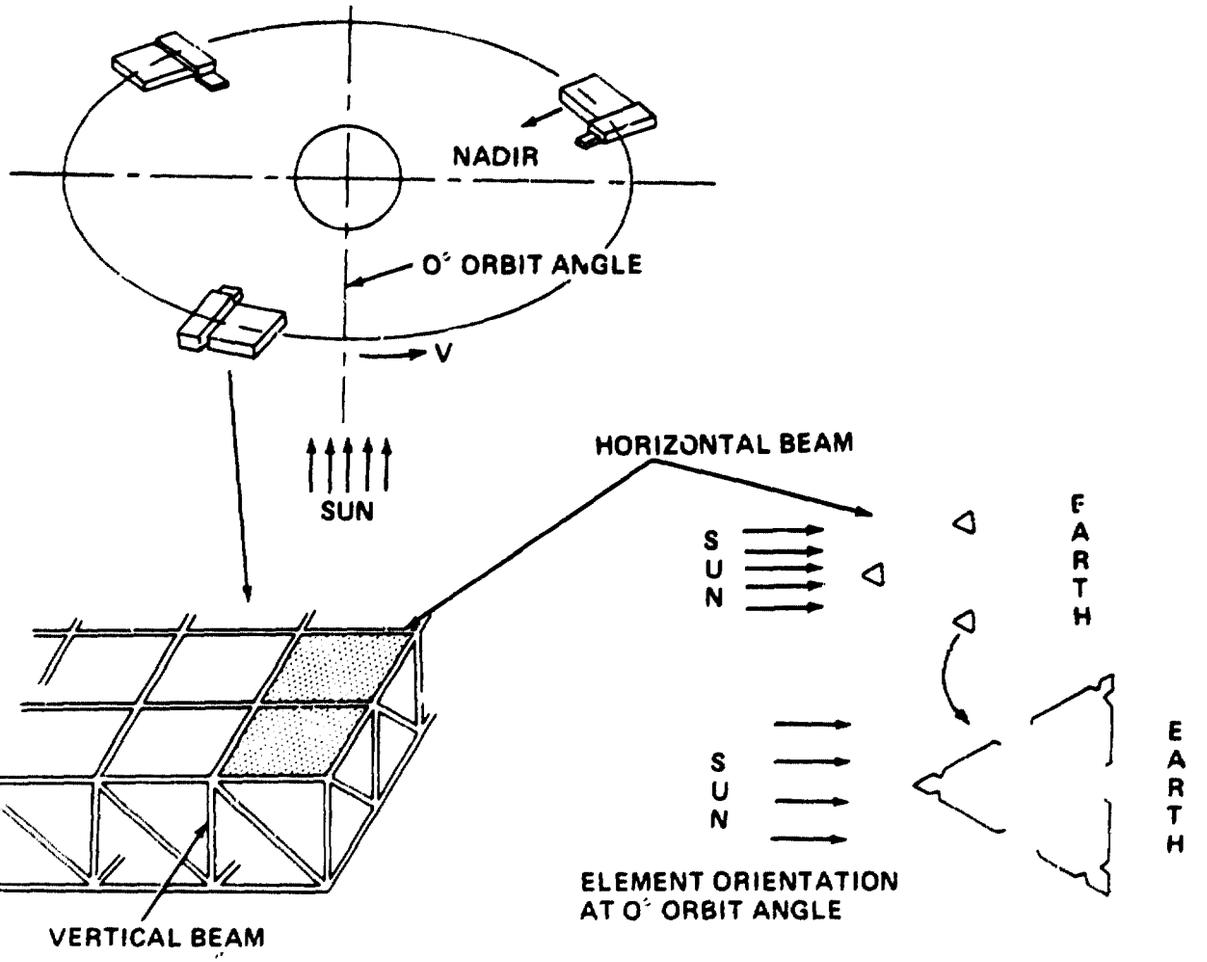

ALUMINUM STRUCTURE STUDY

REMAINING TASKS:

- COMPLETE THERMAL ANALYSES FOR SELECTED ORIENTATION
- EVALUATE STRUCTURAL RESPONSE TO TEMPERATURE EXPOSURE
- COMPARISON WITH COMPOSITE DESIGN

UPDATED EFFICIENCY AND SIZING

The SPS efficiency chain has undergone two minor revisions during this contract period. The regulation, auxiliary, and annealing power factor of 0.983 is lower than the 0.99 factor used previously. The inter-subarray loss factor of 0.976 is an improvement over the 0.956 factor used in the Part III System Definition Study.

The changes to the efficiency chain result in a slight decrease in the solar cell area requirement ($0.6\ km^2$).

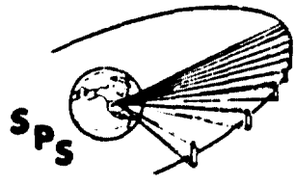

Updated Efficiency and Sizing

	EFFICIENCY	MEGAWATS PER LINK	
MAIN BUS I^2R	0.934	8,876	SOLAR ARRAY OUTPUT
ROTARY JOINT	1.0	8,290	
ANTENNA POWER DISTRIBUTION AND PROCESSING	0.97	8,290	TOTAL INPUT TO ANTENNA
DC-RF CONVERSION	0.85	8,041	
WAVEGUIDE I^2R	0.985	6,836	TOTAL RF POWER
IDEAL BEAM	0.965	6,733	TOTAL RADIATED POWER
INTER-SUBARRAY LOSSES	0.976	6,497	
INTRA-SUBARRAY LOSSES	0.981	6,341	
ATMOSPHERE LOSSES	0.98	6,221	
INTERCEPT EFFICIENCY	0.95	6,097	
RECTENNA RF-DC	0.89	5,792	INCIDENT ON RECTENNA
GRID INTERFACING	0.97	5,155	
	0.563	5,000	NET TO GRID

SOLAR INPUT:	1,353 W/m^2
SOLAR-CELL CONVERSION EFFICIENCY (0.173)	234.1
BLANKET FACTORS (0.9453)	221.3
THERMAL DEGRADATION (0.954)	211.1
ORIENTATION LOSS (0.919)	194.0
APHELION INTENSITY (0.9675)	187.7
NONANNEALABLE RADIATION DEGRATION (0.97)	182.1
ORBIT TRANSFER COMPENSATION (0.99)	180.2
REGULATION, AUXILIARY POWER, AND ANNEALING (0.983)	177.2
EOL BLANKET OUTPUT:	177.2 W/m^2
TOTAL SOLAR-CELL AREA:	50.1 km^2
SOLAR ARRAY OUTPUT:	8,876 MW

5000 MEGAWATT REFERENCE PHOTOVOLTAIC SYSTEM DESCRIPTION

The configuration of the 5000 megawatt SPS is basically that of one-half of the 10,000 megawatt SPS developed in the Part III System Definition Study. This description shows the revised dimensions from the updated efficiency chain, structural resize, and implementation of array shadowing diodes.

Using 12.7 meter beams for array attachment necessitated changing the internal bay dimensions to compensate for increased lost area, for 667.5 x 667.5 meter bay centerlines. In addition to this dimension change, the beam/array clearance for the catenary support system was increased from 2 meters to 3 meters at each bay end.

Incorporation of shadowing diodes in the array panels (to be shown on a later chart) created more lost area on the blanket. To compensate for the combined lost area effects it was necessary to add two array strings to each bay, one string to each end segment.

5000 Megawatt Reference Photovoltaic System Description

SPS-2470

BOEING

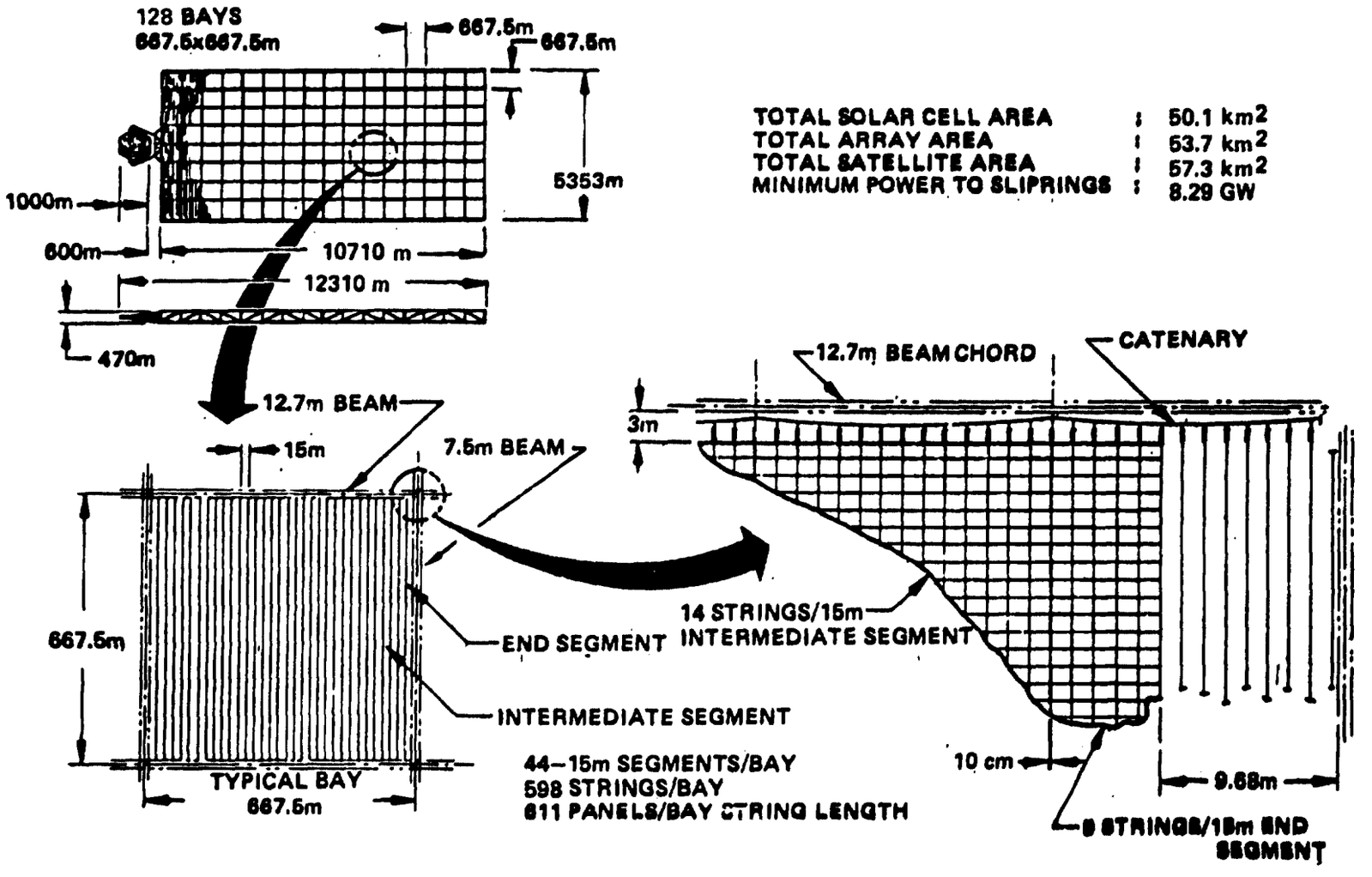

TOTAL SOLAR CELL AREA	:	50.1 km^2
TOTAL ARRAY AREA	:	53.7 km^2
TOTAL SATELLITE AREA	:	57.3 km^2
MINIMUM POWER TO SLIPRINGS	:	8.29 GW

REFERENCE PHOTOVOLTAIC SYSTEM DESCRIPTION

The basic blanket panel configuration has changed slightly. To compensate for the shorter length available within the bay, the solar cell length was degreased from 6.55 cm to 6.48 cm. This was sufficient to allow for the 12.7 meter beams and 3 meter catenary support discussed previously.

The only other change that was made to the basic blanket panel was the incorporation of two shadowing diodes (shunts) per panel. Each panel maintains the 16 cells in series and 14 cells in parallel configuration except on the two end rows where there are 13 cells in parallel. The 13 parallel cells will allow only 3 cell failures, instead of 4 allowed by the other rows, and still pass string current without reverse bias operation.

Reference Photovoltaic System Description

SPS-1849

- 14 CELLS IN PARALLEL WILL TOLERATE 4 CELL FAILURES IN ANY ROW

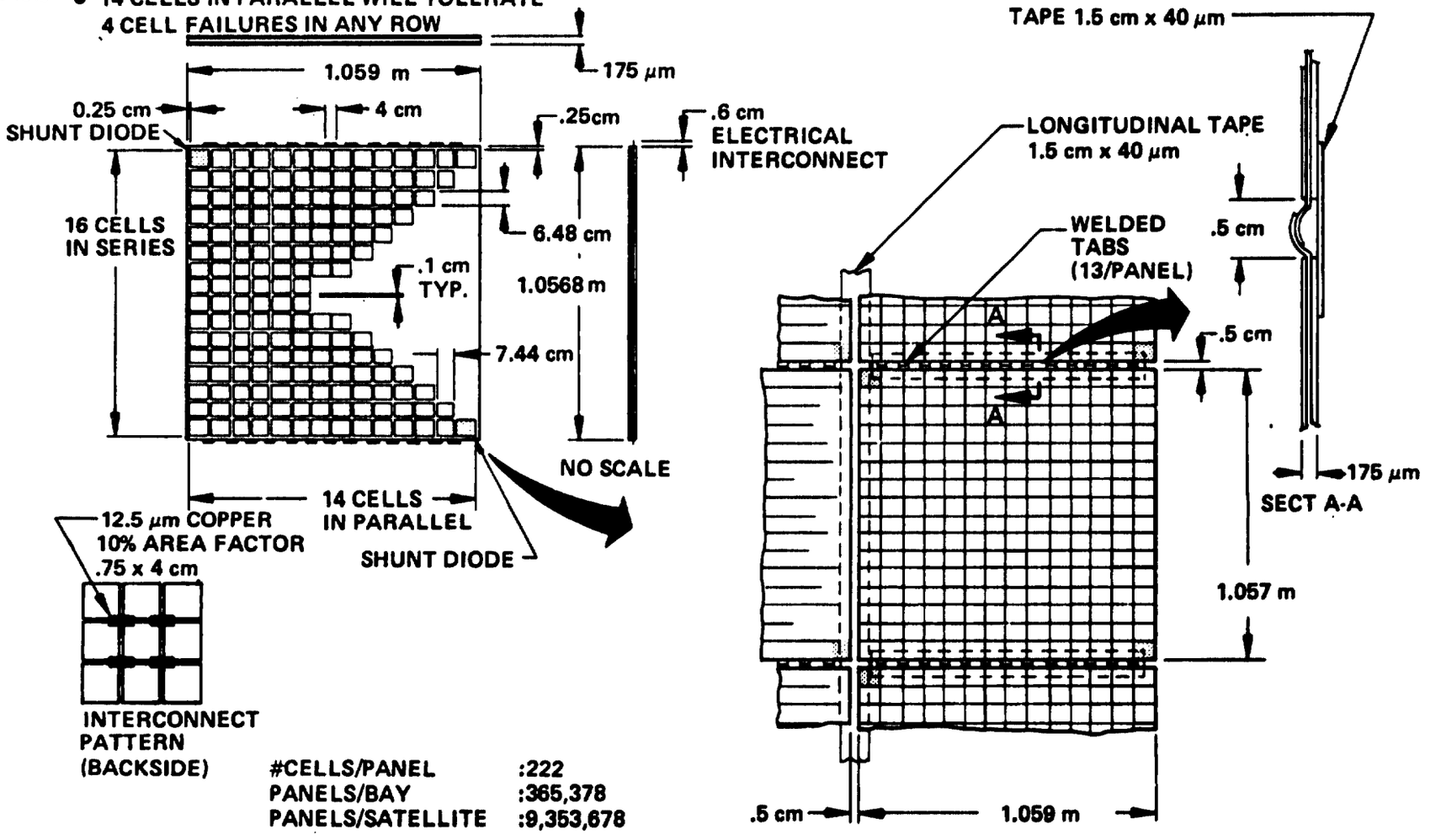

#CELLS/PANEL	:222
PANELS/BAY	:365,378
PANELS/SATELLITE	:9,353,678

IMPLEMENTATION OF ARRAY SHADOWING DIODES

A large shadow moving across an array string could cause the shadowed cells to operate in a reverse-biased mode. This operation can cause "hot spots" (energy consumption instead of generation) and can lead to string failure. To prevent this problem from causing array damage it is necessary to incorporate shadowing diodes to shunt the power around shadowed panels and prevent reverse-bias operation. The rationale and design criteria used to incorporate the shadowing diodes on the SPS blanket are noted on this chart.

Two, redundant, shadowing diodes were added to each blanket panel as shown. The electrical equivalent of a blanket panel with the shadowing diodes is also shown. This configuration will protect array panels from reverse-bias operation. The individual parallel sets of cells on the panel receive their protection by the "four out of fourteen" cell loss method.

Since the shadowing diodes occupy space that would normally be used for solar cells, an increase in the "lost area" of the blanket panel results. If the diodes were placed in another location packaging for transportation penalties would result. Therefore, to compensate for the new "lost area", extra array was added to the system with mass and area penalties shown.

Implementation of Array Shadowing Diodes

RATIONALE:

- PREVENTS ARRAY DAMAGE CAUSED BY UNEVEN ILLUMINATION AND SHADOWING EFFECTS
- PROVIDES MORE GRACEFUL POWER DEGRADATION FROM BLANKET PANEL FAILURES AND SHADOWING EFFECTS

DESIGN CRITERIA:

- REVERSE-BIAS PROTECTION FOR BLANKET PANELS
- LOW REVERSE LEAKAGE CURRENT
- LOW FORWARD-VOLTAGE DROP
- HIGH RELIABILITY
- COMPATIBLE WITH BLANKET PANEL CONFIGURATION

REDUNDANT (PARALLEL) SHUNT DIODES
INCREASE IN SYSTEM SIZE = 0.451 km^2
INCREASE IN SYSTEM MASS = 192.3 MT

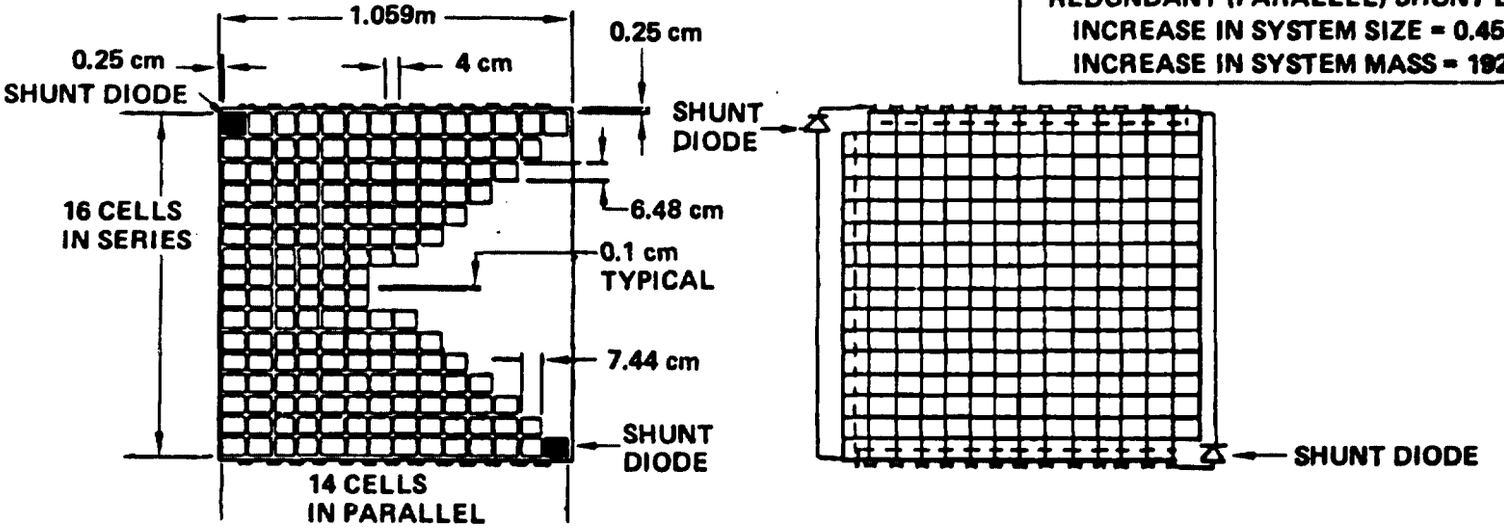

PHYSICAL ARRANGEMENT OF SHUNTING DIODES ON BLANKET PANEL

ELECTRICAL EQUIVALENT

SOLAR ARRAY SUPPORT STRUCTURE EVOLUTION

Illustrated here are the original and revised baseline hexahedral solar array support structure concepts. In the original system the edge cells of each of the eight modules making up the entire SPS used the configuration illustrated. The interior cells employed an absolute minimum of structure. Further analysis indicated that the edge cells were not stable with the result that the entire system was not stable. Further, the 7.5 meter beams were not adequate for solar blanket tension when the solar blanket tension was changed to uniaxial. As a result, the system was revised to the configuration indicated with 12.7 meter beams for solar blanket tension support and all cells incorporating the structural concept shown. The lower-deck-to-upper-deck diagonal provides structural stability.

Solar Array Support Structure Evolution

SPS-2194

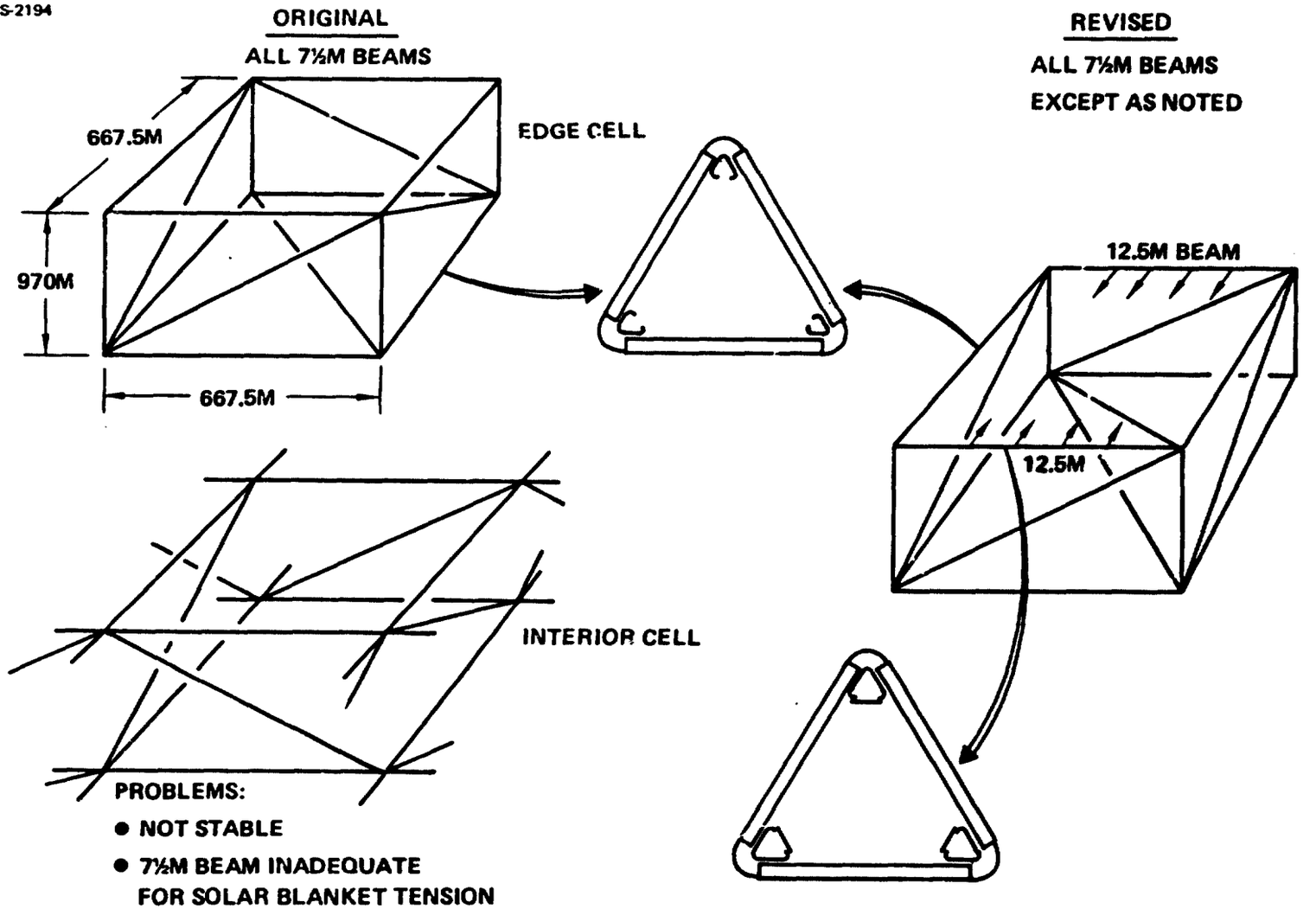

SOLAR POWER SATELLITE STRUCTURAL BAY CONFIGURATION

The revised bay configuration including an index of the location and types of beams used in a typical bay is shown. A loads analysis resulted in using three types of beams in the satellite structure. For construction purposes, type B and C beams differ only in their batten spacing. This will allow the use of only two types of beam machines in the construction facility.

For the SPS constructed at GEO, the type "B" beams are replaced by type "C".

Solar Power Satellite
Structural Bay Configuration

SPS-2473

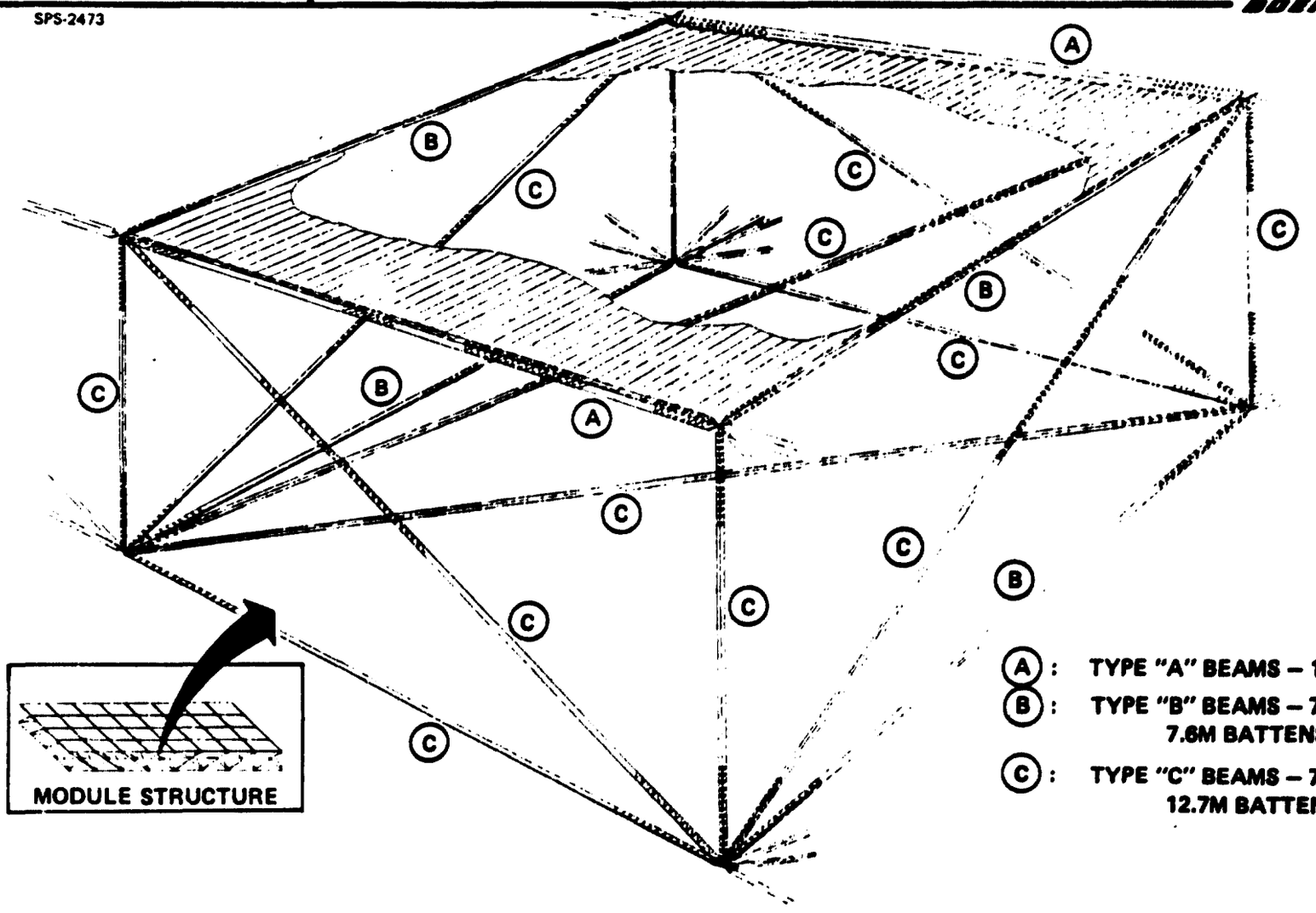

BEAM CONFIGURATIONS

The three types of beams in the satellite primary structure are shown. Also listed for each type of beam are their section and beam characteristics. In previous satellite designs the beams were sized for the "worst case" load condition resulting in a mass penalty on the majority of members which had a significantly lower load. This updated configuration has started to reduce that penalty by having three types of members. The savings can be shown by the difference in mass/length between the 12.7 meter, type A, beam and the 7.5 meter, type C beam. The majority of beams in the satellite are type C beams.

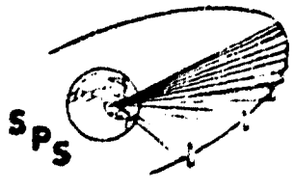

Solar Power Satellite Structural Update Beam Configurations

BOEING

SPS-2468

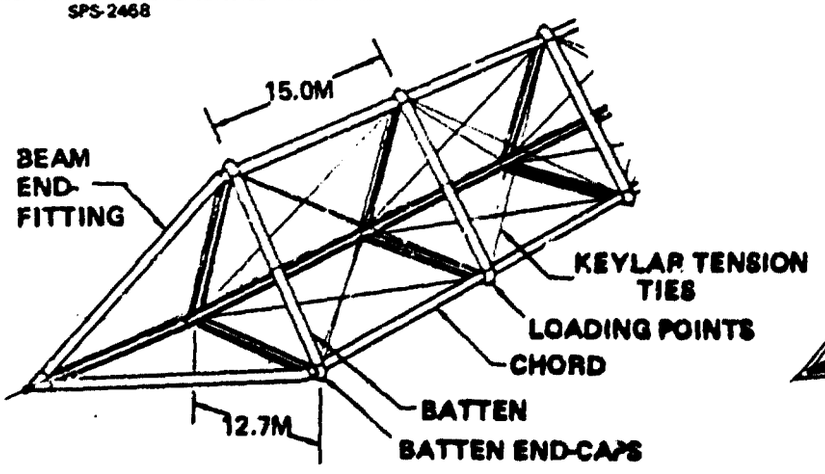

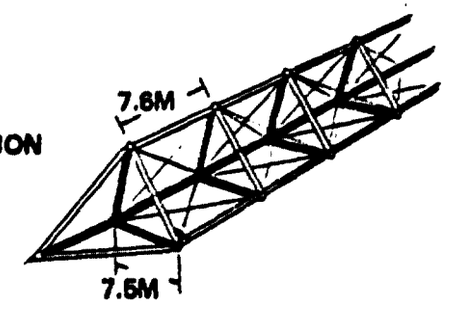

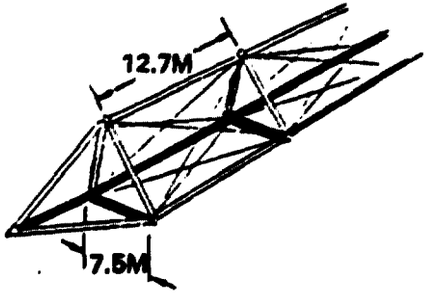

ITEM	TYPE A UPPER SURFACE LONGITUDINAL BEAM	TYPE B UPPER AND LOWER SURFACE LATERAL BEAM	TYPE C BEAM USED IN ALL OTHER LOCATIONS
SECTION	CLOSED	OPEN	OPEN
REF. SIDE LENGTH	38 CM	38CM	38CM
MAT'L THICKNESS	0.86 MM	0.71 MM	0.71 MM
EI_X	3.39 E8 N/CM^2	1.80 E8 N/CM^2	1.80 E8 N/CM^2
BEAM WIDTH	12.7M	7.5M	7.5M
BATTEN SPACING	15.0M	7.6M	12.7M
CRITICAL LOAD	17480N (CRIP. CHORD)	19000 N (BUCK. BEAM)	7090 N(BUCK BEAM)
MASS/LENGTH	7.48 KG/M	5.12 KG/M	4.11 KG/M

MULTIPLE BUS SPS POWER DISTRIBUTION

During the critique of the baseline system concept the system redundancy of the major power system buses were of some concern to both Boeing and TRW personnel who accomplished the critique. In addition, the potential fault currents that could occur with the single-line bus system was also of concern.

A redesign of the main power distribution bus system was accomplished to decrease the possibility of loss of all power to the antenna and to limit potential fault currents. The overall multiple bus system concept is shown.

Multiple Bus SPS Power Distribution

BOEING

SPS-1252

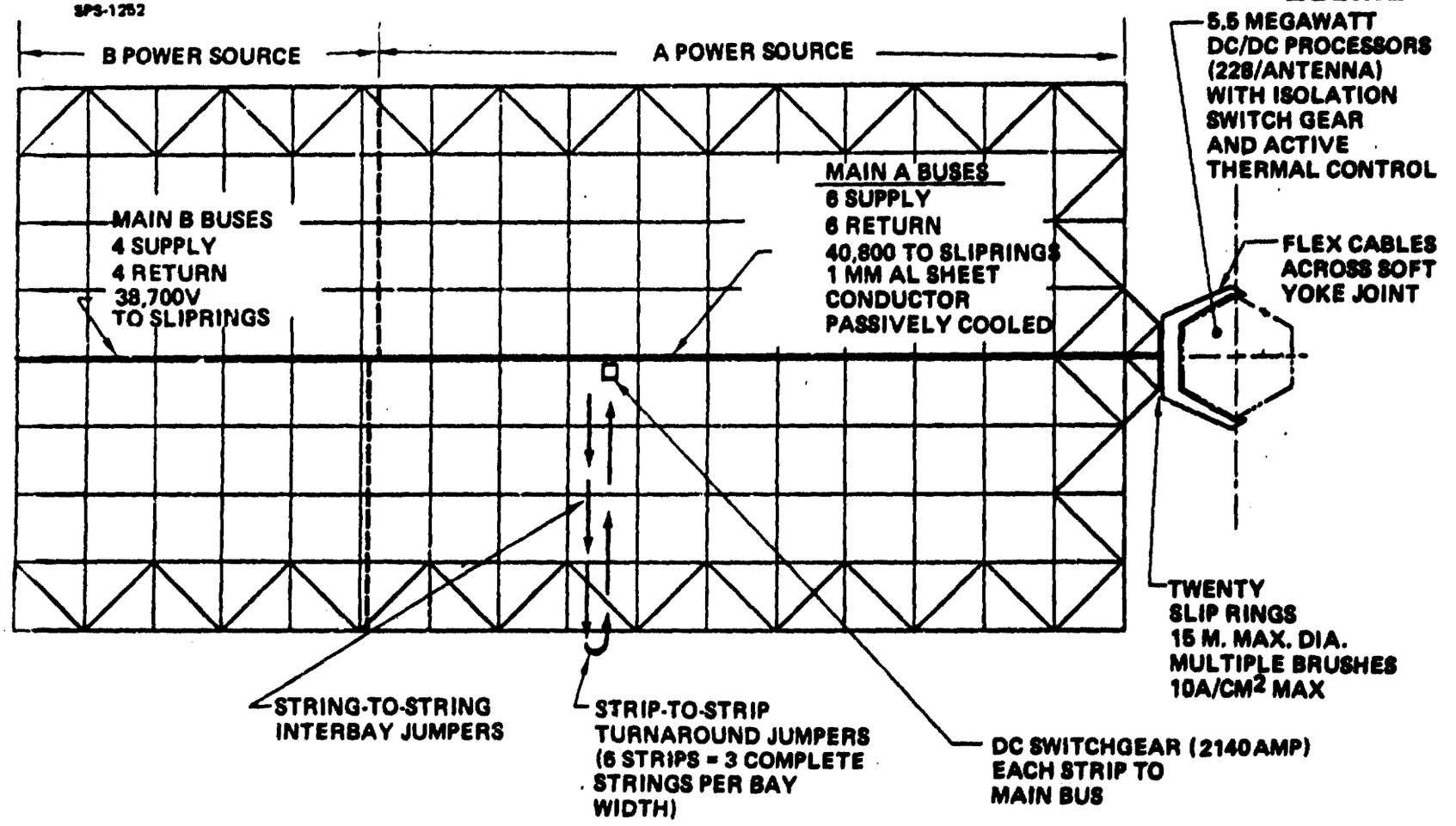

MULTIPLE BUS/ARRAY CONNECTION

One of the problems to be addressed in a multiple bus system is the delivery of power to all sections of the antenna at essentially the same voltage. Shown is a concept that was developed which will enable the delivery of power to the rotary joint with the voltage levels for all buses within 0.25% of each other which should satisfy distribution requirements. By staggering the bus connections as shown the voltage delivered only varies by the voltage drop across 1/3 of a satellite bay. The adoption of this multiple bus scheme will result in the loss of one quadrant of the antenna for faults on any of the main B source power buses and one-sixth of the antenna for faults on the main A source power buses.

Multiple Bus/Array Connection

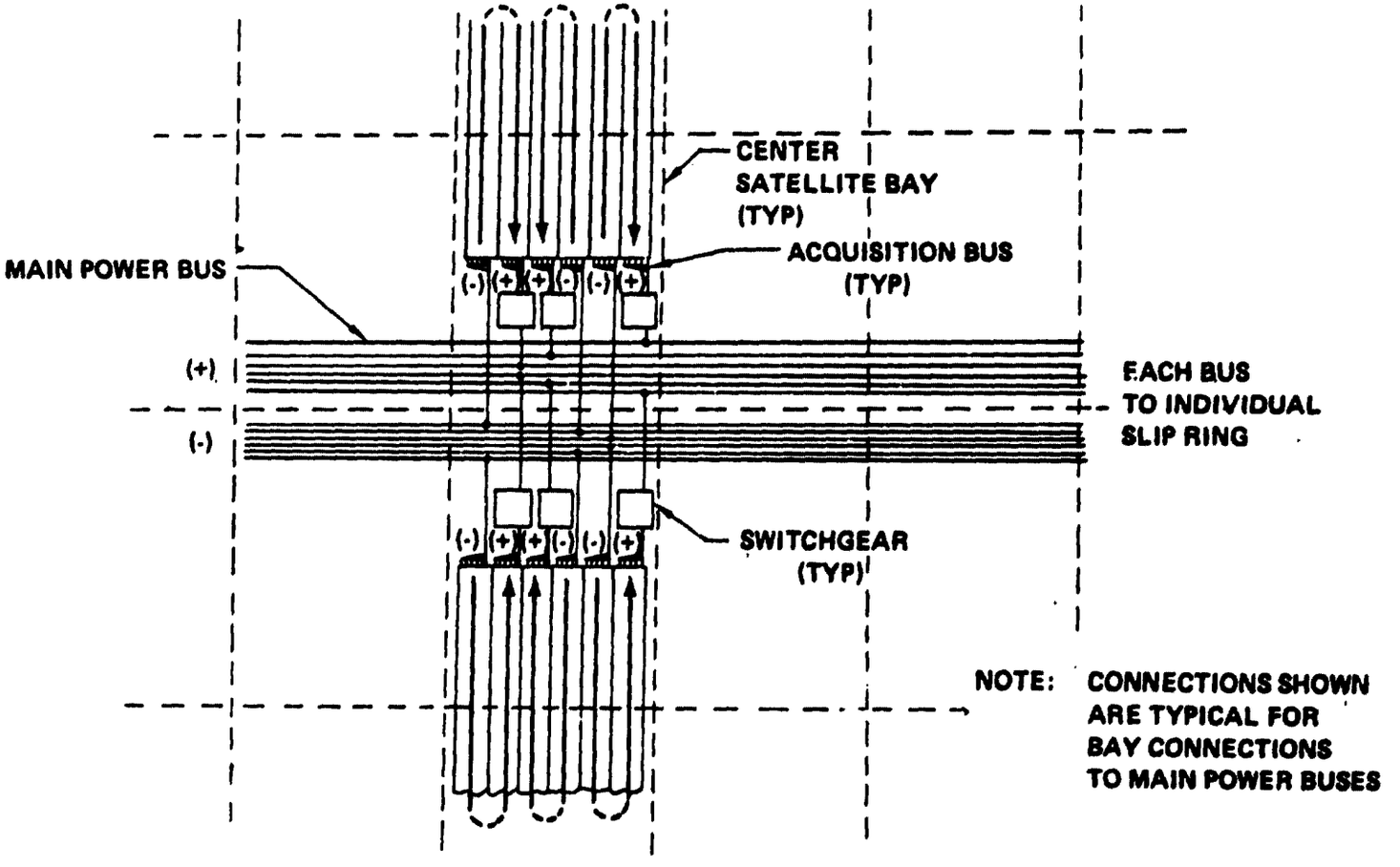

MULTIPLE BUS CONDUCTOR SUMMARY

This table shows a breakdown of the number of buses for each power source, the number of array power sectors per power source, and the normal bus current per bus for each power source. Also shown is the number of DC-DC converters per bus in power source B and the number of klystrons supplied by each bus of each power source.

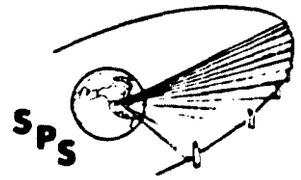

Multiple Bus Conductor Summary

SATELLITE				ANTENNA	
POWER SOURCE	NO. OF BUSES	ARRAY POWER SECTORS	NORMAL BUS CURRENT (PER BUS)	NO. OF CONVERTERS PER BUS	NO. OF KLYSTRONS PER BUS
A	4 (+) 4 (-)	31	15,966	57	25,388
B	6 (+) 6 (-)	65	22,783		16,925

SLIP RING ASSEMBLY FOR MULTIPLE BUS POWER DISTRIBUTION SYSTEM

With the selection of the multiple bus system for SPS power distribution, the requirement for a multiple slip ring rotary joint exists for accomplishing the transfer of power between the power generation (sun-facing) portion and the power transmission (earth-facing) portion of the SPS. A design was developed which provides for twenty slip rings to accomplish power transfer for the ten pairs of power buses.

The concept shown was developed based on the following requirements:

1. Twenty separate slip ring assemblies
2. Normal slip ring current capabilities
3. Maximum brush current density of 10 amperes per square centimeter
4. Brush feeder current density of 400 amperes per square centimeter
5. Brush pressure of 25.9 Kpa (4 psi)
6. Coin silver slip ring (90% silver and 10% copper)
7. Silver-molybdenum disulfide-graphite (85% Ag 12% MOS_2 and 3% Graphite) brushes
8. Maximum outside diameter of 16 meters (fits inside HLLV payload bay)
9. Earth assembled
10. Minimum spacing between different conductor systems of 0.7 meters
11. Positive retraction of the brush assembly from the slip ring contact surface.
12. All feeder conductors to have maximum surface exposure to free space for thermal dissipation purposes.

SPS-2552

Slip Ring Assembly for Multiple Bus Power Distribution System

BOEING

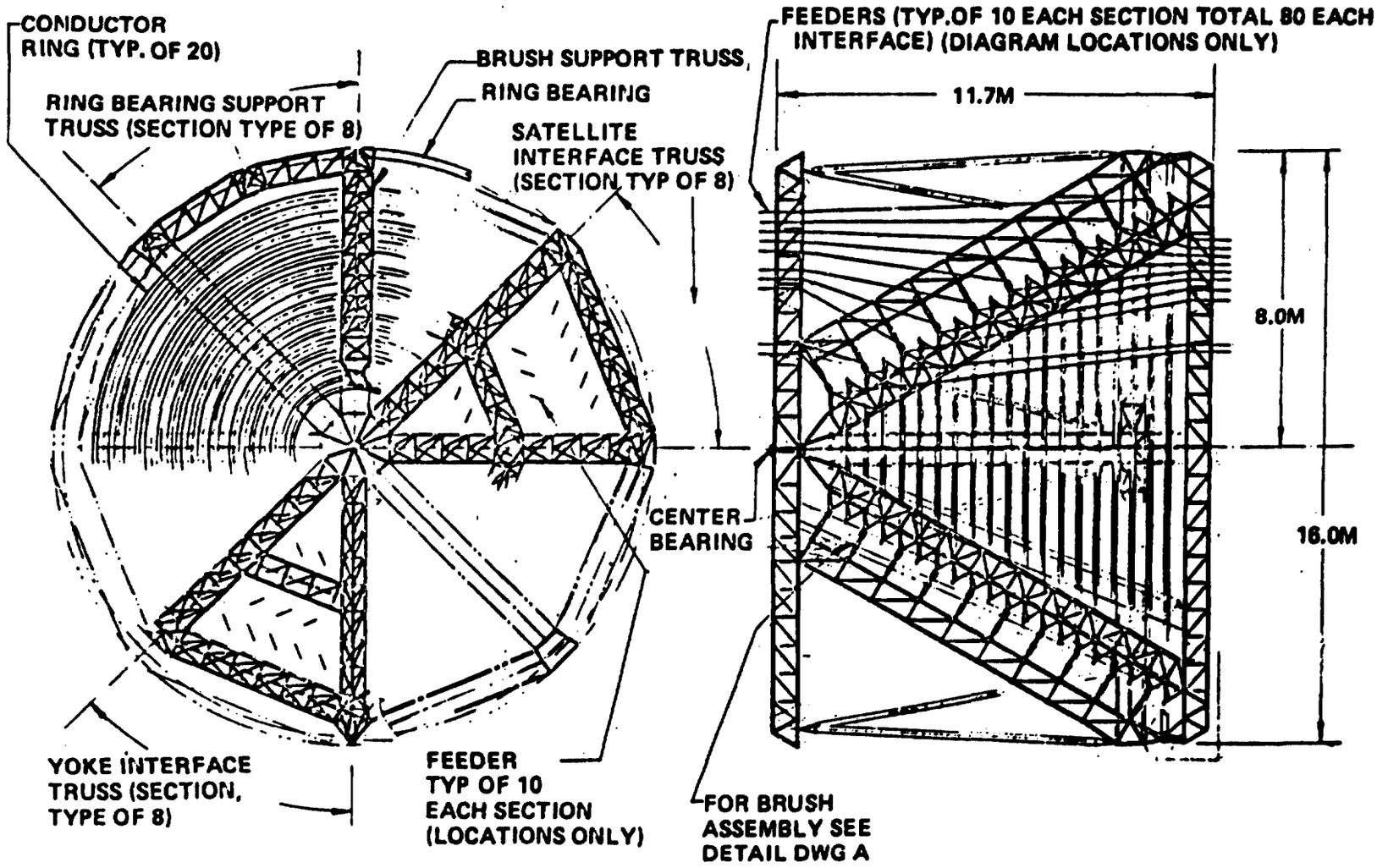

MULTIPLE SLIP RING BRUSH ASSEMBLY

Details of the brush assembly and slip ng arrangement is shown.

Multiple Slip Ring Brush Assembly

SPS-2518

BOEING

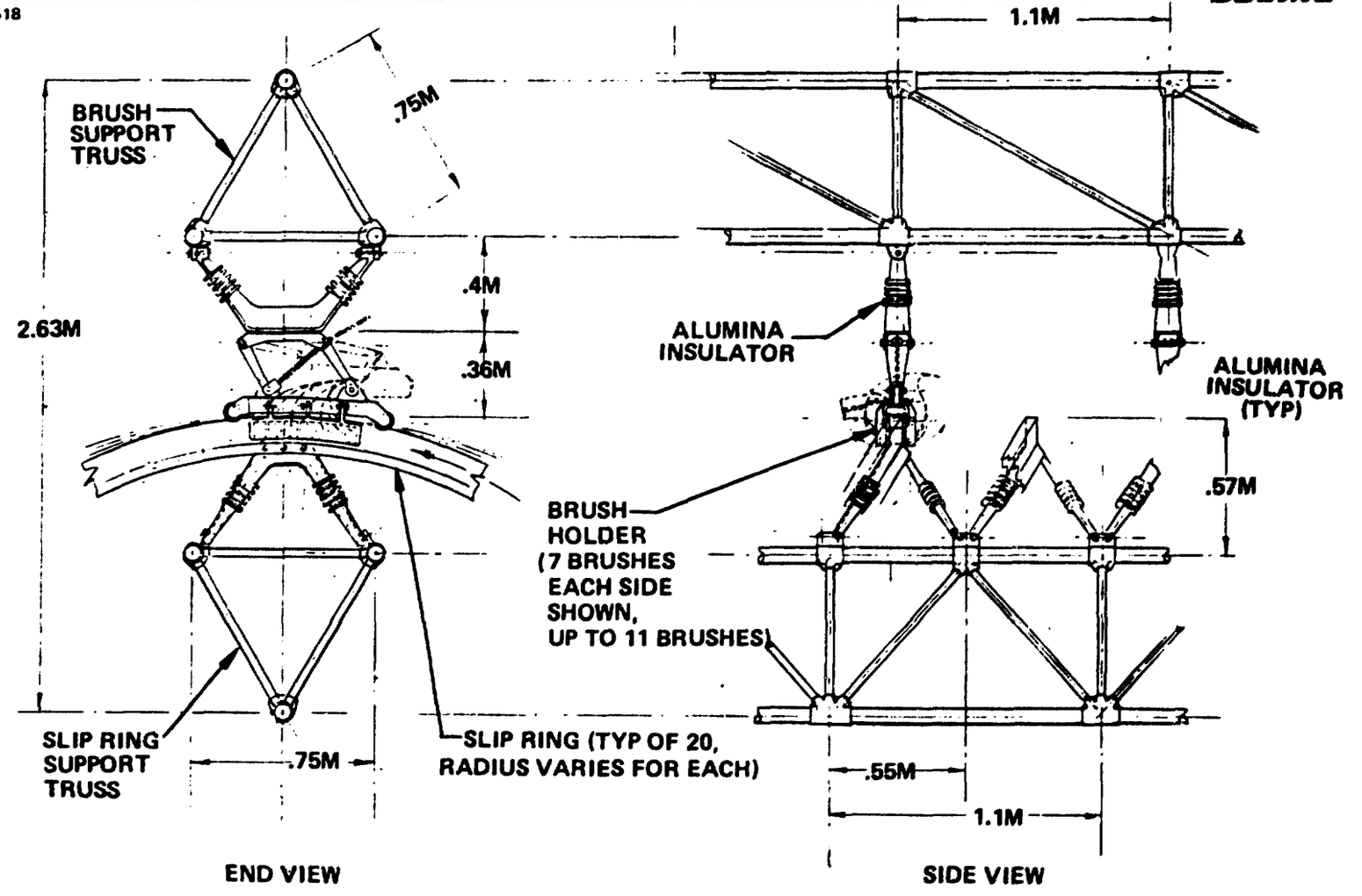

ITEMIZED DC/DC CONVERTER LOSSES—NEW DESIGN

The critique of the reference concept (task 4.1.1) raised the issue of DC to DC converter life based on corona induced failures within transformers and inductors used in filters. The reference DC to DC converter concept was derived by selecting a converter chopping frequency of 20 kilohertz in order that the overall satellite mass was minimized. However, the reliability analysis was performed using failure rate data based on 400 hertz. Corona-induced failures within transformers are dependent upon the total number of AC cycles to which the transformer is subjected. The mean-time-to-failure at 20 kilohertz is 50 times shorter than at 400 hertz.

As a result of the critique, an analysis was accomplished to investigate the following three approaches to increasing the predicted life of the converter.

a) Reduce the converter system chopping frequency
b) Increase the transformer life by derating the dielectric material (i.e., operate at a lower voltage stress)
c) Redesign the transformer to increase its operating life.

Reducing the converter system chopping frequency incurs a significant mass penalty. The converter specific mass including thermal control at 1 kilohertz is approximately 2.9 kg/kw and is approximately 1.7 kg/kw at 20 kilohertz. Derating the dielectrics in the converter results in a converter specific mass (including thermal control) of 2.0 kg/kw.

In order to increase the overall converter lifetime dielectrics were derated for all filters in the converter. The losses for the revised converter are tabulated as a function of frequence in the table.

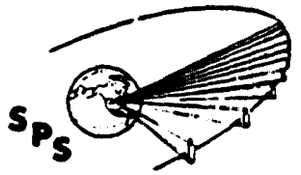

Itemized DC/DC Converter Losses – New Design

179

CONVERTER SECTION	LOSSES IN KW AT CHOPPING FREQUENCY			
	1 KHZ	10 KHZ	20 KHZ	30 KHZ
INPUT FILTER	30	42	48	54
SWITCHING COND	12	12	12	12
SW	2.4	12	24	36
DRIVE AND SUPPRESSION	2.2	5.5	11	16.5
TRANSFORMER	70	70	70	70
RECTIFIERS	2.2	2.2	2.2	2.2
OUTPUT FILTERS	60	120	138	149.5
TOTAL LOSSES	178.8	263.7	305.2	340.2
EFFICIENCY (%)	96.8	95.3	94.7	94.1

DC/DC CONVERTER SWITCHING FREQUENCY SELECTION

In order to select the chopping frequency for the long life processor, the curves shown were developed for the baseline converter design, the baseline converter with de-rated dielectrics, and the baseline converter with de-rated dielectrics in all filters and a liquid cooled transformer as a replacement for the baseline transformer. It is apparent from the curves in this figure that the minimum mass system occurs when the liquid cooled transformer is used (with de-rated dielectrics in all filters) at a chopping frequency in the 15 to 20 kilohertz range. The converter concept selected to replace the baseline converter concept is shown as the lower of the three curves.

DC/DC Converter Switching Frequency Selection

- MASS = CONVERTER MASS + THERMAL CONTROL MASS + ARRAY MASS (REQUIRED TO MAKE UP FOR CONVERTER LOSSES)

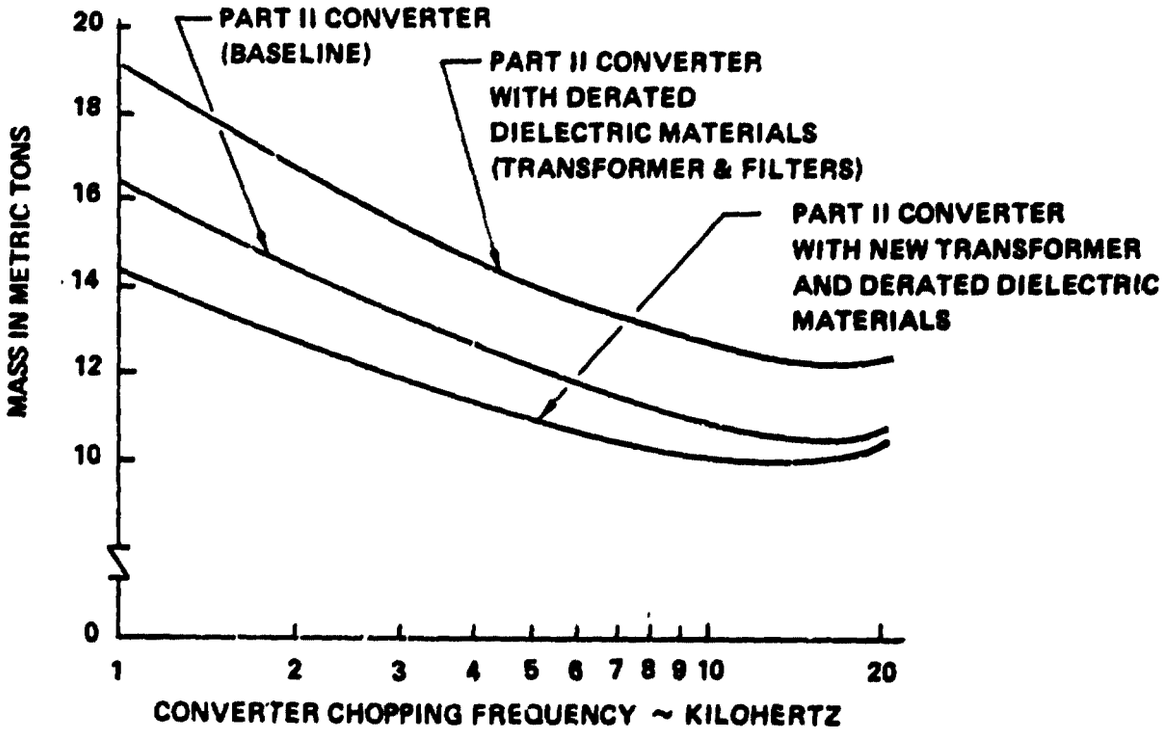

LIQUID COOLED TRANSFORMER

An effort is underway by Thermal Technology Labs (funded by the USAF Aero Propulsion Laboratory) to develop lightweight transformers for airborne power supplies. A computer program has been developed, and a 50 KVA prototype fabricated to verify the computer optimized design, to enable the design of lightweight liquid cooled transformers. The computer optimization was used to develop a design for a 6,000 kw liquid cooled transformer. The selected DC/DC converter transformer characteristics are shown in this table.

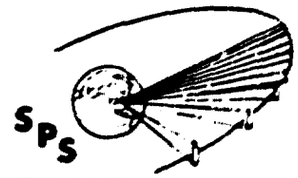

Liquid Cooled Transformer

POWER IN	5610 KW
POWER OUT	5540 KW
EFFICIENCY	98.73%
WEIGHT	170 KG
INTERNAL SIZE	$(14\ IN)^3$
OPERATING FREQUENCY	20 KHZ

KLYSTRON MODULE THERMAL CONTROL SYSTEM CHARACTERISTICS

A revision to the Part III heat pipe thermal control system for the klystron module is an active (pumped) thermal control system with the characteristics shown on this chart. There are several reasons for the proposed changed to an active thermal control system, but they are highlighted by lower mass and less fault impact.

Using an active thermal control system with the characteristics shown could result in a mass advantage of over 570 MT per antenna.

There is a possibility of micrometeoroid penetration or mechanical failure causing a tube leak in the radiator of the module thermal control system. Using the heat pipe system of Part III, such a leakage could cause severe, long lasting electrical problems in the vicinity of the radiator leak because conductive fluids were used in the heat pipes. Thus a leak could have contaminated high voltage electrical insulators with a conductive film of heat pipe fluid. At reasonable pressure, the only heat pipe fluids found to operate in the 500^{o}C temperature range were conductive (i.e., NaK, Hg, CS, etc.).

The active thermal control system adapted for SPS uses air (or Nitrogen) for the high temperature (500^{o}C) section and Dowtherm-A for the low temperature (300^{o}C) section. Both of these fluids are nonconductive.

This work was accomplished by Mr. Ray French of the Vought Corporation, an independent contributor not under contract on this project.

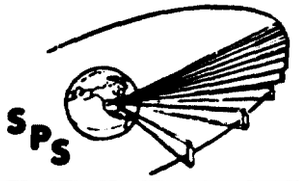

Klystron Module Thermal Control System Characteristics

BOEING

VOUGHT CORPORATION

	500°C	300°C
MATERIAL	COPPER	COPPER
FLUID	STEAM @ 20 ATM	DOWTHERM–A
INLET TEMP	477°C	277°C
OUTLET TEMP	413°C	260°C
LENGTH X WIDTH	0.57m x 1.61m	1.04m x 1.61m
TUBE SPACING	3.7 cm	2.84 cm
TUBE DIAMETER	5.6 mm	1.27 mm
TUBE THICKNESS	0.886 mm	0.71 mm
FIN THICKNESS	0.163 mm	0.066 mm
EMISSIVITY	0.8	0.8
ABSORTIVITY	0.3	0.3
TSINK	36.3°C	36.6°C
PUMP EFFY.	0.3	0.3
FIN EFFECTIVENESS	0.894	0.920
AREA	0.91 m^2	1.67 m^2
MASS/MODULE	7.95 kg	5.13 kg
CURRENT MASS/MODULE – 13.18 kg PART III MASS/MODULE – 18.88 kg		

KLYSTRON PUMPED FLUID THERMAL CONTROL SYSTEM

Shown here is the basic layout of the components of the revised active thermal control system adopted for the klystron module.

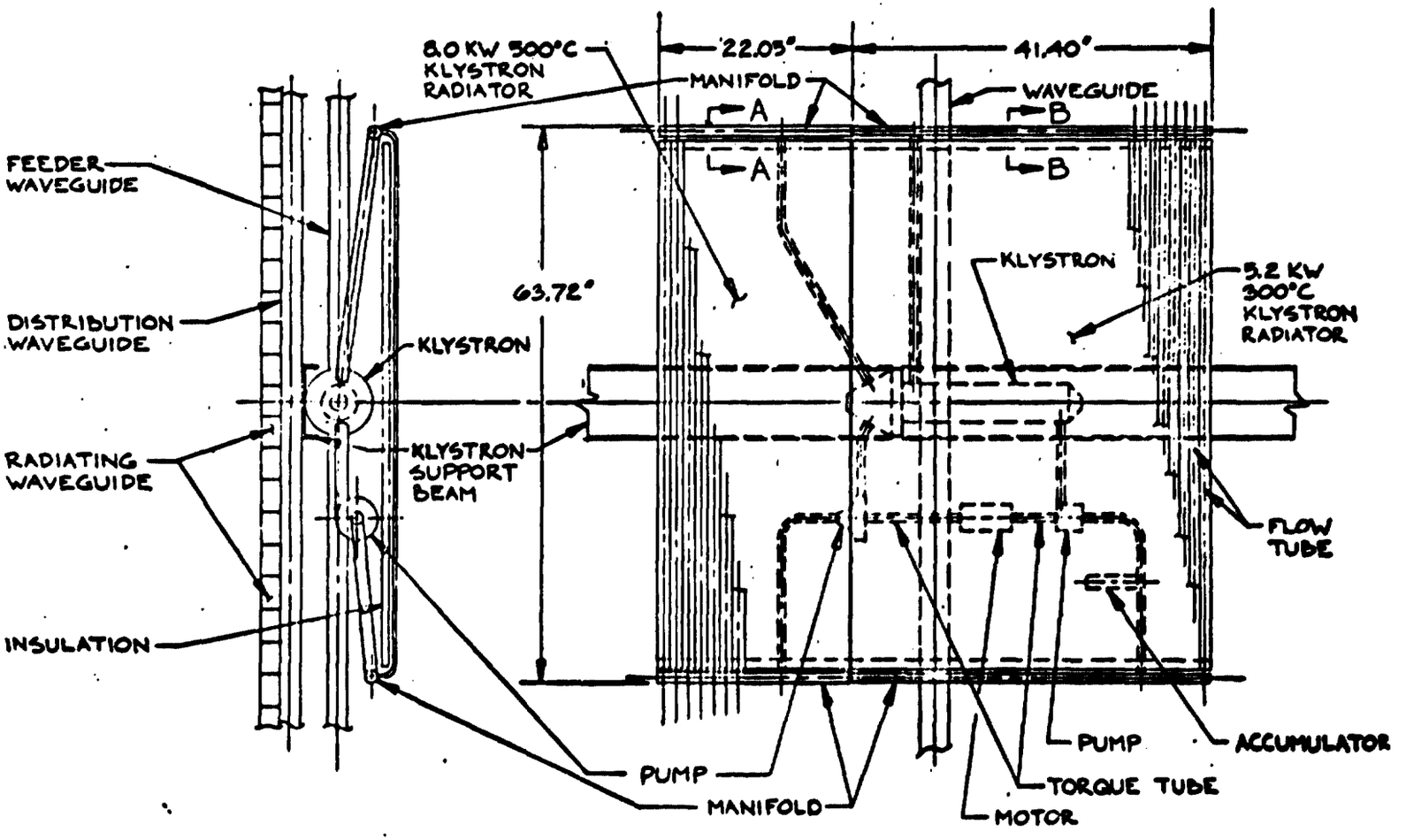

VOUGHT CORPORATION

KLYSTRON PUMPED FLUID THERMAL CONTROL SYSTEM

BOEING THERMAL ANNEALING TEST DATA

The next three charts show some of the results of a Boeing (IR&D) test program to investigate the possibilities of thermal (bulk) annealing radiation damage from unglassed 50 μ m (2-mil) silicon solar cells. The unglassed cells were irradiated with 2 MeV protons and annealed in a laboratory oven at the temperatures and times noted. The cells were also subjected to repeated radiation damage and annealing.

The results of these tests are by no means conclusive but do show recovery of radiation damage. It is anticipated that continued work in this area could lead to the optimation of the thermal (bulk) annealing processes for the type of solar blanket baselined for SPS

BOEING SPS

Thermal Annealing of Proton Damage In Silicon: Boeing Test Data

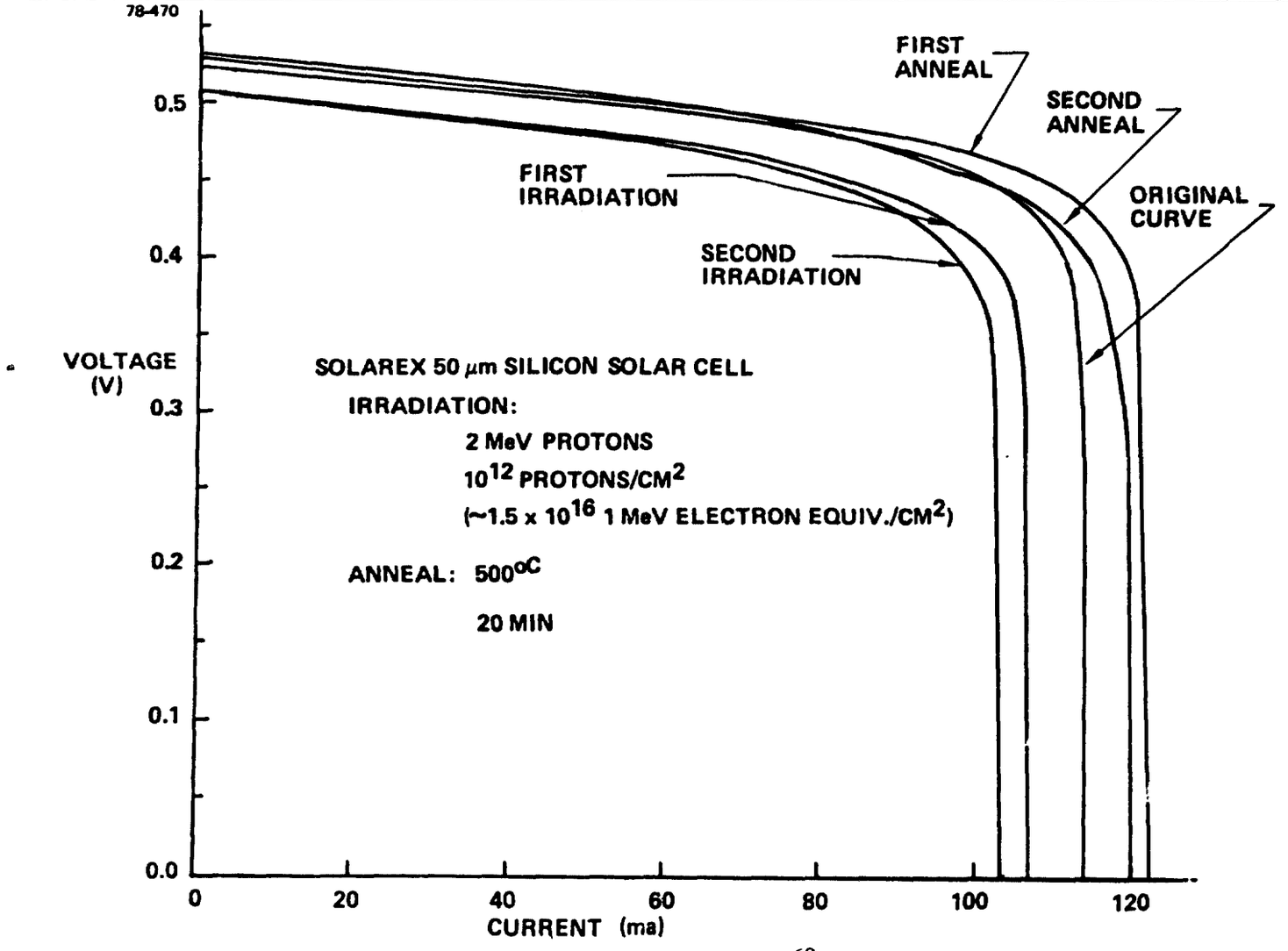

BOEING SPS

Thermal Annealing of Proton Damage In Silicon Cells: Boeing Test Data

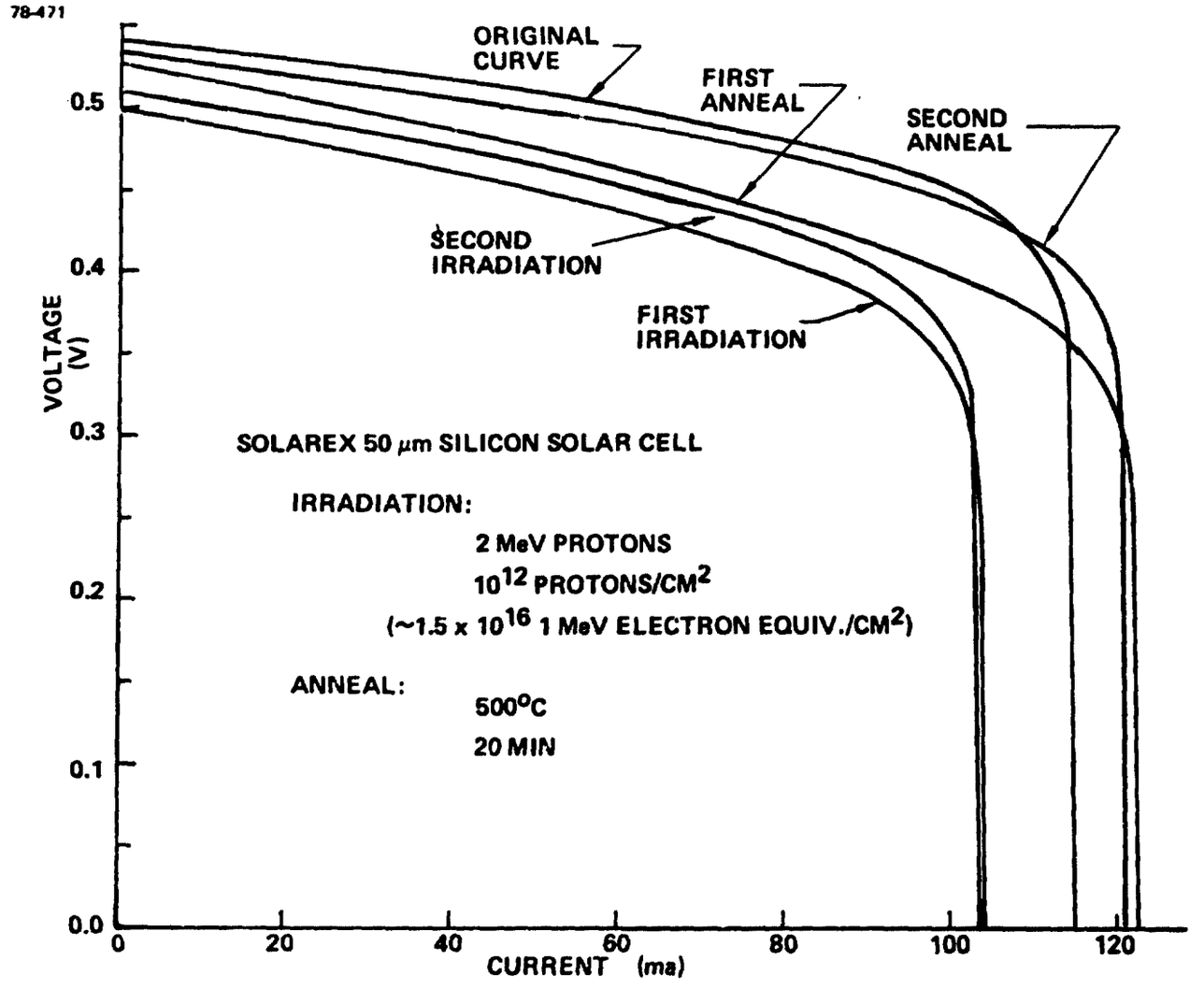

BOEING SPS

Thermal Annealing of Proton Damage In Silicon Solar Cells: Boeing Test Data

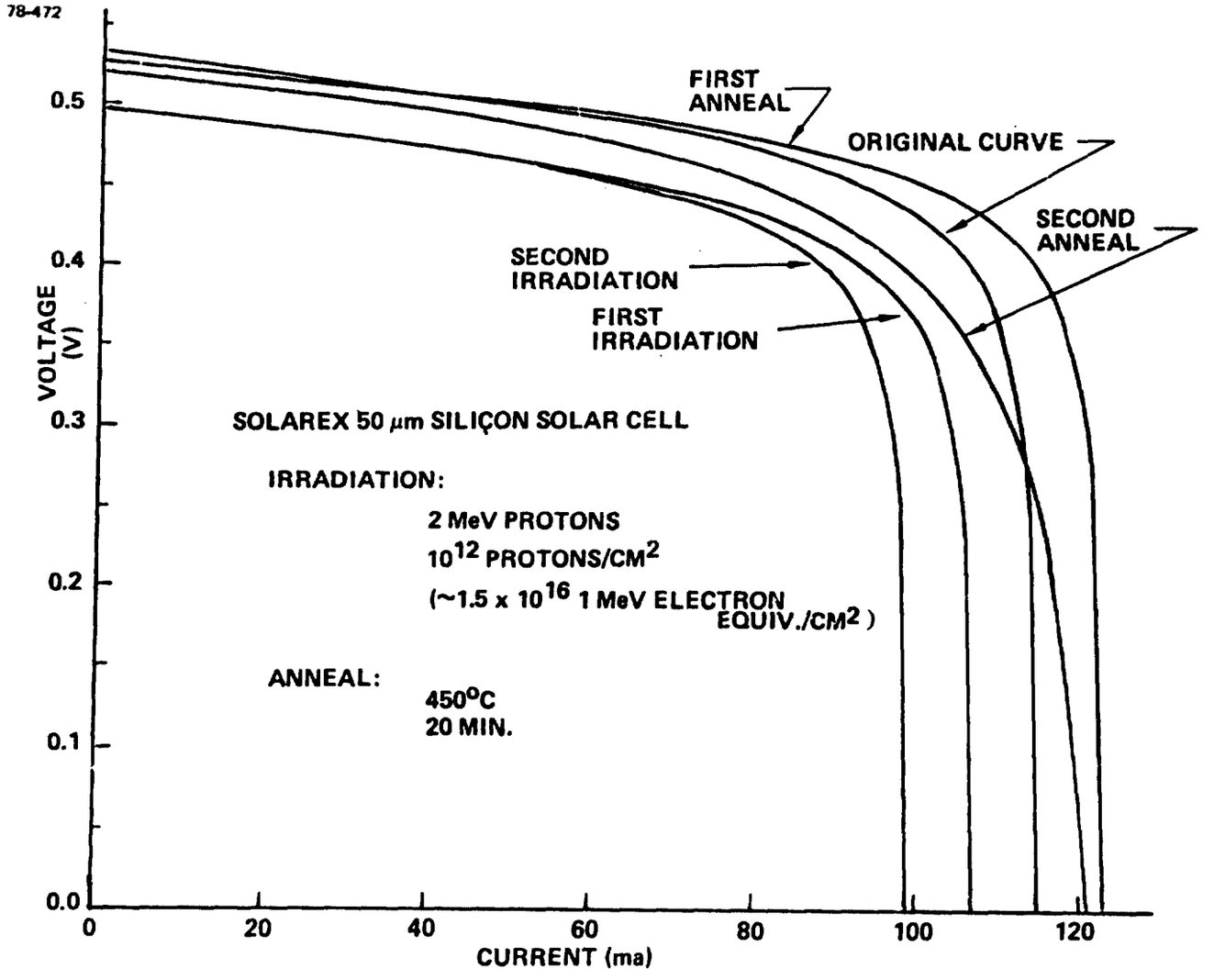

FIRST LASER ANNEALING TEST OF A PROTON IRRADIATED 50 μm SILICON SOLAR CELL

The first laser annealing test results for this contract are shown. The cell that was tested was an unglassed 50 μm (2-mil) silicon solar cell. This cell was irradiated with $1x10^{12}$ 2 MeV protons/cm^2 ($\approx 1.5x10^{16}$ 1 MeV electron equiv./cm^2). The cell was then annealed using a 10.6 μm wavelength CO^2 laser. The time/temperature plots for this test are on the next chart.

After irradiation the cell degraded to approximately 74 percent of its initial output. By annealing the cell the output increased back to 83 percent of its initial power. The small amount of recovery was considered very good considering the fact that no optimization of the laser annealing parameters was accomplished prior to this test.

First Annealing Test of Proton Irradiated 50 μ m Silicon Solar Cell

SPS-2548

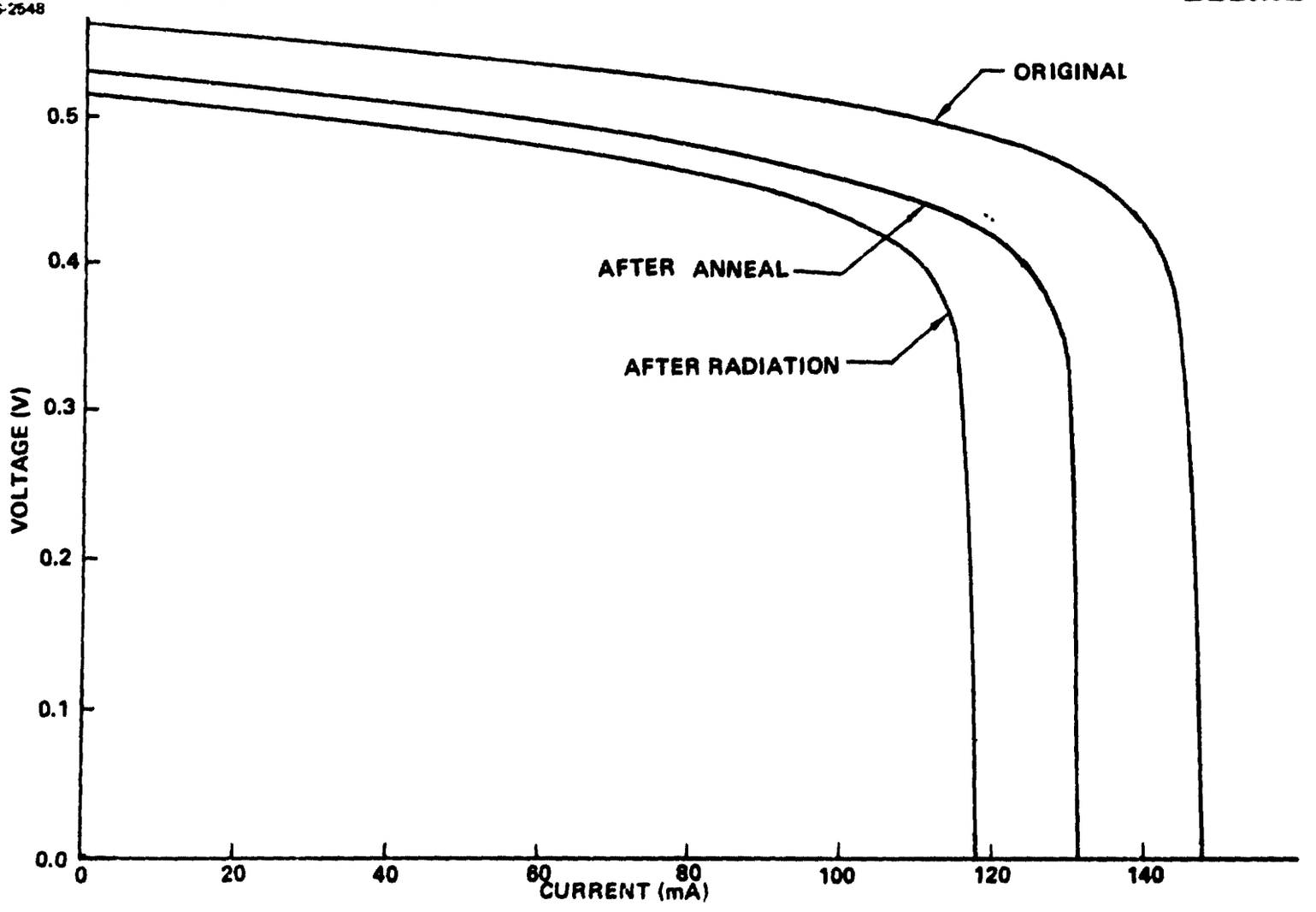

FIRST ANNEALING TEST TEMPERATURE - TIME DATA

In the first attempt to laser anneal a 50 μm (2-mil) silicon solar cell two heating cycles were used. The reason for this is that on the first attempt the duration of the laser pulse was too short. The maximum cell temperature achieved was on the order of 400°C. The second pulse, of longer duration, achieved a cell temperature of 558°C. The time that the cell was above 500°C was on the order of 0.5 seconds. Considering the short "time at temperature" of this test the results are encouraging.

First Annealing Test Temperature – Time Data

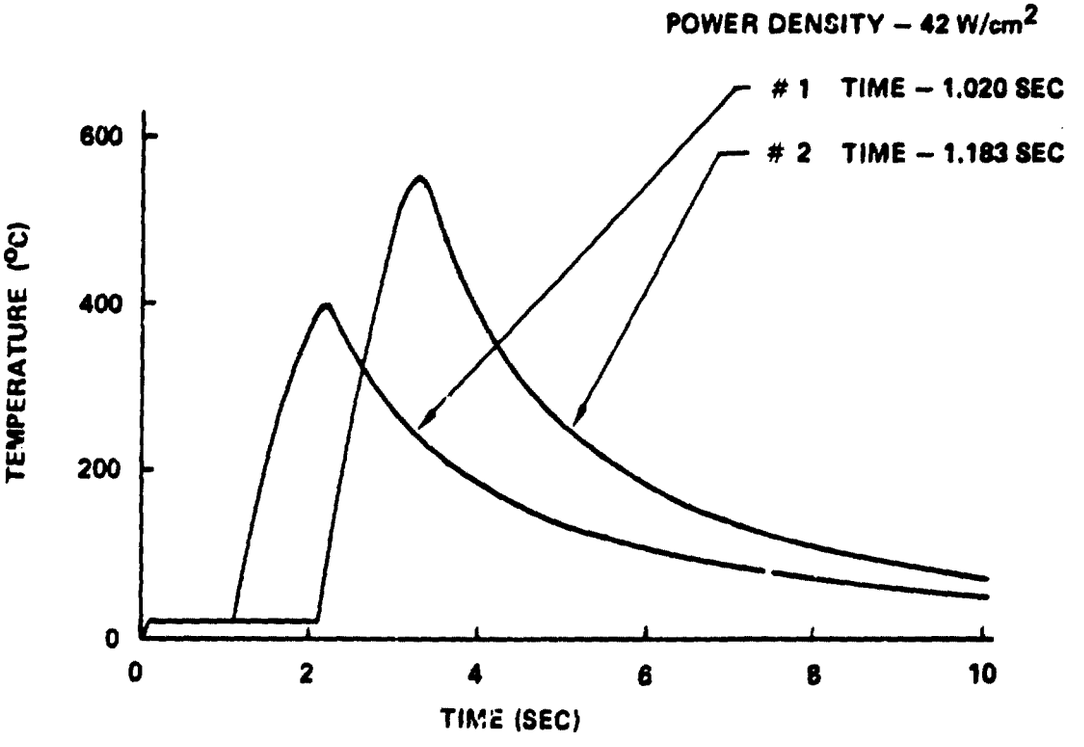

LASER ANNEALING CONCEPT

The concept of how the annealing process would be accomplished is shown. Each laser gimbal would have 8-500 watt CO_2 lasers installed. The laser beams would be optically tailored to provide the desired illumination pattern and energy density.

The gimbals would be mounted on an overhead gantry that would span the entire bay width, one bay of solar array would be annealed in fifteen meter increments. It should be noted that the solar array strings that are undergoing annealing are nonoperational.

Laser Annealing Concept

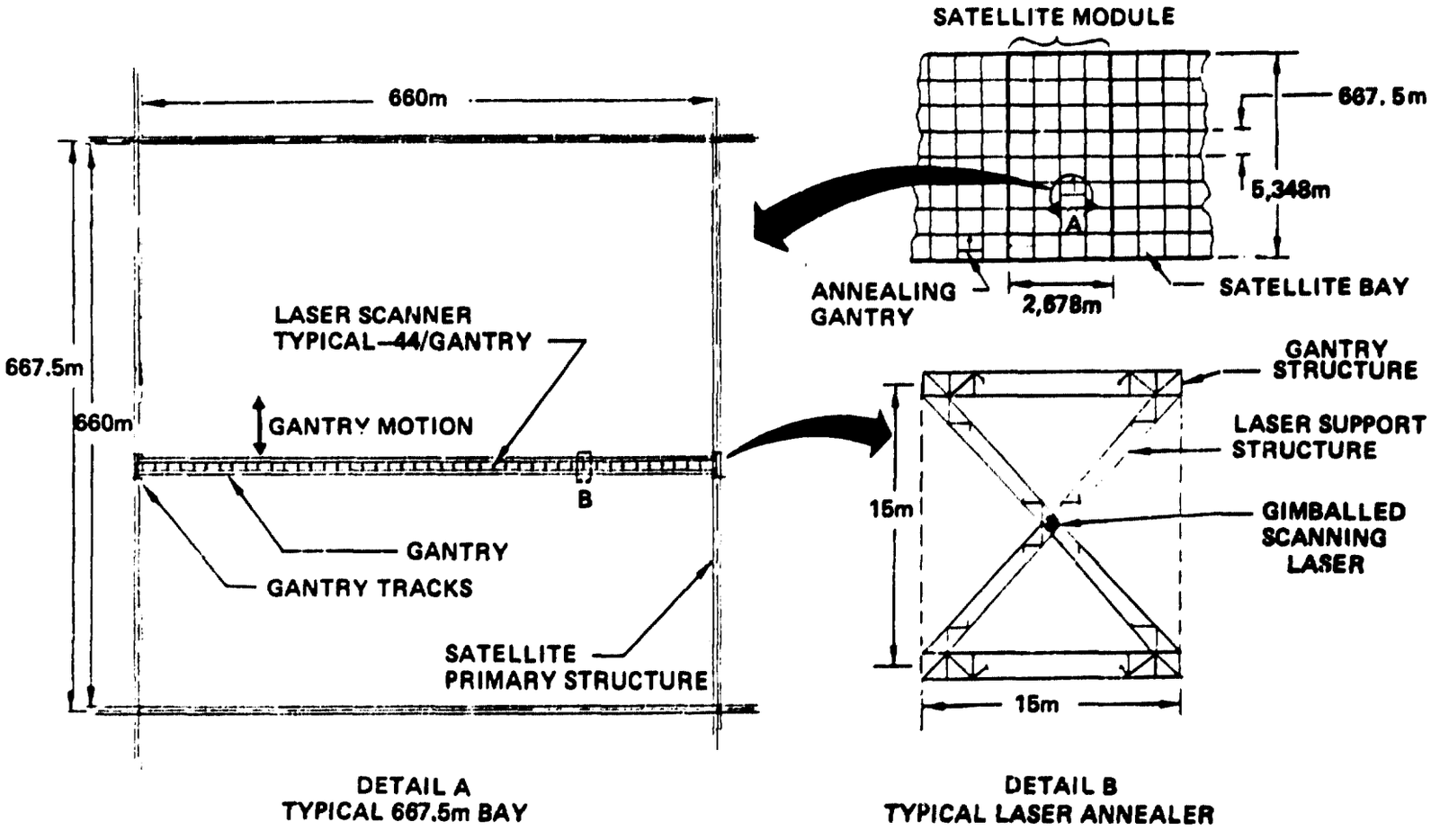

DETAIL A
TYPICAL 667.5m BAY

DETAIL B
TYPICAL LASER ANNEALER

GIMBALLED SCANNING LASER CHARACTERISTICS - UPDATE

As a result of the laser annealing tests being conducted under our current contract and after analyzing the SPIRE annealing test results from the Part III contract, the laser annealing power density and amount of equipment has been decreased by a factor of eight. Shown here are the revised laser annealing system characteristics.

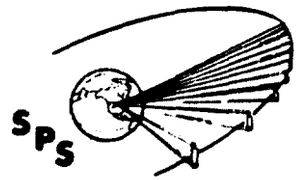

SPS-2157

Gimbaled Scanning Laser Characteristics Update

BOEING

- ANNEALING ENERGY DENSITY: 16 W-sec/cm^2
- POWER DENSITY: 8 W/cm^2
- T_{MAX} (ACTIVE REGION): 550°C
- LASERS/GIMBAL: 8
- SCANNING SPOT SIZE: 500 cm^2 (44.0 x 11.4 cm)
- SPOT SWEEP RATE: 5.7 cm/s
- POWER REQUIRED/LASER GIMBAL: 26.7kW
- POWER REQUIRED/GANTRY: 1.17 MW
- NUMBER OF GANTRIES/SATELLITE: 8 (1/SATELLITE MODULE)
- TOTAL ANNEALING POWER REQUIREMENT: 9.4MW
- TIME REQUIRED TO ANNEAL ARRAY: 147 DAYS

LARGE FLARE EFFECT ON ARRAY PERFORMANCE

Results of a statistical analysis of solar flare size are shown. The flare size probability distribution was assumed to follow a log-normal curve. The available statistical sample is too small to develop detailed conclusions as to flare size. It seems unlikely that a log-normal distribution would hold for very large flares since this distribution places no upper limits on flare size.

The two curves shown represent power law and exponential rigidity models for the proton spectrum. Available data fit either law about equally, yet these spectral distributions predict large differences in proton fluxes in the energy range from 2 MEV to 10 MEV. This energy range is of principal concern for thin solar cells with thin covers, but available data do not extend into this region.

Degradation more than 10% from a single large flare is deemed to be highly unlikely. Much improvement in the confidence in this result can be expected due to continued accumulation of statistical data from the current solar cycle and with direct observation of proton fluxes in the 2 MEV to 10 MEV range.

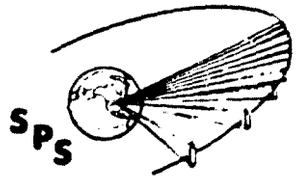

Large Flare Effect on Array Performance

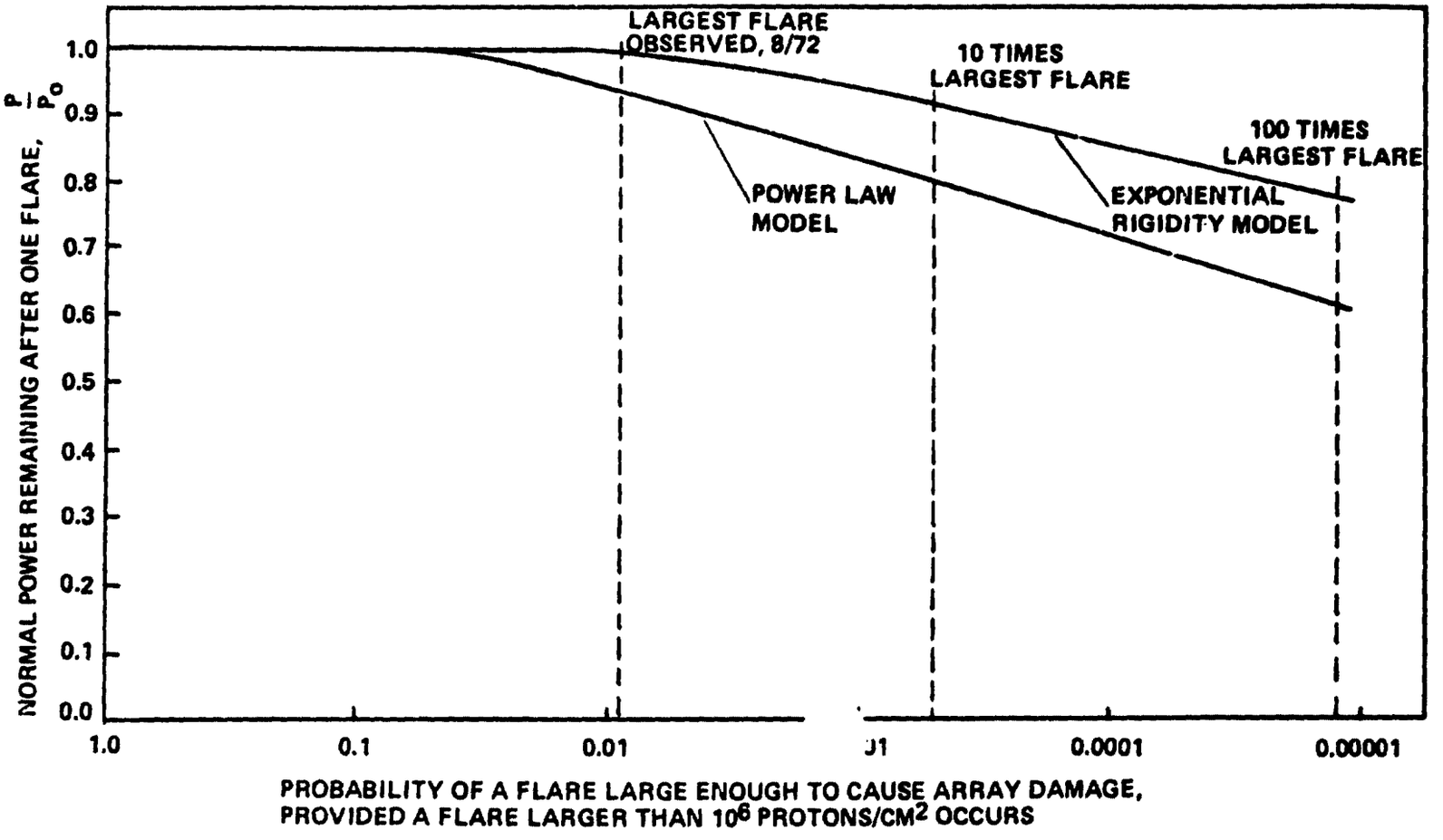

DEGRADATION COMPARISON OR ELECTRON IRRADIATION

Shown here is a comparison of the radiation degradation characteristics of the Boeing/JSC baseline 50 μm silicon solar cell and the published RI/MSFC baseline GaAlAs/GaAs solar cell. It can be noted that very little difference in the degradation characteristics can be seen on this plot. This comparison is significantly different than the comparison made in the Rockwell documentation. The data that Rockwell used for the 2 mil silicon cell could have been that published in the TRW Radiation Handbook which is not a textured surface cell and shows significantly greater degradation.

For a proper system level trade between the Boeing and Rockwell baselines it is necessary to resolve the degradation characteristics issue.

Degradation Comparison For Electron Irradiation

BOEING

SPS-2452

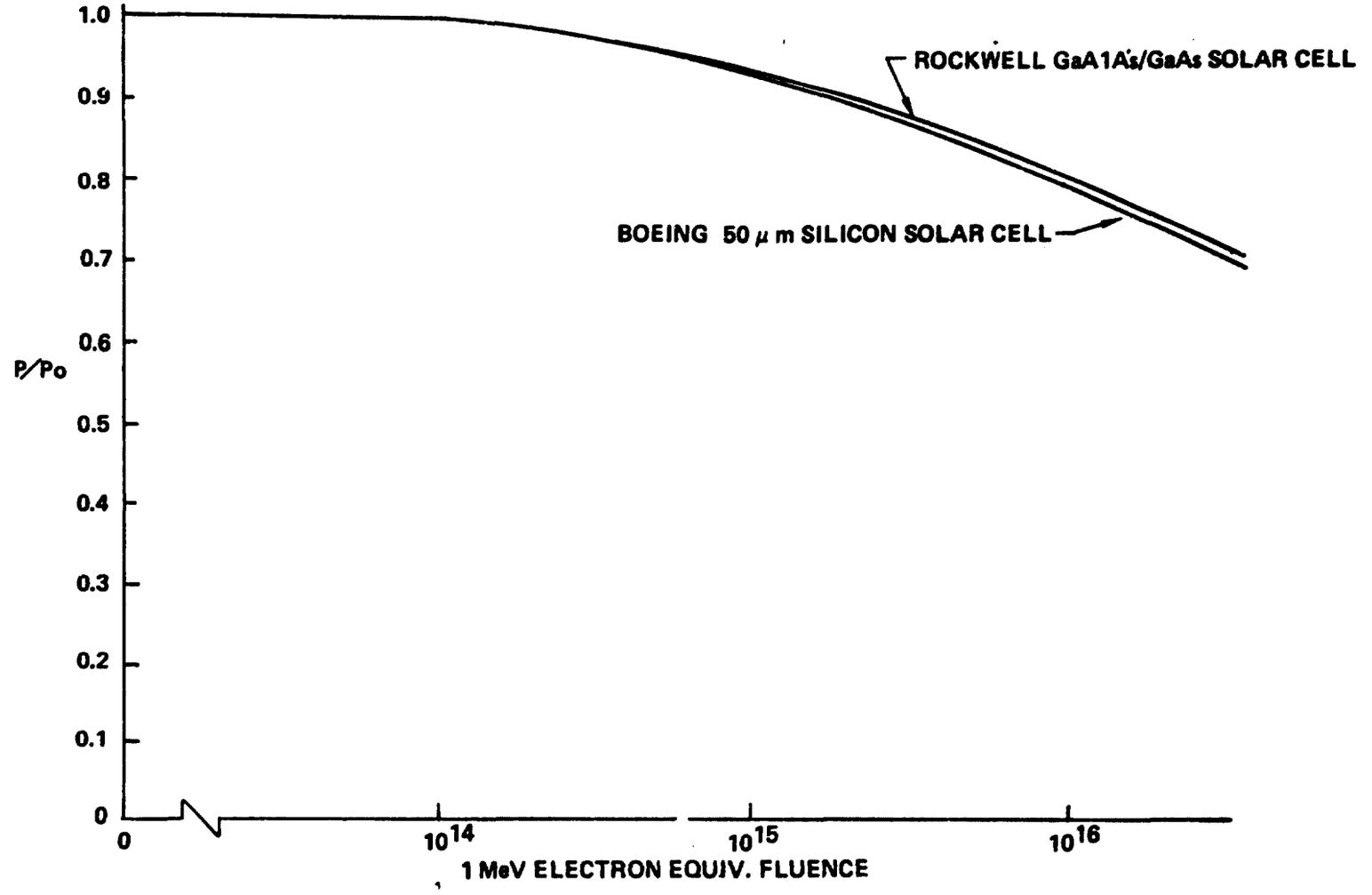

DEGRADATION COMPARISON FOR PROTON IRRADIATION

This chart further shows the differences that exist between the two major SPS contractors. From this chart it would appear that silicon would have less degradation than GaAs solar cells. It is not being suggested that this is the case, however. The point that is being made is that it appears that there is not a significant difference in radiation degradation characteristics between a 50μm silico' (texturized surface) solar cell and the published Rockwell GaAs solar cell data.

Degradation Comparison For Proton Irradiation

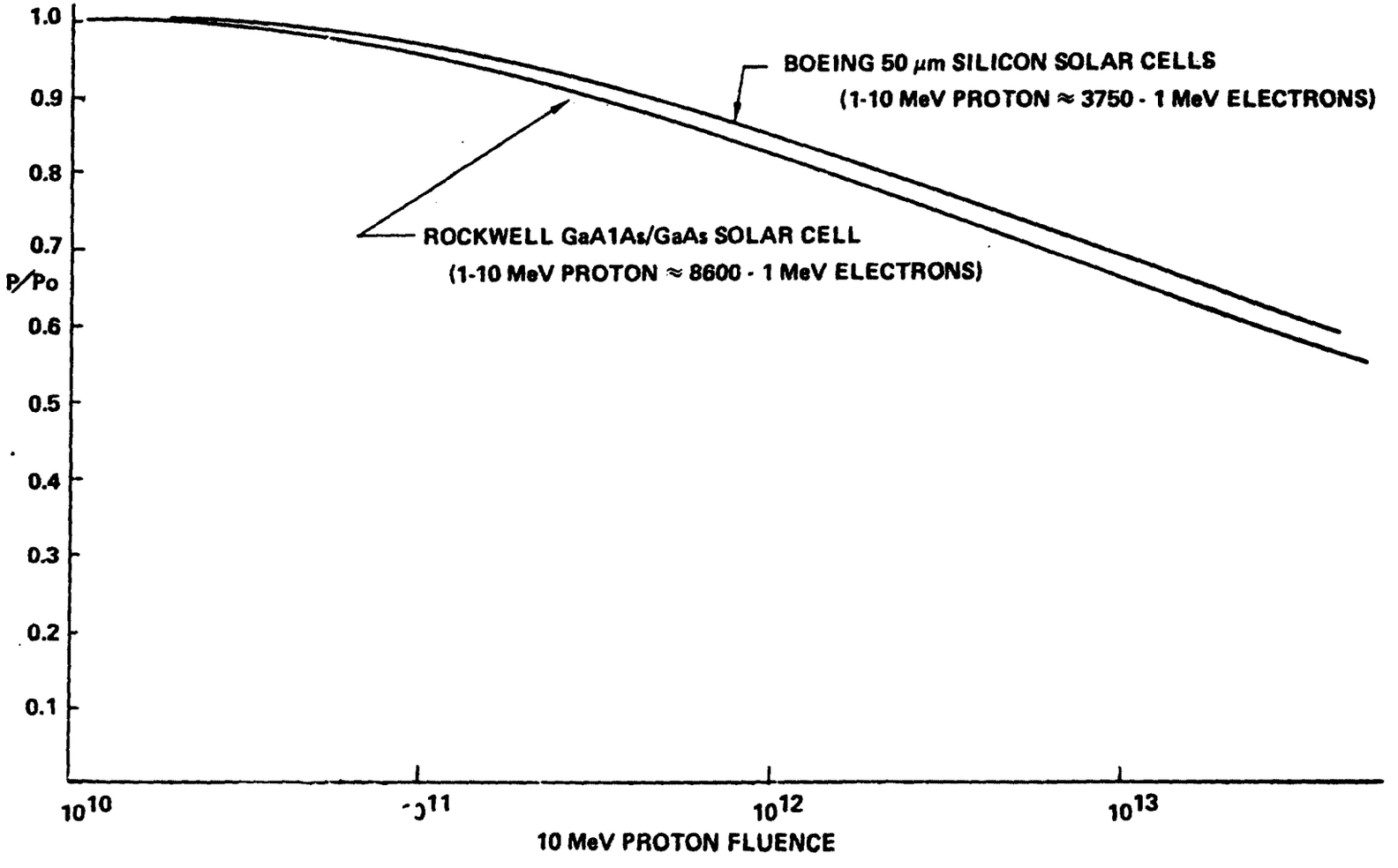

30 YEAR FLUENCE COMPARISON

Another apparent inconsistency that exists between the two major SPS contractors has to do with the model that is being used to predict the fluence the cell will be subjected to during its 30 years of operation.

This table shows the baseline blankets for both systems in terms of amount of shielding afforded in each case. With the silicon being shielded almost twice as much as the gallium system it is doubtful that it could be subjected to a larger fluence unless the environmental models being used are significantly different.

Using the Boeing method for fluence calculations, the Rockwell 5μm GaAlAs solar cell equivalent 1-MeV electron fluence would be approximately 6×10^{16} instead of the 4.9×10^{15} shown.

Again, a system level trade between the two systems should require both systems to be weighed on the same scale.

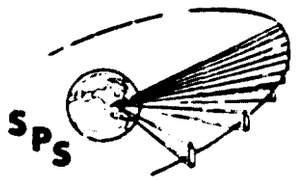

30 Year Fluence Comparison

ITEM	BOEING	ROCKWELL
CELL THICKNESS (mils)	2.0	0.2
FRONT SHIELD (COVER)	BOROSILICATE GLASS	Al_2O_3 (SAPPHIRE)
THICKNESS (mils)	3.0	0.8
MASS/AREA (g/m^2)	167.6 ←	79.6 ←
BACK SHIELD (SUBSTRATE)	BOROSILICATE GLASS	FEP/KAPTON
THICKNESS (mils)	2.0	1.6
MASS/AREA/(g/m^2)	111.8 ←	72.0 ←
30 YEAR FLUENCE (1-MeV ELECTRON EQUIV. /cm^2)	2×10^{16} ←	(1) 4.9×10^{15} ←

(1) BOEING MODEL WOULD PREDICT APPROX. 6×10^{16} 1-MeV ELECTRON EQUIV./cm^2

SPS TELEMETRY REQUIREMENTS

This figure summarizes the telemetry requirements estimated for the spacecraft (solar array) portion of the satellite up to and including the slip rings, and for the MPTS antenna from the slip rings on. The estimates were prepared by examining the satellite design in detail and estimating the instrumentation required to determine the satellite state of health and to make decisions concerning commands in the event of anomalies.

For those subsystems on which very little design information exists, estimates were made based on knowledge of requirements for typical subsystems of existing satellites which were then extrapolated to a system of the magnitude of SPS.

TRW
DEFENSE AND SPACE SYSTEMS GROUP

SPS TELEMETRY REQUIREMENTS

SATELLITE SUBSYSTEM	TELEMETRY TYPE		
	ANALOG	BILEVEL	DIGITAL
SPACECRAFT			
SOLAR ARRAY	89,152	19,200	
ATTITUDE CONTROL & DETERMINATION	26	28	4
ELECTRIC PROPULSION	656	128	
CHEMICAL PROPULSION	112	112	
COMMAND & DATA HANDLING	4,805	9,610	24,025
COMMUNICATIONS	30	48	6
POWER CONTROL	426	204	12
THERMAL CONTROL	200	400	
TOTAL	95,407	29,730	24,047
MPTS ANTENNA			
CENTRAL POWER DISTRIBUTION	1,648	4,120	
POWER SECTORS	4,560	131,708	1,140
KLYSTRONS	970,560	485,280	
PHASE CONTROL/RF DRIVE	679,372	388,224	
ATTITUDE CONTROL & DETERMINATION	26	28	4
CONTROL MOMENT GYROS	48	24	24
COMMAND AND DATA HANDLING	9,194	18,388	45,970
COMMUNICATIONS	30	48	6
THERMAL CONTROL	200	400	
TOTAL	1,665,638	1,028,220	47,144

SPS COMMAND REQUIREMENTS

This figure summarizes the command requirements estimated for the satellite using the same techniques as used for estimating the telemetry requirements. This process necessitates many decisions concerning the component level to which each subsystem will be instrumented and the level to which a command capability will be provided. For example, voltage will be measured on each string in each bay and each string will have a command disconnect capability at the main power bus.

As these figures indicate, the requirements of the MTS are much greater than those of the spacecraft, however, in both cases they are much greater than those of current satellites. The magnitude of these requirements suggest that unusual measures must be taken to keep the data transmission rates relatively low.

TRW

SPS COMMAND REQUIREMENTS

SATELLITE SUBSYSTEM	COMMAND TYPE	
	PULSE	STATE
SPACECRAFT		
SOLAR ARRAY		19,200
ATTITUDE CONTROL & DETERMINATION	84	32
ELECTRIC PROPULSION	1,000	
CHEMICAL PROPULSION	224	
COMMAND & DATA HANDLING	220	2,400
COMMUNICATIONS	54	200
POWER CONTROL	90	96
THERMAL CONTROL		400
TOTAL	1,672	22,328
MPTS ANTENNA		
CENTRAL POWER DISTRIBUTION		1,848
POWER SECTORS	1,140	485,280
ATTITUDE CONTROL & DETERMINATION	84	32
CONTROL MOMENT GYROS	24	
COMMAND AND DATA HANDLING	18,388	9,194
COMMUNICATIONS	54	200
THERMAL CONTROL		400
TOTAL	19,690	496,954

SPS COMMAND & DATA HANDLING SYSTEM (CDHS) CONSIDERATIONS

The impact of the large numbers of telemetry points and commands required by the satellite is to make unsatisfactory the usual practice of sending all data to the ground for information and action. If this practice were followed for SPS, the data rates would be unacceptably large. In addition the data would either have to be processed, commands generated and then sent automatically after it reached the ground or extremely large numbers of ground personnel would be required.

In the recommended concept, a large amount of the automatic data processing and generation of predetermined commands will take place at the local component level in the satellite, with only summary information and configuration changes transmitted to the ground. This concept reduces the amount of data to be transmitted (hence data rates) and also reduces the number of ground personnel required.

TRW

SPS COMMAND & DATA HANDLING SUBSYSTEM (CDHS) CONSIDERATIONS

- CONVENTIONAL TECHNIQUES (I.E., ALL DATA TO GROUND FOR PROCESSING AND COMMAND DECISION GENERATION) UNSATISFACTORY DUE TO LARGE NUMBERS OF TELEMETRY AND COMMAND REQUIREMENTS
  - EXTREME AMOUNTS AT DATA THROUGH SATELLITE AND BETWEEN GROUND AND SATELLITE
  - LARGE GROUND CREWS REQUIRED OR COMPUTER AIDED DATA REVIEW AND COMMAND DECISION GENERATION
- RECOMMENDED CONCEPT CHARACTERICS
  - PERFORM ROUTINE DATA REVIEW AND GENERATE PREDETERMINED COMMANDS ABOARD SATELLITE WITH MICROPROCESSORS NEAR EQUIPMENT (E.G., LIMIT CHECK DATA AND SWITCH OFF FAULTY EQUIPMENT)
  - SEND LIMITED REAL-TIME DATA TO GROUND WHEN SYSTEM IS OPERATING SATISFACTORILY. ALL DATA AVAILABLE TO GROUND UPON REQUEST.

PRINCIPAL FEATURES OF CDHS

In order to process telemetry data and generate commands locally within the satellite, numerous microprocessors and memories are required which are distributed throughout the satellite. These processors are organized into groups, each of which is monitored by a processor that is one of another tier of processors. This tiering process continues up to a Centrol Processor Unit which manages the data traffic to and from the ground.

The recommended approach is essentially two systems connected by a limited data link through the slip rings. The reasons for this approach are:

a) The large amount of information which must be handled
b) Transmission of large amounts of data at high rates across the slip rings will be very difficult
c) A redundant link with the ground is provided

The use of fiber optics is recommended for data transmission because such a system is of lighter weight, is more fault tolerant (because it is a non-conductor it does not propogate faults), has a wide-band multiplexing capability, is inherently immune to EMI and arc discharges, and the raw materials required are in ready supply and inexpensive. It is recognized, however, that a considerable amount of development in fiber optics will be required.

A code format which contains the clock has been selected because the long distances over which the data must be transmitted not only make synchronization with a separate clock signal very difficult, but also results in an appreciable increase in complexity and cost.

TRW

PRINCIPAL FEATURES OF CDHS

- PERFORMS SELECTED DATA PROCESSING AND COMMAND GENERATION LOCALLY ABOARD SATELLITE USING TIERED SYSTEM OF MICROPROCESSORS
- CONSISTS BASICALLY OF TWO SYSTEMS, ONE FOR SPACECRAFT, ONE FOR MPTS ANTENNA, WITH LIMITED DATA LINK THROUGH SLIP RINGS
- EACH SYSTEM HAS SEPARATE GROUND COMMUNICATION LINK
- UTILIZES FIBER OPTICS FOR DATA TRANSMISSION ABOARD SATELLITE
- UTILIZES CODE FORMAT, SUCH AS MANCHESTER II BI-PHASE CODE, WHICH INCLUDES THE CLOCK

SPACECRAFT CDHS USING FOUR TIERS OF PROCESSORS

The spacecraft CDHS shown utilizes four tiers of control including the Central Processor Unit (CPU). The tiers for monitor and control of the solar array are organized in the same order as the solar array. At the lowest tier (4), each RTU monitors and controls two of the 100 strings which constitute a load sector. At the next tier (3), each processor (load sector controller) monitors and controls 50 of the lower tier RTU's plus the other load sector functions. The next tier (2), of processors (module controllers) monitor and control 48 load sector controllers and interface with the CPU. The other spacecraft subsystems require a relatively small number of RTU's, hence there are only three levels of control, with module controller #3 interfacing directly between the RTU's and the CPU.

The CPU manages data traffic to and from the ground, formats telemetry for transmission and checks commands for bit errors. Other functions of the CPU include maintaining stored commands for operating and testing the data subsystem in the absence of ground control and control of telemetry data storage for later transmission.

Each tier monitors operation of the tier below, instigates check on subordinate units and establishes priority for upward communication. The lowest tier interfaces the CDHS to other subsystems through sensor readings, digital data transfers and command outputs. An upper tier may also override a command by a lower tier in order to restore operation or diagnose apparent failures if its information on the status of the RTU involved, or information from another RTU, warrants such action.

TRW
DEFENSE AND SPACE SYSTEMS GROUP

SPACECRAFT CDHS USING FOUR TIERS OF PROCESSORS

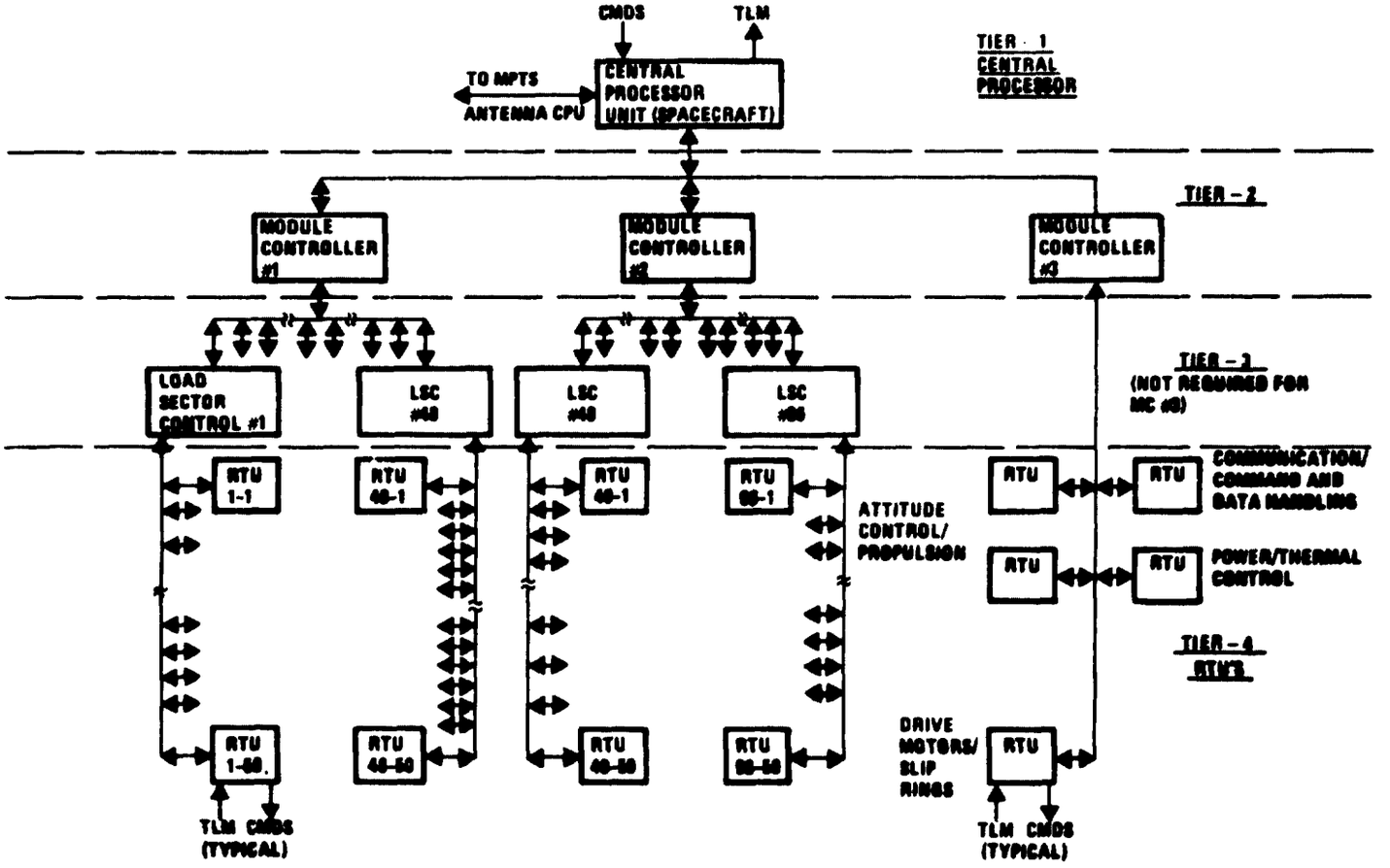

NOTES – RTU – REMOTE TERMINAL UNIT
– 4000 RTU's REQUIRED FOR SOLAR ARRAY
– 5 RTU's REQUIRED FOR REMAINDER OF SPACECRAFT

MPTS ANTENNA CDHS USING FIVE TIERS OF PROCESSORS

The MPTS antenna CDHS requires a five tier system not only because of the much greater telemetry and command requirements, but because much quicker response is required by the power sectors and klystrons of the MPTS in order to prevent extensive damage in the event of an anomaly. The RTU's (5), monitoring these components monitor fewer sensors but sample them at nearly twice the rate of the spacecraft RTU's. Simularly, at the next level above the RTU's, the RTU controllers (4), monitor fewer RTU's but sample their outputs at a higher rate.

Tiers (3) and (2) provide communications management and test programs for the subordinate tiers except in the case of module controllers #4 and #5 which monitor and control the antenna subsystems other than the MPTS. For these subsystems the number of RTU's is much smaller because of the lower requirements. As in the case of the spacecraft the number of intermediate tiers is reduced for the portion of the CDHS associated with these subsystems.

TRW
DEFENSE AND SPACE SYSTEMS GROUP

MPTS ANTENNA CDHS USING FIVE TIERS OF PROCESSORS

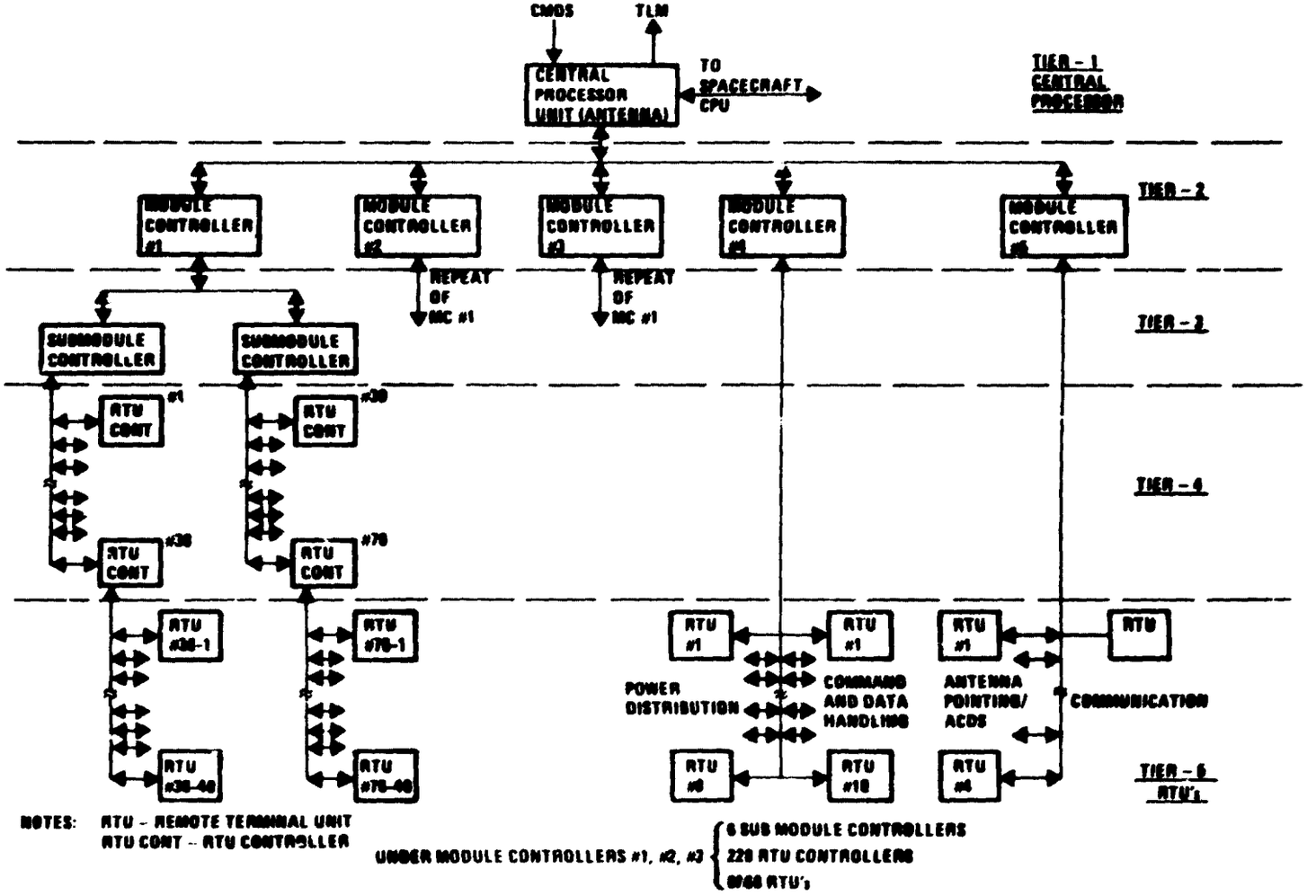

COMMUNICATION SUBSYSTEM CHARACTERISTICS

Separate systems for the spacecraft and MPTS antenna are recommended not only because there are separate CDHS systems which must communicate with the ground, but because the nature of the system mission (i.e., continuous provision of electrical power to the ground) demands high reliability which suggests this redundance.

Alternative systems considered for MPTS communication were use of the retrodirective beam for the command uplink and modulation of the output of one of the klystrons for the downlink. Both of these techniques have certain advantages, however, since in the event of a relatively minor attitude control system deviation the MPTS antenna beam is deliberately despoiled, the result would be severe degradation of the communication link at a critical period of operation. For this reason a separate antenna which provides earth coverage is recommended.

As the figures indicate, the necessary performance is readily provided by an S-Band system using a 20 watt transmitter.

TRW
DEFENSE AND SPACE SYSTEMS GROUP

COMMUNICATION SUBSYSTEM CHARACTERISTICS

- SEPARATE SYSTEMS FOR SPACECRAFT AND MPTS ANTENNA
- EACH SYSTEM HAS 2 FOOT PARABOLIC ANTENNA PROVIDING EARTH COVERAGE GAIN OF 18 dB AT S-BAND
- SPACECRAFT SYSTEM ALSO HAS OMNI-ANTENNA FOR COMMAND RECEPTION IN EVENT OF LOSS OF ATTITUDE CONTROL
- TELEMETRY DOWNLINK CAPABILITY 1-10 MBPS (1 REQUIRED) AT 2.2-2.3 GHZ
- COMMAND UPLINK CAPABILITY 1-5 MBPS (1 REQUIRED) AT 2.05-2.15 GHZ
- KLYSTRON WIDE-BAND NOISE $\sim$ 40 dB BELOW COMMAND RECEIVER THRESHOLD

SPS COMMUNICATION SUBSYSTEM

This figure shows the recommended subsystem and its interface with the CDHS. This system is very similar to existing S-Band systems hence most of the components are currently available. Information to date indicates that little or no development will be required for an SPS communication system.

SPS COMMUNICATION SUBSYSTEM

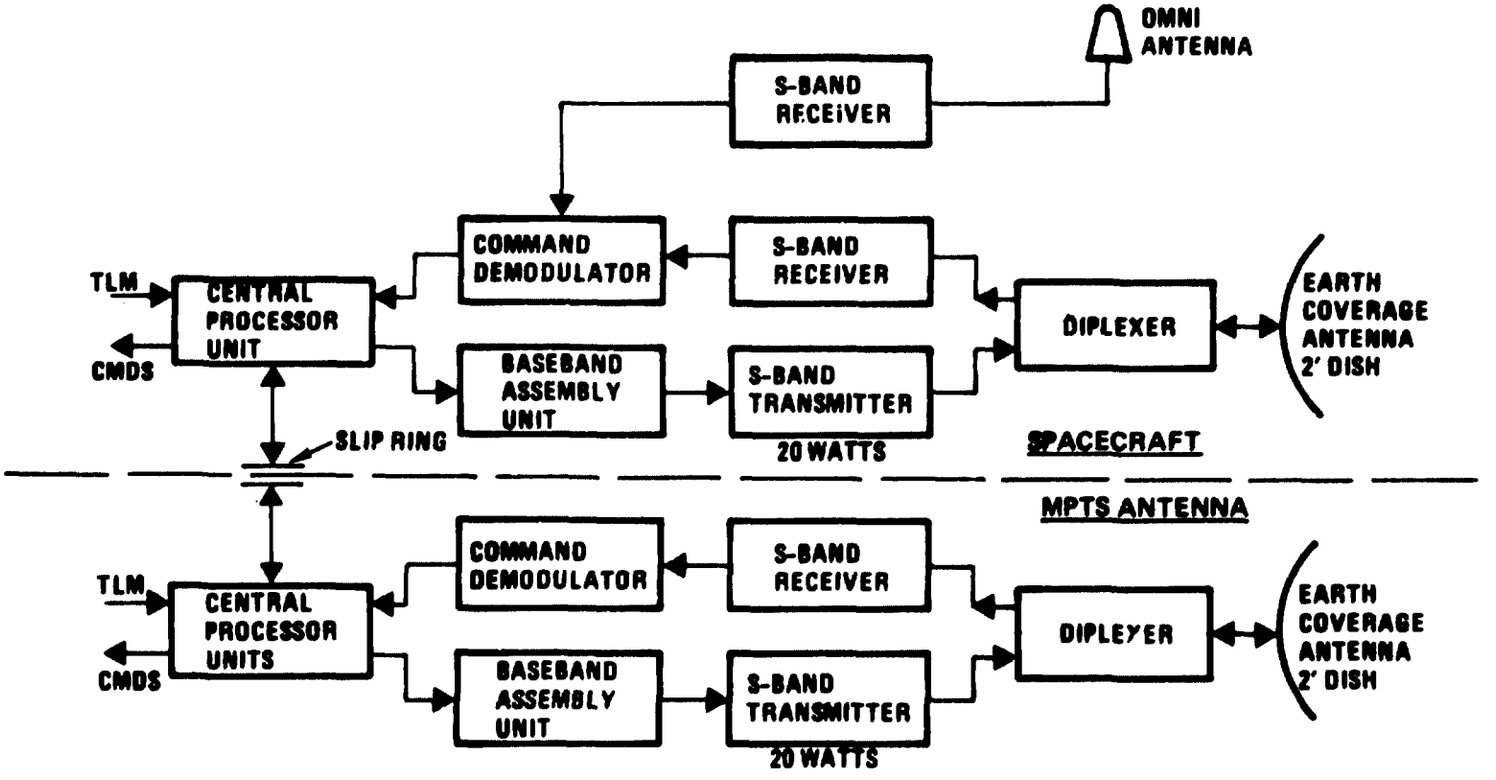

CDHS FAILURE MODES AND EFFECTS ANALYSIS RECOMMENDATIONS

The status of hardware design of the CDHS is such that it was not possible to make such an analysis at the hardware level, however, a preliminary system analysis was made. This analysis resulted in the processor redundancy recommendations shown. At the RTU level it was recommended that the data be distributed among the RTU's such that the condition of a component can be determined from the data on two different RTU's. For example one RTU can monitor the on/off switch position of an electrical component. The temperature of that component could be monitored by another RTU. In the event one RTU failed, the status of that component could still be determined from the data of the remaining RTU. This technique also provides for a cross-check by the next level processor monitoring the RTU's.

This analysis also was an important factor in the recommendation to use fiber optics as well as the provision of earth-coverage antennas and the omni antenna.

TRW
DEFENSE AND SPACE SYSTEMS GROUP

CDHS FAILURE MODES AND EFFECTS ANALYSIS RECOMMENDATIONS

- PROCESSOR REDUNDANCY
  - PROCESSORS IN STANDBY REDUNDANCY AT CPU AND MODULE CONTROLLER LEVEL
  - BANK OF SPARE PROCESSORS AT LEVELS BETWEEN RTU'S AND MODULE CONTROLLERS
  - NON-REDUNDANT RTU'S - REDUNDANCY PROVIDED BY DATA DISTRIBUTION
- DATA BUS
  - USE FIBER OPTICS
  - REDUNDANT PARALLEL BUS BETWEEN MODULE CONTROLLERS AND CPU
- PROCESSOR POWER SUPPLY - USE BUS WITH LOCAL REGULATION
- SATELLITE/GROUND COMMUNICATIONS - USE WIDE BAND (EARTH COVERAGE) ANTENNA

ELECTROMAGNETIC INTERFERENCE SOURCES CONSIDERED

The sources listed are considered to be the most likely sources of internal EMI. Very preliminary consideration of these sources indicated that corona effects and inrush currents were likely to be less severe sources than the others. Since it is not planned to operate high voltage disconnects unless the power has been interrupted previously by circuit breakers it was felt that this source would be less than would otherwise be the case. The status of information on slip rings of the size considered here and on 70 Kw klystrons is such that analysis would be of little value at this time.

Since some data is available on the DC/DC converters, and since they are a continuous EMI source, this source was selected for analysis. This very preliminary analysis indicated that the mean electric field at a distance of 6 meters from the conductors would be 20 volts/meter at 20 Khz, declining at higher frequencies. Current equipment must be designed for 10 volts/meter from 14 Khz to 35 Mhz. The mean magnetic field at the same distance would be 36 milliamperes/meter at 20 Khz. The current requirement on equipment is 2.6 microamperes per meter.

TRW
DEFENSE AND SPACE SYSTEMS GROUP

ELECTROMAGNETIC INTERFERENCE SOURCES CONSIDERED

- * DC/DC CONVERTERS
- HIGH VOLTAGE SWITCH GEAR
- ROTARY JOINTS
- CORONA EFFECTS
- INRUSH CURRENTS
- 70 KW KLYSTRONS

* SELECTED FOR ANALYSIS

SPS-2558

MPTS Phase I Review

Erv Nalos
December 1978

MPTS STUDY AREAS

Primary areas of emphasis in Part 4, Phase I, SPS Microwave Power Transmission System studies were in the three areas defined on the attached chart. The first two high leverage items contribute to the baseline design verification, and the third item, due to its potential impact on r.f. transmitter reliability, offers a viable alternate SPS design worthy of refinement.

SPS-2556

- PHASE CONTROL
- FAILURE ANALYSIS
- SOLID STATE SPS

MPTS PHASE CONTROL

The major accomplishments in the phase control area are summarized on this chart. A comprehensive dialogue has been established through the SPS Program Office with Lincom Inc., the designer of the baseline phase control system. A number of circuit refinements and model simulations were carried out to arrive at an improved compromise design.

The failure analysis of a 4 node system defined in conjunction with General Electric Space Division was accomplished, yielding a 3.8% efficiency degradation due to MPTS system availability.

Initial definition of a fiber-optic cabling system was defined in a supporting IR&D effort, yielding a potential 20:1 reduction in phase error due to cable temperature fluctuations. Laboratory verification is required using coherent and possibly non-coherent GaAs LED's.

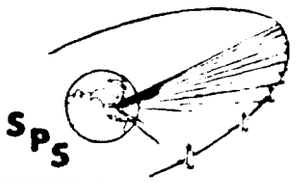

MPTS Phase Control

- PHASE CONTROL CRITIQUE
  - CIRCUIT IMPLEMENTATION
  - COMPUTER PROGRAM VERIFICATION
  - DISTRIBUTION TREE LAYOUT

- FAILURE MODE ANALYSIS
  - BASELINE SYSTEM DEFINED
  - REDUNDANCY LEVEL DEFINED
  - IMPACT ON EFFICIENCY

- FIBER OPTIC CABLING FEASIBILITY
  - CONCEPT AND LINK CALCULATIONS

SPS ARRAY COMPUTER SIMULATION

In the computer simulation area, routine use is now being made of the "Tiltmain" array program in checking grating lobe levels with systematic and random tilt. The "Modmain" program, which overcomes some of the storage limitations of Tiltmain is now 65% complete, and will ultimately enable modeling the SPS array to the klystron module level (100,000 elements). The program flow of each are indicated on the attached chart, and the status of each is indicated below.

- o "TILTMAIN"

  Phase Control Verification
  Grating Lobe Levels, Tilt

- o "MODMAIN"

  Capability to Access NASA-JSC Computer
  Set up files for main program and subroutines

Modmain will have the following features:

- o Capability to model the spacetenna down to the power module level without excessive storage requirements.
- o Incorporation of variable spacing between modules.
- o Capability to define level of phase control.
- o More accurate modeling of grating lobe behavior

So far "Modmain" has been matched to a no-error "Tiltmain" run for a 10 m x 10 m subarray and plan for Phase 2 is to:

- o Incorporate the "error" subroutine into "Modmain" and match to Tiltmain runs.
- o Detail the model by changing the size and spacing of the modules. There will be ten different sizes of klystron modules corresponding to the ten step quantized illumination taper.

Computer Program Flow Comparison

CURRENT "TILTMAIN" FLOW CHART

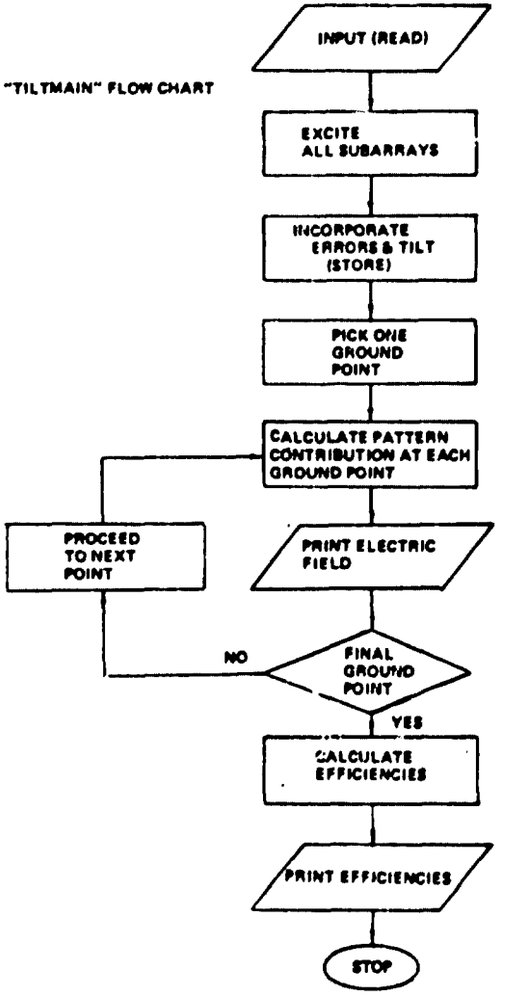

"MODMAIN" PROGRAM FLOW CHART

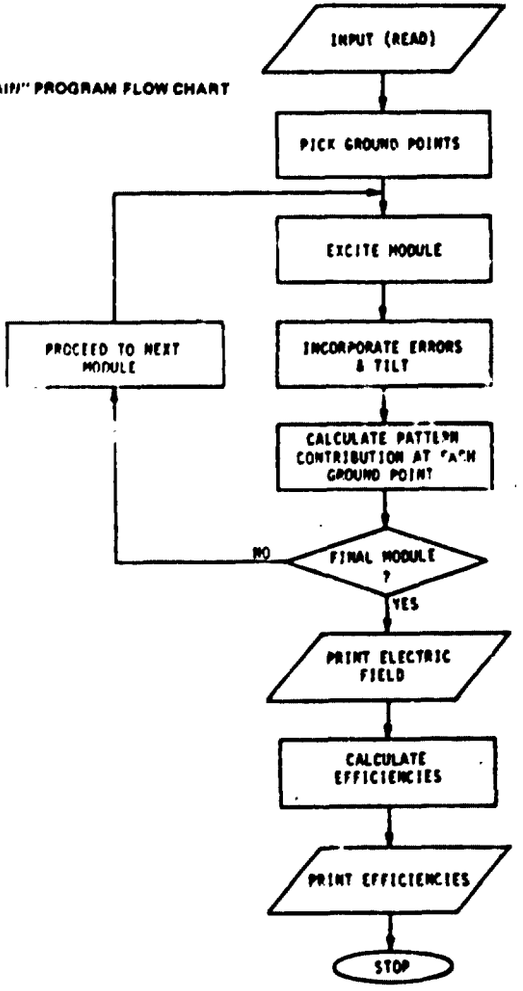

GRATING LOBE LEVELS.

Typical grating lobe level amplitudes are illustrated as a function of distance from the rectenna. The design requirement of 1 arcmin. of systematic tilt are derived from these, to meet the Soviet microwave level standard at the first grating lobe. The random tilts have only second order effect on grating lobe levels and affect primarily the array scanning loss.

The baseline 1 arcmin. random tilt, combined with the above systematic tilt, will combine to give a 0.5% efficiency loss for a 10 m x 10 m subarray. Going to a 5 m x 5 m subarray would allow the tilt requirement to be relaxed to 2 arcmin. systematic and 2 arcmin. random for the same scanning loss of 0.5%.

Grating Lobe Peaks Produced by Systematic Spacetenna Tilt

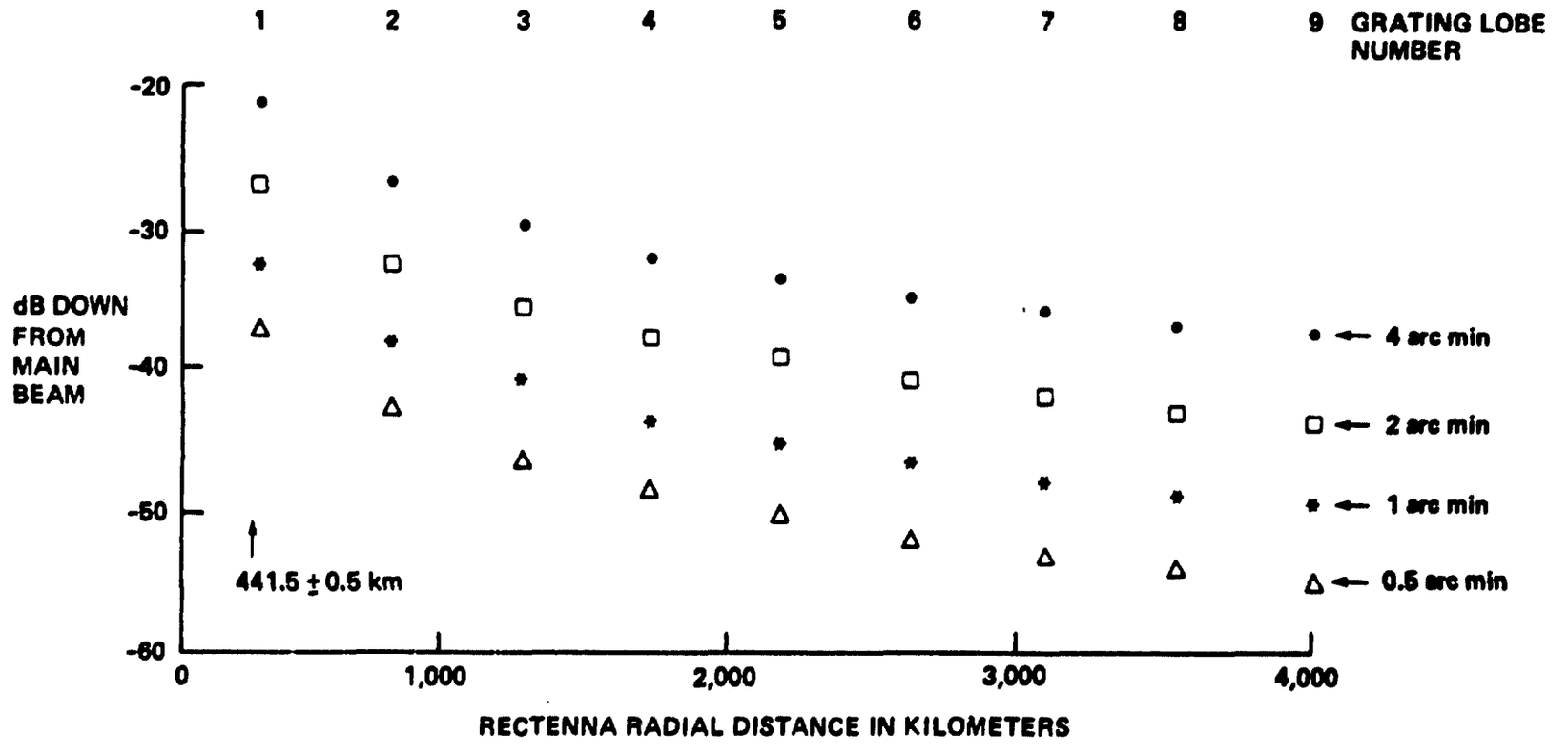

COMPARISON OF ARRAY

PERFORMANCE DEGRADATION WITH TILT

A number of "Tiltmain" runs were made to check some available aspects of the Lincom "Solarsim" program, of which the attached curve is typical. For the use of a 10 m x 10 m subarray, both one dimensional and two dimensional "Tiltmain" runs checked well with the Lincom results, provided that surface irregularity error were accounted for in a similar manner.

Comparison of Array Performance Degradation with Tilt

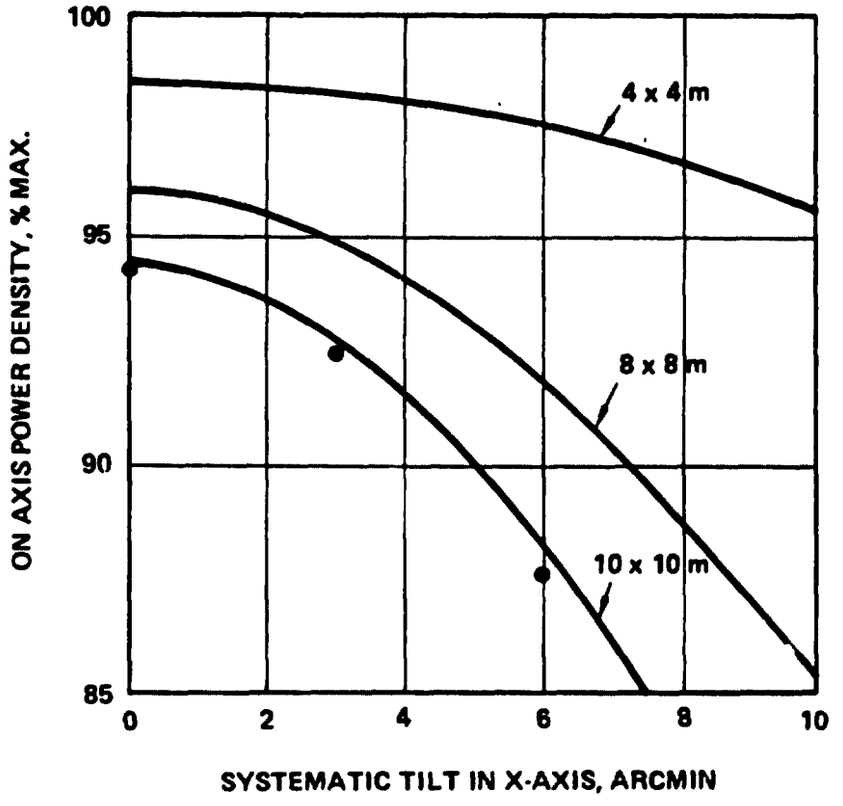

LEGEND

LINCOM RESULTS

3 arcmin SYSTEMATIC Y TILT
3 arcmin RANDOM TILT (1 σ)
Surface ϵ = .01λ (48 mils)

BOEING "TILTMAIN" RESULTS

① 3 arcmin SYSTEMATIC TILT
$3\sqrt{2}$ arcmin RANDOM TILT

② $3\sqrt{2}$ arcmin SYSTEMATIC TILT
$3\sqrt{2}$ arcmin RANDOM TILT

③ $3\sqrt{5}$ arcmin SYSTEMATIC TILT
$3\sqrt{2}$ arcmin RANDOM TILT

Surface ϵ = .01λ corresponds to 1/2% power loss

EFFECT OF PHASE ERROR AND TILT ON BEAM SHAPE

From the designer's point of view, it is important to estimate the effects of various phase control system errors near the rectenna. The attached chart does this in a qualitative manner. One fallout is the fact that correlated phase errors may not be of great importance in a system that has more than, say, ten branches per node.

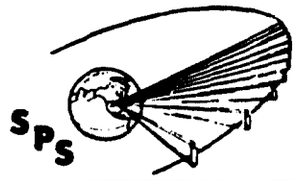

Effect of Phase Error and Tilt on Beam Shape

	EFFECT
PHASE ERROR BUILDUP	
• UNCORRELATED ERRORS	• NO EFFECTS ON MAIN BEAM SHAPE • FAR-OUT SIDELOBE LEVEL PLATEAU INCREASED
• CORRELATED PHASE ERRORS	
• FEW BRANCHES (4) AT FIRST/SECOND LEVEL	• SLIGHT RANDOM WANDER OF MAIN BEAM BEAM BROADENED BY 4%(95% CONFIDENCE)
• MANY BRANCHES	• PROBABLY NEGLIGIBLE
ANTENNA TILT	
• SYSTEMATIC TILT	• MAIN BEAM SHAPE UNAFFECTED BUT POWER REDUCED BY SCAN LOSS WHICH APPEARS AT GRATING LOBES
• RANDOM TILT	• MAIN BEAM SHAPE UNAFFECTED; RESULTING AMPLITUDE MODULATION CAN RAISE ERROR PLATEAU

SPS-2557

- Failure Analysis
- Impact On Efficiency

POTENTIAL PHASE DISTRIBUTION TREE LAYOUTS

The detailed layout of the phase distribution system will depend on the results of a trade study of correlated and uncorrelated phase error buildup per node; redundancy/reliability/ and level at which phase control is exercised. The nine node system suffers from poor reliability, poor phase randomization (.e., resulting correlated phase errors which produce beam pointing errors) and lowest allowable phase error per node. The four node system may be a viable candidate if 10 m x 10 m subarrays are retained and phase control is exercised down to the klystron level. A three node system may be possible if phase control is exercised at the subarray level only, and subarray size is reduced to 5 m x 5 m.

To reduce phase correlation effects, i.e., beam steering errors, the number of branches at the lower levels should be kept high. This also allows higher random phase error per level in the error budget. Even with 4 m x 4 m subarray, the 4-level system will require a total (1 GHz) phase accuracy of 2^{o} per level to achieve a 96% efficiency including tilt. This will require stringent design criteria. A possible 3 m x 3 m subarray could be accommodated by a 32 x 16 x 16 x 8 four node distribution system. Phase error buildup affects only far-out low level sidelobes, i.e., does not constitute a major environmental problem.

Potential Phase Distribution Tree Layouts

● 4-NODE SYSTEM – 7,220 SUBARRAYS, 100,000 KLYSTRON MODULES

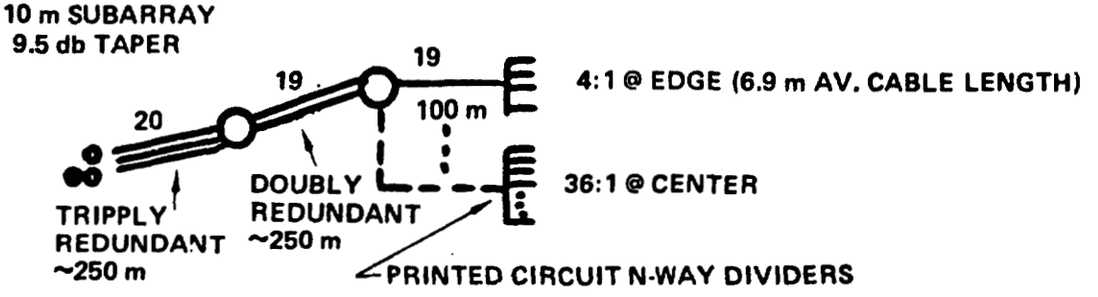

● 3-NODE–32 BRANCH SYSTEM – 28,880 SUBARRAYS

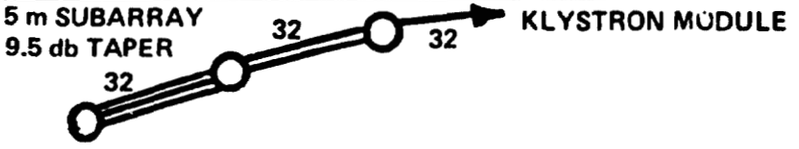

● 4-NODE–13 BRANCH SYSTEM – 28,880 SUBARRAYS

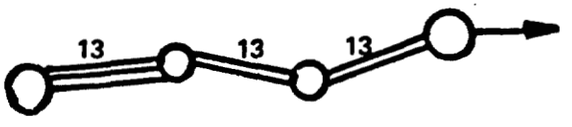

● 9 NODE – 4 BRANCH SYSTEM

262,144 ELEMENTS

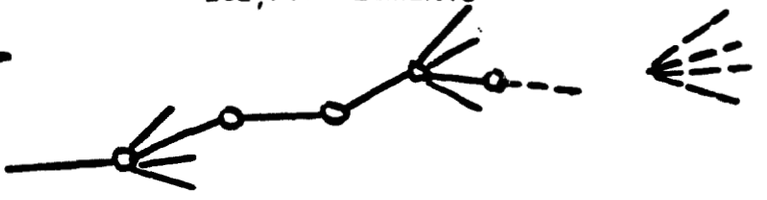

FOUR NODE PHASE DISTRIBUTION SYSTEM LAYOUT

Three sections are shown of the 4 node system selected for reliability analysis by the General Electric Co. This layout uses 20 triply redundant sections at the first level, 19 doubly redundant paths at the second level, and 19 non-redundant paths (cable and electronics) at the third level (i.e., 7220 subarrays). The fourth level provides power dividers down to the klystron module (4:1 at the center and 36:1 at the array edge), to accommodate the quantized 10 db Gaussian power taper indicated in the chart.

GENERAL ELECTRIC

LOCATION OF REFERENCED PHASE REPEATER STATIONS OF SECTORS AND GROUPS

space division

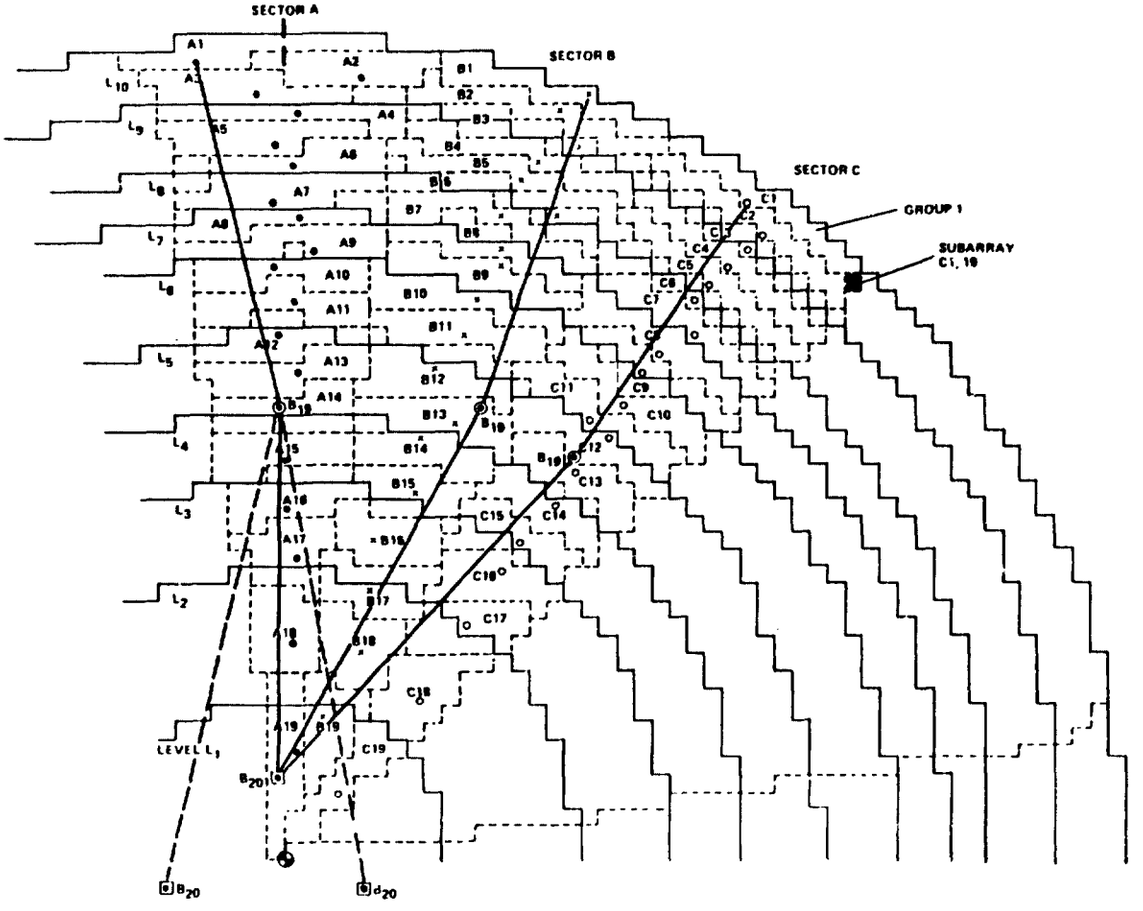

RELIABILITY CALCULATIONS

The MTBF values assigned to each component in the phase distribution path are indicated. These values, together with the redundancy level selected, and the selected maintenance procedure assumed, lead to availability numbers detailed in the Part 4, Phase I, Final Report, Dec. 14, 1978, General Electric Space Division. The overall impact of the failure analysis on efficiency is summarized in the table below.

	Availability, %	Efficiency, η	Comment
Phase Control	.989	.978	Power & Beam Loss Redundant 1st, 2nd Level Conjugator, Receiver 6 Months Maintenance
Klystron & Driver	.98	Previous Budget	No Redundancy 25 Year MTBF 6 Month Maintenance
Rectenna	.984	.984	Diodes Nonredundant No Maintenance DC Panel Open/Short Circuit Continuous Maintenance
		3.8%	Microwave Related
		5.1%	Total MPTS

Note that for the phase control system failure, there is a double penalty: array thinning (% availability), and associated loss of power, since the klystrons are not radiating in the main beam direction. The 5.1% figure includes efficiency degradation due to bussbar failures on the space antenna and the rectenna.

GENERAL ELECTRIC

BLOCK DIAGRAM FOR RELIABILITY CALCULATIONS

space division

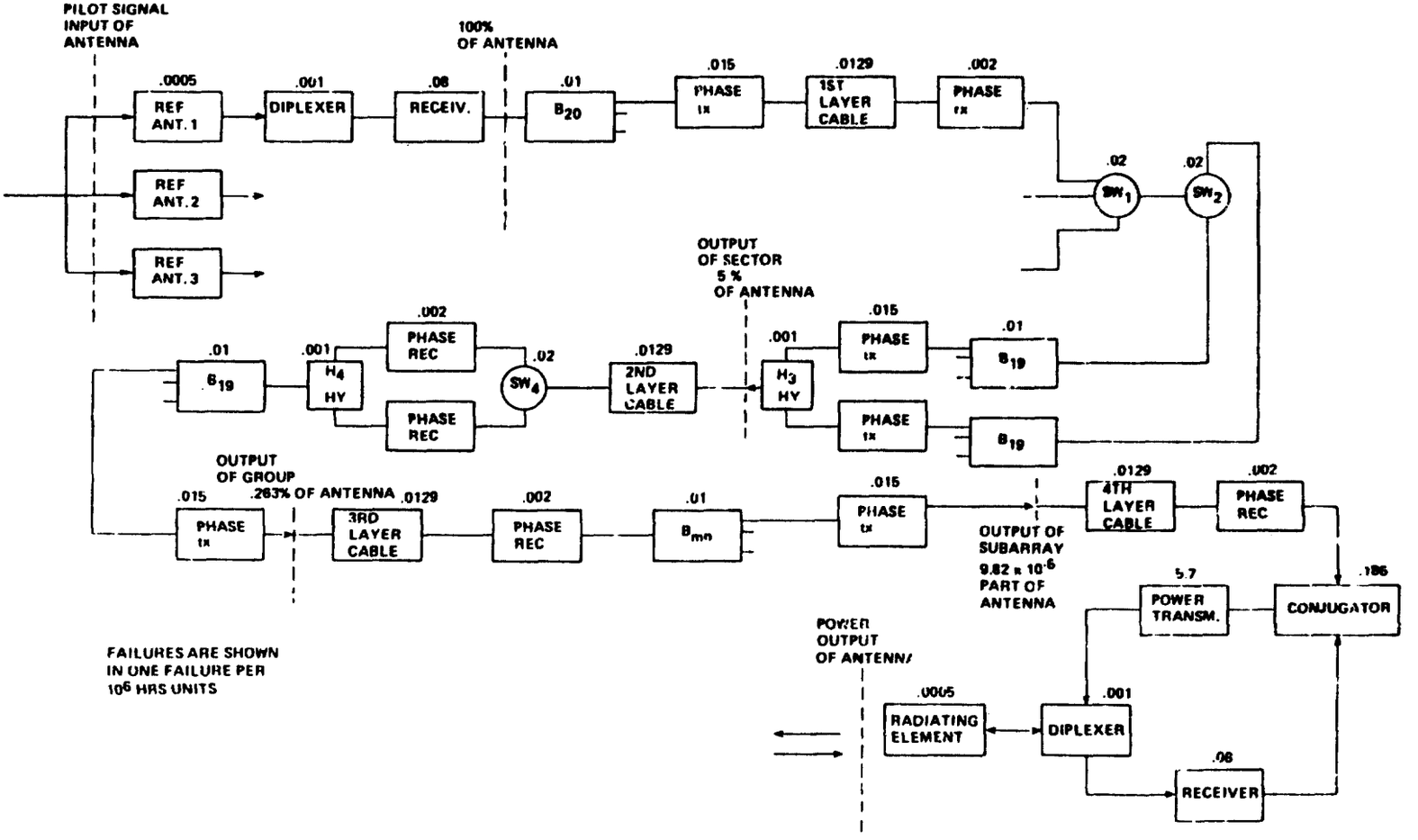

KLYSTRON MODULE LAYOUT

For purposes of illustration, a layout of the klystron module is indicated. It shows possible locations of the solid state phase control modules for good thermal distribution. The selection of a pilot receiving antenna has not been finalized and is indicative of an approach to be considered to achieve good isolation in a system in which the power beam and pilot beam are at the same frequency. The radiator is indicative only and is not representative of an alternate lower mass active cooling system under consideration.

GENERAL ELECTRIC

MECHANICAL LAYOUT OF A TYPICAL KLYSTRON MODULE IN THE OUTER RING OF THE SPACE ANTENNA

space division

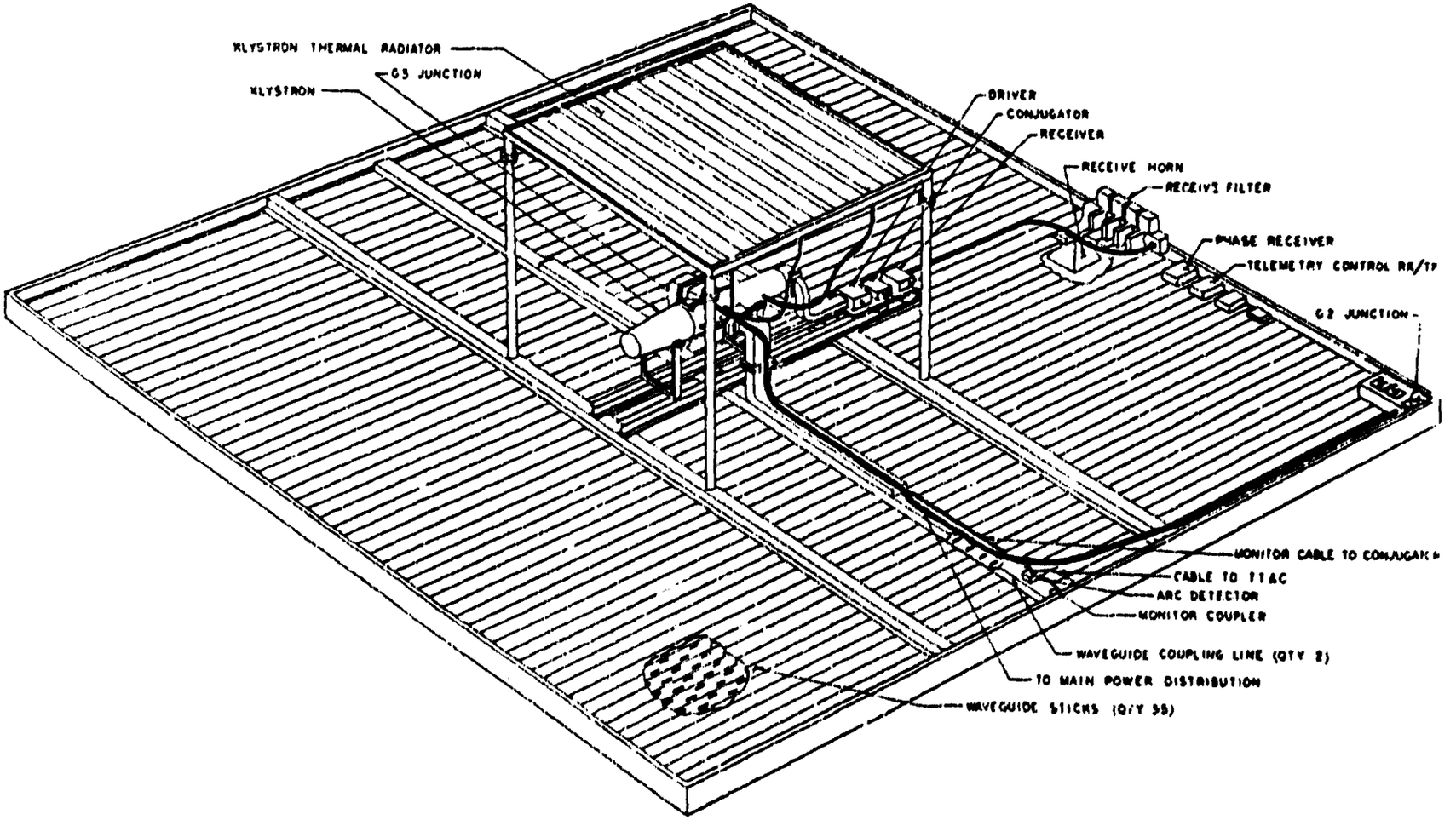

KLYSTRON MODULE THERMAL CONTROL SYSTEM CHARACTERISTICS

Failure analyses also indicated a problem with the heat-pipe-cooled klystron. The difficulty was that the 500°C segment would utilize a mercury vapor heat pipe. In the event of a meteoroid puncture or other leak, the liquid metal would be released into the high voltage environment of the transmitter system and lead to arcing and damage. Plating of liquid metals on insulators might lead to a permanent damage situation that would require repair and replacement. Vought Corporation examined a circulating fluid cooling option and found that a mass reduction was possible and that fluids could be selected that would minimize risk of arcing. Their analysis indicates that a circulating fluid system can be made as reliable as the heat pipe system and certainly more reliable than the expected lifetime of the klystron themselves. The facing page shows principal features of the circulating fluid system for the klystron cooling circuit.

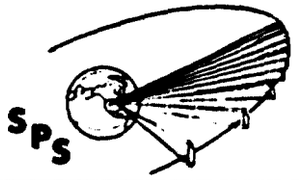

Klystron Module Thermal Control System Characteristics

BOEING

VOUGHT CORPORATION

	500°C	300°C
MATERIAL	COPPER	COPPER
FLUID	STEAM @ 20 ATM	DOWTHERM–A
INLET TEMP	477°C	277°C
OUTLET TEMP	413°C	260°C
LENGTH X WIDTH	0.57m x 1.61m	1.04m x 1.61m
TUBE SPACING	3.7 cm	2.84 cm
TUBE DIAMETER	5.6 mm	1.27 mm
TUBE THICKNESS	0.886 mm	0.71 mm
FIN THICKNESS	0.163 mm	0.066 mm
EMISSIVITY	0.8	0.8
ABSORTIVITY	0.3	0.3
TSINK	36.3°C	36.6°C
PUMP EFFY.	0.3	0.3
FIN EFFECTIVENESS	0.894	0.920
AREA	0.91 m^2	1.67 m^2
MASS/MODULE	7.95 kg	5.13 kg
CURRENT MASS/MODULE – 13.18 kg PART III MASS/MODULE – 18.88 kg		

ANTENNA WAVEGUIDE MATERIAL

Although the plated composite approach is probably a high risk based on today's knowledge because of potential breaks or delamination of the plating under thermal cycling or high RF power conditions, the cost advantages of a low-coefficient-of-thermal-expansion material are sufficient that development of a suitable such approach for waveguides should be identified as a priority development item for SPS.

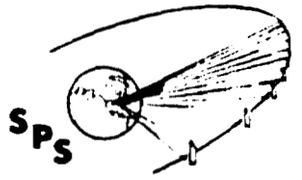

Antenna Waveguide Material

- Low CTE-plated composite detuning loss is 0.2% compared to 1.3% for aluminum.
- Cost of 1% efficiency loss is $75 million per 5-GW SPS.
- Plated composite as high-risk, based on today's knowledge.
- Recommend using low-CTE characteristics for waveguide performance and mass; flag development of suitable material as high-priority research item.

COMPARISON OF LOSSES FOR METAL AND COMPOSITE WAVEGUIDE

Included in the analysis of aluminum structural options was the analysis of use of aluminum for the waveguides in the transmitting antenna. Aluminum has a high coefficient of thermal expansion compared to the graphite used in the earlier baseline. As a result, due to expected temperature changes, the aluminum waveguides will be significantly detuned resulting in power losses as tabulated on the facing page.

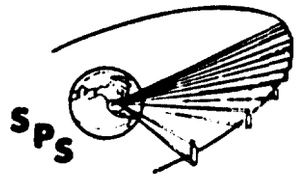

Comparison of Losses for Metal & Composite Waveguide

- AVERAGE STICK = 2.76 METERS
- $\Delta T = 55^{o}C$

	PERCENT POWER LOSS	
	ALUMINUM	COMPOSITE
STICK LENGTH	.67	.02
STICK WIDTH	.42	.12
CROSS GUIDE LENGTH	.17	.02
CROSS GUIDE WIDTH	.11	.03
	1.37%	.19%

COMMENTS ON NOMINAL EFFICIENCY CHAIN - MPTS

The effect on the overall MPTS efficiency is summarized for the case of aluminum waveguide and the baseline tilt requirements. (1 arcmin systematic tilt to control grating lobe levels, and 1 arcmin random tilt to limit total scanning loss to .5%). The additional efficiency reduction due to metal waveguide and failures in the baseline design is (1.18 + 3.8) = 4.98% for the 10 m x 10 m subarray if tilt remains as above. Further refinements in the rectenna subsystem efficiency values are indicated as subject for Phase 2 studies.

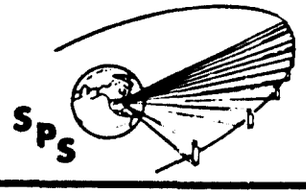

Comments on Nominal Efficiency Chain–MPTS

- CURRENT BUDGET BASED ON COMPOSITE WAVEGUIDE
- SYSTEMATIC TILT 1.75 ARCMIN, NO RANDOM TILT

	EFFICIENCY DEGRADATION	
	10M X 10M	5M X 5M
ALUMINUM WAVEGUIDE	1.18%	1.18%
TILT { 2 ARC MIN SYSTEMATIC, 2 ARC MIN RANDOM }	2.7%	0.5%
RECTENNA	TBD	TBD
FAILURES	3.8%	3.8%
$\Delta\eta$	7.68%	5.48%

FIBER OPTIC CABLE FOR PHASE DISTRIBUTION

The potential advantages of a fiber optic cable for phase distribution are indicated, possibly with the use of a coherent laser emitter or a non-coherent LED emitter. The elements are identified below, with a sample link calculation.

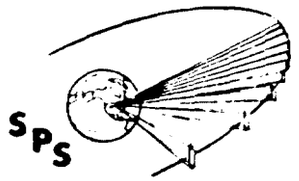

Fiber Optic Design Considerations for SPS Phase Control Distribution

- INCOHERENT LIGHT EMITTING DIODE
  - ONE EMITTER CAN ILLUMINATE BUNDLE OF >100,000 FIBERS
  - REDUNDANT LED EASY TO IMPLEMENT
- MULTIMODE GRADED INDEX FIBER
  - LOSS OF 10 DB/KM COMPATIBLE WITH SPS ($6 PER METER)
  - POTENTIALLY GOOD RADIATION RESISTANCE
  - CABLE BUNDLE ≅ 2.5" FOR DUAL FIBER REDUNDANCY (~200,000 FIBERS)
- SAMPLE LINK CALCULATION

  POWER DIVISION LOSS ≅ 55 db

  FIBER LOSS ≅ 5 db

  FOR 1 mw RADIATED POWER, RECEIVED POWER IS = -60 dbm = 1 nwatt

  AVALANCHE DIODE RECEIVER WILL HAVE S/N > 20 db @ THIS LEVEL FOR 5 MHz BANDWIDTH.

FIBER OPTIC DISTRIBUTION SYSTEM CONCEPT

A potential layout, suitable for accommodating up to 200,000 fibers is indicated, illuminated by a LED or semiconducting (GaAs) laser array of several milliwatts output.

Fiber Optic Distribution System Concept

SPS-2288

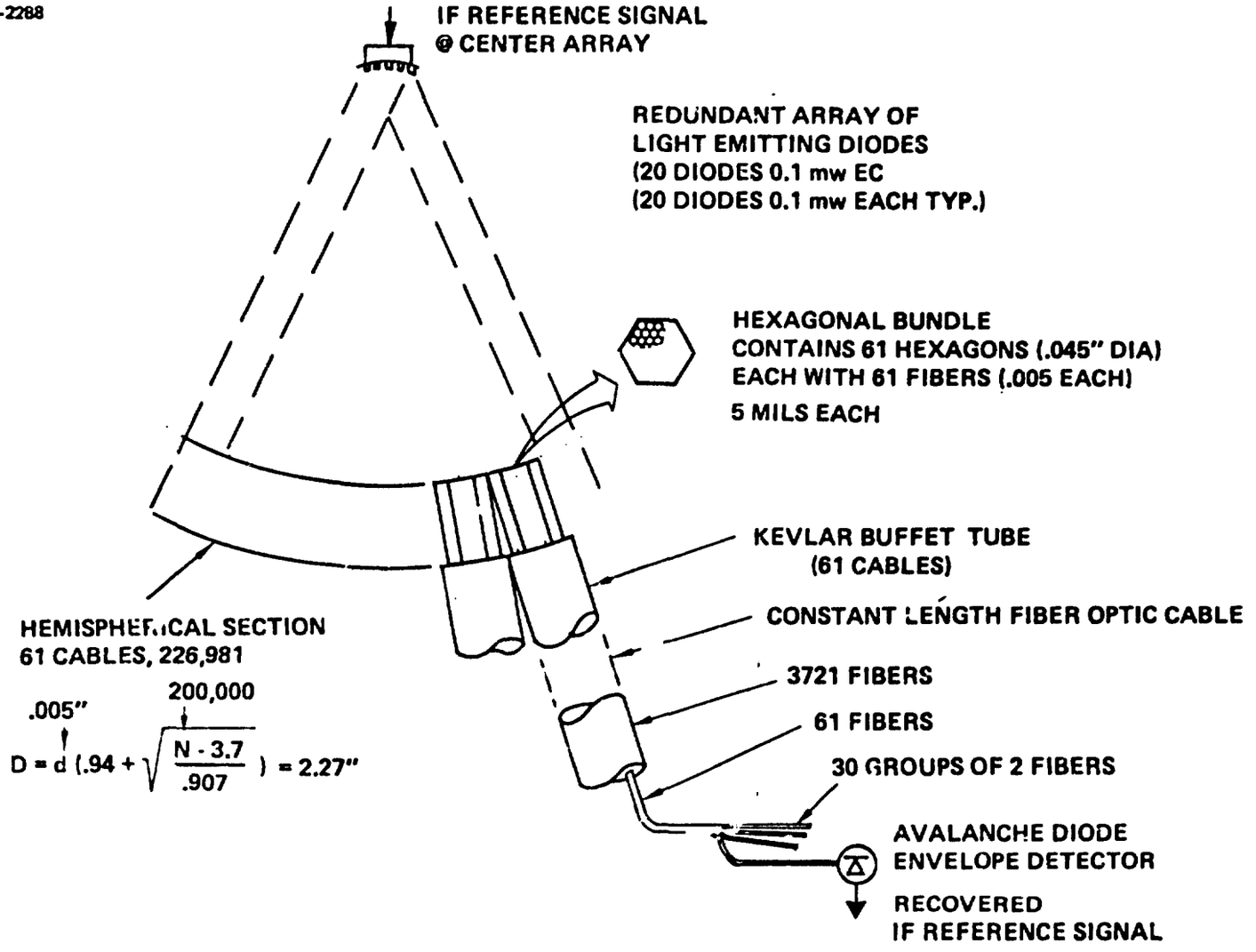

COMPARISON OF COAXIAL AND FIBER OPTIC SYSTEM

A comparison of phase delay for a conventional cable and fiber optic cable indicates a potential reduction in phase chage of nearly 20:1, as well as cabling mass and cost reductions.

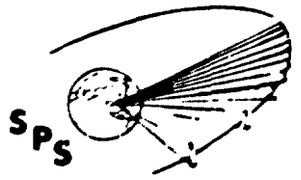

Comparison of Coaxial and Fiber Optic System

	COAXIAL CABLE		OPTICAL FIBER
	RG-58 SOLID DIEL.	LDF-50 FOAM DIEL. (1/2 DIA)	~5 MIL DIA (65 μm ACTIVE CORE)
ATTENUATION db/km (100 MHz)	180 db	35	5
MASS kg/km	43	160	.5
COST $/km	2,000	4,200	1500 (1978)
PHASE DELAY @ f_{IF} = 100 MHz	120°/METER (ϵ=1.0, λ_g=3m)		180°/METER (ϵ=1.5 λ_g=2m)
LINEAR EXPANSION	16.5×10^{-6}/k (COPPER)		5.5×10^{-7}/k (QUARTZ)
PHASE CHANGE FOR ΔT=450°C L=300m	89.1°		4.46°

SOLID STATE DEVICE ASSESSMENT FOR SPS

Progress in Part 4, Phase I, emphasized areas dealing with:

- Device Assessment
  - GaAs FET
  - Switched Mode
  - Initial Noise Analysis
- Power Module Concept
  - Strip Line Cavity Radiator
  - Low Loss Combiner
  - 3-Stage Amplifier Design
- SPS Integration
  - Subarray Layout
  - SPS Sizing Trade Study
  - Power Conditioning Initiated
  - Initial Reliability Assessment

Solid State Power Amplifier

FINDINGS

- IDENTIFIED A PRACTICAL ELEMENT/SUBARRAY DESIGN APPROACH
- SOLID STATE TRANSMITTER IS A MASS/AREA SYSTEM RATHER THAN A MASS/POWER SYSTEM
- GaAs FET'S HAVE ADEQUATE PERFORMANCE—80% EFFICIENCY IS A REASONABLE EXPECTATION
- EFFICIENCY AND THERMAL CAPABILITY YIELD A MAXIMUM TRANSMITTER RATING OF ROUGHLY 2.5 GW GROUND OUTPUT AT 1.4 km DIA.
- EXPECT SIGNIFICANT RELIABILITY ADVANTAGE

ISSUES

- ELIMINATION OF POWER PROCESSING
- EXPERIMENTAL MEASUREMENT OF INTEGRATED DEVICE/CIRCUIT/ RADIATOR PERFORMANCE: EFFICIENCY, GAIN, NOISE, HARMONICS
- DEVICE COST (NOW ≈ $100/WATT IN LOTS OF 100)

SOLID STATE CW POWER STATUS

The device selection of a GaAs Field Effect Transistor (FET) was based on a thorough review of the state of the art of various solid state devices, discussions with NASA-JSC, RCA, and other industries. The power level of 5 watts per device is considered realistic for the SPS time frame

Solid State CW Power Status–1978

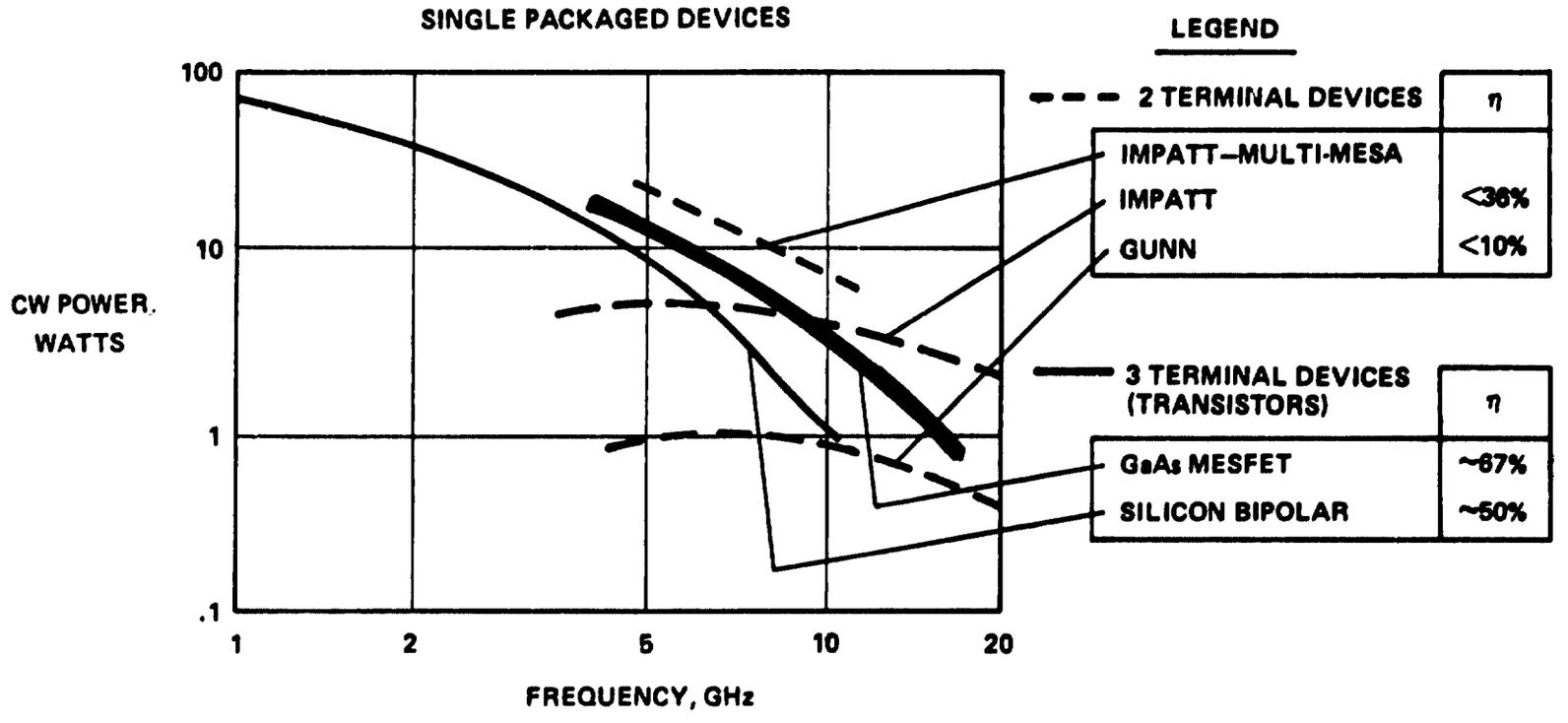

SWITCHING AMPLIFIER STATUS

To achieve efficiencies in excess of 70%, it will be necessary to consider the switched mode of operation where efficiencies in excess of 90% were obtained below 100 MHz. The implementation of these techniques at microwave frequencies will have to be accomplished as part of a proposed experimental task.

BOEING SPS

Switching Amplifier Status

78-336

EFFICIENCY: >95% AT 10 MHZ
>90% AT 100 MHZ

ACTIVE DEVICE: CAN USE BIPOLAR TRANSISTOR OR FET

MICROWAVE IMPLEMENTATION

- NEEDS LABORATORY VERIFICATION
- MICROSTRIP WITH COMMERCIAL FET INTO TERMINATION
- MEASURE EFFICIENCY, SPECTRUM, AND SENSITIVITY TO POWER SUPPLY VARIATIONS

SOLID STATE DEVICE LIFETIME

The failure statistics indicated in the attached chart show that at a channel temperature of 135°C, 98% of the devices will still be operating after 30 years. This suggests that a no-maintenance mode of operation may not be unfeasible. Even if a single FET failure in a power module consisting of 8 output FET's (say 4 watts each) constituted a total loss of the entire module (no graceful degradation), the operation of such modules at 125°C would result in 2% loss after 30 years, compatible with SPS failure rate budget.

Solid State Device Lifetime

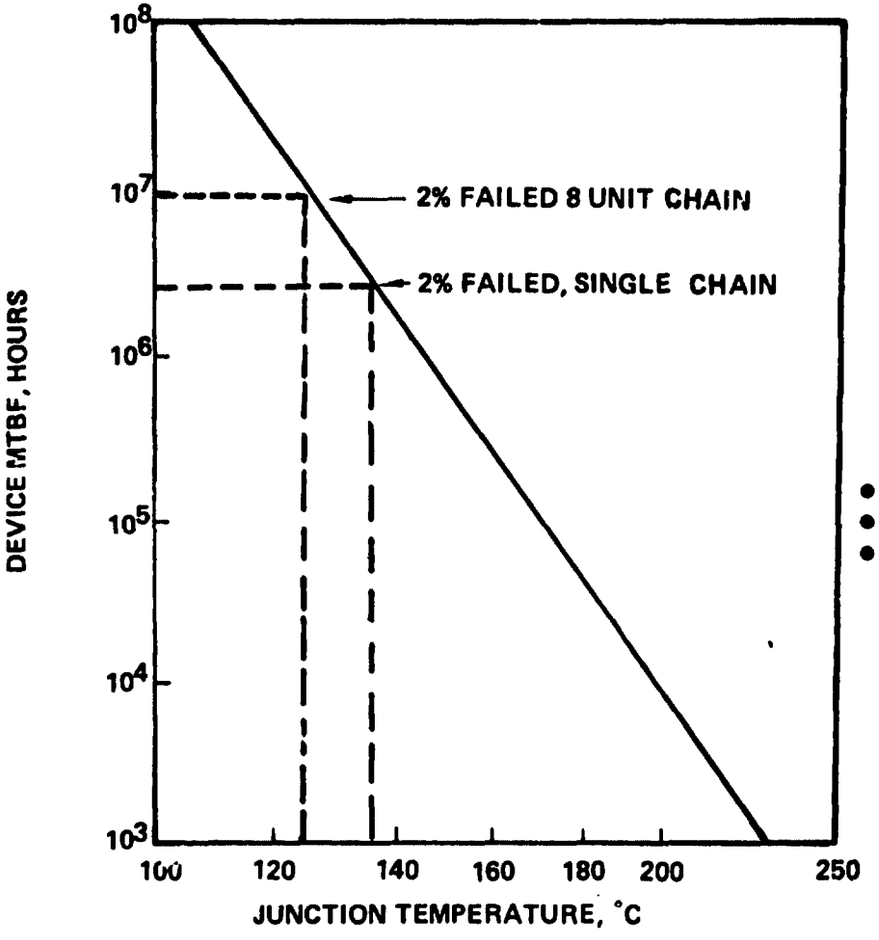

- GaAs FET
- 30 YEAR MAINTENANCE
- LOG NORMAL FAILURE DISTRIBUTION
  $\sigma = 1$

1978 RELIAB. PHYSICS SYMP.

SOLID STATE DEVICE MATURE INDUSTRY COSTING

With a 70% production rate improvement curve (i.e., units produced at the rate of 2n per year cost 70% as much as units produced at the rate of n per year), cost per unit power for GaAs FETS is about the same as the projected cost per unit power for klystrons.

Solid State Device Mature Industry Costing

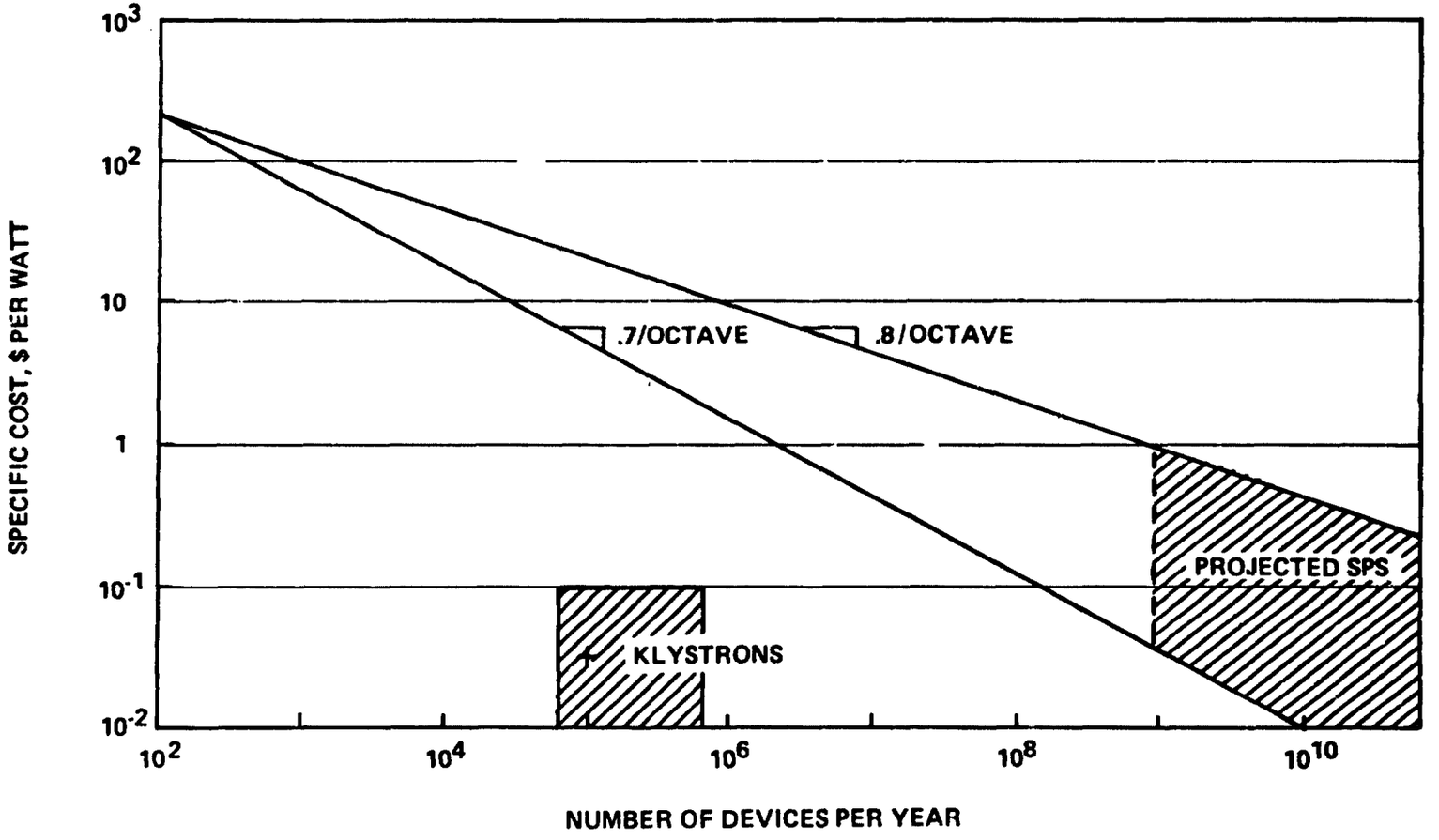

SOLID STATE SUBARRAY LAYOUT

A proprietary module was identified in an associated IR&D program, in which low-loss combining in a cavity type microstrip radiator was achieved. Such a module would use 6 three-stage amplifiers with a 5 watt output stage, totaling 30 watts per module. Further module feasibility tests have been proposed.

A subarray would consist of 144 panels, each panel consisting of 3 strings in parallel, each string consisting of 12 rows in series, and each row of 4 modules in parallel. The subarray would operate at approx. 2 Kv and radiate 622 Kw of r.f. power.

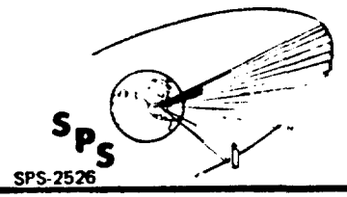

Solid State Subarray Layout

BOEING

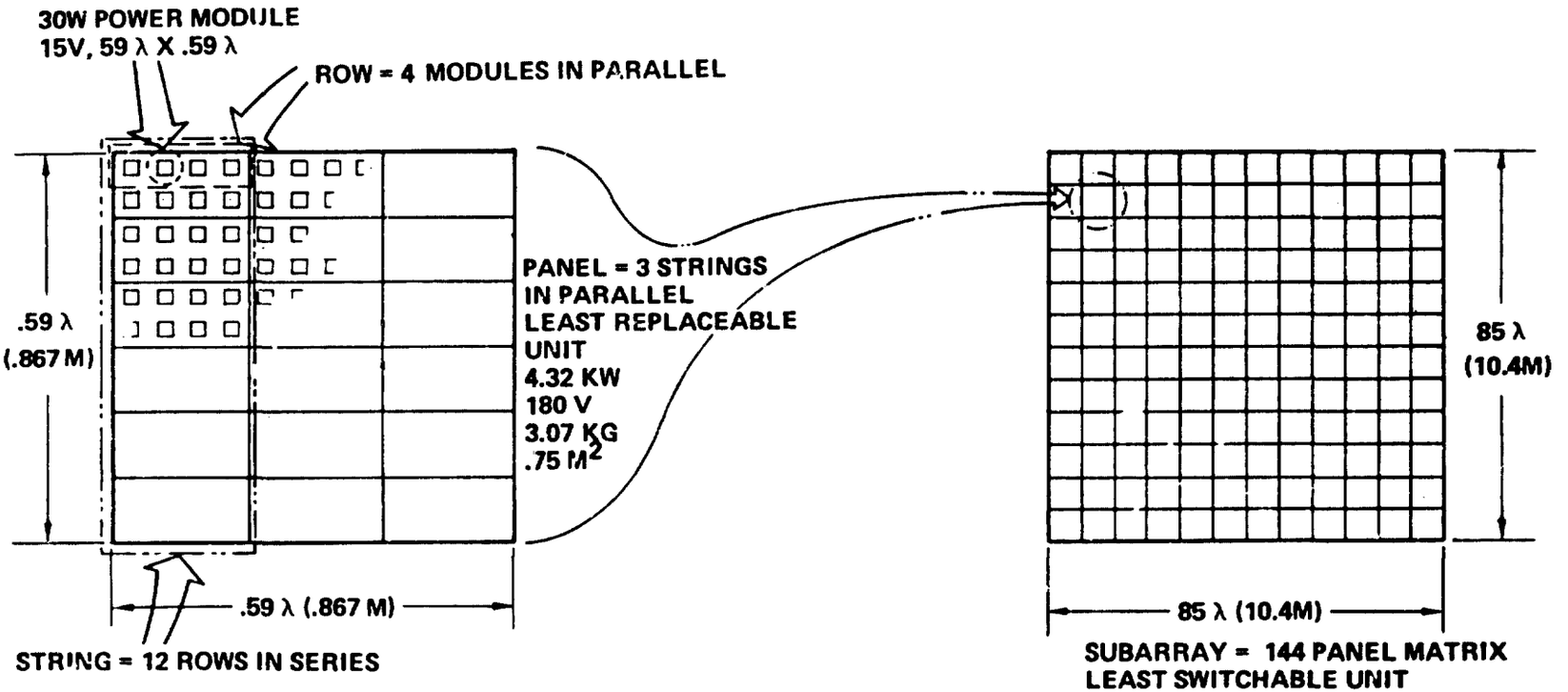

MASS ESTIMATE

COMPONENT	MASS PER UNIT AREA (KGM^{-2})
Al_2O_3 DIELECTRIC	1.99
Al, INCLUDING RADSHIELD	1.39
PHASE FEED AND INTRASUBARRAY STRUCTURE	.70
MPTS SECONDARY STRUCTURE	.72
MPTS PRIMARY STRUCTURE	.07
TOTAL	4.87

SOLAR POWER SATELLITE BEAMING NOMOGRAPH

A nomograph has been developed as a useful design tool to determine potential solid state SPS design parameters. For an 80% efficient GaAs FET and a device temperature of 125°C, a thermal limit of 3-5 Kw r.f. radiated per m^2 is indicated. A nominal design of 2 Gw with a 1.5 km diameter space antenna corresponds to this value, for the ionospheric heating limit of 23 mw/cm^2 and the nominal SPS efficiency chain. Uniform illumination would not be of any advantage in such a design.

Solar Power Satellite Beaming Nomograph

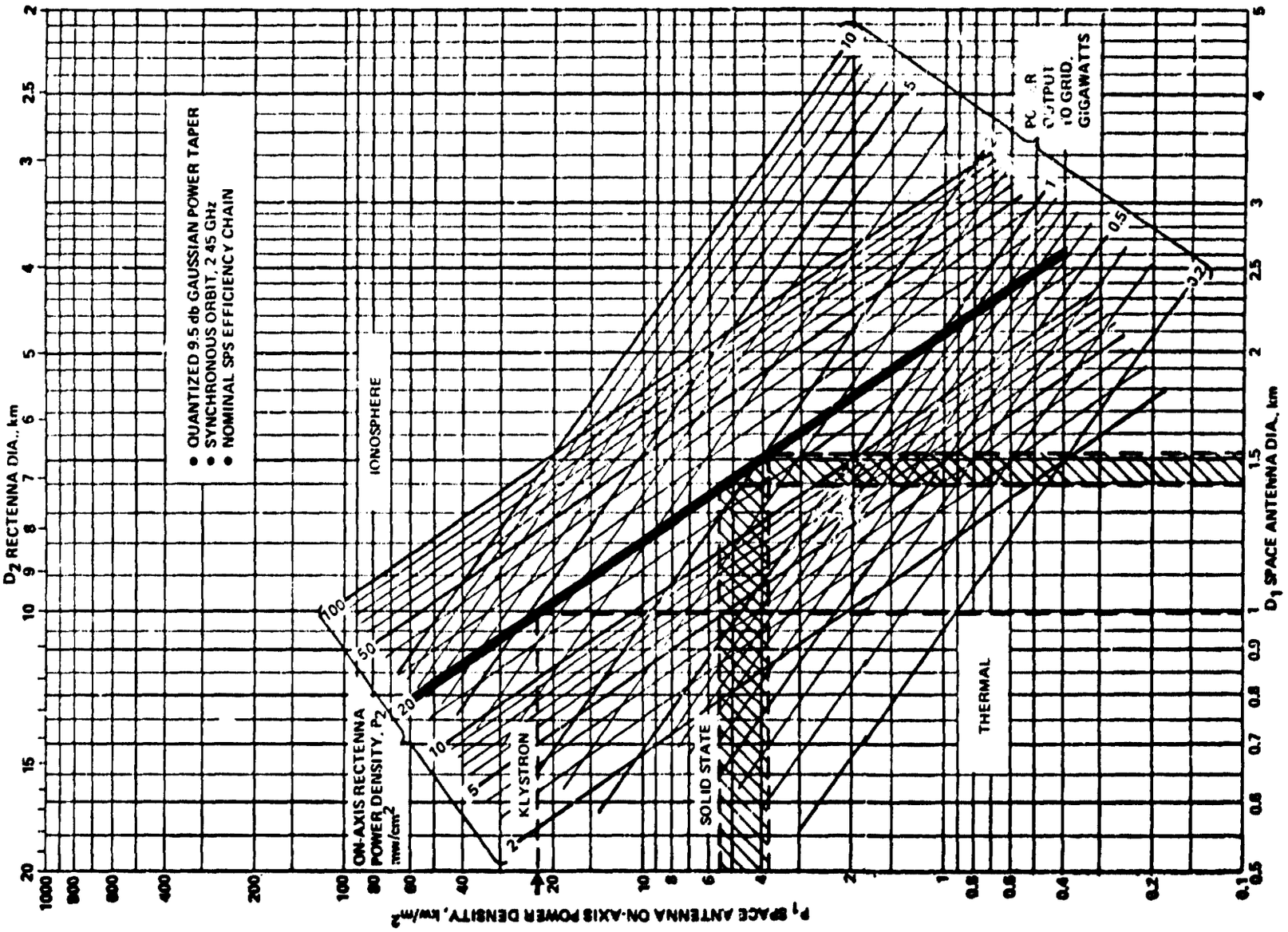

COMPARATIVE CALCULATION OF GROUND NOISE

A preliminary noise analysis near the operating frequency does not indicate a significant advantage for the solid state design, since good oscillators are about at the same level of -160 dBc/Hz as are electron tubes of the klystron type. It is, however, possible to spread this ground noise over a larger area, since the solid state module can be made smaller than a klystron module, and the noise is incoherent (i.e., radiates independently from each module). The attached table shows calculations of the type made by NASA-JSC for the klystron, and indicates a level 14 dB lower for the solid state design for the parameters chosen. Harmonic radiation was not considered in this analysis.

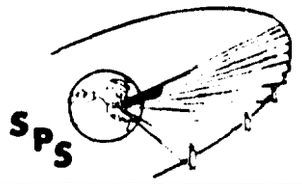

Comparative Calculation of Ground Noise

SOLID STATE

$P_N = 3.5 \times 10^9 \times 10^{-16} = 3.5 \times 10^{-7}$ W/Hz

$G_N = 4\pi AN/\lambda^2 = 308$

N = .5 COHERENCY FACTOR
AREA = $(7\lambda)^2$

NOISE SPECTRAL DENSITY = $P_N G_N / 4\pi R_o^2$

$P' = 7 \times 10^{-21}$ WATTS/m^2/Hz
$= -201.5$ dbw/m^2/Hz

EXTERNAL FILTER
CAN PROVIDE
ADDITIONAL ATTENUATION

KLYSTRON

$P_N = 7 \times 10^9 \times 10^{-16} = 7 \times 10^{-7}$ W/Hz

G_N = 3650 FOR AV. AREA PER KLYSTRON OF 8.7 m^2

$P' = 1.54 \times 10^{-19}$ WATTS/m^2/Mf
$= -187.4$ dbw/m^2/Hz

MULTIPLE CAVITY DESIGN PROVIDES
24db/OCTAVE ATTENUATION

INCOHERENT NOISE POWER DISTRIBUTION

The footprint of the incoherent noise contributions is indicated and compared with that of a klystron module.

Incoherent Noise Power Distribution

SPS-2346

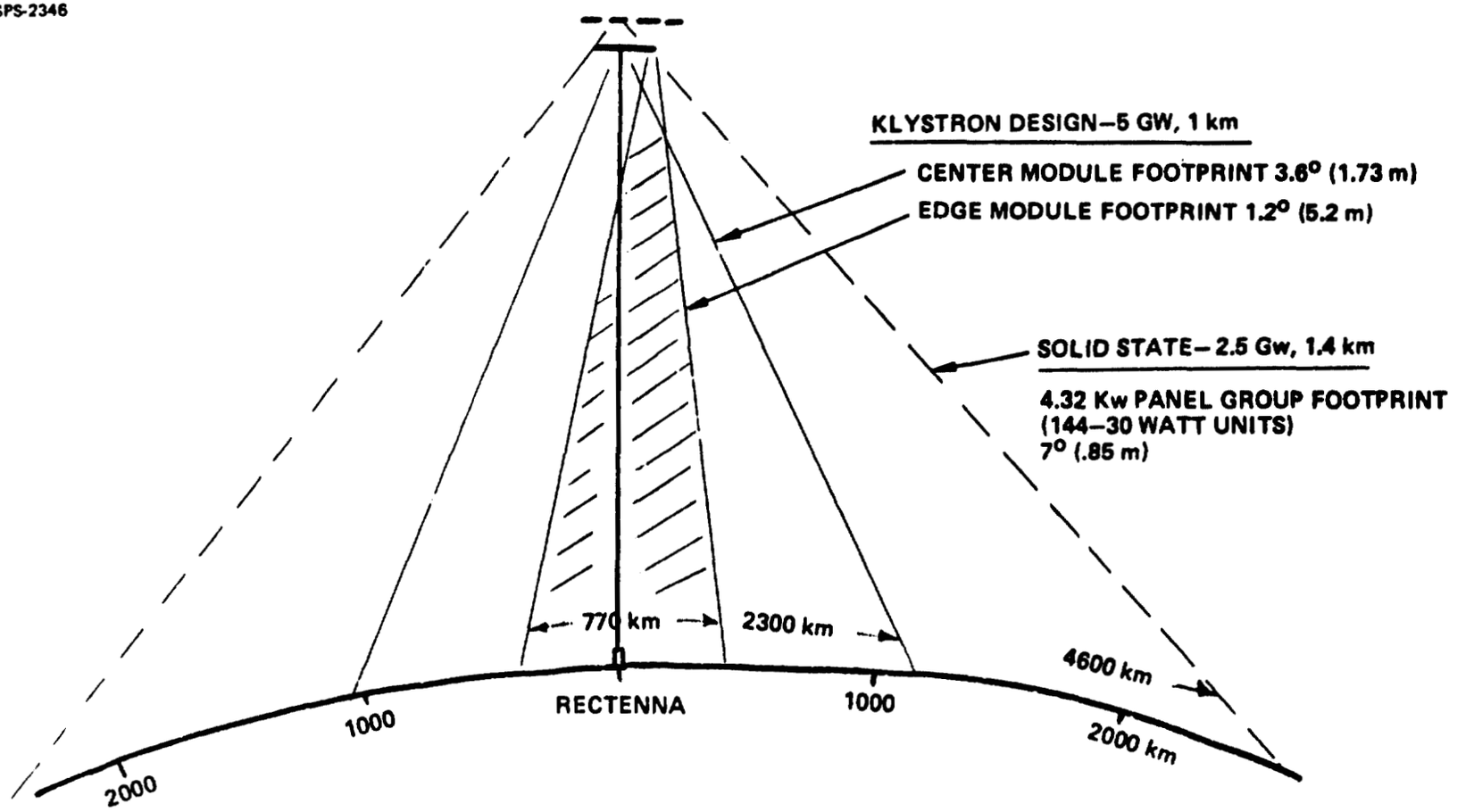

SOLID STATE POWER SUPPLY OPTIONS

Solid state devices suitable for microwave power amplification operate at voltages on the order of 25 volts. Distribution voltages suitable for SPS application range from 20,000 to 40,000 volts. If it were necessary to process all this power down to a voltage of 25 volts, the cost and efficiency of power processing combined with the I^2R losses and conductor mass for such operations might be prohibitive. Therefore, an approach to elimination of power processing is highly desirable and constitutes the first option identified, Direct High Voltage DC (DHV DC). An aspect of this approach is series-parallel connection of the microwave power amplifiers (as regards DC power supply) similar to that used for solar cells in generation of the DC power. Aggregate sets of microwave power generators can then be supplied at comparatively high distribution voltages. This option raises concerns regarding stability, matching, and balance of the power supply and control network.

The minimum risk option is use of DC/DC converters but this will result in significantly greater SPS mass and cost.

AC power distribution may provide a means of minimizing distribution losses and reducing solar array voltage. Mass and cost penalties will be similar to those for full DC/DC processing.

Solid State Power Supply Options

BOEING

SPS-2542

- DIRECT HIGH VOLTAGE DC
  - REQUIRES SUBARRAYS IN SERIES
    - CONNECTION TOPOLOGY A PROBLEM
  - HIGH E-FIELDS NEAR ADJACENT SUBARRAYS
    - MAY CAUSE ARCS, WILL SUSTAIN THEM

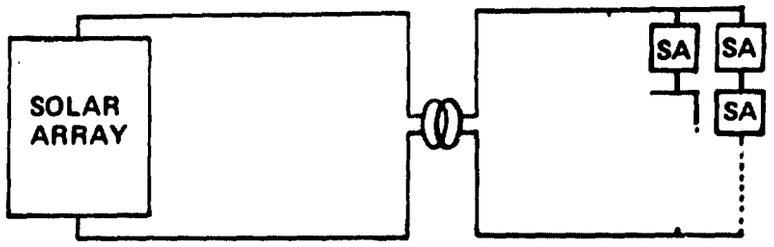

- DC-DC CONVERSION ON MPTS
  - PERFORMANCE PENALTIES
    - DC-DC CONVERTERS ≈ 1kg/kw
    - POWER LOSSES IN CONVERTERS
  - SERIES/PARALLEL CONNECTIONS WITHIN SUBARRAYS STILL REQUIRED

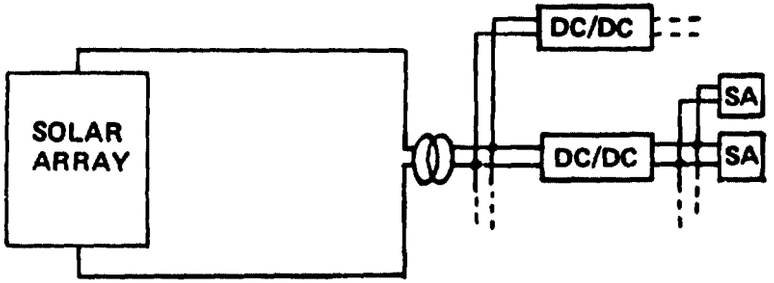

- AC POWER DISTRIBUTION
  - CONVERT
    - DC/AC ON SOLAR ARRAY
    - AC/DC AT SUBARRAY
  - REQUIRES S/P TO SOME EXTENT ON SUBARRAY

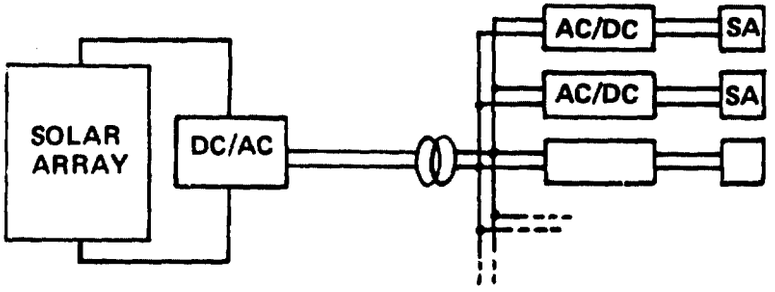

SERIES - PARALLEL INTERCONNECTION

RELIABILITY ASPECTS

The assumptions for an initial reliability analysis are stated and concerns dealing with AC transients and stability are defined for further effort.

Series -Parallel Interconnection Reliability Aspects

- Direct current reliability
  - Single or double failures must not take system down
  - Adequate reliability if devices can take 20% overvoltage
- Turn-on transients
  - Strings of panels like transmission line
  - No problem with $\tau > 10^{-6}$ s
- Alternating current stability
  - Oscillations due to coupling between modules
  - Suppress via damping

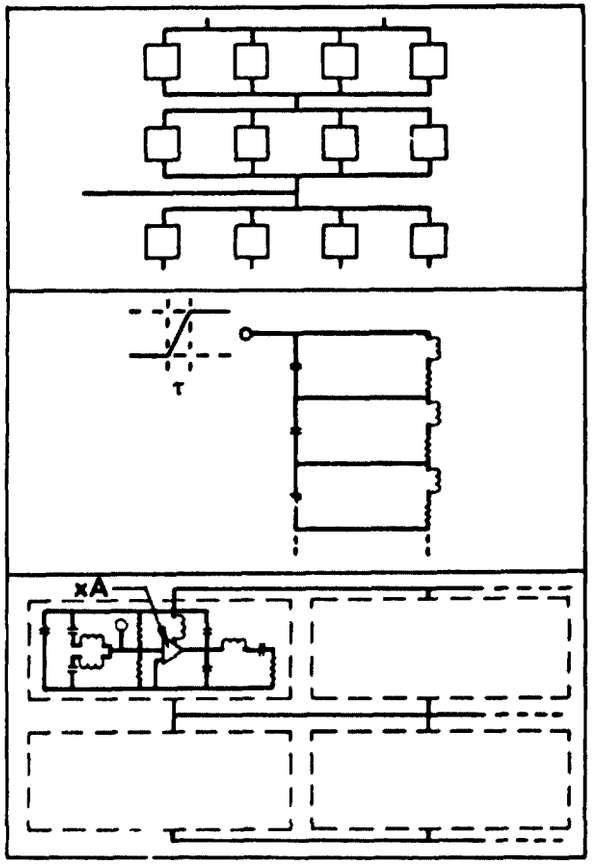

STRING RELIABILITY ANALYSIS CONFIGURATION

The string configuration is defined for the reliability analysis as consisting of 96 amplifiers, in 12 rows of 4 modules, where each module has 2 output amplifiers, each with3 output devices.

String Reliability Analysis Configuration

SPS-2553

SERIES STRINGS OF 12 ROWS
- 4 MODULES PER ROW
- 2 AMPLIFIERS PER MODULE

SINGLE AMPLIFIER FAILURE PROBABILITY = F_P

IF > N AMPLIFIERS PER ROW FAIL STRING GOES DOWN

DESIRED RESULT IS STRING FAILURE PROBABILITY, F_S,
AS A FUNCTION OF F_P AND N

REWORK DESIGN UNTIL $F_S \ll F_P$

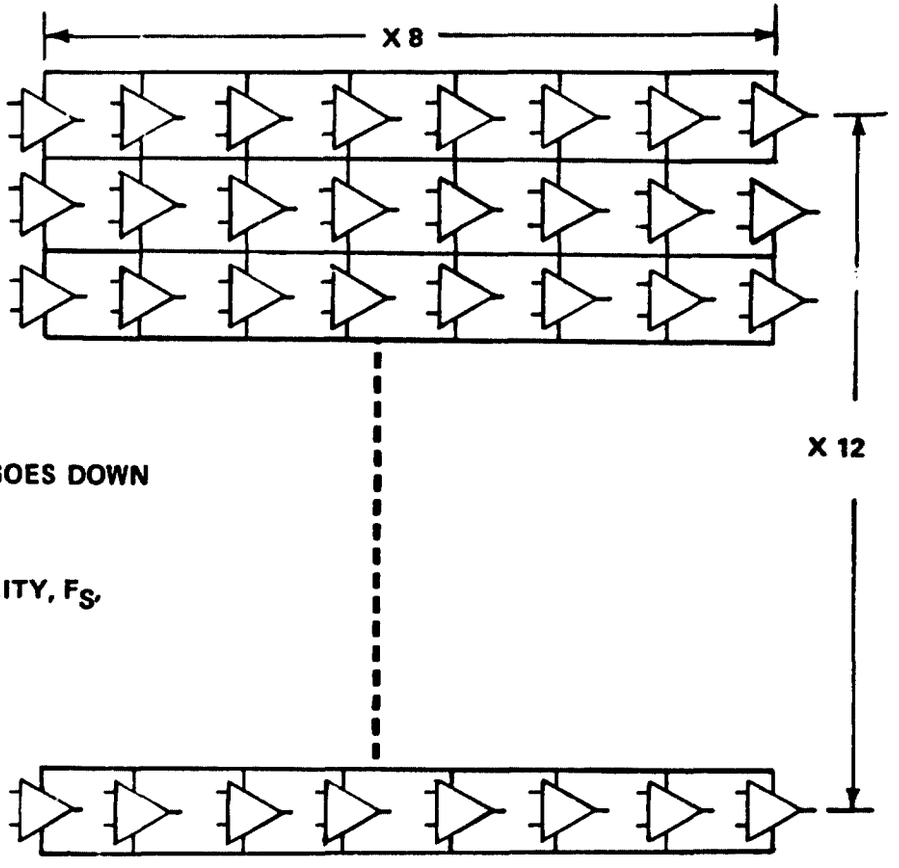

SERIES - PARALLEL STRING FAILURE

The initial results of the reliability analysis indicate that, for the case where 2 amplifiers per row may fail and still maintain an acceptable overvoltage, the string failure rate can be made much lower than the amplifier failure rate for cases where the amplifier is highly reliable. For example, the probability of string failure is 10X lower than amplifier failure at $F_p \cong 04$. This will be even more dramatic for lower F_p's.

Series–Parallel String Failure

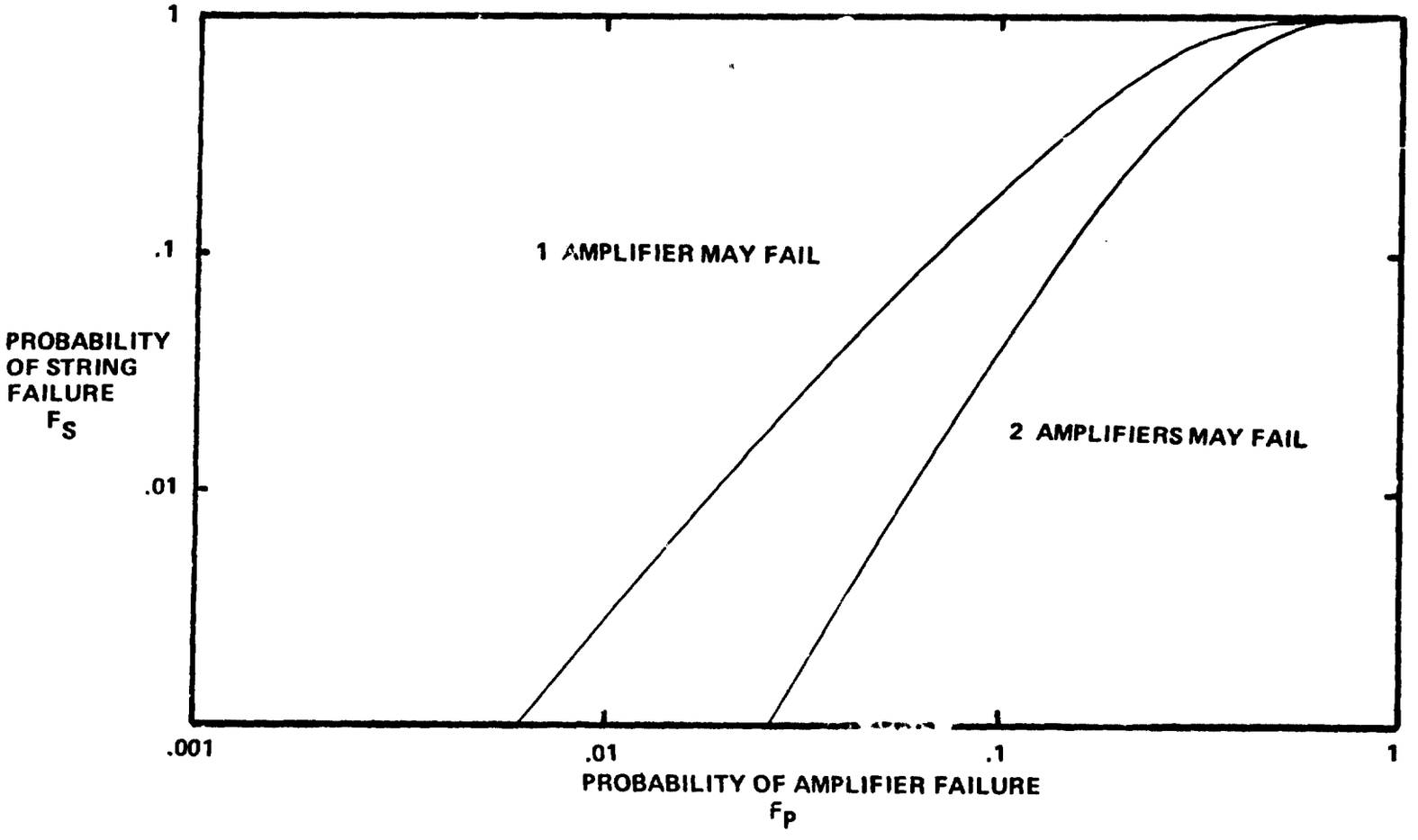

SERIES - PARALLEL UNIT RESPONSES (PRELIMINARY)

Further progress in the reliability analysis is contingent upon understanding of how overvoltages/ overcurrents in a string are to be managed. The matrix chart illustrates some options which are currently being investigated and are subject for further studies in Phase 2.

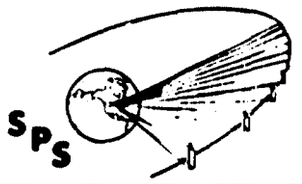

Series – Parallel Unit Responses (Preliminary)

	MODULE	ROW	STRING	PANEL	SUBARRAY
UNDERVOLTAGE	NO RESPONSE	NO RESPONSE	NO RESPONSE	NO RESPONSE	NO RESPONSE
OVERVOLTAGE	NO RESPONSE	OPEN ON 1.2X LOAD ON 1.05X	NO RESPONSE	OPEN AND LOAD ON 1.2X	OPEN AND LOAD ON 1.15X
CURRENT LOW	NO RESPONSE	NO RESPONSE	NO RESPONSE	NO RESPONSE	NO RESPONSE
EXCESSIVE CURRENT	FUSE ON 3X	NO RESPONSE	FUSE ON 2X OPEN ON 1.5X LOAD ON 1.4X	OPEN ON 1.5X	OPEN ON 1.5X

ALL FAILURES SHOULD BECOME OPEN OR SOFT

TURN-ON TRANSIENTS

It has been ascertained by the use of a small computer program, that turn-on transients will not be troublesome, provided turn-on times of $>10^{-6}$ seconds are used.

The assumed unbalanced reactance $C^* = 2C$ and values of R, L, C selected are estimates considered representative of current knowledge of the solid state module.

Turn-On Transients

- CONSIDER STRINGS OF AMPLIFIERS AS RLC NETWORK
  4 MODULE STRING, V_o = 60 V

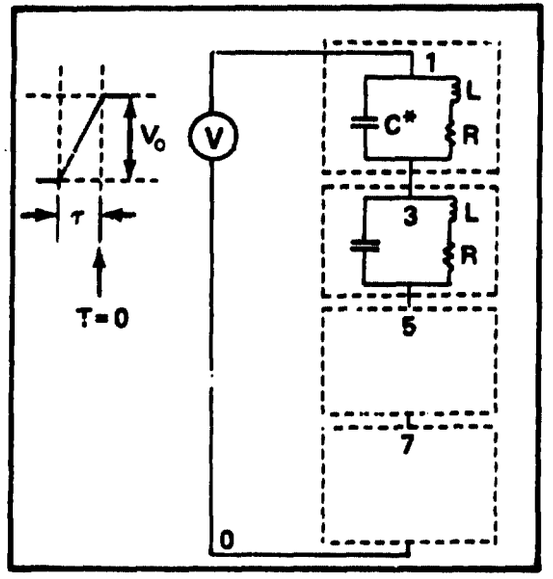

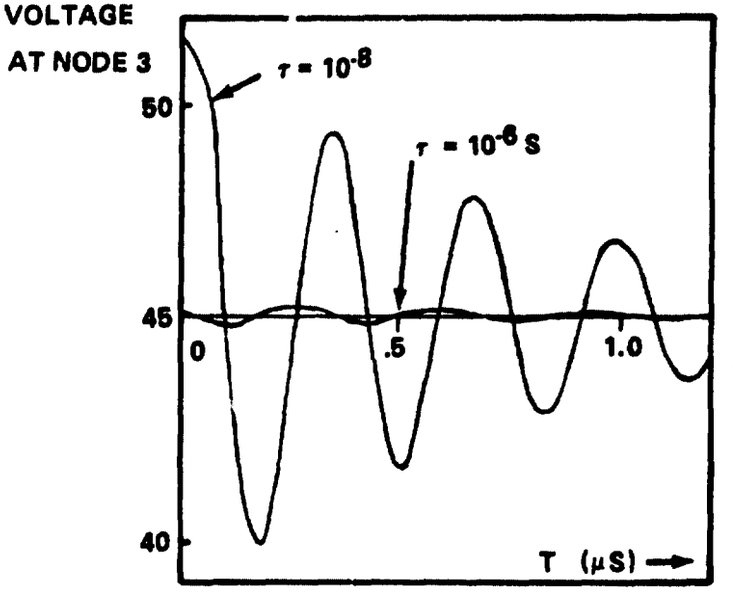

- ROUGH ESTIMATES FOR SOLID STATE MODULES
  ARE C = 500 PF, L = 3μ H, R = 7.5 Ω.

- IF REACTACES ARE UNBALANCED (FOR INSTANCE, IF C = 2C) AND TURNON IS FAST ($\tau = 10^{-8}$ s) RINGING AT SEVERAL MHZ OCCURS. SLOWER TURN-ON TIMES ($\tau = 10^{-6}$ s) LARGELY ELIMINATE THIS PROBLEM.
- SINCE L/R >> $\sqrt{L(C^* - C)}$ MAXIMUM VOLTAGE ACROSS R DOES NOT EXCEED NOMINAL.
- HOWEVER, RINGING MODULATES VOLTAGES ON WAY UP TO FULL VOLTAGE. MAY CAUSE SIDEBANDS DURING TURNON.

REPRESENTATIVE SOLID STATE SPS COSTS AND SIZING

The solid state transmitter is limited by maximum allowable device temperature to a thermal dissipation of roughly 1.5 kilowatts per square meter. At a conversion efficiency of 80% with a 10 dB Gaussian taper, the thermal constraints and ionosphere power density constraints follow characteristics curves as illustrated on this map of SPS power cost indicators versus transmitter diameter and power level. As can be seen, the solid state system is constrained to a total power level of approximately 2½ gigawatts with a transmitter aperture of 1.4 kilometers. Thus, this system is well-suited to the smaller size lower power SPS application and, in fact, may be limited to such lower power transmitter links.

Representative Solid State SPS Costs and Sizing

SPS-2345

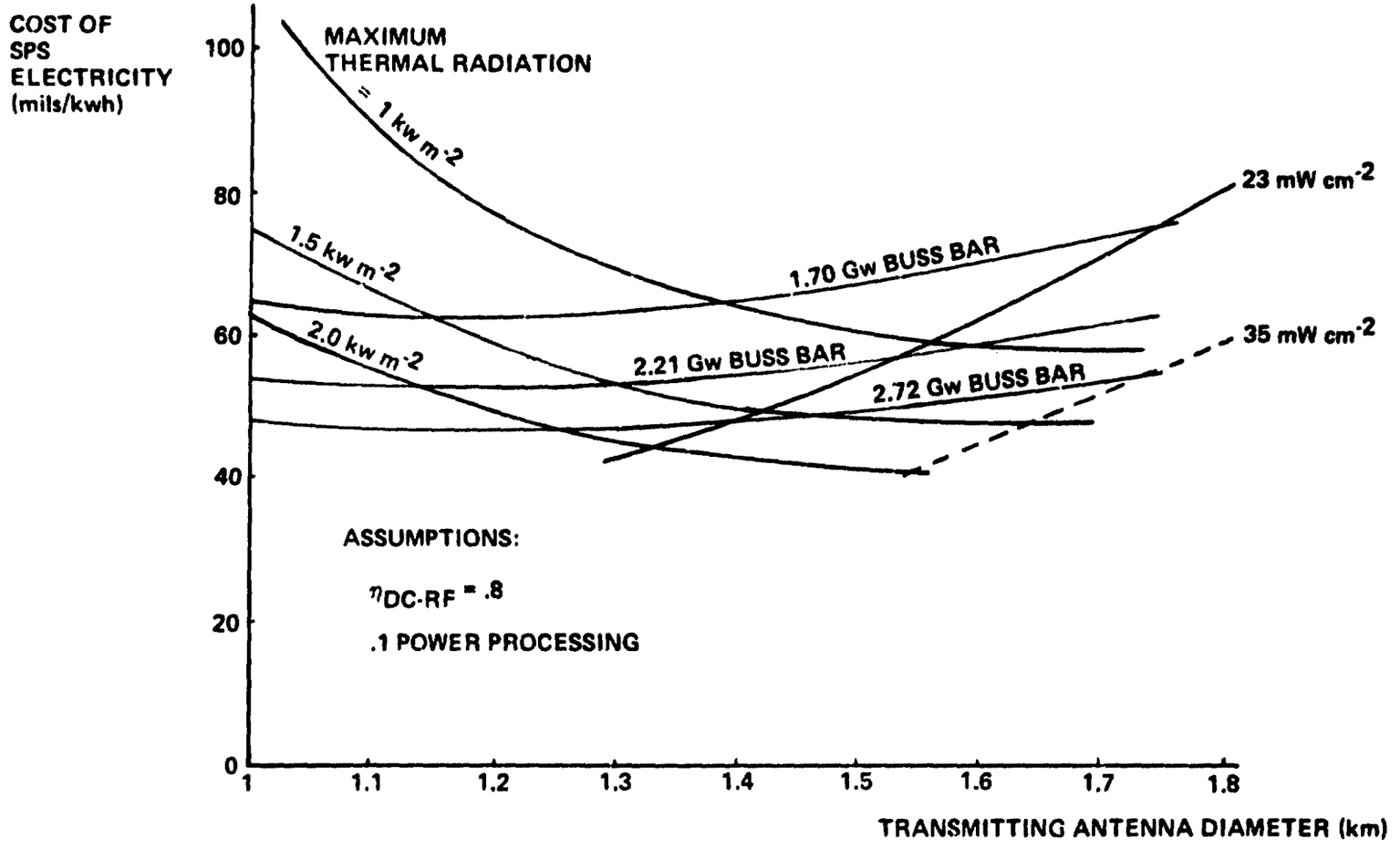

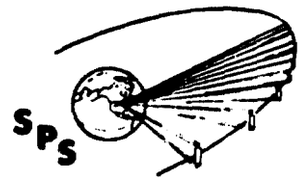

MPTS Phase II Recommendations

- PHASE CONTROL
  - OPTIMUM SUBARRAY SIZE
  - FIRM UP DISTRIBUTION TREE
  - REFINE FAILURE ANALYSIS
  - LABORATORY FEASIBILITY
    - FIBER OPTIC DEMONSTRATION
    - WAVEGUIDE STICK TESTS
  - DEVELOP "MODMAIN" COMPUTER SIMULATION
- SOLID STATE
  - INTEGRATE POWER MODULE INTO SPS DESIGN
    - STRUCTURAL INTERFACE
  - COMPLETE DEVELOPMENT PLAN
    - ALTERNATE CIRCUIT/RADIATOR CONCEPTS
    - LIGHTWEIGHT SUBSTRATE
    - RELIABILITY OF INTERCONNECTION METHODS
- RECTENNA
  - DEFINE RF COLLECTION CIRCUIT CRITERIA
    - SELECT BEST OPTION
  - DEFINE COLLECTION EFFICIENCY CHAIN
    - COMPLETE FAILURE MODE ANALYSIS
  - IMPROVED DEVELOPMENT PLAN

GENERAL ELECTRIC

PART 4 - PHASE 1 PRESENTATION

space division

- SPACE ANTENNA
  - DC POWER DISTRIBUTION AND RF PHASE CONTROL LAYOUT
  - PHASE CONTROL SYSTEM FAILURE MODES AND EFFECTS ANALYSIS
  - PHASE DISTRIBUTION SYSTEM MAINTENANCE ANALYSIS
- RECTENNA SYSTEM
  - ANTENNA LAYOUT
  - POWER CONDITIONING LAYOUT
  - FAILURE MODES AND EFFECTS ANALYSIS
  - MAINTENANCE ANALYSIS

SPACE ANTENNA DC POWER DISTRIBUTION AND RF REFERENCE PHASE DISTRIBUTION SYSTEM

The conceptual mechanical layout of the DC power distribution and RF reference phase distribution was developed during the Part IV, Phase 1 Study. The summary displays some of the most important results.

GENERAL ELECTRIC

SPACE ANTENNA DC POWER DISTRIBUTION AND RF REFERENCE PHASE DISTRIBUTION SYSTEM

space division

SUMMARY

- DC DISTRIBUTION IS USING 228 MAIN SECTO' LINES AND AN AVERAGE OF 446 KLYSTRON LINES ATTACHED TO EACH SECTOR LINE.
- DC TO DC CONVERTERS MUST BE REDUNDANT FOR ACCEPTABLE DC POWER AVAILABILITY.
- FOUR LAYER REFERENCE PHASE DISTRIBUTION NETWORK IS USED WITH 20, 19 AND 19 BRANCHES AT THE CONSECUTIVE NODES (SECTOR, GROUP, SUBARRAY, KLYSTRON). THE POWER DIVISION AT THE LAST (KLYSTRON) LEVEL IS DETERMINED BY THE NUMBER OF KLYSTRONS PER SUBARRAY.
- THE PHASE DISTRIBUTION AND CONJUGATION PROCESS IS COMPLETELY SEPARATED.
- TRIPLE REDUNDANCY IS USED IN THE FIRST AND DOUBLE REDUNDANCY IN THE SECOND LAYER OF THE PHASE DISTRIBUTION TREE.
- THE ELECTRONIC CIRCUIT CONCEPT IS AS PER RECOMMENDATIONS OF THE LINCON REPORT.

DISTRIBUTION OF DC SECTOR LINES FOR THE SPACE ANTENNA

A total of 228 main DC lines enters into the space antenna each carrying about 35 MW power. On the average 11.4 lines serve an 18° wide pie sector of the aperture.

GENERAL ELECTRIC

DISTRIBUTION OF DC SECTOR LINES FOR THE SPACE ANTENNA

space division

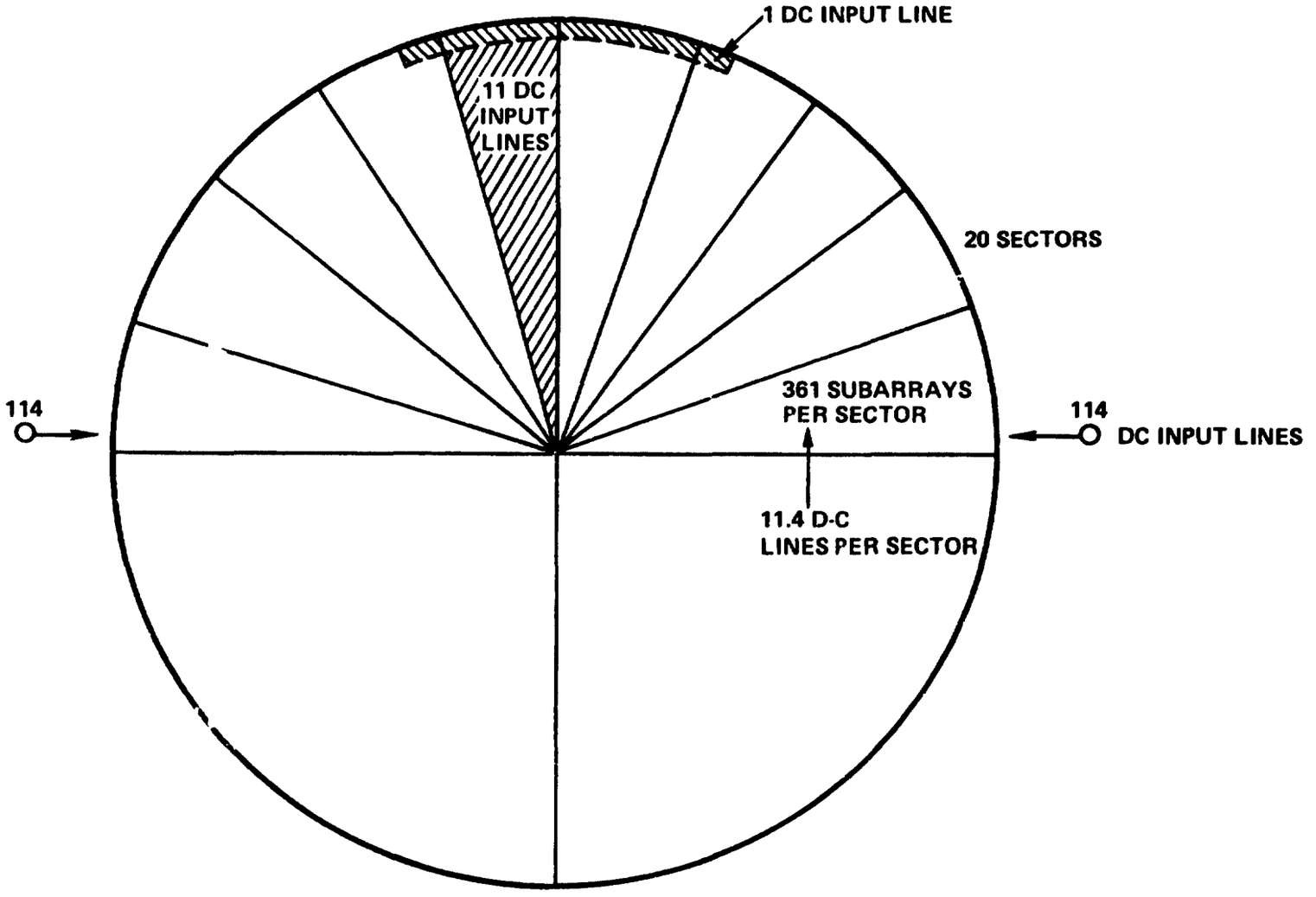

DISTRIBUTION OF DC SECTOR LINES WITHIN 1 OF 20 SECTORS

The DC sector lines and their J_1 end junctions within a typical sector of the space antenna are distributed in such a manner that the density of the junctions correspond to the density of the klystrons over the antenna area. On the average a main DC line serves 31.67 subarrays or 446 klystrons.

GENERAL ELECTRIC

DISTRIBUTION OF DC SECTOR LINES WITHIN 1 OF 20 SECTORS

space division

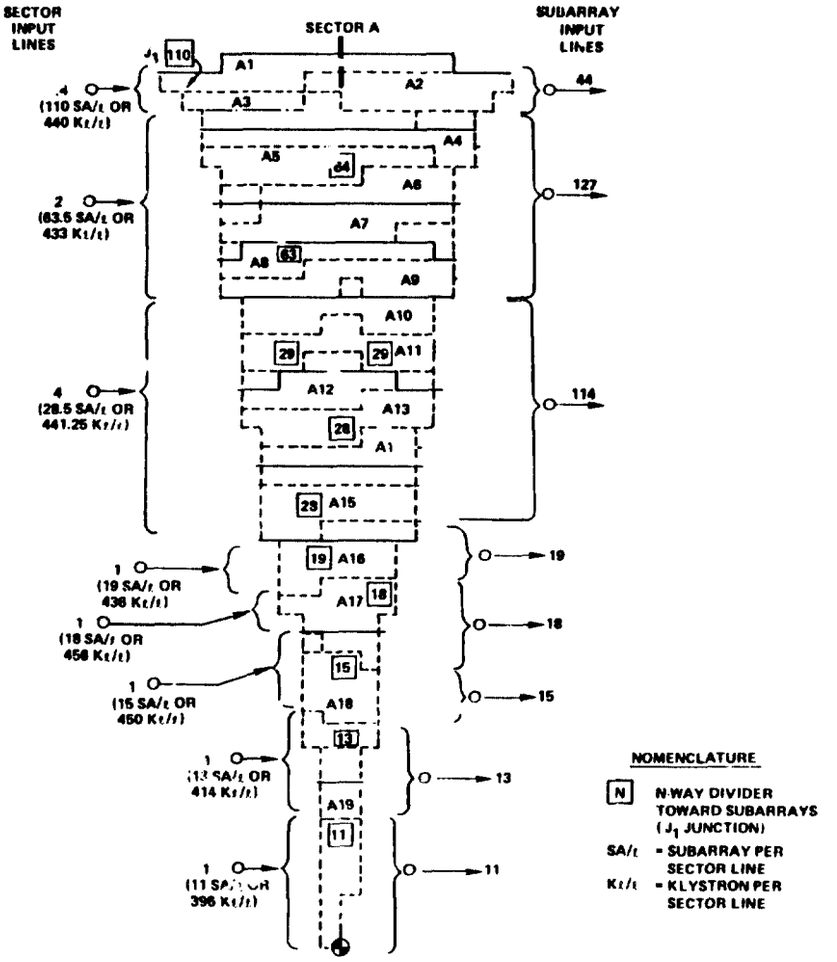

DISTRIBUTION OF DC SUBARRAY (KLYSTRON) LINES WITHIN A TYPICAL (OUTER) PART OF A SECTOR

At the J_1 junction about 16.2% of the power goes through a redundant DC to DC converter. Both the processed and unprocessed power then is divided into subarrays or directly to klystrons. The figure shows this lower level of distribution system covering the A_1, A_2, A_3 and part of A_4 group subarrays in the outer region of a typical sector.

GENERAL ELECTRIC

DISTRIBUTION OF DC SUBARRAY (KLYSTRON) LINES WITHIN A TYPICAL (OUTER) PART OF A SECTOR

space division

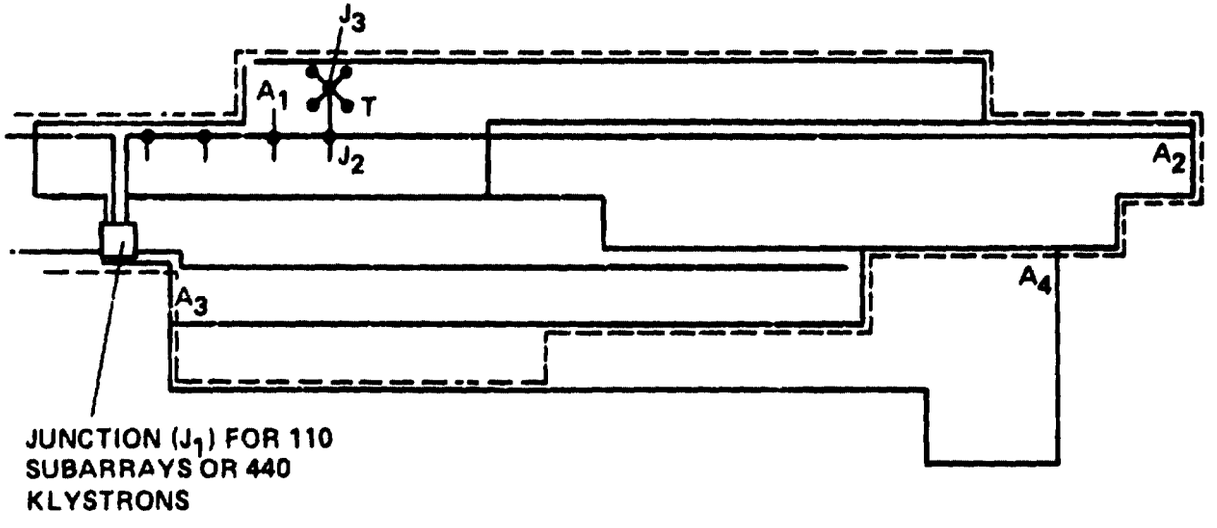

LAYOUT OF THE TEN DIFFERENT TYPES OF SUBARRAYS, SHOWING
KLYSTRON PHASE REPEATER LOCATIONS AND WAVEGUIDE STICK SIZES

The figure shows the ten different types of subarray layouts, the locations of klystrons and the best reference phase distribution power dividers. Only two types of slotted waveguide radiators (sticks) are used in the system.

GENERAL ELECTRIC

LAYOUT OF THE TEN DIFFERENT TYPES OF SUBARRAYS, SHOWING KLYSTRON PHASE REPEATER LOCATIONS AND WAVEGUIDE STICK SIZES

space division

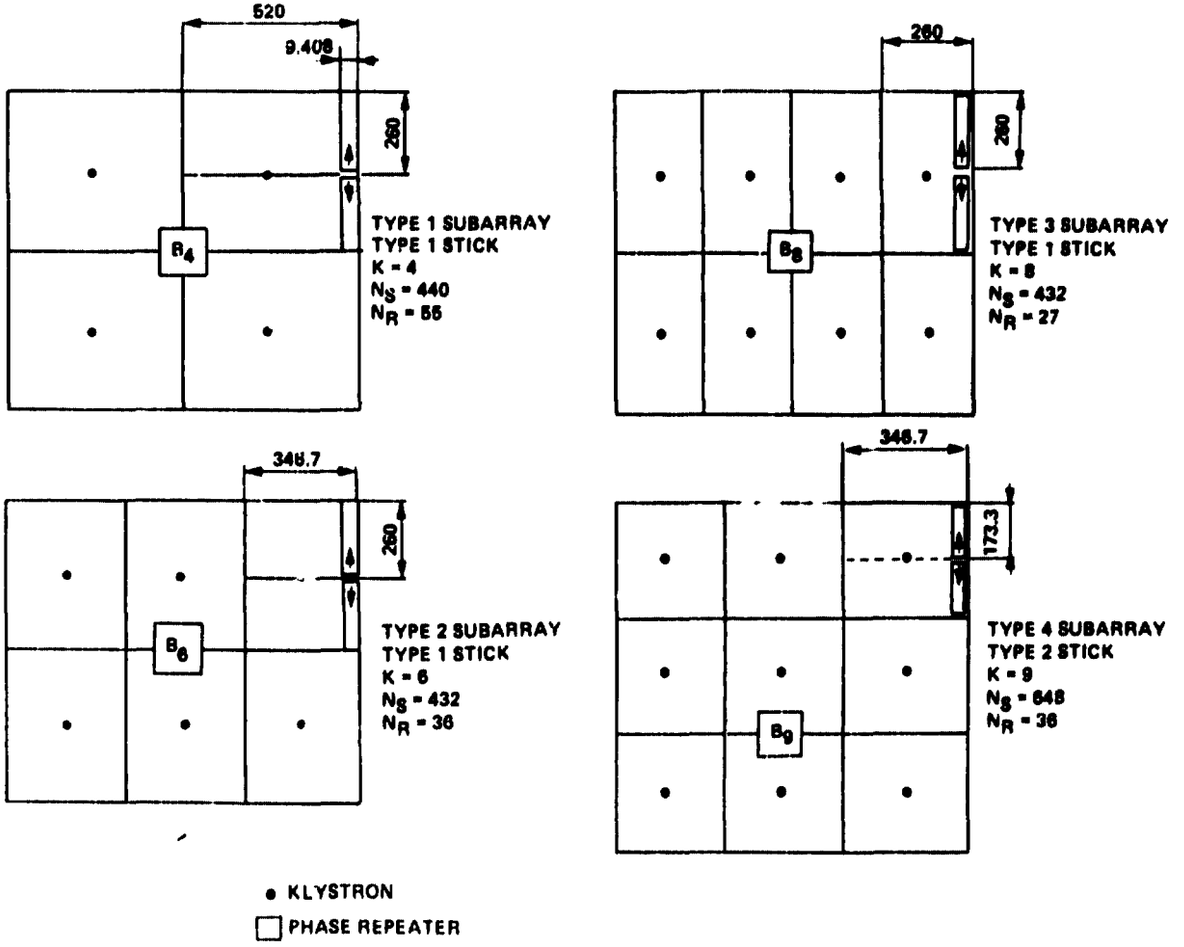

GENERAL ELECTRIC

LAYOUT OF THE TEN DIFFERENT TYPES OF SUBARRAYS, SHOWING KLYSTRON PHASE REPEATER LOCATIONS AND WAVEGUIDE STICK SIZES (Cont'd)

space division

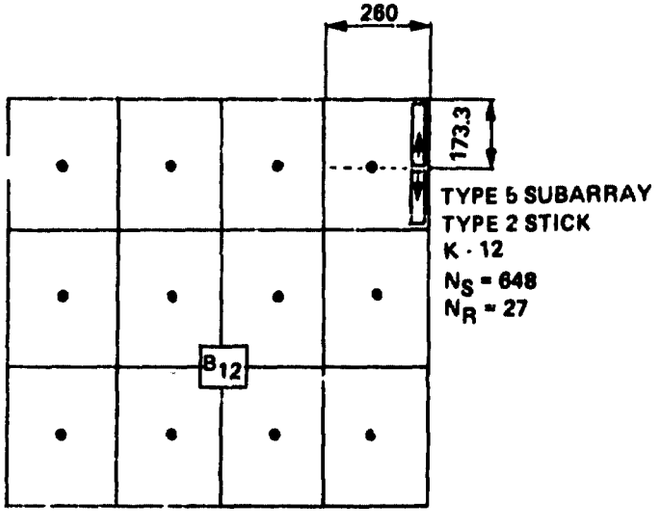

TYPE 5 SUBARRAY
TYPE 2 STICK
K = 12
N_S = 648
N_R = 27

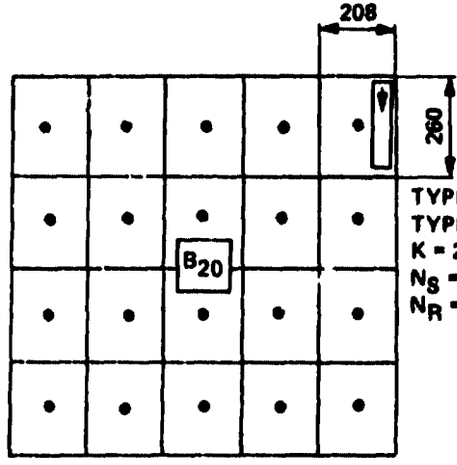

TYPE 7 SUBARRAY
TYPE 1 STICK
K = 20
N_S = 400
N_R = 22

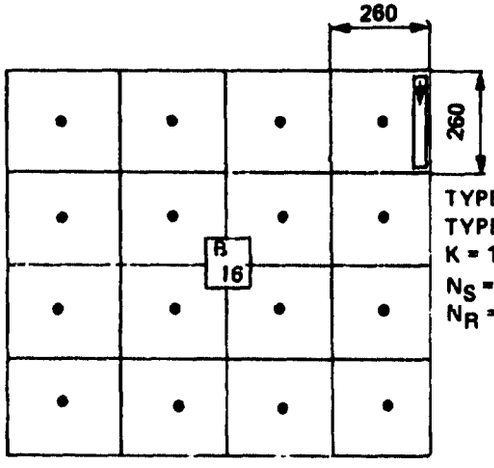

TYPE 6 SUBARRAY
TYPE 1 STICK
K = 16
N_S = 432
N_R = 27

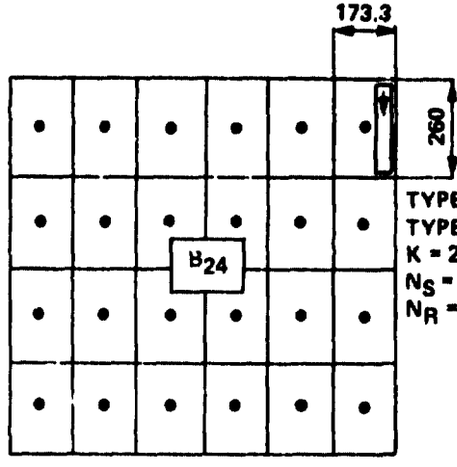

TYPE 8 SUBARRAY
TYPE 1 STICK
K = 24
N_S = 432
N_R = 18

GENERAL ELECTRIC

LAYOUT OF THE TEN DIFFERENT TYPES OF SUBARRAYS, SHOWING KLYSTRON PHASE REPEATER LOCATIONS AND WAVEGUIDE STICK SIZES (Cont'd)

space division

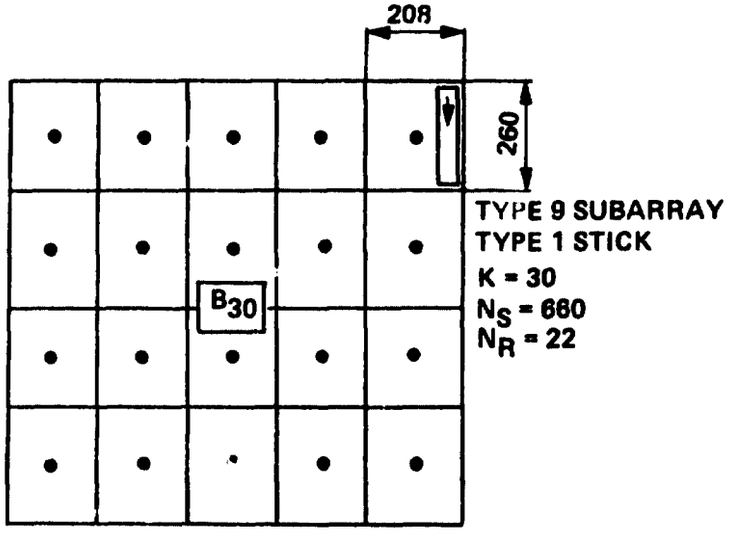

TYPE 9 SUBARRAY
TYPE 1 STICK
K = 30
N_S = 660
N_R = 22

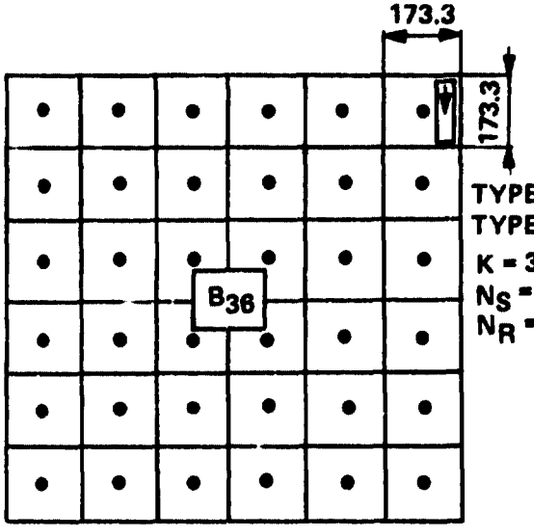

TYPE 10 SUBARRAY
TYPE 2 STICK
K = 36
N_S = 648
N_R = 18

GENERAL ELECTRIC

DIVISION OF 7220 ELEMENT SPACE ANTENNA INTO 10 POWER LEVEL RINGS

space division

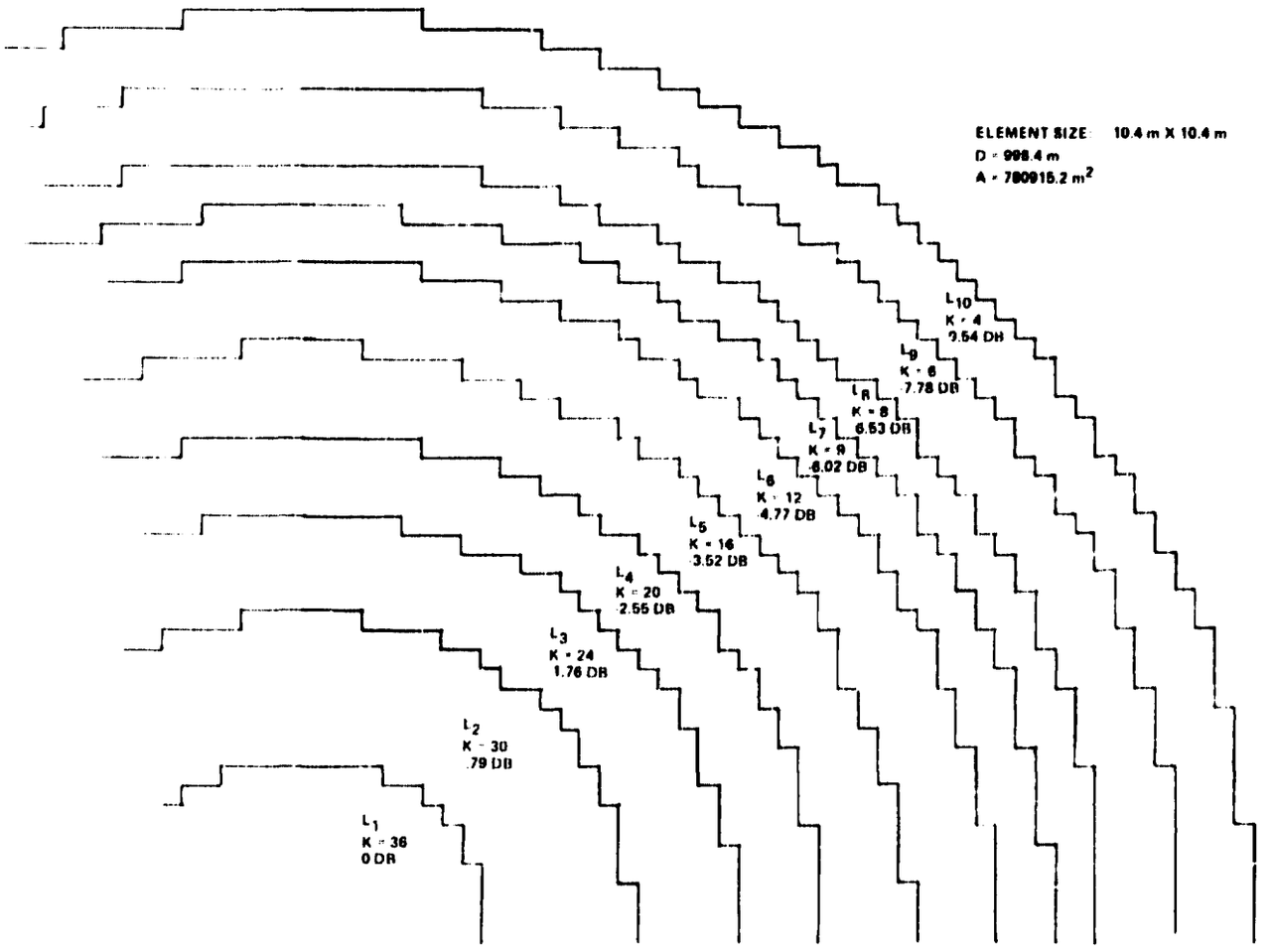

GENERAL ELECTRIC

LAYOUT OF PHASING SECTORS AND GROUPS

space division

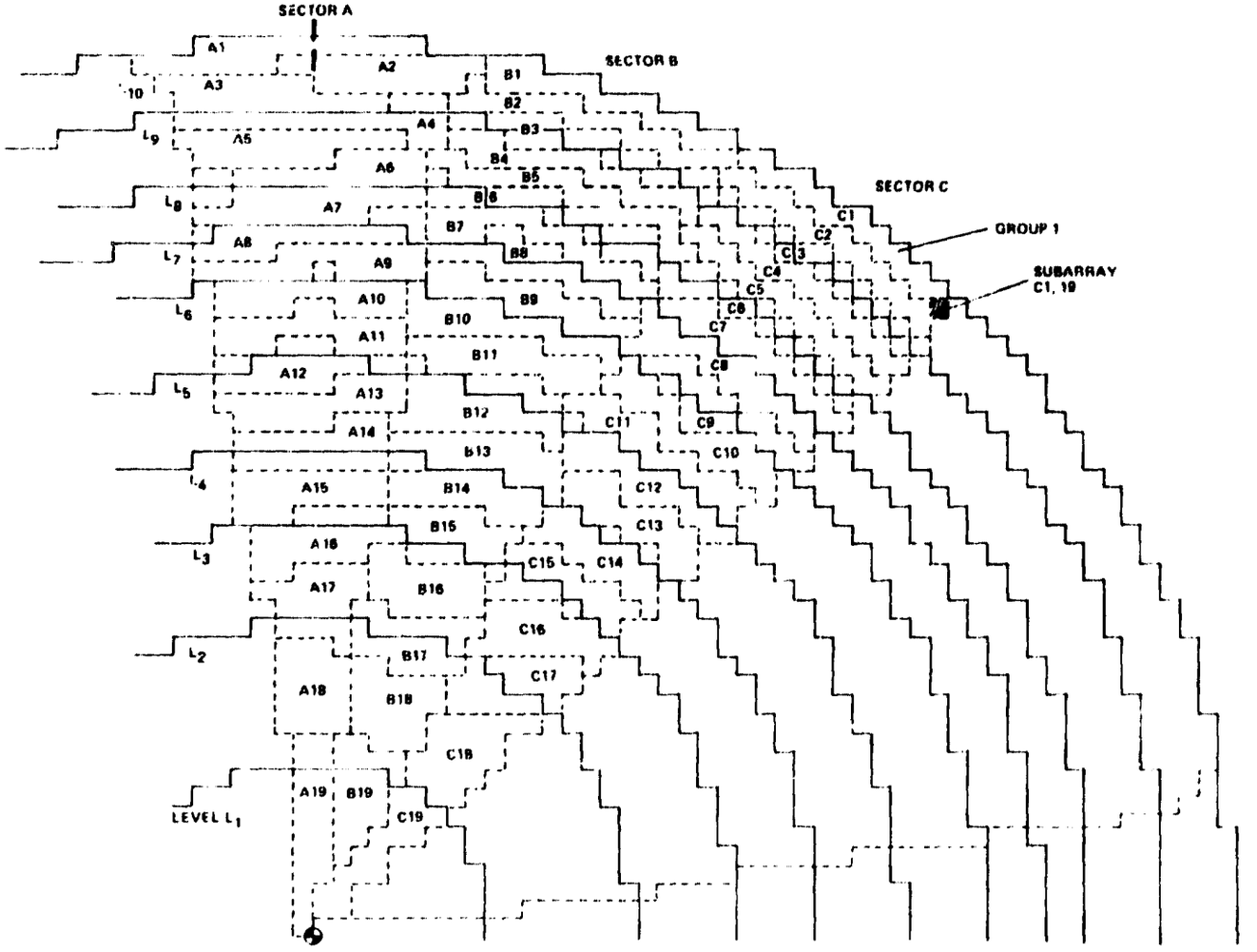

LOCATION OF REFERENCED PHASE REPEATER STATIONS OF SECTORS AND GROUPS

The figure shows the layout of the reference phase distribution network and the location of the phase repeater stations. The phase distribution network is a four layer tree. The first, second and third layers have 20, 19 and 19 way power dividers respectively at the nodes of the network. The first layer is called sector, the second group, the third unit, the fourth subarray. The power dividers at the fourth layer correspond to the number of klystrons carried by the subarray.

GENERAL ELECTRIC

LOCATION OF REFERENCED PHASE REPEATER STATIONS OF SECTORS AND GROUPS

space division

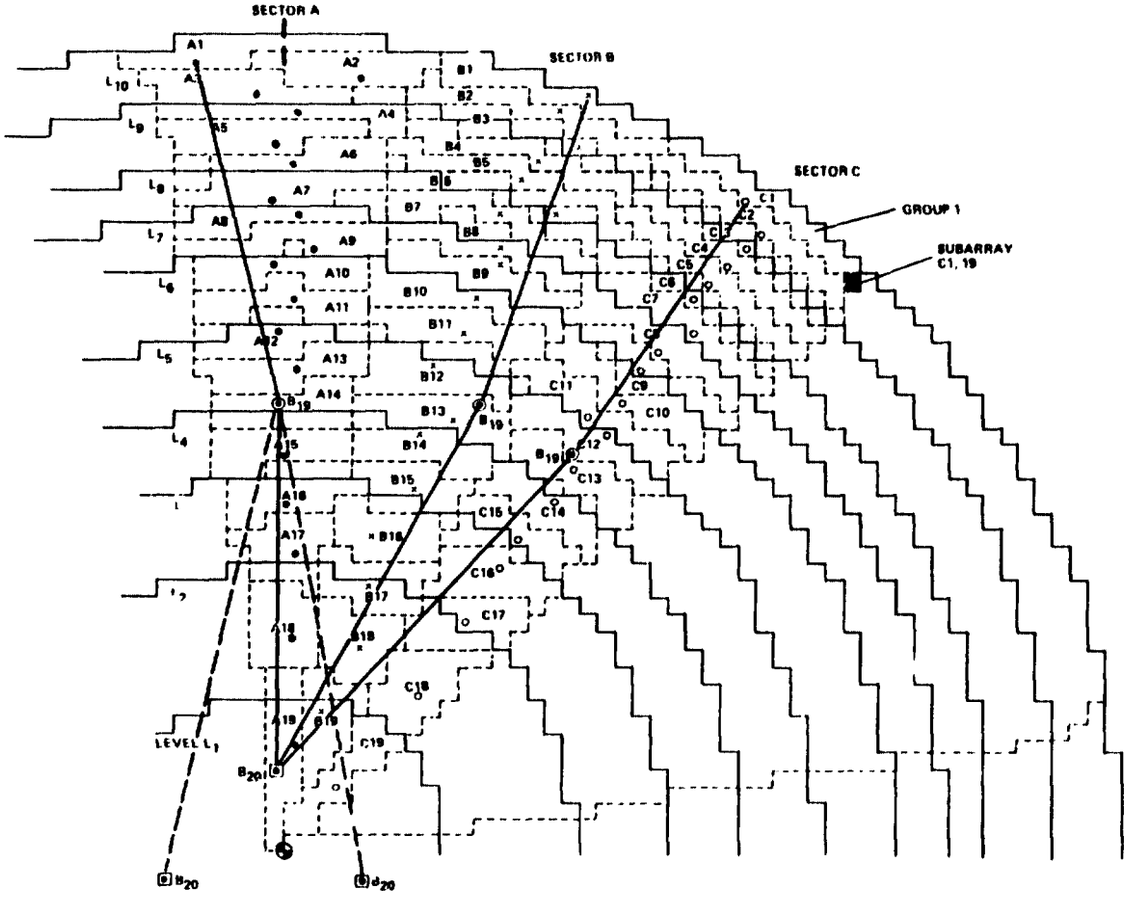

MECHANICAL LAYOUT OF A TYPICAL KLYSTRON MODULE IN THE OUTER RING OF THE SPACE ANTENNA

The figure shows the conceptual layout of all the components which are related to a "klystron" module of the space antenna. The example shown is for a subarray, at the edge of the antenna, which carry a total of four klystrons.

GENERAL ELECTRIC

MECHANICAL LAYOUT OF A TYPICAL KLYSTRON MODULE IN THE OUTER RING OF THE SPACE ANTENNA

space division

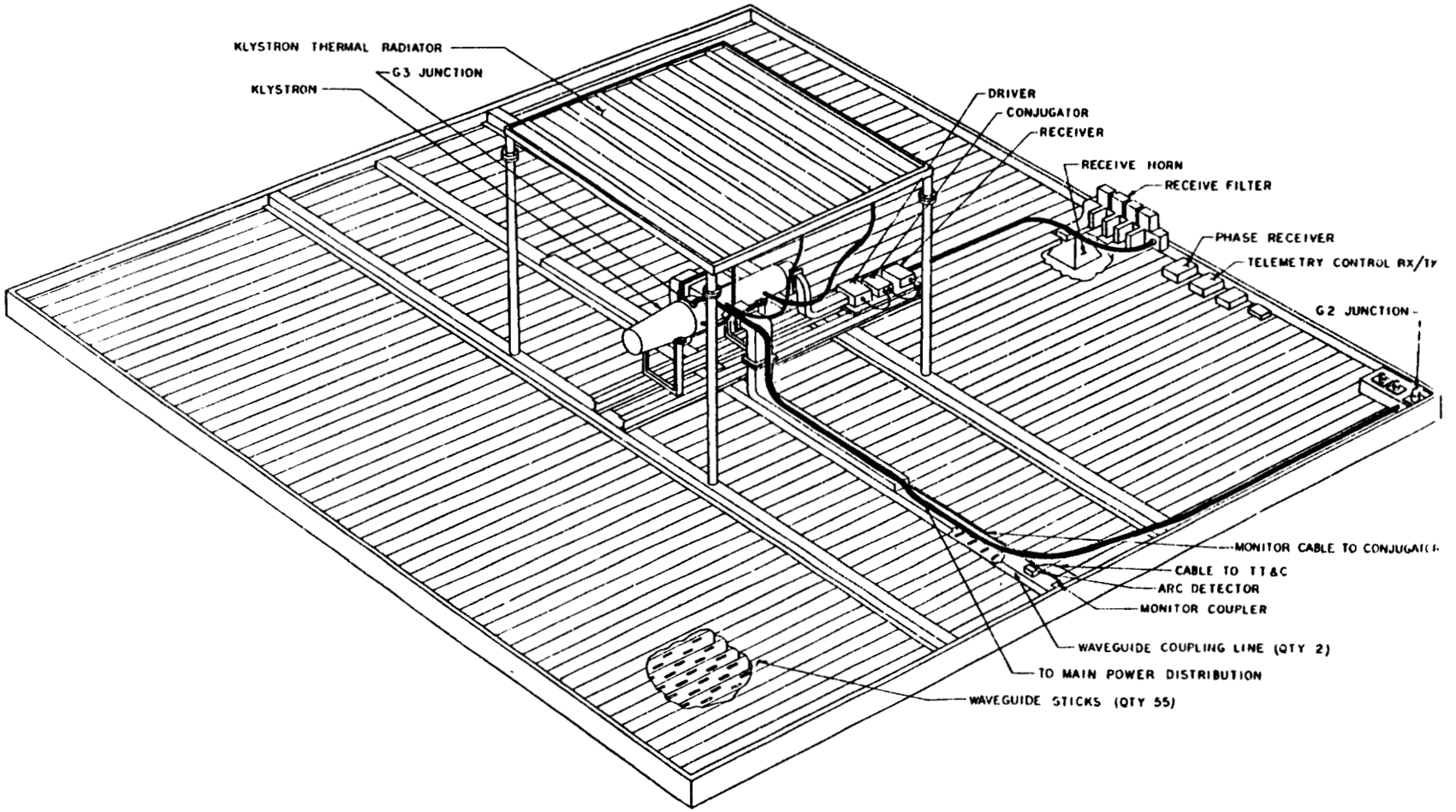

GENERAL ELECTRIC

REDUNDENCY CONCEPT OF PHASE DISTRIBUTION NETWORK

space division

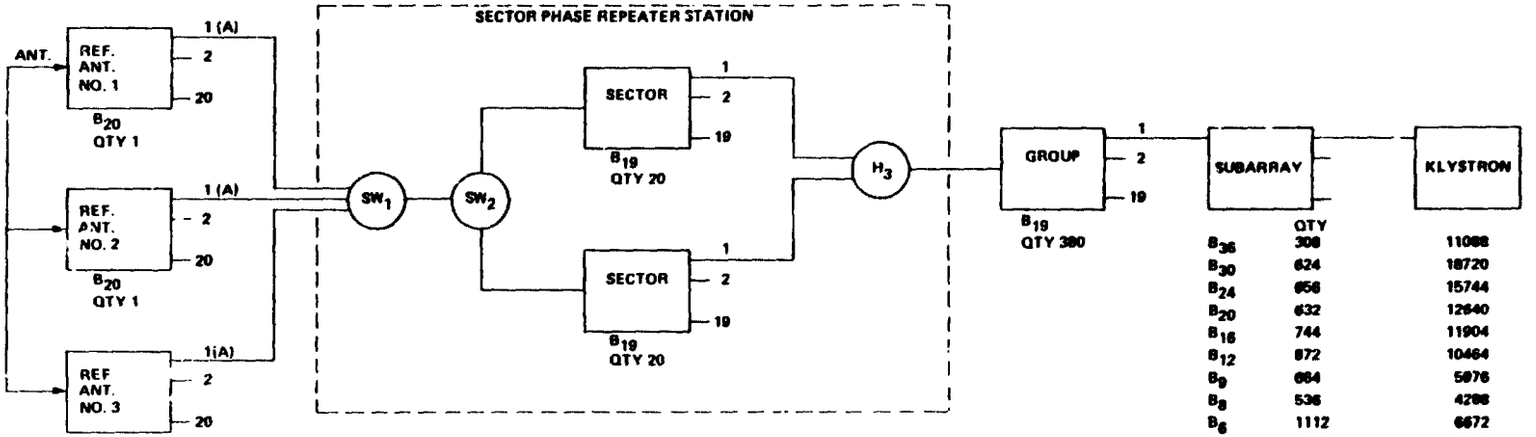

BLOCK DIAGRAM FOR RELIABILITY CALCULATIONS

The figure shows the redundancy and failure rate assumptions in the phase distribution network. The first layer is triple, the second is doubly redundant.

GENERAL ELECTRIC

BLOCK DIAGRAM FOR RELIABILITY CALCULATIONS

space division

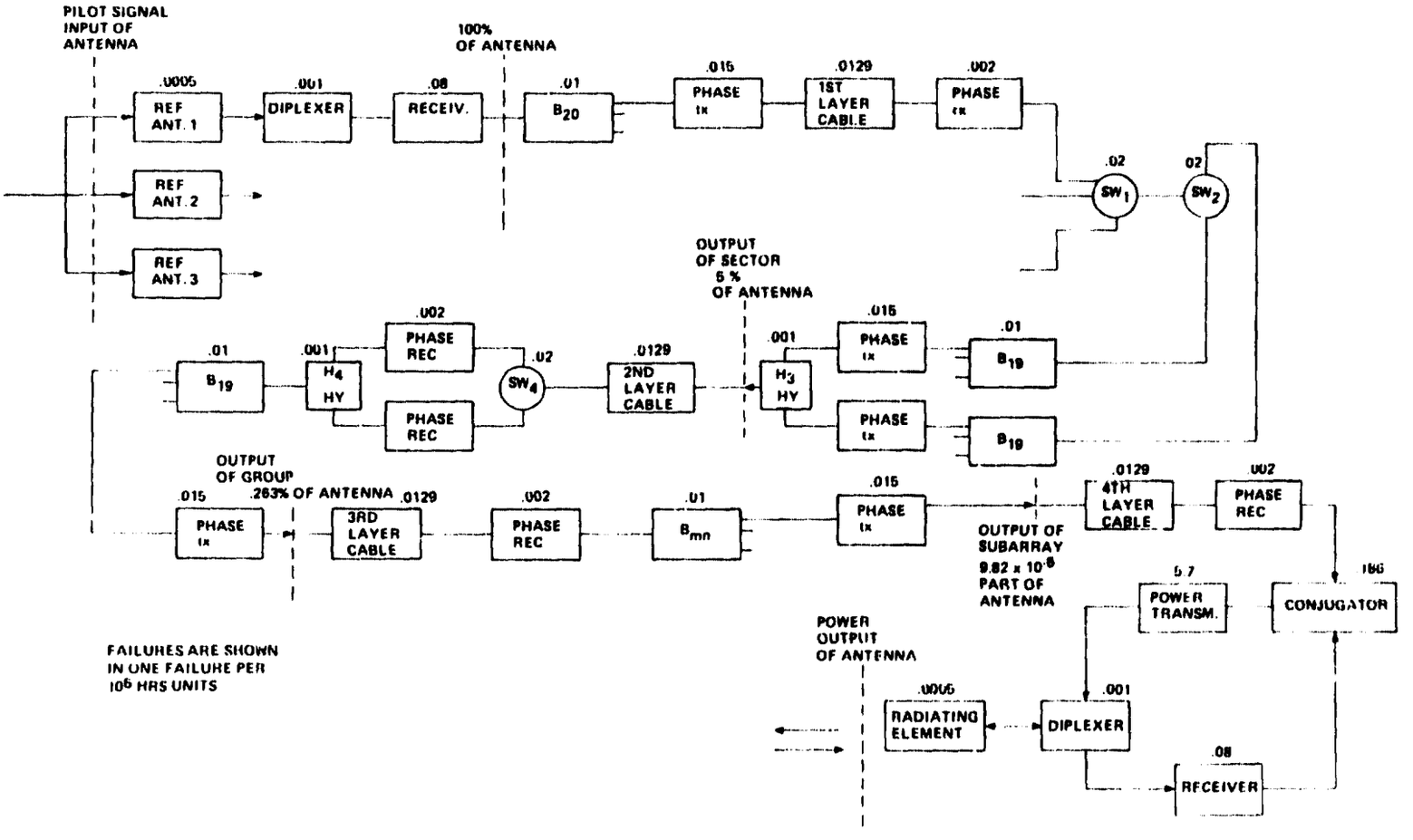

RECTENNA POWER CONDITIONING

The rectenna power conditioning network from input aperture plane to utility grid interface was developed conceptually including detailed geometry and conductor sizes. The summary displays some of the most important results.

GENERAL ELECTRIC

RECTENNA POWER CONDITIONING SUMMARY

space division

- MECHANICAL AND ELECTRICAL LAYOUT OF A TYPICAL RECTENNA WAS DEVELOPED FOR A TEXAS SITE.
- THE FOLLOWING COMPONENTS ARE DISTINGUISHED: DIPOLE, ARRAY, PANEL, UNIT, GROUP.
- A LOW VOLTAGE AND A LOW CURRENT DESIGN WAS CONCEIVED, THE LOW VOLTAGE, USING MAX. 3 KV (NOMINAL) WAS SELECTED AS THE BASELINE.
- FOUR DIFFERENT TYPES OF PANELS AND SEVEN DIFFERENTLY WIRES UNITS ARE NECESSARY TO FORM THE OVERALL NETWORK.
- ALL PANEL DIMENSIONS ARE IDENTICAL (3 M X 3.33 M) AND THE NS DIMENSIONS OF ALL UNITS ARE EQUAL (117.18 M).
- MOST OF THE LOSS IS IN THE PANEL WIRING, MOST OF THE WEIGHT IN THE UNIT LINES. USING ALUMINUM CONDUCTORS TOTAL NETWORK LOSS IS 1.39% AND TOTAL NETWORK WEIGHT IS 225,490 METRIC TONS.
- HIGH VOLTAGE DESIGN CAN CONSIDERABLY REDUCE THE NECESSARY WEIGHT OF CONDUCTORS, BUT IT INCREASES THE WEIGHT OF INSULATORS.
- LOSS IN THE AC SYSTEM IS APPROXIMATELY 1.5%.

GENERAL ELECTRIC

RECTENNA RF POWER DISTRIBUTION

space division

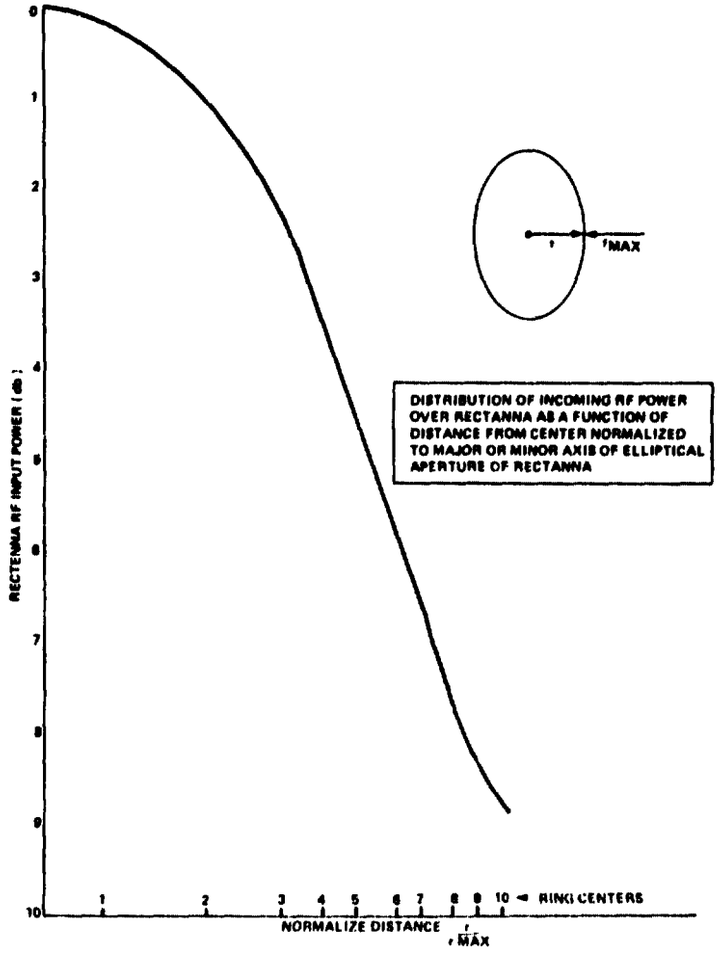

RECTENNA PANEL LAYOUT WITH 1849 DIPOLES AND DIODES

Figure shows the typical dimension of a panel in the rectenna and the highest applicable voltages in the so-called "low voltage" design. There are 1849 dipoles on one panel in the middle of the rectenna. Each dipole receives over an average of 54.1 cm^2 area. There are 1.305×10^{10} dipoles, 7.654×10^9 diodes, 7.06×10^6 panels in a typical rectenna.

GENERAL ELECTRIC

RECTENNA PANEL LAYOUT WITH 1849 DIPOLES AND DIODES

space division

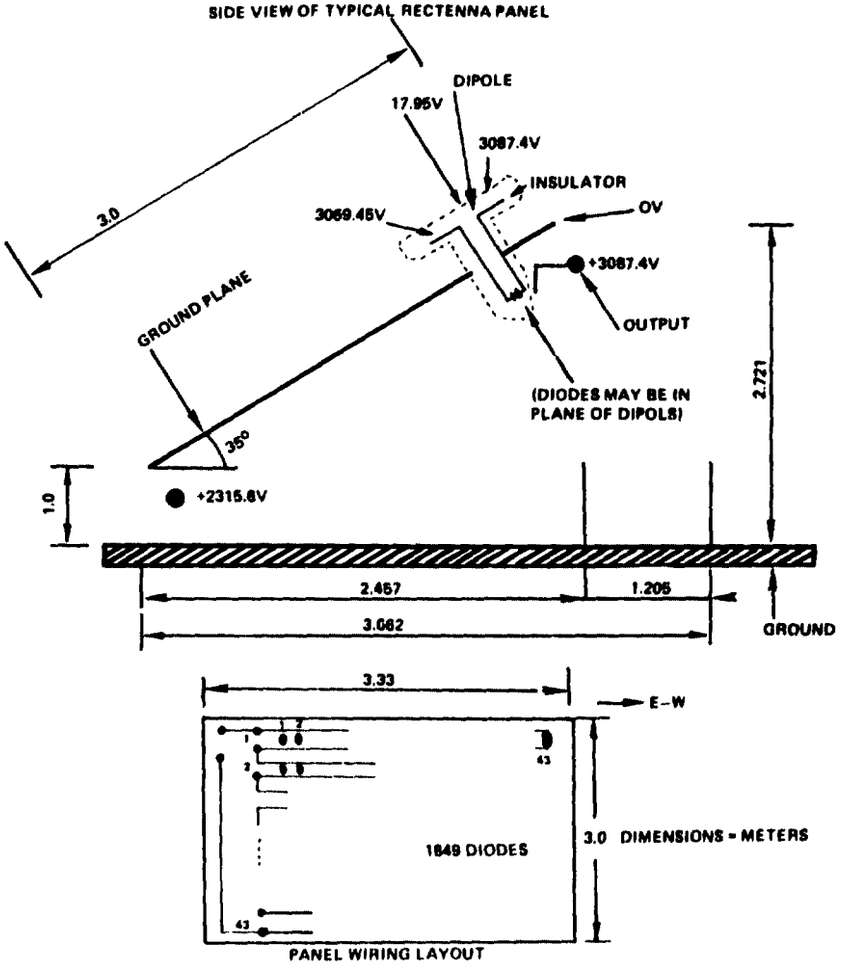

CHARACTERISTICS OF THE PANELS

A nominal panel size of 3m (NS) and 3.33m (EW) is assumed carrying between 1800 and 1849 dipoles. Dipoles are forming 1, 2, 4 or 8 element radiators in various rings of rectenna. Approximately 1.305×10^{10} dipoles and 7.654×10^{9} diodes are used. The voltage of panels vary between 283.5V and 772.3V.

GENERAL ELECTRIC

CHARACTERISTICS OF THE PANELS

space division

Ring	$P^{\frac{mw}{cm^2}}$	$P_{RF}^{\frac{w}{Panel}}$	η_r	$P_{DC}^{\frac{w}{Panel}}$	Dipoles	Diodes	$V_{DC}^{\frac{V}{Diode}}$	$P_{DC}^{\frac{w}{Diode}}$	$V_{DC}^{\frac{V}{Panel}}$	$I_P^{\frac{A}{Panel}}$	$R_{DC}^{\frac{ohm}{Panel}}$
1	23.33	2333	.7453	1738.8	43 x 43 = 1849	1849	17.96	.9398	772.3	2.25	1100
2	18.76	1876	.7366	1375.2	1849	1849	16.11	.7437	692.7	1.98	1100
3	14.38	1438	.7255	1043.3	1849	1849	14.11	.5642	606.7	1.72	1100
4	11.42	1142	.7251	828.1	2x30x31 = 1860	930	17.73	.8904	549.6	1.50	1136
5	8.67	867	.7216	625.6	1860	930	15.44	.6727	478.6	1.31	1136
6	6.72	672	.6966	468.1	1860	930	13.59	.5033	421.3	1.11	1136
7	5.34	534	.6842	365.4	1860	930	12.12	.3929	375.7	.973	1136
8	4.24	424	.6889	292.1	4x21x22 = 1848	462	15.32	.6322	337.0	.866	1152
9	3.49	349	.6776	236.5	1848	462	13.90	.5119	305.8	.773	1152
10	3.14	314	.6815	214.0	8x15x15 = 1800	225	18.90	.9511	283.5	.755	1100

WIRING LAYOUT OF THE FOUR DIFFERENT RECTENNA PANELS

The figure shows the four different panel wiring layouts necessary in the overall rectenna. The different panel layouts are necessary to keep the received power per diode relatively constant in the gradually decreasing power density rings of the rectenna.

GENERAL ELECTRIC

WIRING LAYOUT OF THE FOUR DIFFERENT RECTANNA PANELS

space division

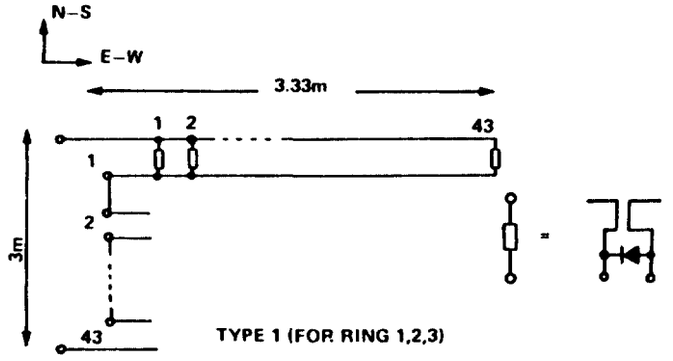

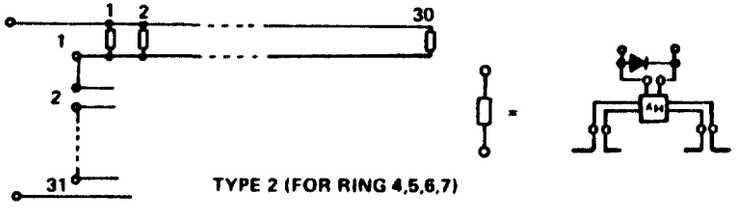

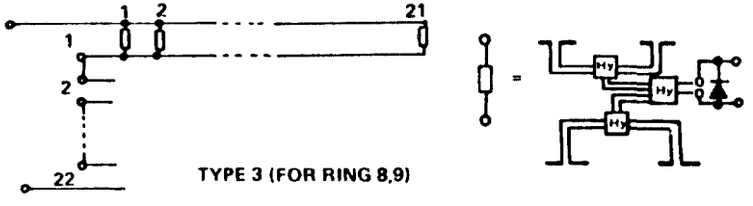

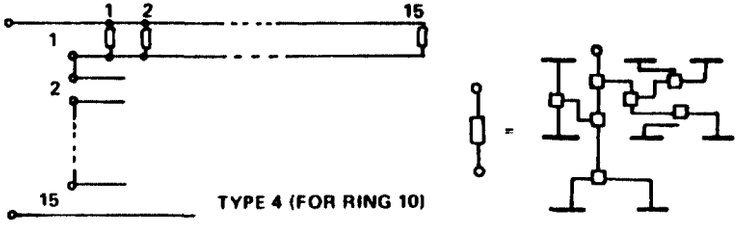

CHARACTERISTICS OF THE UNITS

From the panels panel strings are formed by parallel connection using between 50 to 160 panels. From the panel strings units are formed by series connections using 8 or 16 panel strings. The NS dimension of all units are identical, 117.18 m, determined by 32 rows of panels. The EW dimension varies for the different power rings of the rectenna. 7270 units are formed and their number roughly corresponds to the number of subarrays in the space antenna. The voltage of units varies between $\pm$ 1685.2 V and $\pm$ 3087.4 V. The power output from units varies between .585 Mw and 1.502 Mw.

GENERAL ELECTRIC

CHARACTERISTICS OF THE UNITS

space division

Ring		No. of Panels Per Unit	No. of Rows of Par. Panels	No. of Panels Per String	No. of Serier Strings	V_{unit}	P_{unit}^{Mw}	I_{unit}^{A}	R_{unit}^{ohm}	No. of Units	Total Power ^{Mw}	Normalized Total Power
1		864	4	108	8	6174.8	1.302	243.2	81.48	518	778.0	.1590
2		1024	4	128	8	5541.6	1.408	254.1	68.75	716	1008.3	.2061
3		960	4	120	8	4853.6	1.002	206.4	73.33	908	909.4	.1859
4		800	4	100	8	4396.8	.6624	150.6	90.88	588	389.5	.0796
5		992	4	128	8	3828.8	.6206	162.1	71	776	481.6	.0984
6		1280	4	160	8	3370.4	.5991	177.7	56.8	820	491.3	.1004
7	*	800	2	50	16	6011.2	.2923			800		
	**	400					.5846	97.25	181.76	400	233.8	.0478
8	*	1024	2	64	16	5392	.2991			688		
	**	512					.5982	110.9	144	344	205.8	.0421
9	*	1280	2	80	16	4892.8	.3027			704		
	**	640					.6054	123.7	115.2	352	213.5	.0436
10	*	1120	2	70	16	4536	.2397			752		
	**	280					.9587	211.3	125.71	188	180.2	.0368

*Subunit
**Unit

Total DC Power Without Conductor Losses: 4891.4

Input Power to Rectenna: 6792.7

Efficiency Without Conductor Losses: 72.01%

WIRING LAYOUT OF THE SEVEN DIFFERENT RECTENNA UNITS

The figure shows the seven different unit layouts, formed from the panels. There are 7270 units in the rectenna. The NS dimension for all units are 117.18 m.

GENERAL ELECTRIC

WIRING LAYOUT OF THE SEVEN DIFFERENT RECTENNA UNITS

space division

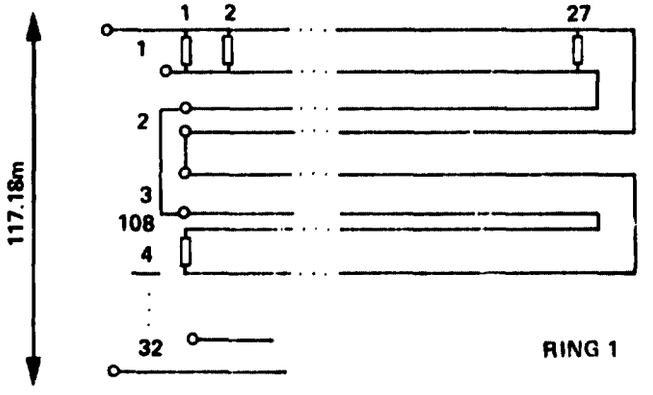

TYPE 1 (FOR RING 1)	1,2 . . . .27 2 4 32	TYPE 2 (FOR RING 2)	1,2 . . . .32 2 4 32	TYPE 3 (FOR RING 3)	1,2 . . . .30 2 4 32	TYPE 4 (FOR RING 4)	1,2 . . . .25 2 4 32	TYPE 5 (FOR RING 5)	1,2 . . . .31 2 4 32
TYPE 6 (FOR RING 6)	1,2 . . . .40 2 4 32	TYPE 4 (FOR RING 7)	1,2 . . .25 2 32	TYPE 2 (FOR RING 8)	1,2 . . . .32 2 32	TYPE 6 (FOR RING 9)	1,2 . . . .40 2 32	TYPE 7 (FOR RING 10)	1,2 . . . .35 2 32

RECTENNA BOUNDARIES OF UNITS

The different types of units are arranged into rings. The figure shows the boundaries between these rings, the number of units in each ring, the incident RF power to the corresponding units (P_U) and the total RF power (P_T) received within the corresponding rings.

GENERAL ELECTRIC

RECTENNA BOUNDARIES OF UNITS

space division

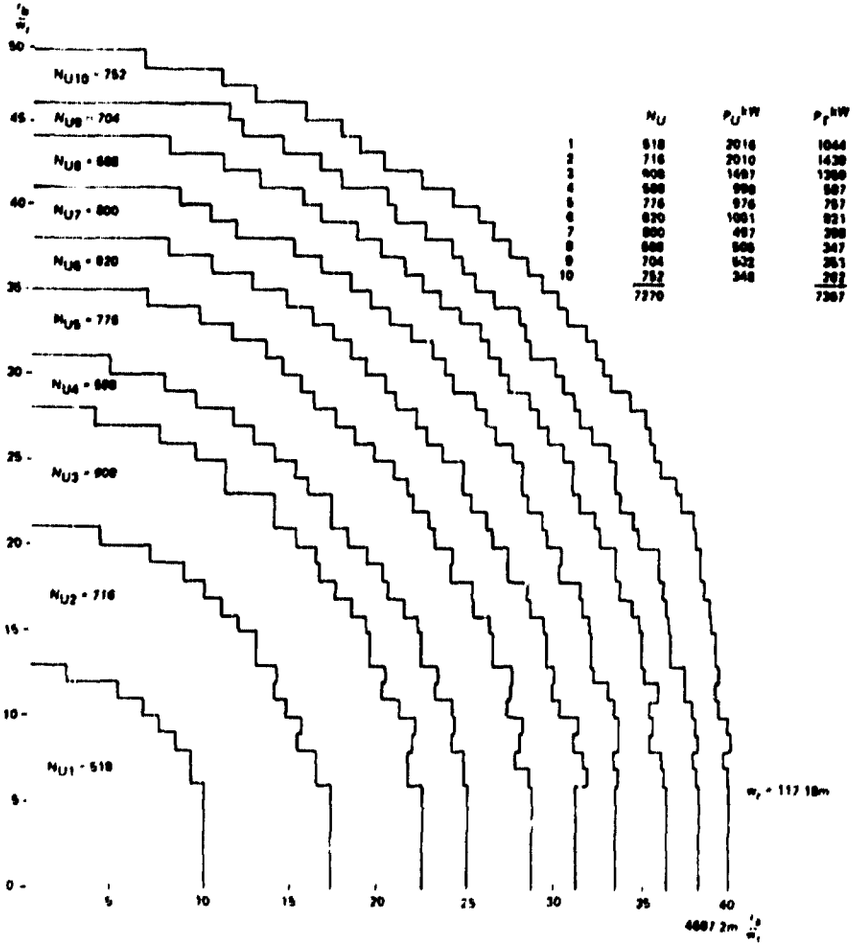

	N_U	P_U kW	P_r kW
1	518	2016	1044
2	716	2010	1439
3	908	1497	1360
4	688	998	687
5	776	976	757
6	820	1051	821
7	800	487	388
8	688	508	347
9	704	522	361
10	752	348	262
	7370		7367

CHARACTERISTICS OF THE GROUPS

From the units groups are formed by parallel connection using four to ten units. A total of 784 groups are in the rectenna. The voltage of the groups varies between $\pm$ 1685.2V and $\pm$ 3087.4V. The power output from groups varies between 2.923 MW and 9.012 MW. The group covers a total area of 84.75 km^2, with a nominal 9.4 km E-W and 11.48 km N-S dimension.

GENERAL ELECTRIC

CHARACTERISTICS OF THE GROUPS

space division

Ring	Parallel Units	N_G	No. of Residual Units	V^V	R^Ω	P^{Mw}	I^A
1	6	85	8	6175	13.58	9.012	1459.2
2	4	179	0	5542	17.18	5.632	1016.4
3	8	112	12	4854	9.166	8.016	1651.2
4	8	72	12	4397	11.36	5.299	1204.8
5	8	97	0	3829	8.875	4.965	1296.8
6	10	82	0	3370	5.68	5.991	1777
7	10	40	0	6011	18.18	2.923	972.5
8	8	43	0	5392	18	4.786	887.2
9	8	44	0	4893	14.4	4.843	989.6
10	8	22	4	4536	15.71	7.669	1690.4

Specials

1	4	2	0	6175	20.37	6.008	972.8
3	6	2	0	4854	12.22	6.012	1238.4
4	6	2	0	4397	15.15	3.974	903.6
10	6	2	0	4536	20.95	5.7522	1267.8

BLOCK DIAGRAM OF A TYPICAL LOW VOLTAGE RECTENNA GROUP
(GROUP 1, RING 1)

The figure shows the block diagram from diodes to "groups" of the rectenna for Group 1 of Ring 1. (Example shows a group close to the center of the rectenna.)

GENERAL ELECTRIC

BLOCK DIAGRAM OF A TYPICAL LOW VOLTAGE RECTANNA GROUP (GROUP 1, RING 1)

space division

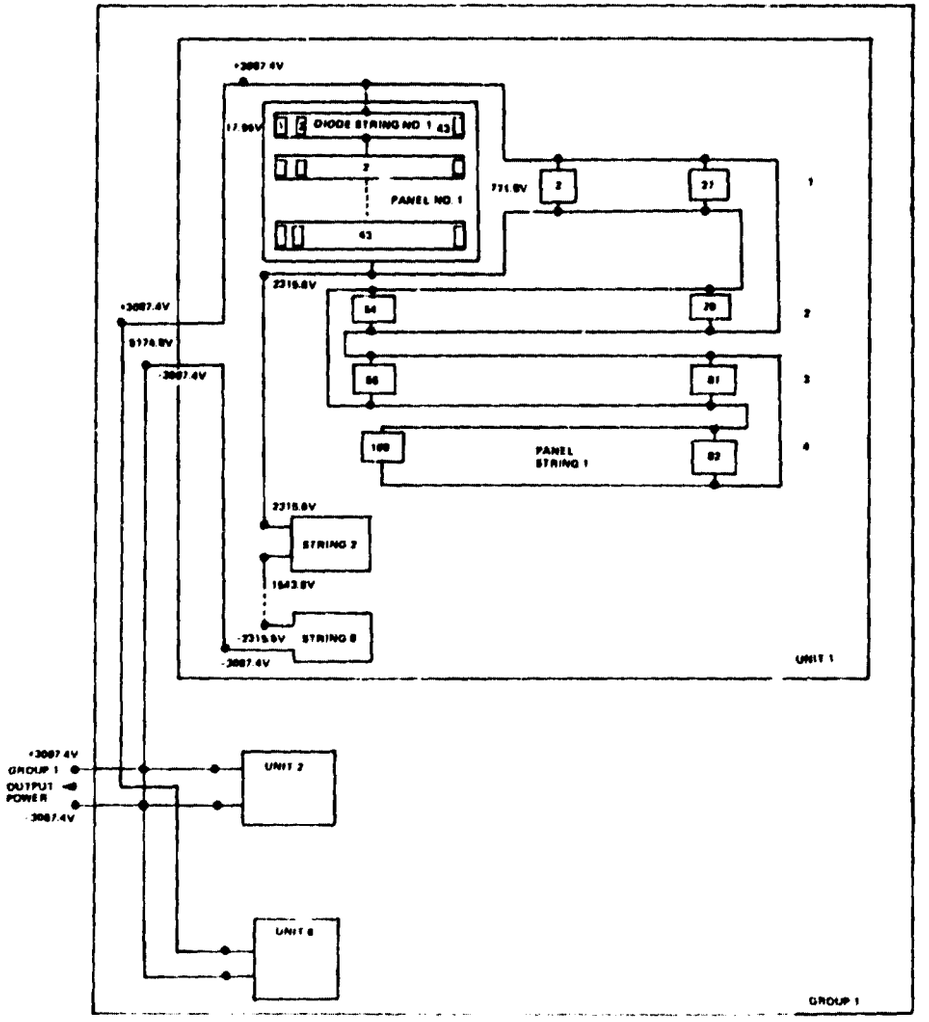

GENERAL ELECTRIC

LOW CURRENT RECTANNA WIRING LAYOUT FOR SEVEN DIFFERENT UNIT DESIGNS

space division

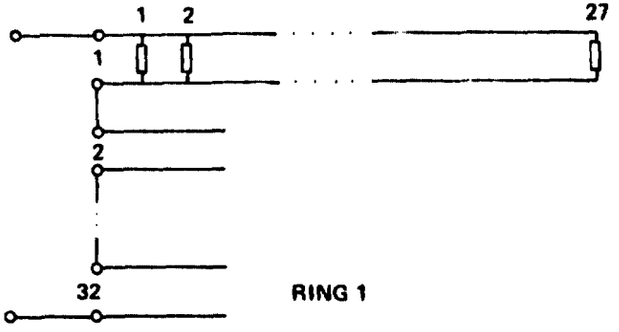

TYPE 1 (FOR RING 1)	1,2 . . . .27 2 ⋮ 32	TYPE 2 (FOR RING 2)	1,2 . . . .32 2 ⋮ 32	TYPE 3 (FOR RING 3)	1,2 . . . .30 2 ⋮ 32	TYPE 4 (FOR RING 4)	1,2 . . . .25 2 ⋮ 32	TYPE 5 (FOR RING 5)	1,2 . . . .31 2 ⋮ 32
TYPE 6 (FOR RING 6)	1,2 . . . .40 2 ⋮ 32	TYPE 4 (FOR RING 7)	1,2 . . . .25 2 ⋮ 32	TYPE 2 (FOR RING 8)	1,2 . . . .32 2 ⋮ 32	TYPE 6 (FOR RING 9)	1,2 . . . .40 2 ⋮ 32	TYPE 7 (FOR RING 10)	1,2 . . . .35 2 ⋮ 32

SUMMARY OF LOSSES AND TRANSMISSION LINE WEIGHTS

The table displays the loss and weight characteristics of the DC power collection system of the rectenna. Using the previously described "low voltage" design the loss can be kept at 1.393% at the cost of 253490 metric tons of aluminum conductor. The bulk of the loss is in the panel lines and the bulk of the weight in the unit lines, thus the system can be improved by further optimization. Conductor weight can be reduced to 32424MT (to 12.8%) by allowing $\pm$ 27.2 kV within the rectenna. ("High voltage" design.)

GENERAL ELECTRIC

SUMMARY OF LOSSES AND TRANSMISSION LINE WEIGHTS

space division

Ring	Loss MW				Weight T			
	Panel	Unit	Group Line	Total	Panel	Unit	Group Line	Total
1	7.40	1.98	.12	9.50	535	12991	406	13932
2	9.41	3.54	.08	13.03	876	21299	333	22508
3	8.44	2.77	.25	11.46	1042	12661	1187	14890
4	4.03	1.59	.14	5.76	272	6832	320	7424
5	5.03	3.02	.28	8.33	445	11181	524	12150
6	4.92	2.48	.46	7.86	620	30491	2859	33970
7	2.30	.90	.15	3.35	185	18591	1743	20519
8	1.44	1.29	.16	2.89	146	20469	1279	21894
9	1.46	1.03	.06	5.44	187	52357	1636	54180
10	1.80	1.40	.18	3.38	30	48931	3059	52020
	46.23	20.02	1.88	66.13	4339	235803	13348	253490

Total DC Power at Diode Output 4891.4

Loss % 1.353

Total DC Power at Inverter Input 4823.3

GROUND POWER COLLECTION AND TRANSMISSION SYSTEM

The integration of SPS power into electric utility power system will depend largely on the local system characteristics. The work in this area included an assessment of using AC at different voltage levels and/or using DC for long distance power transmission.

The failure characteristics and modes for the elements in the rectenna AC power collection system were developed and integrated into reliability profiles describing the availability of the various rectenna layouts studied.

The maintenance requirements both periodic and unscheduled were assessed and tabulated.

GENERAL ELECTRIC

GROUND POWER COLLECTION AND TRANSMISSION SYSTEM

space division

TASKS IN PHASE 1

- **INTEGRATION OF SPS POWER INTO A TYPICAL ELECTRIC UTILITY POWER SYSTEM**
- **FAILURE MODE AND RELIABILITY ANALYSIS OF RECTENNA AC POWER COLLECTION SYSTEM**
- **MAINTENANCE REQUIREMENTS FOR THE AC POWER COLLECTION SYSTEM – SCHEDULED AND UNSCHEDULED**

INTEGRATION OF SPS POWER INTO A TYPICAL ELECTRIC UTILITY POWER SYSTEM

The critical parameters when considering what kind of transmission system and what voltage levels will be feasible for connecting SPS power plants to the power grid is first, the distance between the SPS plant and the load centers served. The existing AC transmission system may be applicable for part of the power but stability and system reliability considerations may well indicate a mixed AC and DC system.

Since the SPS system is likely to be far more stable than a conventional power plant of the same rating the breakeven between AC and DC might well be different than in conventional systems. Due to the possibility of extreme reliability criteria being imposed on a SPS system, the conventional transmission planning contingency criteria will also need review in site specific studies.

GENERAL ELECTRIC

INTEGRATION OF SPS POWER INTO A TYPICAL ELECTRIC UTILITY POWER SYSTEM

space division

CRITICAL PARAMETERS

- LOCATION OF LOAD CENTERS RELATIVE TO SPS RECTENNA LOCATION
- EXISTING POWER TRANSMISSION SYSTEM
  - –DISTANCE FROM SPS LOCATION
  - –STABILITY
- TRANSMISSION PLANNING CONTINGENCY CRITERIA

INTEGRATION OF SPS POWER INTO A TYPICAL ELECTRIC UTILITY POWER SYSTEM

Previous arrangements shown using a redundant set of transmission lines has been restudied and the arrangement shown in this figure using a total of six 500 kV circuits would be applicable if the SPS would serve one major and a couple of minor load areas. It is anticipated that any two of the 6 circuits could be removed from service without reduction of the rectenna output. The remaining four circuits, together with the normal utility transmission interconnections should be capable of carrying the 5000 MW output required.

GENERAL ELECTRIC

INTEGRATION OF SPS POWER INTO A TYPICAL ELECTRIC UTILITY POWER SYSTEM

space division

CONSIDERATIONS FOR AC BULK POWER TRANSMISSION

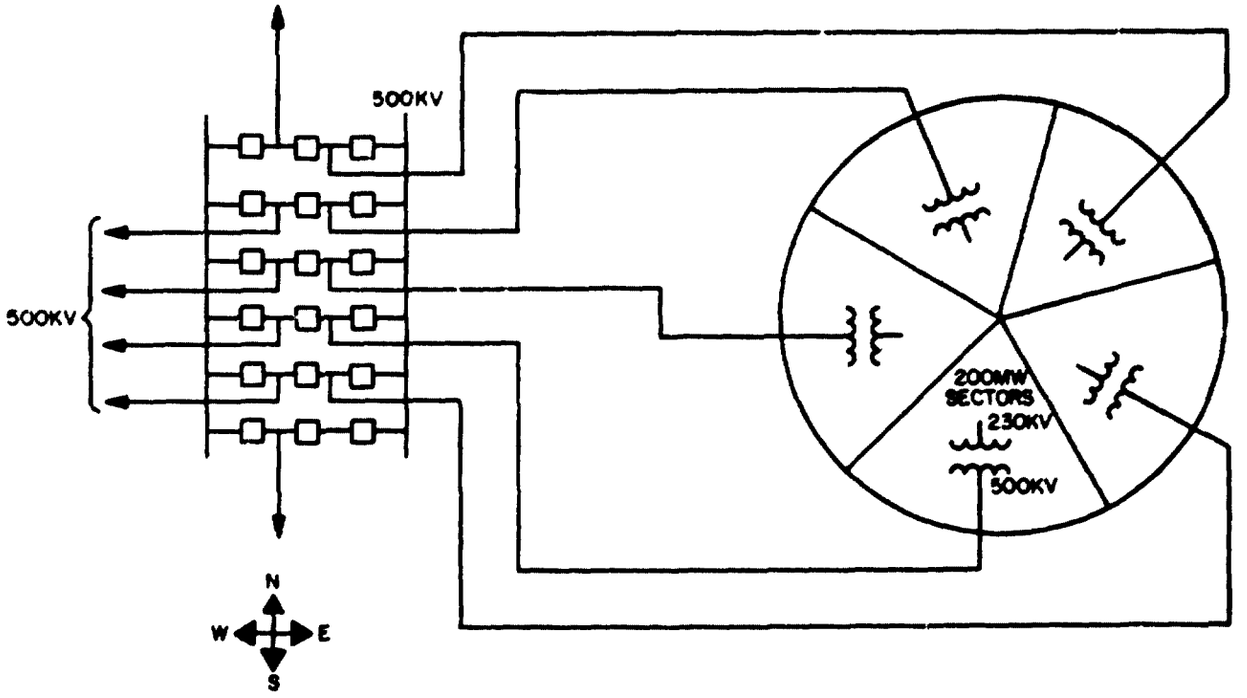

TRANSMISSION REQUIREMENTS FOR UTILITY INTERPHASE

INTEGRATION OF SPS POWER INTO A TYPICAL ELECTRIC UTILITY POWER SYSTEM

For conventional generation stations, depending on the distance to the load center, some series capacitor compensation of the AC transmission lines would normally be expected when considering contingency line loadings. Typical line loadings versus distance and amount of series compensation for AC transmission lines is shown in this figure.

When considering contingency loadings as discussed before with 2 lines down and 4 lines carrying the full 5000 MW the line loadings would be 1.25 times the surge impedance loading (SIL). The surge impedance loading for various voltage levels are shown in the table and for 500 kV, the SIL would be about 1000 MW. From the curves it would appear that a reasonable transmission distance with no series compensation for this example would be about 200 miles, which could be increased to 350 or 400 miles with up to 70% series compensation.

GENERAL ELECTRIC

INTEGRATION OF SPS POWER INTO A TYPICAL ELECTRIC UTILITY POWER SYSTEM

space division

CONSIDERATIONS FOR AC BULK POWER TRANSMISSION

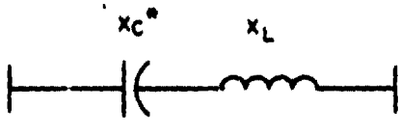

* NOTE: SERIES COMPENSATION TYPICALLY APPLIED BEYOND 150 - 250 MILES

TYPICAL ECONOMIC LINE LOADINGS

REPRESENTATIVE LINE SURGE IMPEDANCE LOADINGS (BIL)

LINE VOLT kV	THREE CONDUCTOR MW	FOUR CONDUCTOR MW
242	209	–
362	468	504
550	1080	1160
800	2280	2460

INTEGRATION OF SPS POWER INTO A TYPICAL ELECTRIC UTILITY POWER SYSTEM

When substantial amounts of power are to be transported for distances of 400 miles or more, the consideration of a high-voltage DC (HVDC) as the transmission load is often indicated. The HVDC system is ideally suited for long distance bulk power transport since it does not suffer from stability effects and can even be used to improve the stability of the AC system to which it is connected.

There are, however, certain specific requirements to be met. At each of its terminals the DC transmission system absorbs reactive power which must be supplied by static capacitors, rotating machines, like synchronous condensers or from the connected AC network. Reactive volt-amperes equal to approximately 60% of the transmitted active power are required.

The current on the AC side of the terminals contains substantial harmonic components which must be removed, generally by shunt-connected tuned circuits.

Lastly, the DC terminal must be connected to an active AC network having a short circuit capacity (in volt-amperes) equal to a minimum of two times the transmitted power.

When the requirements for filtering, reactive supply, and short circuit capacity are met, the HVDC system is a reliable, efficient, and readily controlled power transmission medium.

GENERAL ELECTRIC

INTEGRATION OF SPS POWER INTO A TYPICAL ELECTRIC UTILITY POWER SYSTEM

space division

CONSIDERATIONS FOR DC BULK POWER TRANSMISSION

DC INDICATED FOR

- LONG TRANSMISSION DISTANCES > 400 MILES
- STABILITY PROBLEMS IN EXISTING AC SYSTEM
- RELIABILITY AND EASY CONTROLABILITY

DC REQUIREMENTS

- REACTIVE POWER SUPPLY ~ 60% OF ACTIVE POWER
  - STATIC CAPACITORS
  - SYNCHRONOUS CONDENSERS
  - CONNECTED AC NETWORK
- CONTROL OF HARMONICS BY FILTERS
- MUST BE CONNECTED TO AN ACTIVE AC NETWORK WITH SUFFICIENT SHORT CIRCUIT CAPACITY

INTEGRATION OF SPS POWER INTO A TYPICAL ELECTRIC UTILITY POWER SYSTEM

A typical HVDC power transmission circuit is shown in this figure. The synchronous condensers and AC filters are shown connected to the AC switchyard. The DC terminal consists of three phase bridge converters connected in parallel on the AC side and in series on the DC side. Although only two bridges are shown between ground and the DC conductor, it is not uncommon for four such bridges to be applied when the DC voltage exceeds $\pm$ 400 kV.

The DC system is balanced with respect to ground and is firmly held this way by fully rated ground electrodes. In normal operation there is no current in these ground electrodes, but in an emergency if one conductor or its converters are lost, the other conductor and the ground circuit will continue to transmit half power. Such emergency use can usually be tolerated. The transformers which couple the AC system to the bridges are shown equipped with load tap changers (LTC) which insure that the converter operates at the proper voltage and firing angle regardless of normal smaller variations in the AC system voltage.

GENERAL ELECTRIC

INTEGRATION OF SPS POWER INTO A TYPICAL ELECTRIC UTILITY POWER SYSTEM

space division

CONSIDERATION FOR DC BULK POWER TRANSMISSION

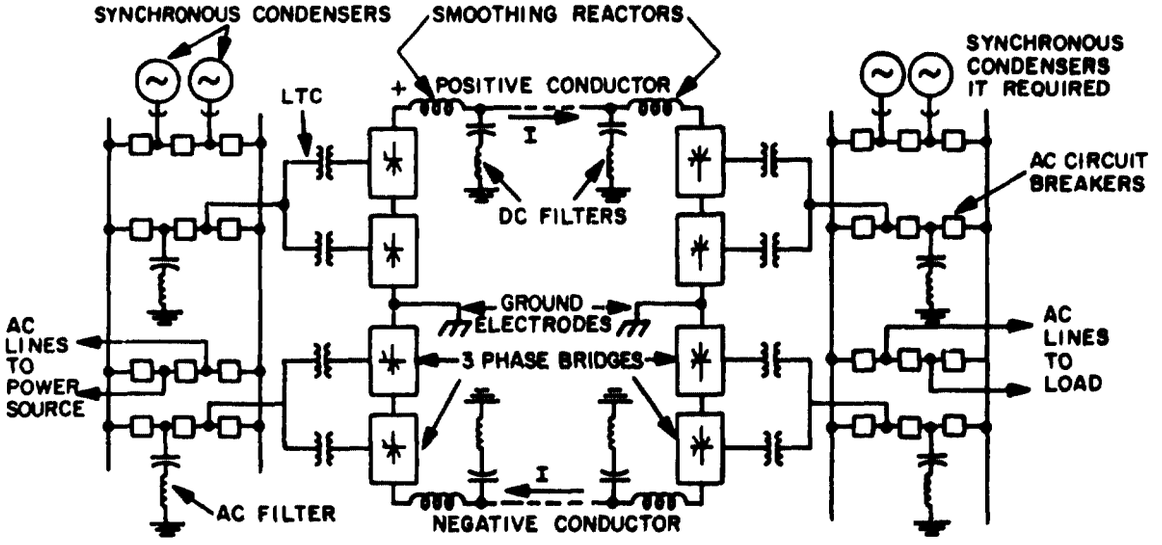

ELEMENTS OF A HVDC TRANSMISSION SYSTEM

FAILURE MODES AND EFFECTS ANALYSIS

The failure modes and their effects was analyzed for the power transmission system between the elevation flexible joint on the spacecraft to the utility interface on the ground. The summary presents some of the most important results.

GENERAL ELECTRIC

FAILURE MODES AND EFFECTS ANALYSIS SUMMARY

space division

- WITH CONVERTER REDUNDANCY THE SPACE ANTENNA DC SYSTEM HAS A MEAN AVAILABILITY OF APPROXIMATELY 99.5%.
- THE PHASE CONTROL SYSTEM MEAN AVAILABILITY IS 99%. THIS CAN BE IMPROVED IF THE FOURTH LAYER IS DUPLICATED, BUT THE COST PENALTY IS VERY LARGE. ANOTHER POTENTIAL IMPROVEMENT IN AVAILABILITY (AND COST) MAY BE POSSIBLE BY OMITTING THE FOURTH LAYER ALTOGETHER.
- THE MEAN AVAILABILITY OF THE KLYSTRON AND ITS DRIVER IS 97.45% WITH 20 YEAR LIFETIME TUBE AND HALF YEARLY MAINTENANCE. POWER LOSS CAN BE CUT BY NEARLY A FACTOR OF TWO IF QUARTER YEARLY MAINTENANCE IS IMPLEMENTED.
- COMBINED EFFECTS OF RANDOM ERRORS IN THE APERTURE DISTRIBUTION AND LOSSES IN THE PROPAGATION MEDIA ARE COMPARABLE TO THAT OF THE KLYSTRONS.
- MEAN AVAILABILITY ASSOCIATED WITH DIODE FAILURES IS APPROXIMATELY 99.45%, ASSUMING NO DIODE OR PANEL RELATED MAINTENANCE.
- THE RESULTANT DC POWER COLLECTION SYSTEM CAN HAVE A MEAN AVAILABILITY OF 98.4%.
- THE RESULTANT AC POWER COLLECTION SYSTEM MEAN AVAILABILITY IS 99.7%.
- RESULTANT SYSTEM EQUIPMENT AVAILABILITY BETWEEN ELEVATION FLEXIBLE JOINTS AND UTILITY GRID IS APPROXIMATELY 90%, POWER AVAILABILITY IS HIGHER THAN 86%.
- NUMBER OF POTENTIAL AREAS WERE DETECTED WHERE AVAILABILITY IMPROVEMENT CAN BE IMPLEMENTED IN COST EFFECTIVE MANNER.

AVAILABILITY VS. PROBABILITY FOR SPACE ANTENNA D-C DISTRIBUTION SYSTEM
FROM OUTPUT OF FLEXIBLE JOINT TO KLYSTRON INPUT

The figure shows the availability of the spacecraft DC power distribution system. The resultant curve is shown for .075 failure/.5 year failure rate DC to DC converters in a redundant configuration. The available power for this case falls below 99.5% of its maximum in no more than 2980.4 Hrs./year or otherwise it stays above this value in 66% of the time. This value may be taken as the average (rms) value of the available DC power.

GENERAL ELECTRIC

AVAILABILITY VS. PROBABILITY FOR SPACE ANTENNA D-C DISTRIBUTION SYSTEM FROM OUTPUT OF FLEXIBLE JOINT TO KLYSTRON INPUT

space division

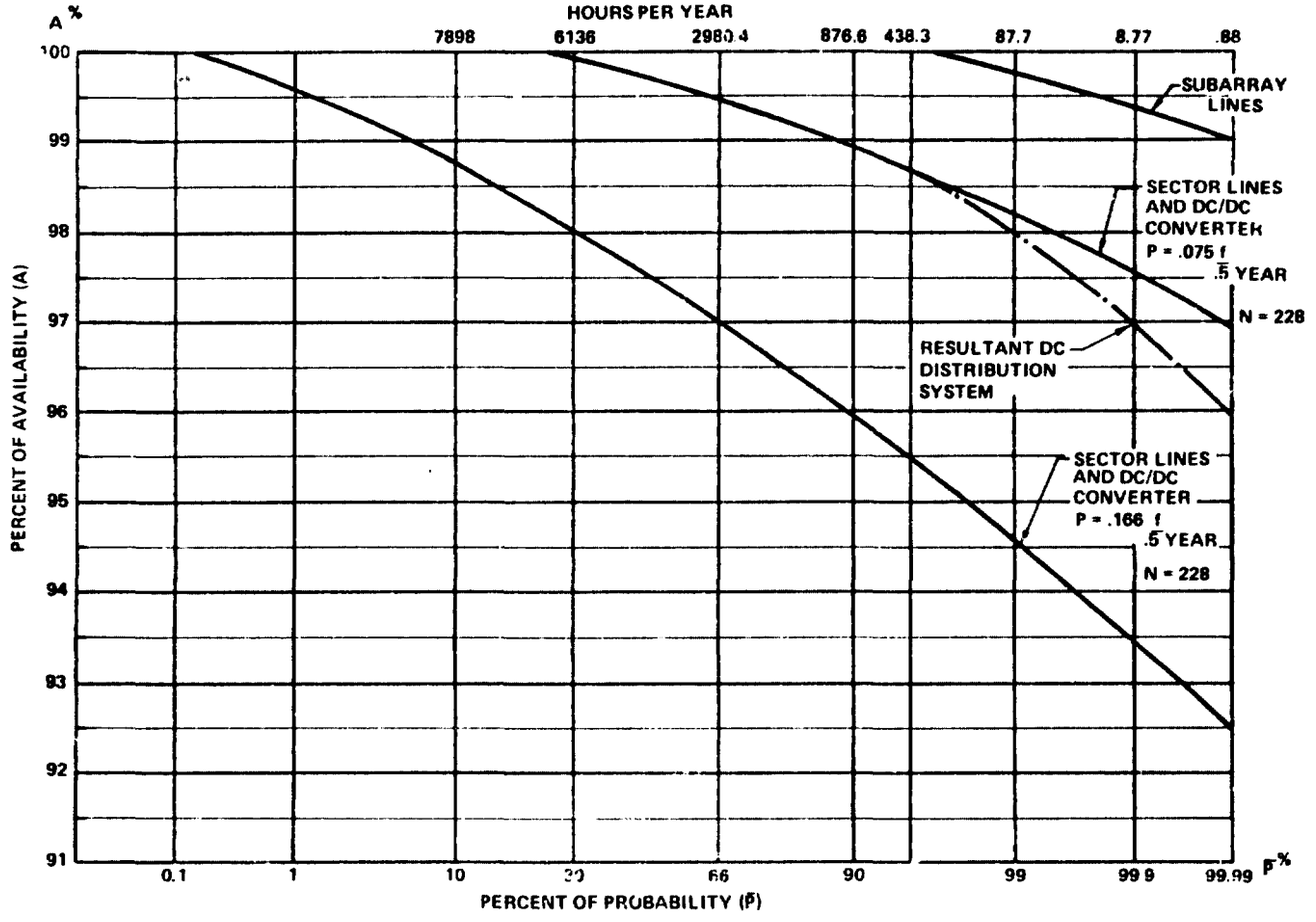

GENERAL ELECTRIC

AVAILABILITY VS. PROBABILITY OF A STRING OF RECTENNA DIODES CONTAINING $N_{DS} = 43$ PARALLEL DIODES

space division

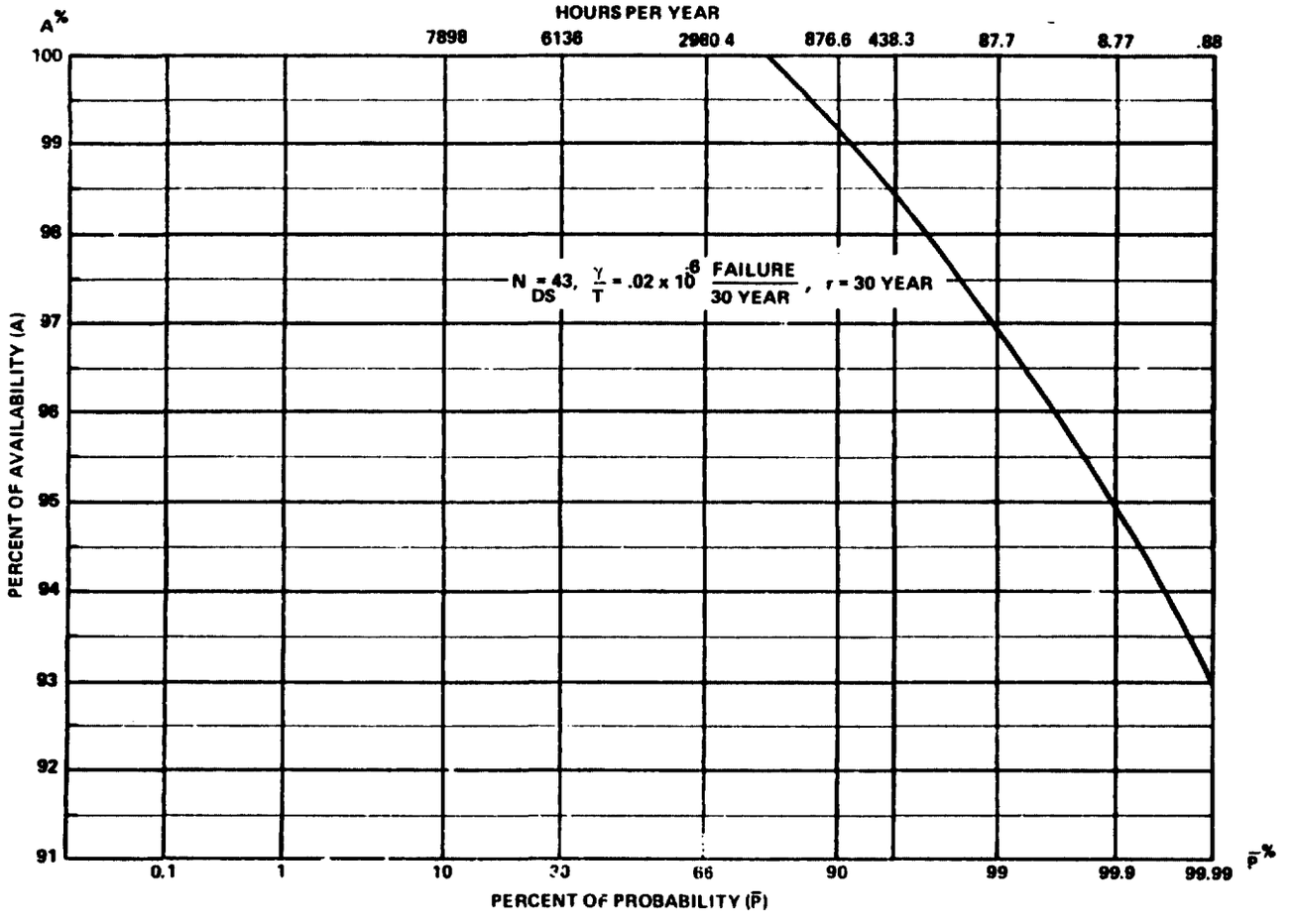

AVAILABILITY VS. PROBABILITY OF THE SPACE ANTENNA PHASE CONTROL SYSTEM
FROM INPUT OF PILOT RECEIVE ANTENNA TO KLYSTRON INPUT

The figure shows the availability of the spacecraft phase distribution system. The average value is 99%.

GENERAL ELECTRIC

AVAILABILITY VS. PROBABILITY OF THE SPACE ANTENNA PHASE CONTROL SYSTEM FROM INPUT OF PILOT RECEIVE ANTENNA TO KLYSTRON INPUT

space division

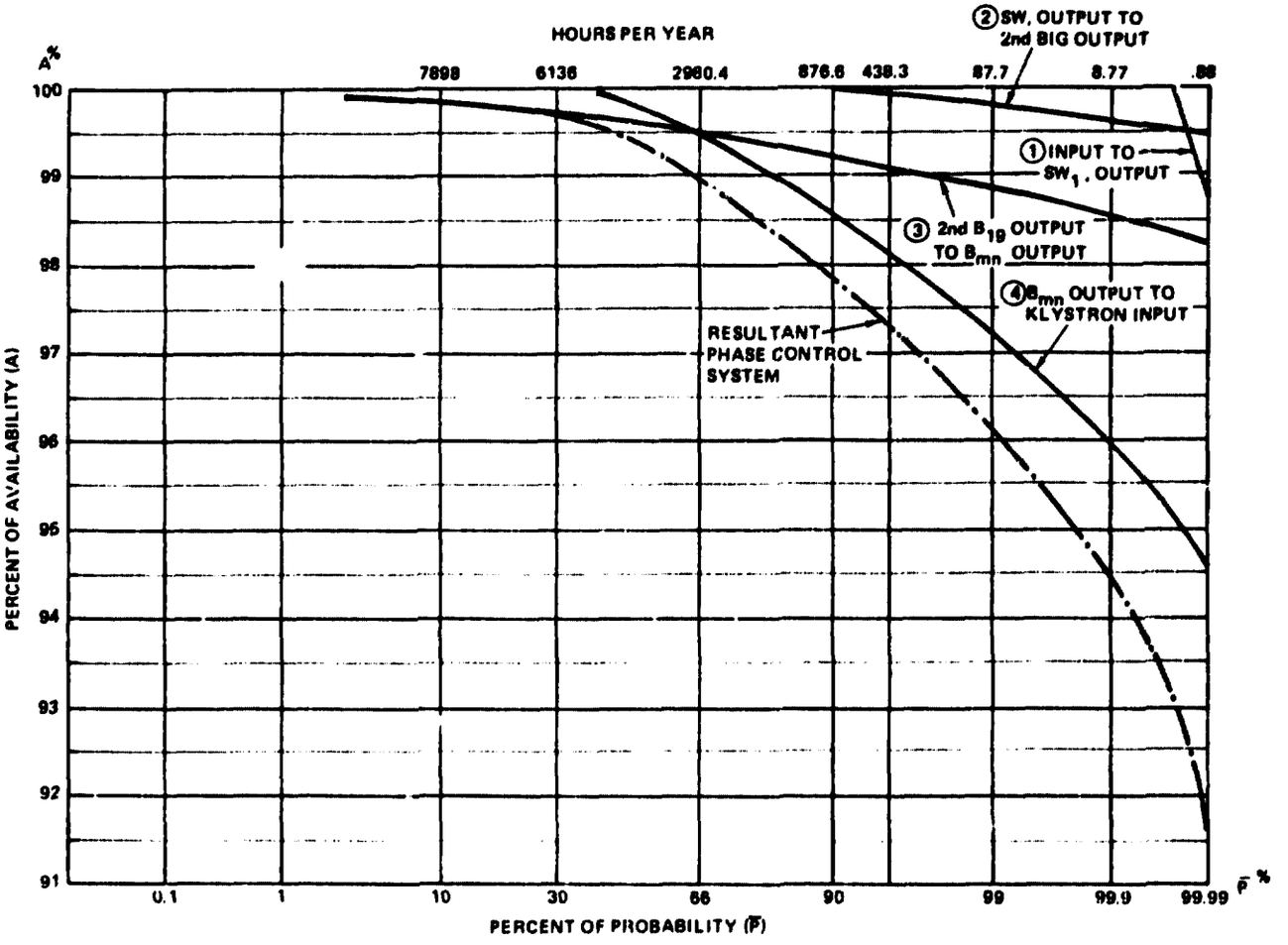

AVAILABILITY VS. PROBABILITY OF KLYSTRONS
BASED ON AVAILABILITY OF A GROUP OF N_G = 380

The figure shows the availability of klystrons and their associated drives. Twenty year lifetime is assumed for this assembly and refurbishment is provided half yearly. The average value of availability is 97.45%. On the average 2544.6 klystrons have to be replaced biyearly out of the 101784 operational units.

GENERAL ELECTRIC

AVAILABILITY VS. PROBABILITY OF KLYSTRONS BASED ON AVAILABILITY OF A GROUP OF N_G= 380

space division

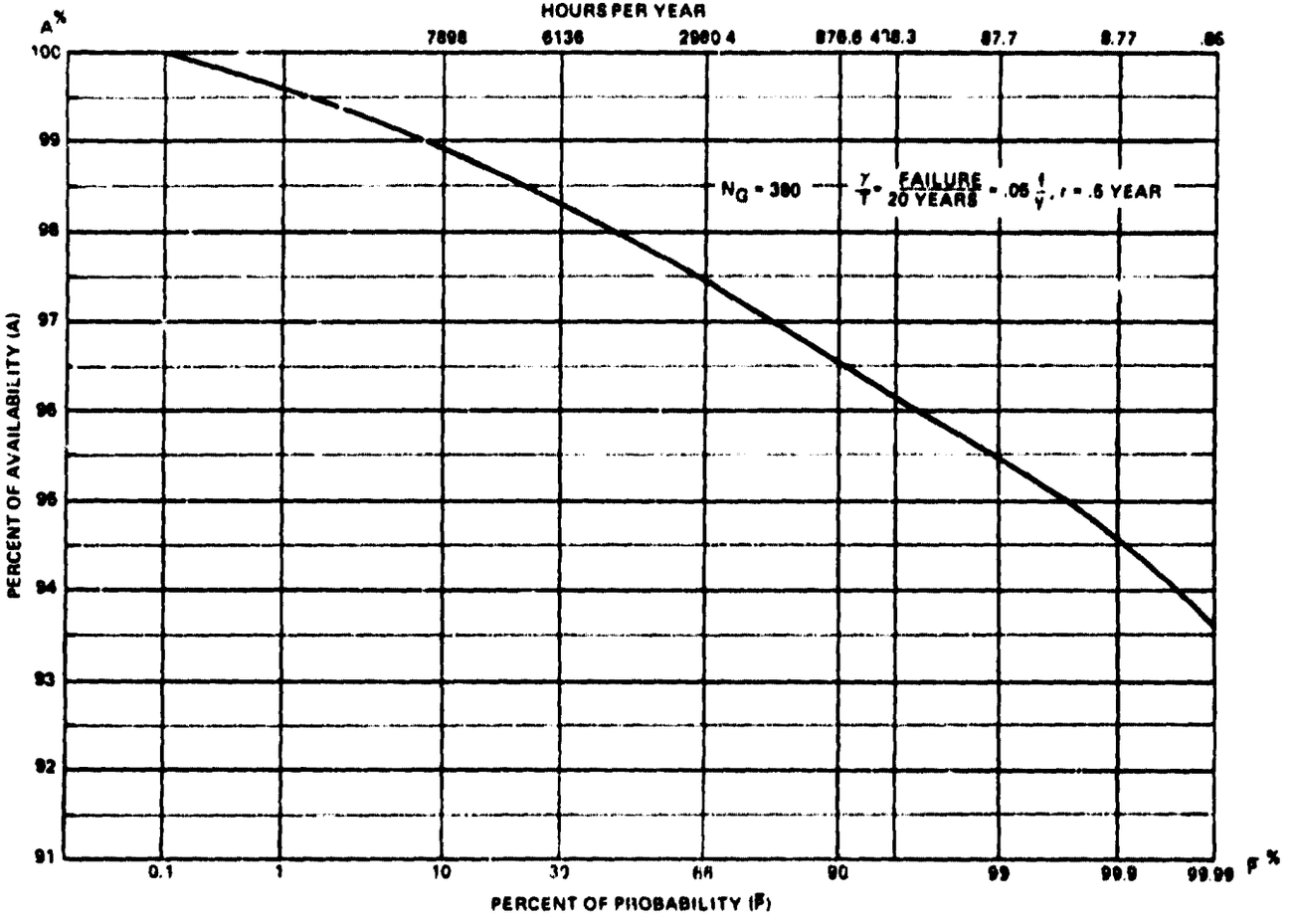

AVAILABILITY VS. PROBABILITY OF POWER OUTPUT FROM IDEAL SPACE ANTENNA DUE TO RANDOM APERTURE ERRORS AND PROPAGATION CONDITIONS

The figure shows the availability of effective antenna gain as it is influenced by random variables. Effects of aperture phase errors, aperture amplitude errors, attenuation in the media and effects caused by Faraday rotation.

GENERAL ELECTRIC

AVAILABILITY VS. PROBABILITY OF POWER OUTPUT FROM IDEAL SPACE ANTENNA DUE TO RANDOM APERTURE ERRORS AND PROPAGATION CONDITIONS

space division

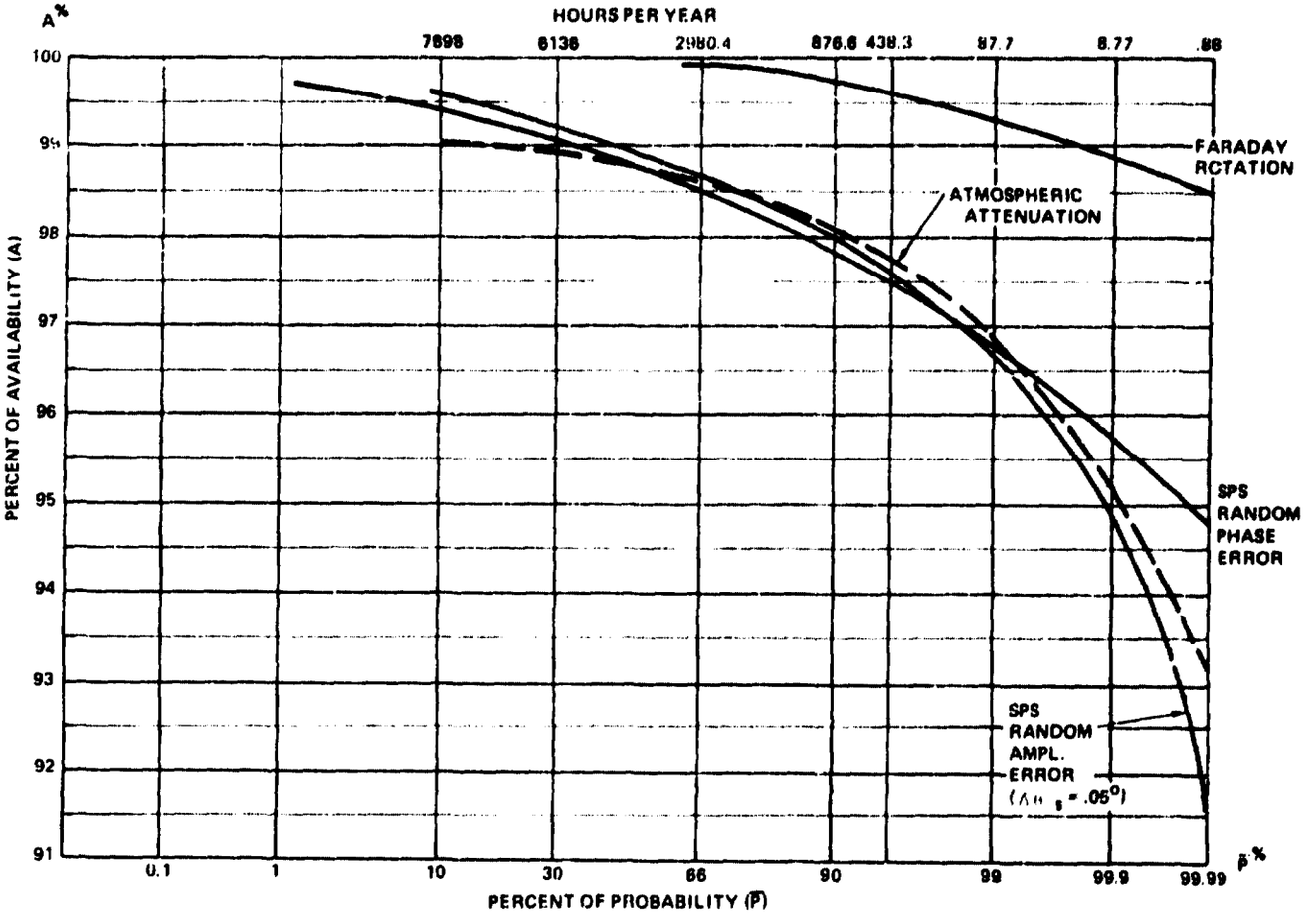

AVAILABILITY VS. PROBABILITY OF A TYPICAL RECTENNA PANEL CONTAINING N = 1849 DIODES

The mean value of availability of a typical rectenna panel is 98.85% with state-of-the-art failure rates ($.04 \times 10^{-6}$ failure/hours). A factor of 2 improvement in failure rates increases the mean availability to 99.45% at the end of the 30 year lifetime. The improved value is assumed for system availability calculations. The dipole panels will be refurbished only after 30 years.

GENERAL ELECTRIC

AVAILABILITY VS. PROBABILITY OF A TYPICAL RECTENNA PANEL CONTAINING N = 1849 DIODES

space division

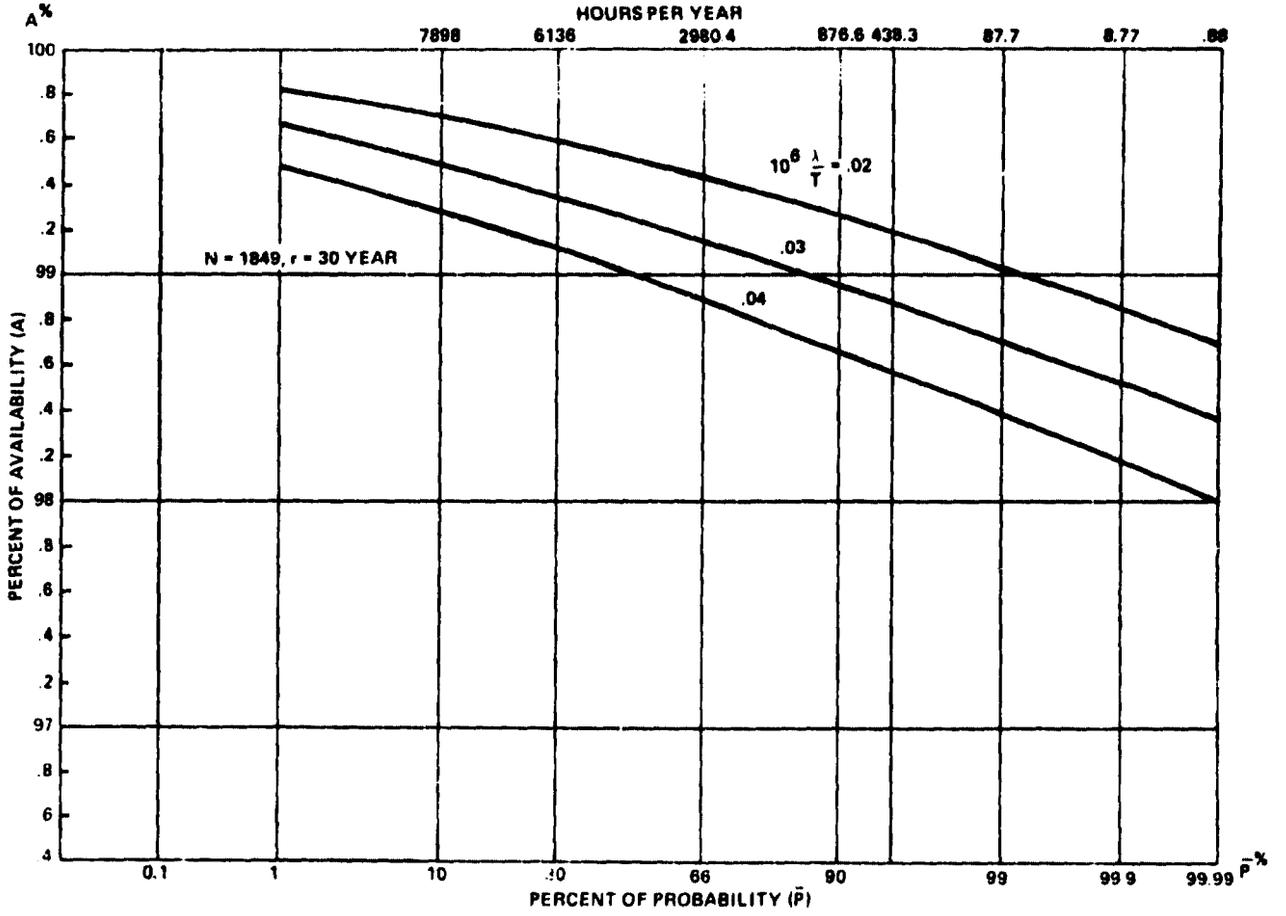

AVAILABILITY VS. PROBABILITY OF A TYPICAL RECTENNA STRING
OF PANELS CONTAINING N_{PS} = 872 PANELS

The mean availability of a typical rectenna panel string (unit) is 99.38% on the account of DC bus line failures if the mean time to repair is r = 876 Hrs. Lines are continuously maintained.

GENERAL ELECTRIC

AVAILABILITY VS. PROBABILITY OF A TYPICAL RECTENNA STRING OF PANELS CONTAINING N_{PS} = 872 PANELS

space division

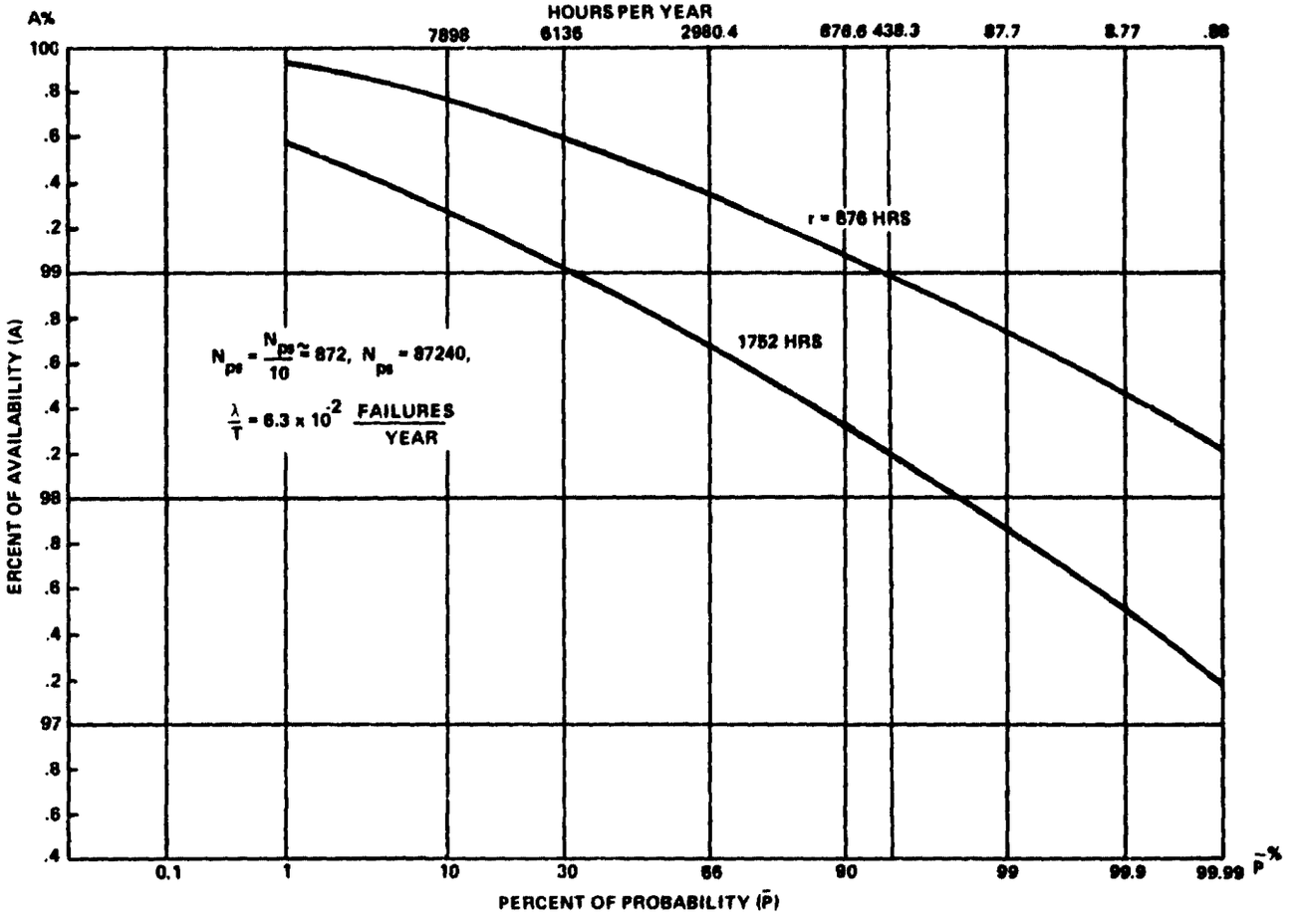

AVAILABILITY VS. PROBABILITY OF UNIT TO GROUP CENTER LINES FOR N_G = 784

The mean availability of rectenna unit to group center connecting line is 99.65% if the mean time to repair is r = 876 Hrs. Lines are continuously maintained.

GENERAL ELECTRIC

AVAILABILITY VS. PROBABILITY OF UNIT TO GROUP CENTER LINES FOR $N_G = 784$

space division

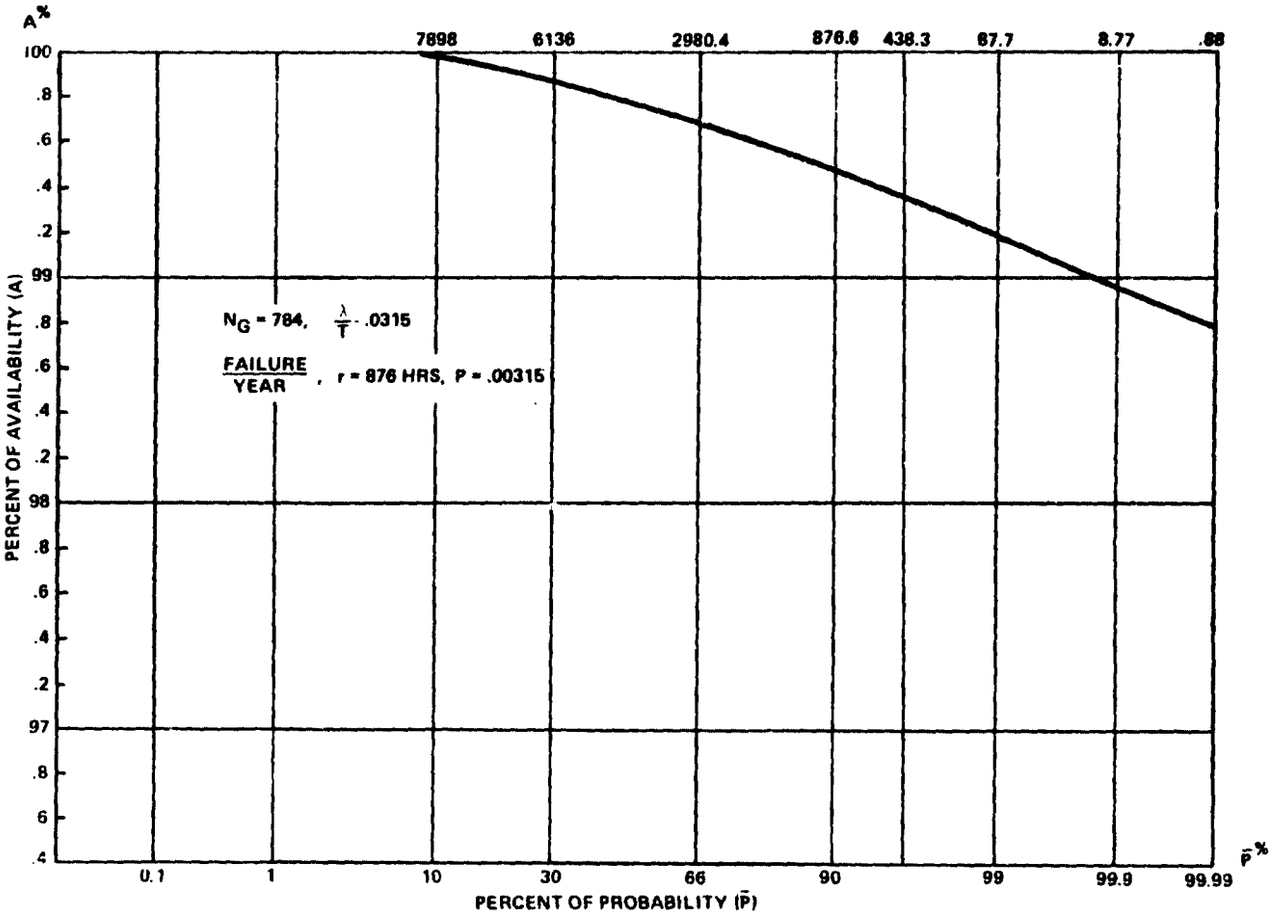

AVAILABILITY VS. PROBABILITY OF RECTENNA D-C POWER COLLECTION SYSTEM FOR VARIOUS FAILURE CHARACTERISTICS COMBINATIONS

The mean availability of the rectenna resultant DC power collection system is 98.4% with .02 x 10^{-6} failure/Hrs. diodes and 876 Hrs. mean time for repair allowance on the DC lines. For the predicted failure rates a crew of 29 is necessary to maintain the DC power collection system.

GENERAL ELECTRIC

AVAILABILITY VS. PROBABILITY OF RECTENNA D-C POWER COLLECTION SYSTEM FOR VARIOUS FAILURE CHARACTERISTICS COMBINATIONS

space division

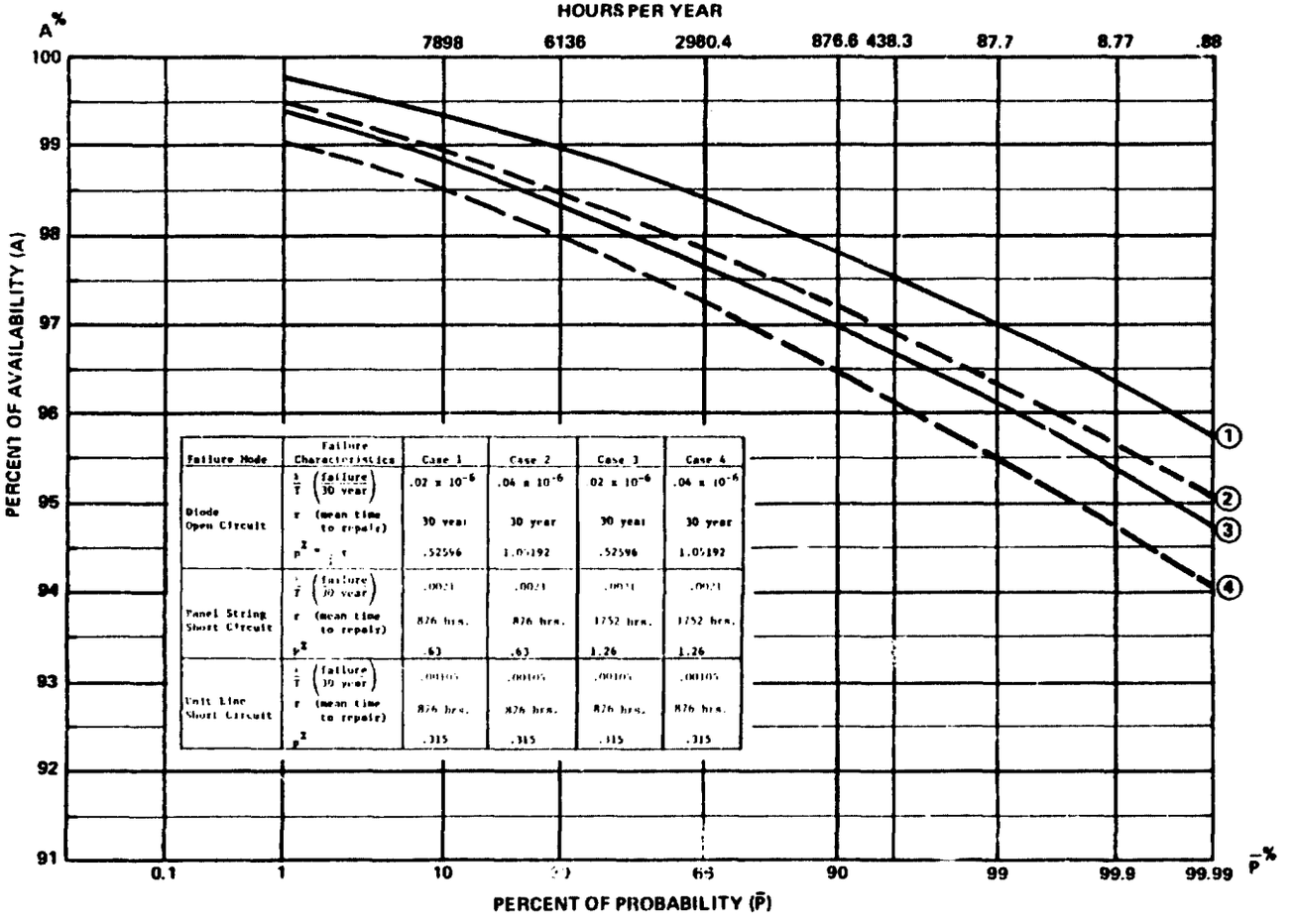

Failure Mode	Failure Characteristics	Case 1	Case 2	Case 3	Case 4
Diode Open Circuit	$\frac{1}{T}\left(\frac{\text{failure}}{30\ \text{year}}\right)$	$.02 \times 10^{-6}$	$.04 \times 10^{-6}$	$.02 \times 10^{-6}$	$.04 \times 10^{-6}$
	r (mean time to repair)	30 year	30 year	30 year	30 year
	$p^2 = \frac{1}{T} r$	.52596	1.05192	.52596	1.05192
Panel String Short Circuit	$\frac{1}{T}\left(\frac{\text{failure}}{30\ \text{year}}\right)$	.0021	.0021	.0021	.0021
	r (mean time to repair)	876 hrs.	876 hrs.	1752 hrs.	1752 hrs.
	p^2	.63	.63	1.26	1.26
Unit Line Short Circuit	$\frac{1}{T}\left(\frac{\text{failure}}{30\ \text{year}}\right)$	.00105	.00105	.00105	.00105
	r (mean time to repair)	876 hrs.	876 hrs.	876 hrs.	876 hrs.
	p^2	.315	.315	.315	.315

RECTENNA AC POWER COLLECTION SYSTEM

The diagram shows an idealized AC power collection network, developed during the Part III study, which can be used for availability calculations.

GENERAL ELECTRIC

RECTENNA AC POWER COLLECTION SYSTEM

space division

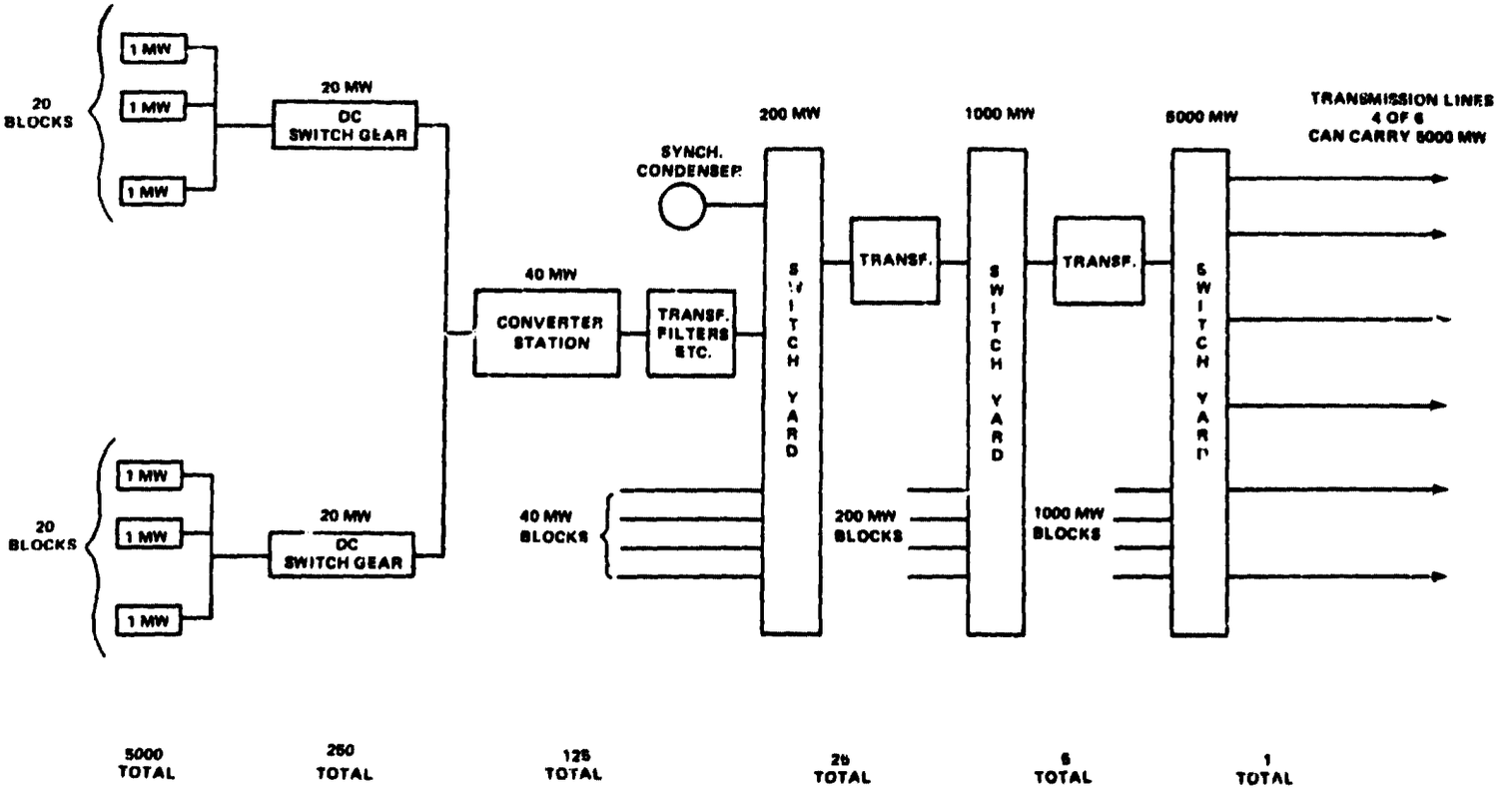

AVAILABILITY VS. PROBABILITY OF OVERALL RECTENNA AC POWER COLLECTION SYST[illegible]

Mean availability of the AC power collection system is 99.7%, limited by the 20 MW stations.

GENERAL ELECTRIC

AVAILABILITY VS. PROBABILITY OF OVERALL RECTENNA AC POWER COLLECTION SYSTEM

space division

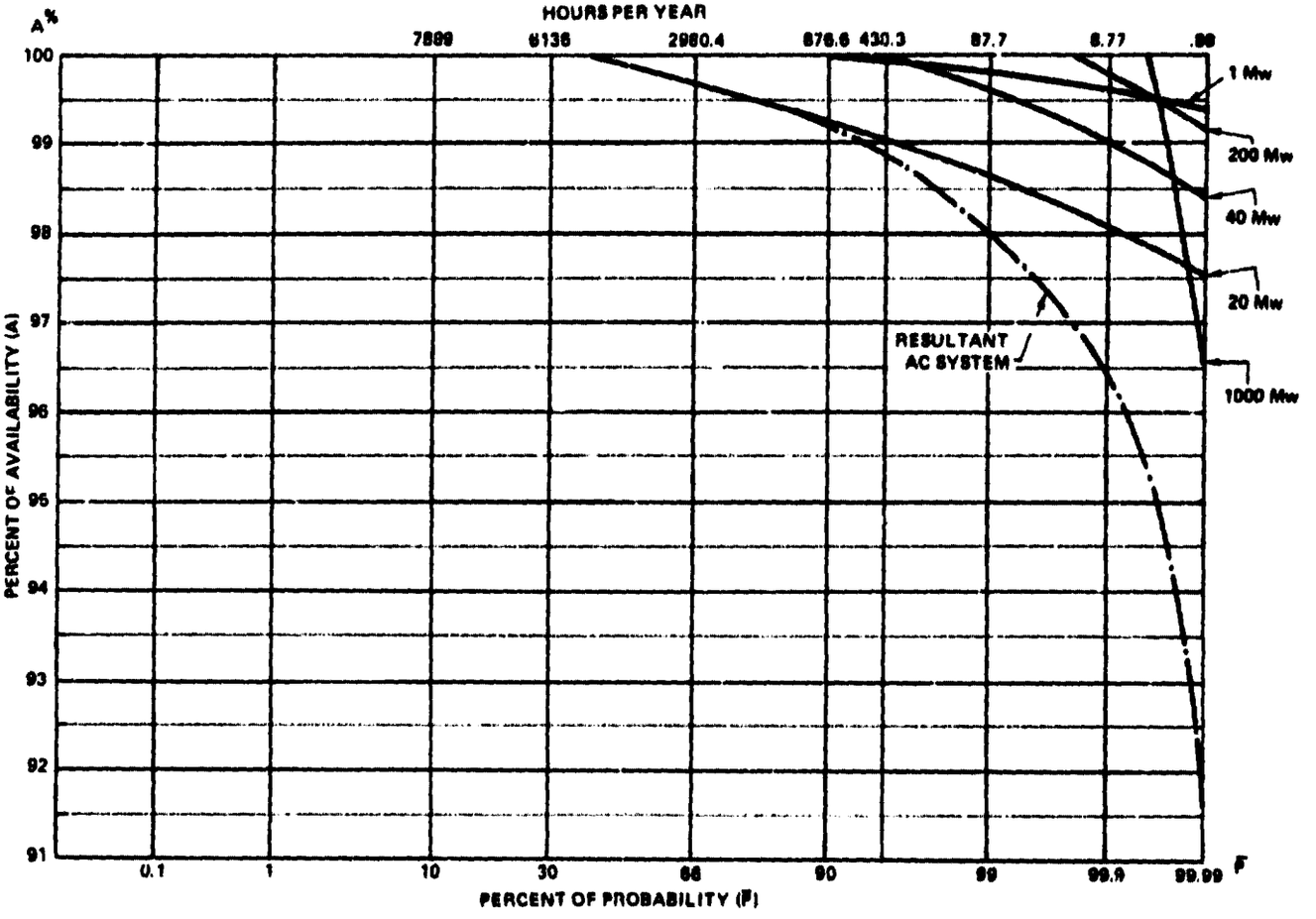

FAILURE MODE AND RELIABILITY ANALYSIS

The calculation of a reliability profile of the AC power collection system was performed for all three layout options. The reliability profile calculated will show the power output from a 625 MW rectenna sector as a function of the percent of time in a year. The block diagram in this figure shows the flow of the probability calculations. The failure characteristics are indicated on the figure.

Mathematically the calculations are performed by using the binomial probability function for each of the groups in each design to which it applies and then combining the probabilities of component outages and the associated power lost to develop the data needed to draw the reliability profiles. The assumptions used are:

1. The exposure period is 8760 hours

2. The switchyards and the synchronous condensers are designed not to contribute to power outages.

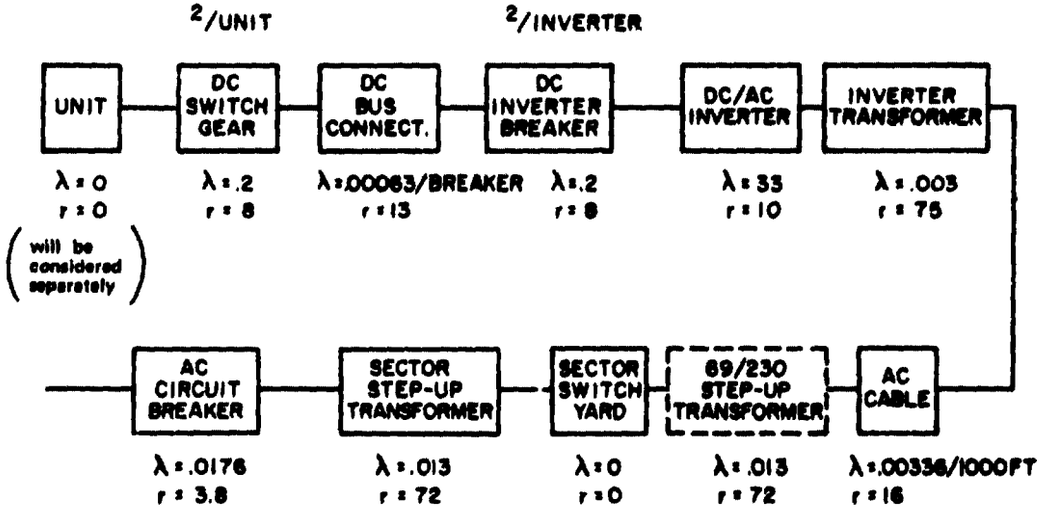

BLOCK DIAGRAM FOR RECTENNA SECTOR
RELIABILITY CALCULATIONS

FAILURE MODE AND RELIABILITY ANALYSIS

The reliability profile for the 625 MW sector considering the elements in the AC power collection system is shown in this curve.

The reliability profile is shown in the figure. The reliability of the rectenna AC power collection system is very high compared to current utility generating equipment, both in the baseline design as well as the other designs studied, and the choice of any of these three designs will not depend on these reliability considerations.

GENERAL ELECTRIC

FAILURE MODE AND RELIABILITY ANALYSIS

space division

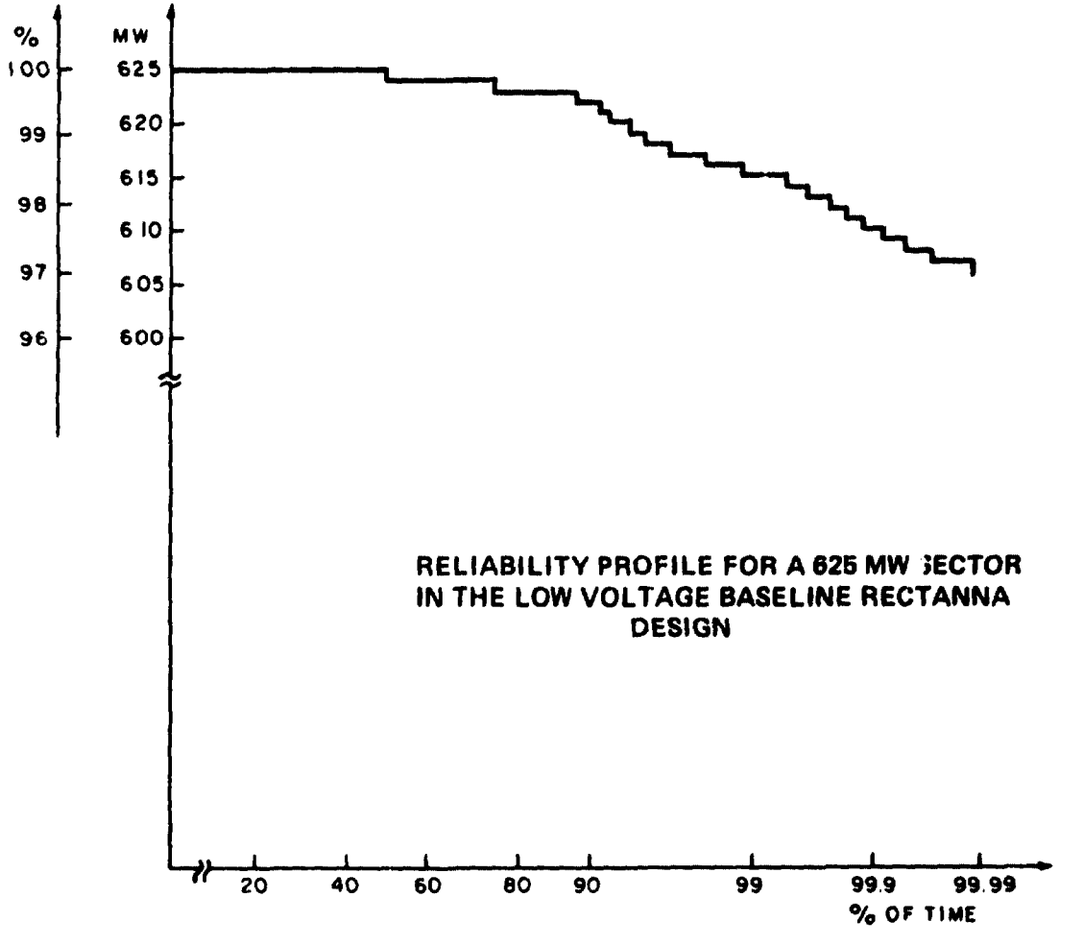

RELIABILITY PROFILE FOR A 625 MW SECTOR IN THE LOW VOLTAGE BASELINE RECTANNA DESIGN

SUMMARY OF EQUIPMENT AND POWER AVAILABILITY CALCULATIONS

The table summarizes the equipment availability and AC power to utility grid availability on the account of the analyzed part of the SPS system. Input interface is at the output of a flexible DC cable on space antenna, output interface is at input to utility grid. All effects which cause statistical variation of availability (failures, errors, propagation) are included. Some of the major assumptions:

- Space antenna DC to DC converter is redundant.
- Phase control uses four layer tree, down to klystron level, only first and second layers are redundant.
- Nonredundant, 20 year lifetime klystrons are used. (This is a factor of ten better than state-of-the-art).
- Random phase and amplitude errors of space antenna are the same as calculated in Part III Study.
- Elevation angle toward satellite is 55°.
- Diode failure rate is .02 per million hrs. Diode is not refurbished for 30 years. (Failure rate is a factor of two better than state-of-the-art).
- Critical components in AC power collection system are redundant, rest are covered by on-site spares.
- Space antenna is refurbished within 84 hrs biyearly periods.
- No power recovery is assumed when a failure occurs in space antenna aperture segment related to items (1), (2) or (3) in table.

Note that with power recovery methods the power availability (89.85% mean value) can be improved to the equipment availability (90.12% mean value).

GENERAL ELECTRIC

SUMMARY OF EQUIPMENT AND POWER AVAILABILITY CALCULATIONS

space division

$\bar{P}^{\%}$	10	66	80	90	99	99.9	99.99
Hrs/Year	7889	2980	1753.2	876.6	87.66	8.766	.8766
A. Space Antenna	97.75	93.20	91.56	89.59	84.12	78.62	71.28
1 DC Distribution	100.00	99.50	99.22	98.95	98.00	97.00	95.95
2 Phase Control	99.84	98.92	98.44	97.83	96.10	94.40	91.30
3 Klystron	98.90	97.50	97.02	96.55	95.48	94.58	93.60
4 Random Phase	99.40	98.50	98.20	97.82	96.80	95.75	94.80
5 Random Amp.	99.60	98.60	98.40	98.00	96.65	94.90	91.70
B. Propagation	99.05	98.54	98.28	97.84	96.24	94.17	91.77
6 Attenuation	99.05	98.62	98.40	98.10	96.90	95.20	93.15
7 Faraday Rotation	100.00	99.92	99.98	99.74	99.32	98.92	98.52
C. Rectenna	98.38	98.13	97.61	97.03	95.06	92.96	87.65
8 DC power Collection	99.38	98.45	98.15	97.81	97.00	96.38	95.80
9 AC Power Collection	100.00	99.68	99.45	99.20	98.00	96.45	91.50
Total Power Transmission System Equipment Availability	96.22	90.12	87.78	84.99	76.96	68.88	57.33
Power Availability at Power Grid Interface Relative to Equipment Without Failure	95.00	85.85	83.19	79.43	69.20	59.65	47.01

AVAILABILITY VS. PROBABILITY OF OVERALL SPS POWER TRANSMISSION SYSTEM FROM OUTPUT OF FLEXIBLE JOINT ON SPACE ANTENNA TO POWER GRID INTERFACE

The chart shows the variation of equipment availability in the overall SPS power transfer system. If power recovery methods are used in the space antenna, then the output power at the power grid interface is determined by the equipment availability. Without power recovery (redirecting the available DC power for DC to RF conversion to the still available part of the space antenna radiating components) the available power at the utility interface is lower because a lost radiating component in the space antenna represents loss of power as well as loss of antenna area.

The mean availability for the two cases is approximately 90% and 86% respectively.

GENERAL ELECTRIC

AVAILABILITY VS. PROBABILITY OF OVERALL SPS POWER TRANSMISSION SYSTEM FROM OUTPUT OF FLEXIBLE JOINT ON SPACE ANTENNA TO POWER GRID INTERFACE

space division

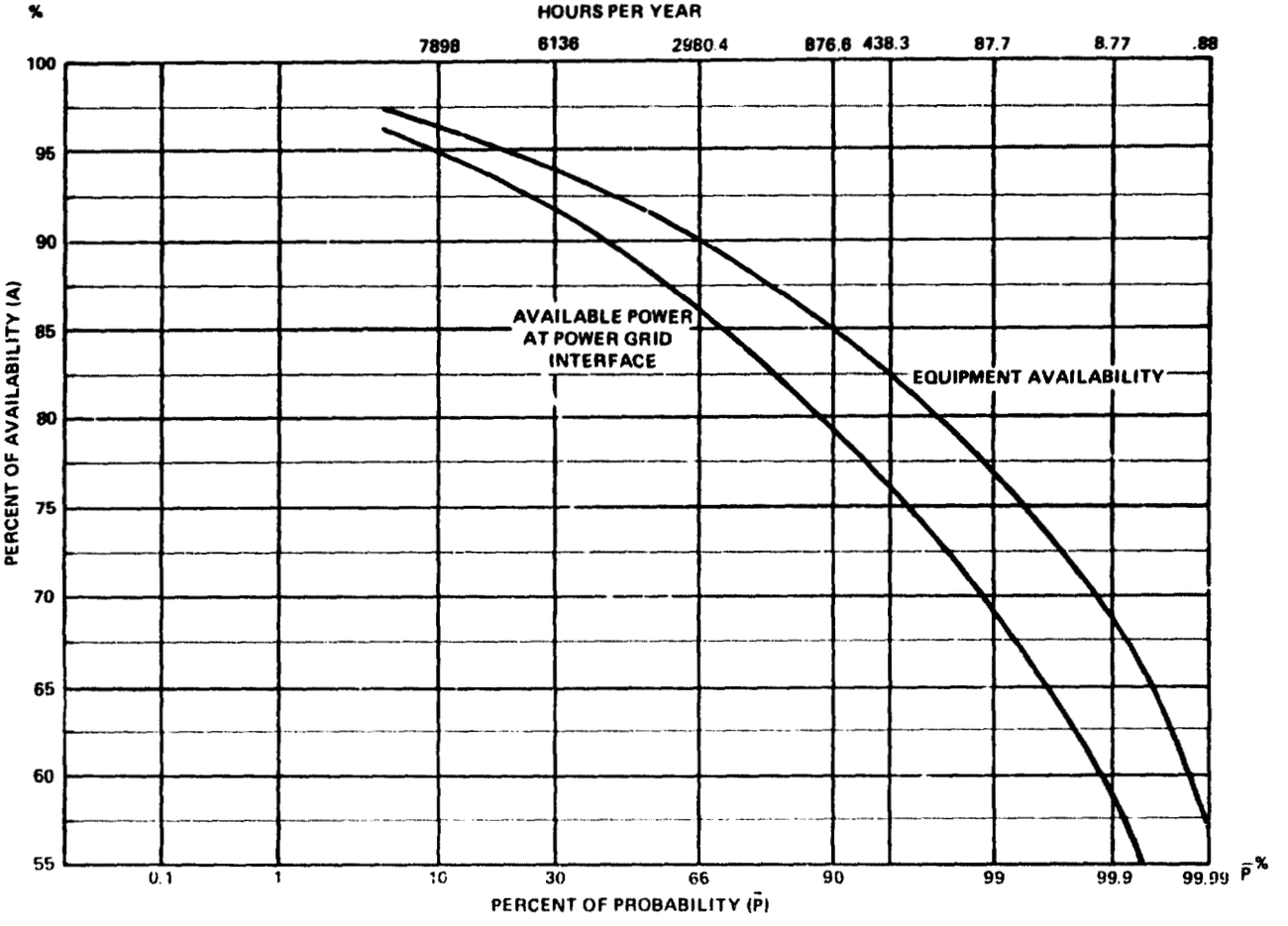

AVAILABILITY OF EFFICIENCY AND POWER INTO POWER GRID

Table shows the worst case efficiency and power into utility grid as a statistical variable. using results of the availability analysis. If diode efficiency is improved by 5% and power recovery methods are successful and spacecraft then the figures shown in the table must be multiplied by 1.1.

GENERAL ELECTRIC

AVAILABILITY OF EFFICIENCY AND POWER INTO POWER GRID

space division

$\bar{P}$ %	10	66	80	90	99	99.9	99.99
Hrs/Year	7889	2980	1753.2	876.6	87.66	8.766	.8766
Available Efficiency %	63.33	57.23	55.46	52.29	46.13	39.76	31.34
Available Power MW	4513.3	4078.6	3952.3	3773.6	3287.6	2833.9	2233.4

EFFECT OF DEVIATION FROM BASELINE SPS ON RELATIVE OUTPUT POWER

This table shows the impact of various output power increasing options on output power and cost.

EFFECT OF DEVIATION FROM BASELINE SPS ON RELATIVE OUTPUT POWER

Option	A % Increase of Output Power	B % Increase of System Cost	B/A
A. Increase 4 and 3 by 1.068 for 23 mw/cm^2 max. Received Power Desnity	6.8	3.88	1.75
B Increase 4 and 3 by 1.1 Reduce 2 by 1.1 Increase 1 by 1.1	10.0	5.71	1.75
C. Increase 1 by 1.1211 for 96.77% beam efficiency	1.5	1.73	.87
D. Implement klystron Maintenance in Every 3 Months	2.5	1.58	1.58
E. Make Last Layer of Phase Control System Fully Redundant	.4	3.0	.13
F. Refurbish Rectenna Panel Asssembly After 15 Years	.58	3.57	.16
G. Reduce r to 438 Hours on Panel String Maintenance	.37	.35	1.06
All the above options are implemented. Average Power Output	23.88 (5052 MW)	26.50	.901
Only Cost Effective Options A, B and D are Implemented Average Power Output	20.42 (4911.4 MW)	11.50	1.77

AVAILABLE SPS POWER TO UTILITY GRID

The figure shows the statistical variation of the available power of the utility interface if power recovery is not used. Improved diodes and power recovery methods can improve the predicted values by about 9%. Chart considers all random failures and scheduled maintenance of 84 Hrs./half year, however, it neglects eclipse and start up/shut down caused power output losses.

GENERAL ELECTRIC

AVAILABLE SPS POWER TO UTILITY GRID

space division

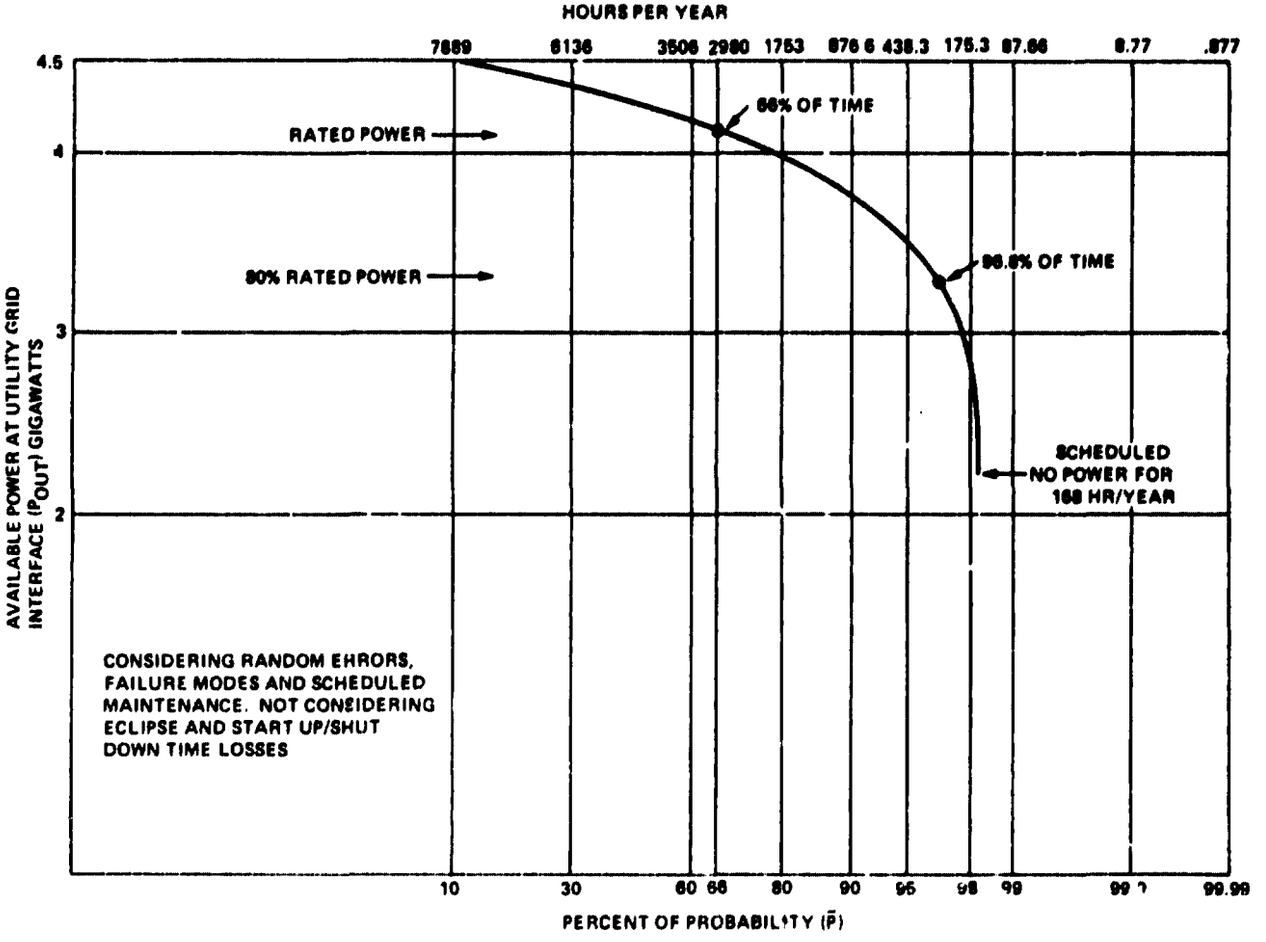

MAINTENANCE REQUIREMENTS SUMMARY

The maintenance tasks for the SPS power transmission system were studied and preliminary manpower requirements were established both for the space and ground operation. The summary shows the manpower needs.

GENERAL ELECTRIC

MAINTENANCE REQUIREMENTS SUMMARY

space division

- SPACE ANTENNA MAINTENANCE HOURS FOR 2 MAN CREWS, PER BIYEARLY CYCLES

DC DISTRIBUTION	281.2
RF REFERENCE PHASE DISTRIBUTION	680.5
KLYSTRONS	2544
TOTAL CREW HOURS PER REPAIR CYCLE	3506.3
TOTAL MAN HOURS PER REPAIR CYCLE	7012.7
TOTAL MAN HOURS PER YEAR	14025.4

- RECTENNA DC PER YEAR 5762.5

- RECTENNA AC PER YEAR 69457

- THE MANPOWER REQUIREMENT IS EQUIVALENT TO APPROXIMATELY SEVEN MAN YEARS PER YEAR IN SPACE (ON THE AVERAGE) AND 64 MAN YEARS PER YEAR ON THE GROUND FOR 5 GW SPS SYSTEM.

NUMBER OF FAILURES AND ASSOCIATED MAINTENANCE TIME REQUIREMENTS IN THE SPACE ANTENNA POWER TRANSMISSION SYSTEM

Table summarizes number of failures in space antenna power transmission system within half year period and associated total repair horns requirement. Klystron maintenance represents 72.6% of total time.

GENERAL ELECTRIC

NUMBER OF FAILURES AND ASSOCIATED MAINTENANCE TIME REQUIREMENTS IN THE SPACE ANTENNA POWER TRANSMISSION SYSTEM

space division

Item	$\frac{f}{.5 \text{ year}}$ p	N	F	$\frac{\text{Hrs.}}{\text{Repair}}$ m	Total Repair Time
DC Convertor	.075	456	34.2	4	136.8
DC Vector Line	.00594	228	1.35	12	16.2
Subarray Line	.000315	101784	32.06	4	128.2
SW_1 Output	.01859	60	1.11	8	8.9
2nd B_{19} Output	.006048	380	2.29	6	13.8
B_{mm} Output	.005246	7220	37.87	2	75.7
Klystron Input	.007626	101784	776.2	.75	582.1
Klystron and Drive	.025	101784	2544.6	1	2544.6
Total			3429.68		3506.3
Man hours for two man team					7012.7

NUMBER OF FAILURES AND ASSOCIATED MAINTENANCE TIME REQUIREMENTS IN THE RECTENNA DC POWER COLLECTION SYSTEM

Table summarizes number of failures in rectenna DC power collection system within 1/10 year maintenance period and the associated repair time requirements. Approximately 29 man can maintain this part of the system.

GENERAL ELECTRIC

NUMBER OF FAILURES AND ASSOCIATED MAINTENANCE TIME REQUIREMENTS IN THE RECTENNA DC POWER COLLECTION SYSTEM

space division

	$\frac{f}{.1 \text{ year}}$ p	N	F	$\frac{\text{Hrs}}{\text{Repair}}$ m ·	Tot. Repair Hrs. Per Maintenance Cycle	Man Hours
Panel String	.0063	87240	549.6	5 (2 man)	2748	5496.1
Unit to Group Center Lines	.00315	784	2.47	18 (6 man)	44.4	266.4
				Total		5762.5

FAILURE MODE AND RELIABILITY ANALYSIS RECTENNA AC POWER COLLECTION SYSTEM

The modular nature of the rectenna design will always contribute to the reliability of the rectenna power output.

The components used in the AC power collection system are shown in this table. The AC power collection system is based on the baseline system with the low voltage system layout.

GENERAL ELECTRIC

FAILURE MODE AND RELIABILITY ANALYSIS RECTENNA AC POWER COLLECTION SYSTEM

space division

FAILURE CHARACTERISTICS OF ELEMENTS IN RECTENNA AC POWER COLLECTION SYSTEM

	FAILURE RATE λ (FAILURES/YR)	MEAN TIME TO REPAIR r (HRS)*
DC SWITCHGEAR	.2	8
DC BUS CONNECTIONS	.00063/BREAKER	13
DC CONVERTER BREAKER	.2	8
DC/AC CONVERTER	.33	10
CONVERTER TRANSFORMER	.003	75
AC CABLE	.00336/1000 FT	16
STEP-UP TRANSFORMER	.013	72
AC CIRCUIT BREAKERS	.0176	3.8

*ASSUMES AVAILABLE PARTS AND SPARES ON SITE

MAINTENANCE REQUIREMENTS FOR THE AC POWER COLLECTION SYSTEM

The values for repair time given in the failure rate and effects analysis were used as a basis for developing the unscheduled maintenance requirements. The values used are typical electric industry statistical data. The values found in the SPS rectenna system may be considerably lower than the values shown due to specially trained maintenance personnel and a well stocked replacement parts supply. Particularly in the area of transformer maintenance the value of a sufficient number of spares would be quite significant. This table shows the expected values of failures per year calculated as Repair time x number of components/8760.

GENERAL ELECTRIC

MAINTENANCE REQUIREMENTS FOR THE AC POWER COLLECTION SYSTEM

space division

EXPECTED VALUES OF FAILURES PER YEAR

	PART III BASELINE	LOW CURRENT DESIGN	LOW VOLTAGE DESIGN
DC BREAKERS	1.917	2.833	2.942
D/A CONVERTERS	.047	.205	.295
CONVERTER TRANSFORMER	.003	.014	.020
AC CABLE	.004	.017	.024
SYNCHRONOUS CONDENSER	.16	.16	.16
AC SWITCHGEAR	.003	.002	.002
SU TRANSFORMER	.001	.0008	.0008

MAINTENANCE REQUIREMENTS FOR THE AC POWER COLLECTION SYSTEM

The normal or scheduled maintenance requirements are defined as being inspections and performance tests causing either no curtailment of power or performed during periods in which the power generation from the rectenna system is zero for other reasons than rectenna AC Power Collection System maintenance.

The scheduled maintenance requirements for the components in the rectenna AC power collection system are quite nominal. There are few standard practices in this area in electric utility systems, since each user would tailor the maintenance practices to fit with his specific situation. Contamination from particles and chemicals, the impact of weather and duty cycles and manufacturers specifications would all be variables in determining frequency and maintenance activities.

Based on available survey results of maintenance activities the data given in this table shows scheduled maintenance in terms of manhours per year for the components in the rectenna AC system.

GENERAL ELECTRIC

MAINTENANCE REQUIREMENTS FOR THE AC POWER COLLECTION SYSTEM

space division

SCHEDULED MAINTENANCE REQUIREMENTS

	MANHOURS/YEAR/DEVICE
DC SWITCHGEAR	2
DC/AC CONVERTERS	16
CONVERTER TRANSFORMER	16
AC CABLE	2
SYNCHRONOUS CONDENSER	40
AC SWITCHGEAR	20
STEP-UP TRANSFORMER	16

SUMMARY OF MAINTENANCE HOURS REQUIREMENTS FOR THE AC POWER COLLECTION SYSTEM

Table summarizes scheduled and unscheduled maintenance time requirement with a 1/10 year maintenance period. Approximately 35 men can maintain this part of the system.

GENERAL ELECTRIC

SUMMARY OF MAINTENANCE HOURS REQUIREMENTS FOR THE AC POWER COLLECTION SYSTEM

space division

	HRS.
UNSCHEDULED	495.7
SCHEDULED	6450
	6945.7